Diss. ETH NO. 23880

Trifluoromethyl *P*-stereogenic ligands: synthetic development and catalytic applications

A thesis submitted to attain the degree of

DOCTOR OF SCIENCES of ETH ZURICH

(Dr. sc. ETH Zurich)

presented by

RIMA DRISSI

MSc in Molecular and Biological Chemistry, EPFL

born on 03.12.1987

citizen of Thônex (GE)

accepted on the recommendation of

Prof. Dr. Antonio Togni, examiner
Prof. Dr. Hansjörg Grützmacher, co-examiner

2016

Our imagination is stretched to the utmost, not as in fiction, to imagine things which are not really there, but just to comprehend those things which are there.

Richard Feynman in *The Character of Physical Law*

Jamais la nature ne nous trompe; c'est toujours nous qui nous trompons.

Jean-Jacques Rousseau in *Émile ou De l'Éducation*

Acknowledgements

A great number of individuals have contributed to the successful completion of this doctoral thesis, and I wish to personally acknowledge them here.

First and foremost, a big thank you goes to my supervisor, my *Doktorvater* Prof. Antonio Togni. Not only has he given me the opportunity to carry out my thesis at the great academic institution that is ETH Zurich, he trusted me to work completely independently on a challenging topic. It has been a privilege to spend my doctoral studies in this work environment. His interest for teaching, his humanity, and his open door have been greatly appreciated. Thank you Antonio!

Prof. Hansjörg Grützmacher is kindly acknowledged for readily agreeing to co-supervise this doctoral thesis and his insightful comments on the content of my work.

A special thank you goes to Prof. Antonio Mezzetti, who has not only given me the opportunity to teach one of the most interesting lab courses in chemistry, but has also showed me what it means to be passionate about science; I highly appreciate his constructive criticism. Antonio, thank you for your support!

Andrea Sachs, our secretary, is kindly acknowledged for her intrinsic role in the Togni group, her administrative competence, organizational skills, and general wisdom, all which allow our group to move forward smoothly.

Although the completion of a doctoral thesis remains a relatively solitary path, this journey would not be what it is without supportive and competent co-workers. The past and present members of our combined research group are therefore kindly acknowledged. Those with whom I have collaborated more closely deserve a special mention:

Rino Schwenk and Barbara Czarniecki: following your suggestion, I embarked on the $P-CF_3$ chemistry. Although extremely laborious at moments, I have learned an incredible amount by working on this topic. Your help, guidance, and patience has been especially helpful during the first two years of my thesis, allowing me to become independent. You really are my Enlightened Mentors! Thank you for everything, be it our time in H230 or at (numerous) social gatherings; I greatly appreciate the time we spent together and the friendship which has emerged.

Remo Senn, it was a pleasure working alongside you as the "GC-MS team", either when dismantling the old GC-MS, or when learning how to troubleshoot the new system. I also highly appreciate your (seemingly unlimited) theoretical and practical knowledge, which have more than once helped me move forward. *Alba gu bràth!*

Lukas Sigrist and Ewa Pietrasiak: thank you for always taking the time to measure my not-always-easy-to-measure crystals! Lukas, thank you for giving me tips on how to crystallize my compounds efficiently (although I usually failed), and for making me tip towards the ferrocenes (probably the best scientific decision of my thesis). Ewa, thank you for your patience and persistence whilst measuring the phenylethylferrocenes.

Alex Lauber, thanks for your endless patience (and knowledge!) concerning HPLC, NMR, and other matters. In general, a big thank you to all members who took the time for their group

jobs and allowed us to have a perfectly running system, contributing to the group dynamic. Václav Matoušek (Vasek), thank you for teaching me valuable lessons in organic and practical chemistry, and for the social times we have shared. More generally, thank you to the "Czech Connection": Jirka and Alena, I very much appreciated the time with you in the group.

Lukas Sigrist, Raphael Bigler, Julie Charpentier, Martin Schwarzwälder, Giuseppe Lapadula, and Erik Schrader, thank you for the friendly and uncomplicated collaboration in the course of the *Praktikum*. Raphi, *merci vilmol für din* Wort vom Tag *chalender; du bisch en super schwiizerdütschlehrer gsii!*

Over the last four years, I have had the privilege to work with highly motivated and competent students. Marius Lutz, Franziska Elterlein, and Manuel Kober-Czerny have contributed considerably to this thesis in the course of their projects. I have learned a lot through them as I hope they have learned from me and the tricky $P-CF_3$ chemistry. Marius, thank you for your consistency and efficiency in the lab. Your first catalytic results with the Fcox ligands are to date still the best! Franziska, thank you for your incredible motivation during a very challenging project, as well as your patience whilst I was teaching the *Praktikum*. Your hard work has not been in vain as we have learned a lot on the 1,1' system, and I greatly appreciate your significant investment of time and effort during your Master thesis! Manu, it was a pleasure for me to supervise you during your first semester project and my last semester in the lab. Your work has been extremely valuable and has allowed a side project to become a full chapter of my thesis. Thank you for being a great student and person!

I have also had the opportunity to supervise other excellent students, in the course of the third semester *Praktikum* and SiROP projects: thank you to all for the generally smooth and disciplined collaboration. Special thanks to Adriano D'Addio, Jonas Bösken (Thor), Moritz Hansen, Salome Heilig, and Fabian Kirschbaum for the synthesis of many project-related compounds and/or the stimulating collaboration on the geosmin project!

My past and present labmates: thank you for making the big lab so diverse (not only musically...). Harutake Kajita (Harusake!) and Carl-Philipp Rosenau (CP), the last two years have been exceptional with you "on my side" (although the former time with the student corner with the infamous Lukas Leu (Lulu) and Peter Müller (Petmüll) remains fondly in my memory). It has also been a joy to share the "cursed spot" with my many "back-to-back" neighbors: Michael Schneider, Marius Lutz, Fabian Brüning, Franziska Elterlein, Ewa Pietrasiak, Lukas Rochlitz (Schnaxi) and, last but not least, Pascal "F." Tripet (who will help restore balance to the EPFL/ETH Force).

To all the ETH staff we collaborate with, the HCI shop personnel, Bruno Strebel, Guido Krucker, the *Werkstatt* personnel, the MS Service team: thank you for supporting us in an excellent fashion.

All my colleagues and friends who were by my side in all locations and events possible and made my doctoral years memorable, a big THANK YOU: Peter, Amos, David, Florent, Laurent, Amira, Nadia, Flalena, Céline, Alix, Maude, Jorge, Simon, Robin (Hawk 12!), Lorena, the St Gallen Open Air team, our various SOLA teams, and all those I may have forgotten to mention personally but who will recognize themselves...

Special thanks are long due to Lukas, Helmo, and Lexi for, well, everything really. Thank you for being by my side and helping me get through the last four years.

Last but not least, I am highly indebted to my parents, who have done everything possible to allow me to be where I am now. They have always supported me the best they could, irrespective of the situation. I am therefore eternally grateful for all they have done for me.

R. D.
Zurich, 02.12.2016

List of contributions

Part of the work completed in the course of this thesis was presented at national and international conferences:

Novel Trifluoromethylated P-Stereogenic Ligands, Oral presentation, 14th Ferrocene Colloquium, 21-23rd February **2016**, University of Konstanz, Germany.

Novel Trifluoromethylated P-Stereogenic Oxazoline Ligands, Poster presentation, 13th Ferrocene Colloquium, 22-24th February **2015**, University of Leipzig, Germany.

Novel Trifluoromethylated P-Stereogenic Oxazoline Ligands, Poster presentation, SCS Fall meeting, 11th September **2014**, University of Zurich, Switzerland.

Novel Trifluoromethylated P-Stereogenic Oxazoline Ligands, Poster presentation and short oral presentation, 5th EuCheMS Chemistry Congress, 31st August-4th September **2014**, Istanbul, Turkey.

Towards a New Class of P-Trifluoromethylated BINAP-Derived Ligands, Poster presentation, SCS Fall meeting, 6th September **2013**, EPFL, Lausanne, Switzerland.

Table of Contents

Abstract

The thesis at hand mainly focuses on the synthetic development of new trifluoromethyl *P*-stereogenic phosphane-based ligands. Their characterization as well as their application in catalytic asymmetric homogeneous processes were considered. The structures investigated comprise various types of backbones, originating from privileged ligand classes, which possess different elements of chirality. The main feature of the ligands developed is phosphorus stereogenicity. This underused chiral motif combined with electron-poor trifluoromethyl substituents at phosphorus renders these ligands unique. This work aims to gain insight on preparative routes to access them and their activity in enantioselective catalysis.

In a first instance, the investigation of axially chiral BINAP-derived ligands was carried out (figure 1). It was found that the high rotation barrier of the binaphthyl backbone does not allow for straightforward modifications in the 2,2' positions. The pathway to the existing bistrifluoromethyl BINAP derivative could not be optimized. The ligand could nevertheless be tested for the first time in the asymmetric alkylative ring opening of 7-oxabenzonorbornadiene. It showed a high level of stereoselection, inducing enantioselectivities up to 84%. No new BINAP derivatives could be prepared in a synthetically reasonable manner. An unhindered biaryl ligand was thus chosen as alternative (figure 1), and a simple P-CF_3 biphenyl ligand was successfully synthesized and shown to coordinate to gold(I).

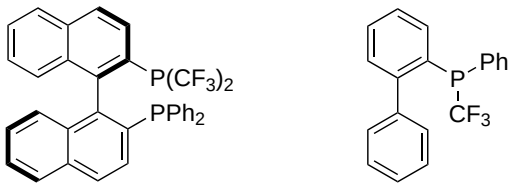

5 **20**

Figure 1: Biaryl ligands investigated (chapter 2).

In a second instance, oxazoline ligands were studied (figure 2). Phenyloxazoline (PHOX) derivatives could be prepared in reasonable amounts via lithium-bromine exchange of the corresponding bromophenyl precursors followed by electrophilic substitution with $PPh(CF_3)_2$. The diastereoselectivity of this reaction could however not be controlled. Furthermore, no means were found to separate the diastereomers. A simple coordination experiment to palladium(II) was successfully carried out with one of the prepared representatives of this ligand class.

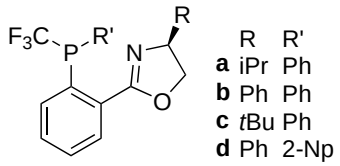

	R	R'
a	iPr	Ph
b	Ph	Ph
c	*t*Bu	Ph
d	Ph	2-Np

(R_P)+(S_P)-**26**

Figure 2: Phenyloxazoline ligands investigated (chapter 3).

1,2-Ferrocenyloxazolines were subsequently investigated (figure 3). It was found that the corresponding planar chiral ligand diastereomers could be easily separated by standard column

chromatography. The ligands were shown to coordinate to palladium(II) and platinum(II), and were subsequently applied in various stereoselective catalyses. The best results were found in the palladium-catalyzed allylic alkylation of cinnamyl acetate. Enantioselectivity was shown to be higher than that of the parent ligand, and the linear to branched ratio was also favorably influenced. In other catalytic transformations, the ligands either displayed no conversion or very little enantioselectivity. Additionally, the absolute configuration at phosphorus seemed to have little to no influence on the catalytic processes tested.

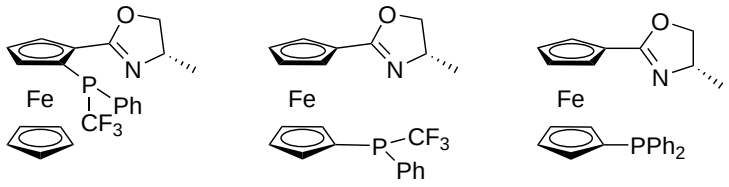

(R_P)/(S_P)-**34a** (R_P)+(S_P)-**49a** **45a**

Figure 3: Ferrocenyloxazoline ligands investigated (chapter 3).

As the synthesis of 1,2 substituted ferrocenyloxazolines suffered from major reproducibility issues, the preparation of the corresponding 1,1' derivatives was instigated (figure 3). The sterically less hindered environment was thought to allow much less restriction with respect to lithiation and electrophilic substitution at the ferrocene backbone. This was however experimentally found to be untrue, as these transformations were also problematic with this substitution pattern. During the course of this work, a new pathway was developed for the synthesis of the 1,1'-ferrocenyl parent ligand (figure 3).

Finally, the study of trifluoromethyl counterparts derived from phenylethylferrocenyl ligands was initiated (figure 4). New synthetic pathways were developed to access the bis- and monotrifluoromethyl congeners of this family, and the processes could be scaled up.

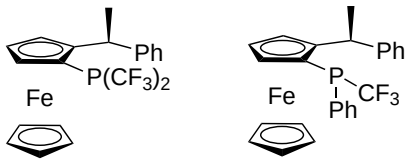

59 (R_P)/(S_P)-**60**

Figure 4: Phenylethylferrocenyl ligands investigated (chapter 4).

The obtained ligands were compared to their parent ligand in the solid state, and their coordination behavior to ruthenium(II) and gold(I) was investigated. Finally, a preliminary activity test was carried out by applying the ligands in the transfer hydrogenation of acetophenone. Under unoptimized conditions, the ligands were found to yield racemic product.

Zusammenfassung

Die vorliegende Dissertation fokussiert sich hauptsächlich auf die synthetische Entwicklung von neuen Trifluormethyl *P*-stereogenen Phosphan-basierten Liganden. Sowohl ihre Charakterisierung als auch ihre Anwendung in katalytischen asymmetrischen homogenen Prozessen wurden betrachtet. Die untersuchten Liganden beinhalten diverse Strukturentypen, welche von privilegierten Ligandklassen abstammen, und besitzen unterschiedliche Chiralitätselemente. Das Hauptmerkmal der entwickelten Liganden ist die Phosphor-Stereogenizität. Dieses unterbenutzte chirale Motiv kombiniert mit elektronarmen Trifluormethylsubstituenten am Phosphor machen diese Liganden einzigartig. Die vorliegende Arbeit gibt einen Einblick in die präparativen Wege zur Herstellung dieser und deren Aktivität in enantioselektiver Katalyse.

Als Erstes wurden BINAP Derivate mit axialer Chiralität untersucht (Abbildung 1). Wie sich zeigte, erlaubt die hohe Barriere der Rotation von Binaphthyl keine direkte Modifikation in den 2,2'-Positionen. Die Syntheseroute zum existierenden Bistrifluormethyl BINAP-Derivat konnte nicht optimiert werden. Der Ligand wurde trotzdem das erste Mal in der asymmetrischen alkylierenden Ringöffnung von 7-Oxabenzonorbornadien getestet. Ein hoher Grad an Stereoselektivität wurde beobachtet, mit Enantioselektivitäten bis zu 84%. Neue BINAP-Derivate konnten in keiner akzeptablen Weise synthetisiert werden. Als Alternative wurde ein ungehinderter Biaryl-Ligand gewählt (Abbildung 1). Ein solcher P-CF_3 Biphenyl-Ligand wurde erfolgreich hergestellt und an Gold(I) koordiniert.

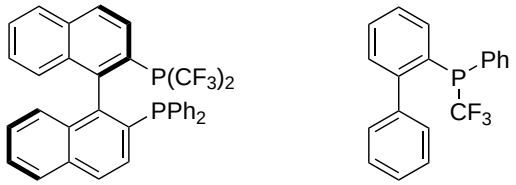

5 **20**

Abbildung 1: Untersuchte Biaryl-Liganden (Kapitel 2).

Im zweiten Teil wurden Oxazoline-Liganden untersucht (Abbildung 2). Phenyloxazoline (PHOX) Derivate konnten in vernünftigen Mengen via Lithium-Brom Austausch von dem entsprechenden Bromophenyl Vorläufern hergestellt werden, gefolgt von einer elektrophilen Substitution mit $PPh(CF_3)_2$. Die Diastereoselektivität dieser Reaktion konnte nicht kontrolliert werden und es wurde keine Methode zur Trennung der Diastereomere gefunden. Ein einfaches Koordinationsexperiment mit einem der Vertreter dieser Ligandklasse zu Palladium(II) wurde erfolgreich durchgeführt.

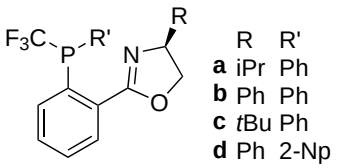

	R	R'
a	iPr	Ph
b	Ph	Ph
c	*t*Bu	Ph
d	Ph	2-Np

(R_P)+(S_P)-**26**

Abbildung 2: Untersuchte Phenyloxazoline-Liganden (Kapitel 3).

Anschliessend wurden 1,2-Ferrocenyloxazoline studiert (Abbildung 3). Es wurde gezeigt, dass sich die entsprechenden planar-chiralen Ligandendiastereomere säulenchromatographisch einfach trennen lassen. Die Koordination der Liganden zu Palladium(II) und Platin(II) wurde gezeigt. Die Liganden wurden in diversen stereoselektiven Katalysen angewandt. Die besten Resultate wurden in der Palladium-katalysierten allylischen Alkylierung von Cinnamylacetat erzielt. Die Enantioselektivität war höher und das Verhältnis von linearem zu verzweigtem Produkt wurde im Vergleich mit dem ursprünglichen Ligandentyp ebenfalls positiv beeinflusst. In anderen katalytischen Anwendungen wiesen die Liganden entweder kein Umsatz oder wenig Enantioselektivität auf. Die absolute Konfiguration von Phosphor scheint wenig oder kein Einfluss auf die Stereoselektivität der getesteten katalytischen Prozesse zu haben.

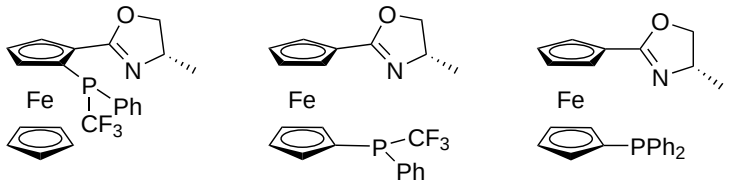

(R_P)/(S_P)-**34a** (R_P)+(S_P)-**49a** **45a**

Abbildung 3: Untersuchte Ferrocenyloxazoline-Liganden (Kapitel 3).

Da die Synthese von 1,2-substituierten Ferrocenyloxazoline unter grossen Reproduzierbarkeitsproblemen leidet, wurde die Herstellung der entsprechenden 1,1'-Derivate initiiert (Abbildung 3). Die Überlegung war, dass die weniger sterisch gehinderte Umgebung der 1'-Position am Ferrocen die Lithiierung und die darauffolgende elektrophile Substitution erleichtern sollte. Experimentell zeigte sich, dass der Schritt der Substitution dennoch problematisch ist. Im Laufe dieser Arbeit wurde ein neuer Syntheseweg zum ursprünglichen 1,1'-Ferrocenylligandensystem entwickelt (Abbildung 3).

Abschliessend wurden Trifluormethyl-Analoga von Phenylethylferrocenyl-Liganden untersucht (Abbildung 4). Neue Synthesewege wurden entwickelt um die Bis- und Monotrifluormethyl Analoga dieser Familie herzustellen. Diese konnten für grössere Massstäbe optimiert werden.

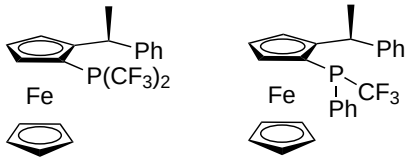

59 (R_P)/(S_P)-**60**

Abbildung 4: Untersuchte Phenylethylferrocenyl-Liganden (Kapitel 4).

Die erhaltenen Liganden wurden röntgenspektroskopisch untersucht und mit dem ursprünglichen Ligand verglichen. Ihre Koordination zu Ruthenium(II) und Gold(I) wurde ebenfalls untersucht. In einem Vorversuch wurde die Aktivität der neuen Liganden in der Transferhydrierung von Acetophenon untersucht. Unter nicht-optimierten Bedingungen wurde nur racemisches Produkt erhalten.

Résumé

La présente thèse se focalise principalement sur le développement synthétique de nouveaux ligands phosphanes trifluorométhyles *P*-stéréogènes. Leur caractérisation ainsi que leur application dans des procédés de catalyse asymétrique homogène ont été considérées. Les ligands étudiés comprennent des types de structures diverses, issues de classes de ligands privilégiés, et possèdent différents éléments de chiralité. La caractéristique principale des ligands développés est la stéréogénicité du phosphore. Ce motif chiral peu répandu en combinaison avec des substituants trifluorométhyles électroniquement pauvres sur le phosphore rend ces ligands uniques. Ce travail vise à établir un procédé préparatif pour y accéder ainsi qu'à tester leur activité en catalyse énantiosélective.

En premier lieu, des ligands dérivés de BINAP avec chiralité axiale ont été étudiés (figure 5). L'importante barrière rotationnelle de la structure binaphthyle n'a pas permis une modification directe des substituants en positions 2,2'. La synthèse du ligand dérivé de BINAP bistrifluorométhyle existant n'a pas pu être optimisée. Le ligand a néanmoins pu être testé pour la première fois dans l'ouverture alkylative asymétrique du cycle 7-oxabenzonorbornadiène. Une haute stéréosélection a été démontrée, le ligand induisant une énantiosélectivité jusqu'à 84%. Aucun nouveau dérivé de BINAP n'a pu être synthétisé de manière raisonnable. Un biaryle non encombré a par conséquent été choisi comme alternative (figure 5). Un ligand biphényle P-CF_3 simple a été préparé avec succès et coordiné à un atome or(I).

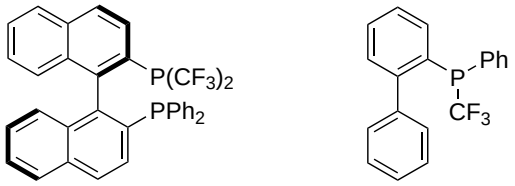

5 **20**

Figure 5: Ligands biaryles étudiés (chapitre 2).

Dans un deuxième temps, des ligands oxazolines ont été étudiés (figure 6). Des dérivés phényloxazolines (PHOX) ont pu être préparés en quantités raisonnables via un échange lithium-brome du précurseur bromophényle correspondant, suivi par substitution électrophile avec $PPh(CF_3)_2$. La diastéréosélectivité de cette réaction n'a pas pu être contrôlée. De plus, aucun moyen n'a été trouvé pour séparer les diastéréomères. Une simple expérience de coordination au palladium(II) a été réalisée avec succès avec un des représentants de cette classe de ligands.

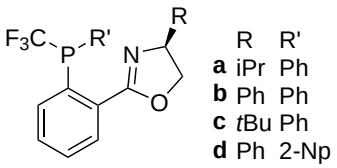

	R	R'
a	iPr	Ph
b	Ph	Ph
c	*t*Bu	Ph
d	Ph	2-Np

(*R*P)+(*S*P)-**26**

Figure 6: Ligands phényloxazolines étudiés (chapitre 3).

Des ligands 1,2-ferrocényloxazolines ont été examinés par la suite (figure 7). Il a été trouvé que ces ligands à chiralité planaire peuvent être facilement séparés par chromatographie sur colonne standard. Les ligands ont démontré leur capacité à coordiner au palladium(II) et platine(II), et ont été ensuite utilisés dans diverses catalyses stéréosélectives. Les meilleurs résultats ont été obtenus dans l'alkylation allylique de l'acétate de cinnamyle catalysée au palladium. L'énantiosélectivité a été plus élevée que celle du ligand parent, et le rapport de produits linéaire à branché a aussi été influencé favorablement. Dans d'autres réactions catalytiques, les ligands ont soit montré aucune conversion, soit très peu d'énantiosélectivité. Par ailleurs, la configuration absolue du phosphore a semblé n'avoir que très peu ou aucune influence sur les procédés catalytiques testés.

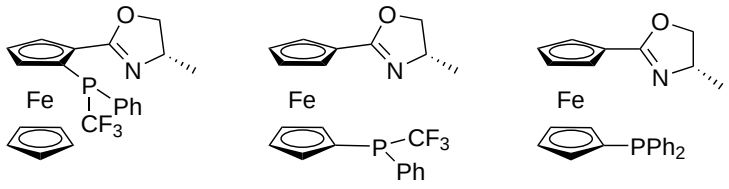

(R_P)/(S_P)-**34a** (R_P)+(S_P)-**49a** **45a**

Figure 7: Ligands ferrocényloxazolines étudiés (chapitre 3).

Étant donné que la synthèse des ferrocényloxazolines 1,2-substitués a souffert de gros problèmes de réproductibilité, la préparation des dérivés 1,1' correspondants a été initiée (figure 7). L'encombrement stérique étant réduit par rapport à la position devant être lithiée, la substitution électrophile devrait être moins restreinte. Il a cependant été démontré expérimentalement que cela n'était pas le cas, vu que la lithiation et substitution électrophile ont aussi été problématiques avec ce type de substitution au ferrocène. Pendant ce travail, un nouveau chemin de synthèse a été développé pour le ligand 1,1'-ferrocényle parent (figure 7).

En dernier lieu, les analogues trifluorométhyles dérivés de ligands phényléthylferrocényles ont été examinés (figure 8). De nouveaux moyens synthétiques ont été développés pour accéder aux ligands bis- et monotrifluorométhyles de cette famille, et les procédés ont pu être optimisés pour une synthèse à plus grande échelle.

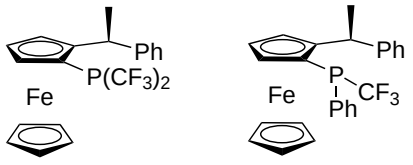

59 (R_P)/(S_P)-**60**

Figure 8: Ligands phényléthylferrocényles étudiés (chapitre 4).

Les ligands obtenus ont été comparés à leur ligand parent par leur structure en phase solide, et leur coordination au ruthénium(II) et or(I) a été étudiée. Finalement, un test d'activité préliminaire a été exécuté, en utilisant ces ligands dans le transfert d'hydrogène de l'acétophénone. Dans des conditions non optimisées, les ligands ont donné lieu à un produit racémique.

Introductory remarks

The author would like to make a few remarks before the actual thesis begins, to help the reader understand a few formalisms which have been used throughout the manuscript at hand.

The chemical name *phosphane* is used according to the most recent IUPAC recommendations on nomenclature.[1] It corresponds to a λ^3-phosphane, i.e. a trivalent phosphorus molecule, and as a substituent it is called *phosphanyl*. Concerning phosphane ligands, the term *parent* ligand refers to what is viewed as standard, i.e. the phosphanyl moiety bearing two phenyl substituents. The non IUPAC name *oxazoline* is used colloquially in place of *4,5-dihydro-1,3-oxazole* for convenience. The term *side chain* refers to the substituent in position 4 of the oxazoline (see figure 9).

Ferrocenes are drawn as shown in figure 9. The iron-cyclopentadienyl bonds are omitted for clarity reasons. The η^5 binding mode of the Cp ligands to iron is thus implicit. Ferrocene and binaphthyl numbering is also shown below.

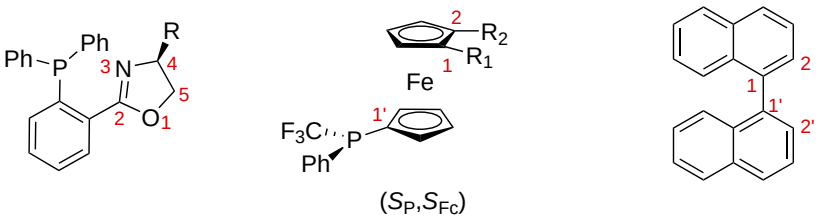

Figure 9: Depiction of an oxazoline parent ligand (left), a substituted ferrocene (middle), and a binaphthyl backbone (right).

In order to have a clear and consistent way of describing planar chirality and absolute configuration of stereogenic atoms, the following system was applied for generating stereodescriptors: phosphorus absolute configuration is denoted by a subscript capital P (R_P or S_P), whereas ferrocene planar chirality is denoted by a subscript Fc suffix (R_{Fc} or S_{Fc}). This is to avoid confusion with the IUPAC defined stereodescriptors for planar chirality (R_p) and (S_p).

Concerning planar chirality stereodescriptors, they are defined as follows (see figure 9): if R_1 has higher priority than R_2, then the adequate stereodescriptor is (S_{Fc}). Stereodescriptors for stereogenic phosphorus atoms are determined by considering the lone pair as the lowest priority substituent following the standard CIP rules.

Finally, following the recommendations that Robert E. Gawley provided in his benchmark publication concerning the use of *ee* and *de* to quantitate stereoselectivity,[1] the use of er, the enantiomeric ratio, and dr, the diastereomeric ratio, is preferred as a measure of stereoselective outcome of a reaction. The obsolete *ee* values are nevertheless given for comparative reasons, as most chemists still solely report and use these values for quantitation of enantioselectivity in catalytic reactions.

[1] Nomenclature of organic compounds – Preferred IUPAC names (Provisional recommendations 2004) and Nomenclature of Inorganic Chemistry – IUPAC Recommendations 2005.

1 General introduction

1.1 Setting the scene

Since the discovery of phosphorus in the most unorthodox manner over three centuries ago by a German alchemist,[2] this element central to life engages thousands of chemists over the world today.[3] Its essentialness is translated in its ubiquity: phosphorus, which is primarily found in the form of phosphate (PO_4^{3-}), is not only one of the most important building blocks present in human bodies in the form of DNA, ATP or as a constituent of bones, but it is also massively used as fertilizer to feed most of the population worldwide.

In nature, phosphorus occurs solely as the phosphate ion, and is found in various minerals, at least two thirds of which are located in North Africa.[4] The phosphate rock is processed to produce either phosphoric acid, which is used to generate suitable phosphate sources for agriculture, or elemental phosphorus, part of which is then further converted to organophosphorus precursors for chemical synthesis.[5]

1.2 General structural considerations

Phosphorus is part of group 15 of the periodic table of elements, also known as the pnictogens.[2] Trivalent pnictogen compounds adopt a pyramidal geometry (see figure 10) and their oxidation states range from –3 to +3. The bond angles of such compounds depend not only on the pnictogen atom considered, but also on the electronic and steric nature of the substituents.

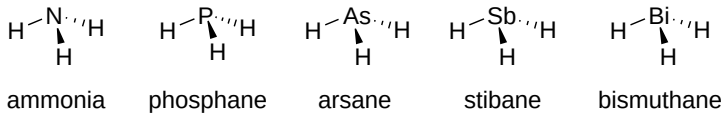

Figure 10: Group 15 hydrides with their IUPAC names.

Different models have been used to explain the bonding mode in phosphanes.[3] Gilheany has written an excellent review taking a look at the different models used to explain the bonding geometry of trisubstituted phosphanes and analyzing the calculations made to predict the geometry of phosphanes.[7] Gilheany notes that "In any event size is important in chemical bonding!". The electronegativity of the substituents is nevertheless not neglected, as it has also been shown to be central in determining the geometry of such molecules. For example, Walsh has noted: "If a Group X attached to Carbon is replaced by a more Electro-negative Group Y, then the Carbon Valency towards Y has more *p* Character than it had towards X. (*sic*)"[12]

This was the basis for the conception of Bent's rule, which he formulated when discussing valence-bond structures and orbital hybridization of first row elements:

[2] For the origin of the term, see the second footnote in Arduengo's publication which notes the use of *pnictogen* to refer to group 15 elements.[6]

[3] Although an important controversy[7][8][9] has existed concerning the involvement of d orbitals in the bonding of phosphorus compounds, that dispute has been put to rest[10][11] and the concept that d orbitals play a role in bonding in main group compounds has become redundant.[7]

"Atomic s character concentrates in orbitals directed toward electropositive substituents. Or, atomic p character concentrates in orbitals directed toward electronegative substituents."[13]

This conclusion was drawn after considering selected experimental data on certain physical properties such as bond lengths, dipole moments, and heats of addition. Bent considered lone pair electrons as electrons in bonds to very electropositive substituents.[13] In other terms, the introduction of an electron-withdrawing group on a phosphorus atom results in an increased s character of the lone pair. This is directly due to the increase in p character of the orbitals involved in bonding to the substituents.

1.2.1 Pyramidal inversion

An important aspect of group 15 trisubstituted compounds is their configurational stability. Two intrinsically distinct conformations of such molecules can exist. These two conformations arise by transposition of the three substituents directly bound to the pnictogen center from one side of the central tricoordinate atom plane to the other (scheme 1).

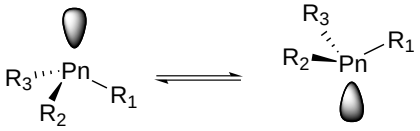

Scheme 1: Pyramidal inversion of trisubstituted pnictogen molecules.

Three different mechanisms of pyramidal inversion are recognized.[8][14][4] The classical view consists of the tricoordinate tetragonal molecule going through a trigonal planar configuration, before flipping to its invertomer (scheme 2).

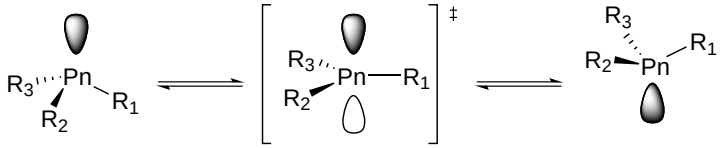

Scheme 2: Classical pyramidal inversion of tricoordinate pnictogens via a trigonal planar transition state.

In the non-classical view, inversion can occur by quantum mechanical tunneling. This can be considered in practice only if at least one of the substituents bound to the central atom is a hydrogen or deuterium, the invertomers are not diastereomers, and at temperatures at which vibrational levels at 5-6 kcal/mol below the potential barrier are substantially populated.[8]

The third inversion mechanism was discovered much later, in the mid 80s, by Arduengo *et al.*,[14] and postulates that tricoordinate pnictogen molecules bearing appropriate electronegative substituents can invert through a T-shaped structure (see scheme 3). This mechanism was at first supported by calculations, and later by experiments.[15] This *edge* inversion process can be stabilized by σ-acceptors in the axial positions and π-donors in the equatorial position.[6]

[4]The mechanisms considered concern pyramidal inversion which occurs without bond formation or breaking.[8]

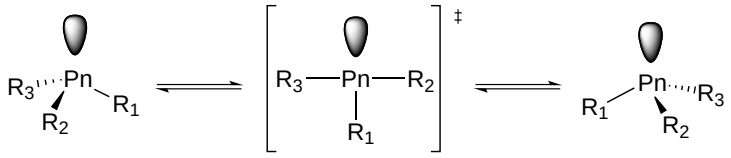

Scheme 3: *Edge* inversion process of electron-poor pnictogens.[14]

It must be noted that the distinction between classical and non-classical inversion mechanism is not important when discussing inversion barriers, although it must be kept in mind that the rates of inversion from which inversion barriers are extracted depend on the relative importance of the two mechanisms.[8]

The inversion barrier depends on the pnictogen center, as supported by experiments and calculations.[6][16] There is a periodic trend, in which the barrier rises when going down the pnictogen series, from ammonia to arsane (see table 1).

Table 1: Calculated inversion barriers for group 15 hydrides with the electronegativity according to Allred

	NH_3	PH_3	AsH_3	SbH_3
Barrier[9] (kcal/mol)	5.60	27.00	34.00	29.00
Electronegativity[17]	3.04	2.19	2.18	2.06

Whereas the energetic inversion barrier of most amines is very low (5.6 kcal/mol for ammonia,[9] see table 1), this barrier is much higher for phosphanes. The direct consequence is that the rapid interconversion taking place for amines does not allow the isolation of single enantiomers, in contrast to phosphanes which encompass configurationally stable compounds due to much higher inversion barriers. Arsanes are even more stable and do not undergo inversion unless sufficient energy is imparted to the system (e.g. by UV irradiation[18]).[19]

The influence of substituents on the rate of inversion was experimentally studied in a systematic manner by Mislow *et al.*,[16] as there had been up till then only sparse reports on the configurational instability of phosphanes at high temperatures. The rates of thermal racemization of a set of optically active phosphanes was determined polarimetrically in hydrocarbon solvents, and all were found to be cleanly first order.

Table 2: Activation free energy of $PMeR_1R_2$ measured by polarimetry at 130 °C in decalin[16]

Entry	R_1	R_2	$\Delta G^{\ddagger}_{130}$ (kcal/mol)
1	Cy	*n*-C_3H_7	35.6
2	Ph	*n*-C_3H_7	32.1
3	Ph	*t*-Bu	32.7
4	Ph	*p*-(MeO)Ph	30.8
5	Ph	*p*-MePh	30.3
6	Ph	*p*-CF_3Ph	29.1

Steric effects seem to play a minor role, as can be extracted of the similar activation free energy values obtained (see table 2). When comparing, for example, a branched analogue

(entry 3) to its linear counterpart (entry 2), the rate of racemization is essentially the same, the values diverging at most by 3.5 kcal/mol. Aromatic substituents slightly decrease the barrier (entries 4–6), as the electrons of the lone pair can take part in the delocalization of the aromatic system. This stabilizes the transition state thereby lowering the activation energy, which is not the case when alkyl substituents are present (entry 1). When electron-withdrawing groups are present on the aryl group, delocalization is more pronounced, thereby lowering the inversion barrier (entry 6).

Mislow has also found a linear correlation between the electronegativity (according to Allred) of atoms attached to phosphorus with the inversion barrier of the corresponding phosphane.[20] Substituents such as fluorine or methoxy, which possess a high electronegativity, cause the corresponding phosphanes to display a very high inversion barrier (~54 kcal/mol), in contrast to phosphanes possessing electron-donating groups which exhibit lower inversion barriers (e.g. MeS with ~32 kcal/mol). Considering Bent's postulations (see section 1.2),[13] this means that the electron lone pair possesses an increased s character in the presence of such electron-withdrawing substituents at the phosphorus atom. The energy needed for the change in hybridization is consequently larger and logically results in a higher inversion barrier.

The configurational stability of phosphanes combined with their high activity and selectivity in stereoselective reactions makes them desired synthetic targets. The next section will delve into important aspects concerning their preparation.

1.3 *P*-stereogenic compounds

1.3.1 Initial work

Although it is unclear who was first to discover an optically active phosphane, most books and articles refer to Meisenheimer and Lichtenstadt's report from 1911[21] as being the original contribution. They reported the synthesis of a *P*-stereogenic phosphane oxide and isolation of one of its enantiomers by resolution with *d*-bromocamphorsulfonic acid (scheme 4)

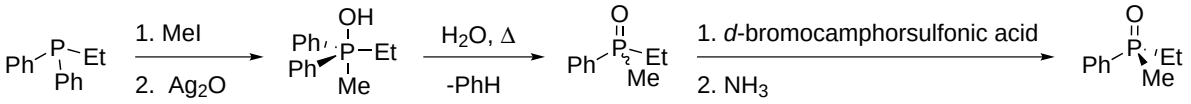

Scheme 4: Synthesis and resolution of an optically active phosphane oxide as first reported by Meisenheimer and Lichtenstadt.[21]

Half a century later, the first reports on the use of *P*-stereogenic phosphanes in asymmetric transformations appeared, thereby opening a new chapter in enantioselective catalysis.[22][23] The question arose of how to synthesize these compounds, and various methods were developed.

1.3.2 Synthetic approaches to *P*-stereogenic phosphanes[24][25]

The early methods only resolved quaternary phosphonium species, and Horner *et al.* were the first to report the *isolation* of tertiary phosphanes.[26] Due to the continued interest in *P*-stereogenic phosphanes, various methods to prepare such molecules have been developed since the first isolation of a *P*-stereogenic compound. Three different approaches have

emerged as pathways commonly used to access such compounds. The traditional and tedious resolution of racemates has made way for more convenient methods, with the development of efficient stereoselective synthetic protocols making use of chiral auxiliaries and the emergence of transition-metal catalyzed reactions using chiral ligands. A selection of the aforementioned methods will be briefly discussed hereafter. For more details, the numerous reviews[24][27][28] and books[25][29] are recommended for further reading.

Chiral palladium(II) complexes are considered to be the most efficient resolving agents, at least for certain types of phosphanes.[24][28] This method developed in the 70s by Otsuka *et al.* makes use of chiral dinuclear Pd(II) complexes with which the phosphanes reacts, resulting in a diastereomeric mixture of mononuclear complexes as shown in scheme 5 (or, alternatively, if half an equivalent of resolving agent is used then possibly only one phosphane enantiomer reacts while the other remains in solution). The diastereomers can then be isolated either by chromatographic techniques or recrystallization. The palladium auxiliary is then removed by ligand substitution yielding the enantiopure phosphane.[30]

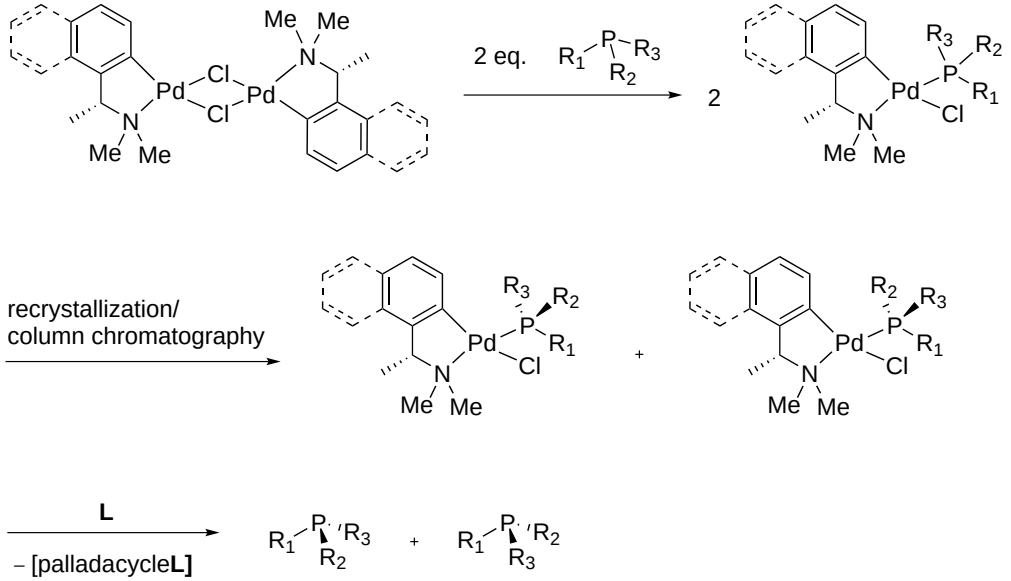

Scheme 5: Otsuka's resolution of racemic phosphanes via a chiral palladacycle auxiliary.[30]

The success of this method depends not only on the selected chiral auxiliary but also on the phosphane substituents. The preparative isolation also usually provides low yields. Alternative methods were thus being developed in parallel.

Stereoselective syntheses make direct use of auxiliaries from the chiral pool and can ideally be recycled as they are used stoichiometrically. The first method developed in the late 60s made use of (–)-menthol as chiral auxiliary. It was found that menthyl phosphinates could be separated by crystallization or chromatography and the corresponding enantiomers substituted by alkyl or aryl Grignard reagents with inversion of the stereocenter (scheme 6). It was later shown that the P–O bond can also be cleaved by a single electron lithium reducing reagent, and subsequent quenching with an alkyl halide yields the phosphane oxide under retention of configuration (scheme 6). The desired trivalent *P*-stereogenic phosphane is then accessed by reduction of the phosphane oxide.[25]

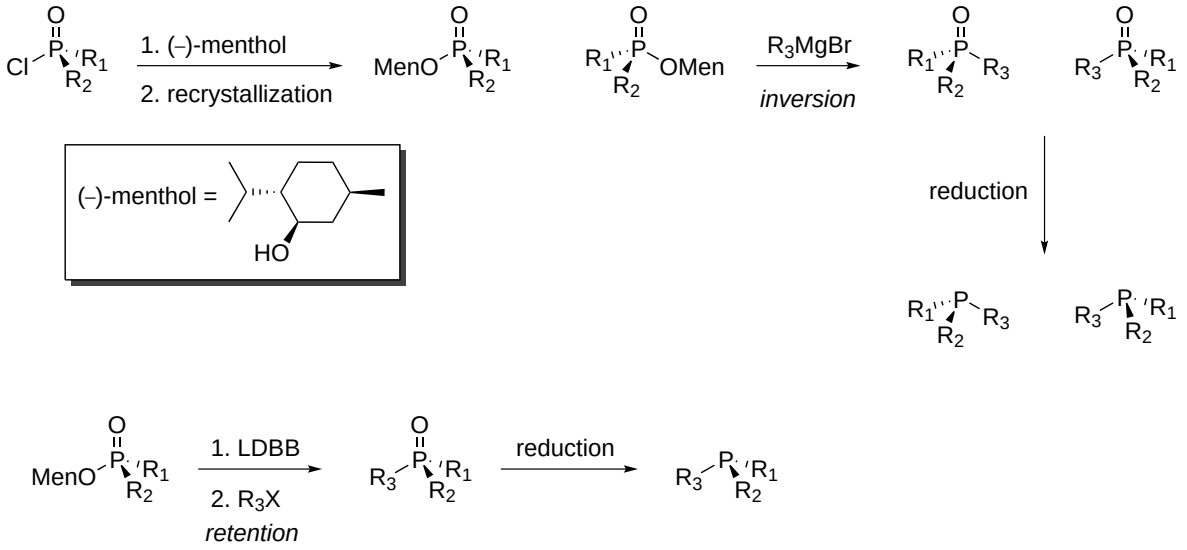

Scheme 6: Stereoselective synthesis of phosphanes using (–)-menthol as chiral auxiliary.[24]

A prominent example is the preparation of the ligand DiPAMP, for which Knowles *et al.* used this methodology to prepare (scheme 7).[31]

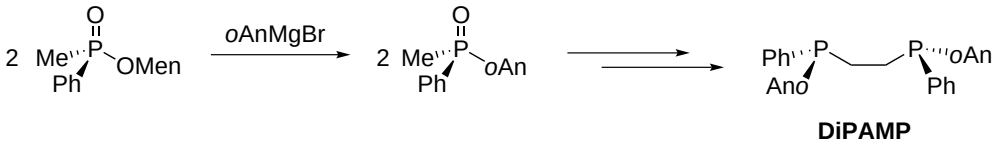

Scheme 7: Knowles' synthesis of DiPAMP using (–)-menthol as chiral auxiliary.[31]

As the nucleophilic substitution of an alkoxy group was established to proceed with high stereoselectivity, the idea that two sequential substitutions of a phosphinate could also lead to enantiopure phosphanes emerged. This led to the development of heterobifunctional chiral auxiliaries comprising of phospholidine derived heterocycles.

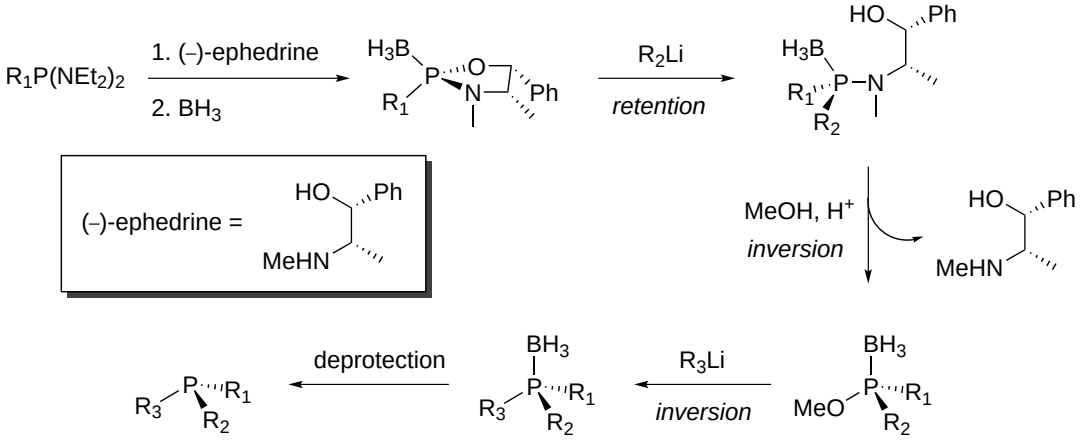

Scheme 8: Jugé's stereoselective synthesis of phosphanes using (–)-ephedrine as chiral auxiliary.[32]

Jugé *et al.* developed a powerful method using (–)-ephedrine as chiral auxiliary to prepare stereogenic phosphanes, via an oxazaphospholidine intermediate (scheme 8). The overall

method allows retention of configuration at the phosphorus atom, and the chiral auxiliary can be recycled. A similar method using a camphor derivative has been established by Corey *et al.*, and proceeds through diastereoselective formation of an oxathiaphospholidine intermediate.[33] Jugé's method is however by far the most successful in terms of versatility, stereoselectivity and availability of the chiral auxiliary, making it more widely used.[24]

This method nevertheless has some drawbacks, as it was found by Mezzetti *et al.* that *o*,*o*'-disubstituted aryllithium compounds did not react with the oxazaphospholidine.[34] Van Leeuwen *et al.* have also reported that 1,1'-dilithioferrocene reacts with low yields and diastereoselectivity when introduced in the first nucleophilic substitution.[35] The Jugé method has nonetheless become widespread and allows the preparation of a range of enantiopure *P*-stereogenic phosphanes.

Another method making use of a chiral auxiliary is based on the observation that methylphosphane boranes and methylphosphane oxides can undergo deprotonation at the methyl group with strong bases with retention of configuration. Evans *et al.* have thus developed a method using (−)-sparteine as chiral auxiliary to allow selective deprotonation of one of the enantiotopic methyl groups (scheme 9).[36]

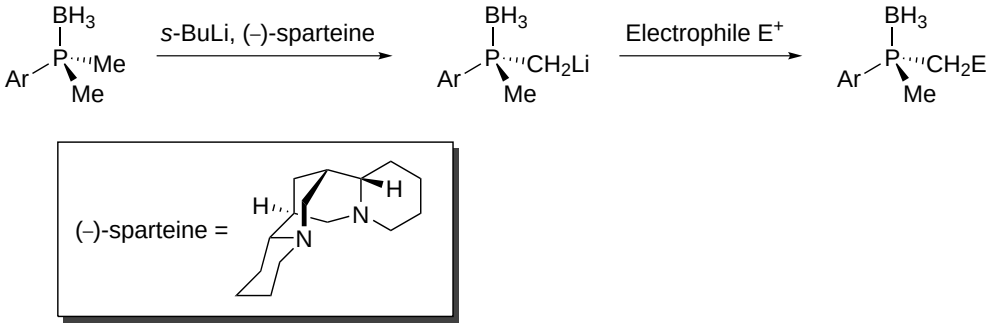

Scheme 9: Evans' stereoselective synthesis of phosphanes using (−)-sparteine as chiral auxiliary.[36]

Although the methods employing chiral auxiliaries allow access to various *P*-stereogenic phosphanes, they all possess a major drawback: the need of a stoichiometric amount of expensive chiral agent, which cannot always be recycled in an convenient fashion. A relatively new field is thus concerned with the preparation of enantiopure phosphanes using catalytic amounts of chiral reagents. Several groups have shown that this approach is in fact feasible, although it remains a limited method (for now). For more insight on this matter, the interested reader is referred to the literature cited in the beginning of this section.

1.4 The advent of phosphorus-based ligands

Since the discovery by Wilkinson *et al.* that a triphenylphosphane-based rhodium catalyst allows not only the homogeneous hydrogenation but also hydroformylation of alkenes,[37][38] much interest in the preparation and application of such catalysts emerged.

A few years after Wilkinson's reports, the first publications concerning the application of an optically active phosphane ligand in asymmetric catalysis by Knowles[22] and Horner[23] appeared quasi simultaneously in 1968. Knowles *et al.* showed that a simple *P*-stereogenic

ligand, mppp, combined with rhodium(I) could enantioselectively catalyze the hydrogenation of α-phenylacrylic acid (see scheme 10). This was one of the first reports of a non-enzymatic asymmetric catalysis, and it triggered the active development of phosphorus-based trivalent ligands with high expectations for their catalytic applications.

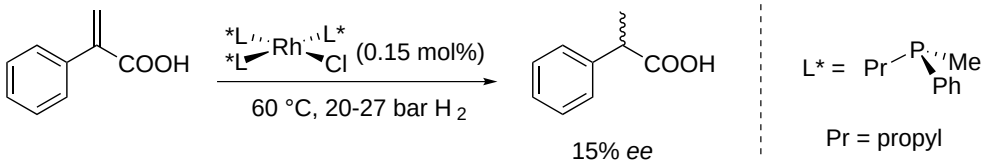

Scheme 10: Knowles' first report on the enantioselective catalytic reduction of α-phenylacrylic acid.[22]

The 70s witnessed the birth of *P*-stereogenic ligands such as CAMP[39] and DiPAMP[40][31] (see figure 11), which have been shown to be extremely valuable in catalysis and instigated the quest of *P*-stereogenic ligands. DiPAMP was used by Monsanto not only in the synthesis of L-DOPA, a pharmaceutical drug for the treatment of Parkinson's disease, but also for the preparation of other amino acids.[41]

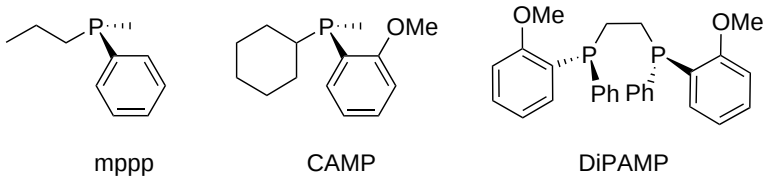

Figure 11: Examples of *P*-stereogenic phosphane ligands.

Knowles, who was very active in this field while working at Monsanto, thought the chirality had to be directly on the phosphorus to achieve high enantioselectivities.[41] However, after the report from Kagan[42][43] of a new phosphane ligand called DIOP which possessed a chiral backbone derived from tartaric acid, Knowles' reasoning was shown to not be completely true and that high stereoselectivity could also be achieved with backbone-chiral ligands (figure 12).

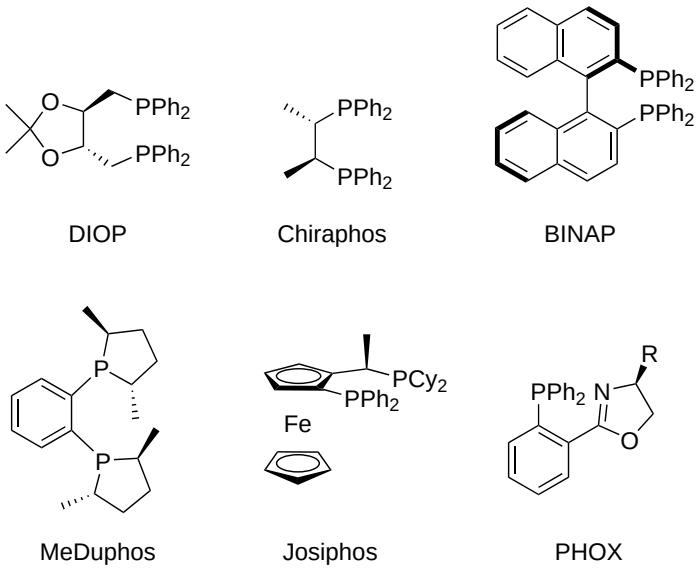

Figure 12: Examples of bidentate phosphane ligands with chiral backbones.

Furthermore, synthetic drawbacks of *P*-stereogenic compounds and the concomitant highly successful development of ligands with chiral backbones profoundly slowed down the development of their *P*-stereogenic counterparts. The event which however more or less reversed the interest in *P*-stereogenic ligands occurred with the discovery of BINAP in 1980 by Noyori[44] and its huge success in homogeneous asymmetric catalysis, which made research prefer further development of ligands with chiral backbones over *P*-stereogenic compounds.

1.4.1 *BINAP, a Beautiful Chiral Molecule*[45]

Motivated by its molecular beauty,[46] and the boom in phosphane ligand development, Noyori and Takaya set out to synthesize this axially dissymmetric molecule. They encountered more difficulties than expected. The first route they found was unreproducible, but after six years of intensive research with many collaborators, the first publication concerning the synthesis (see scheme 11) and catalytic use of BINAP appeared.[44] This seminal work spawned the further development of synthetic methods towards BINAP, as well as research focused on BINAP modifications.[47]

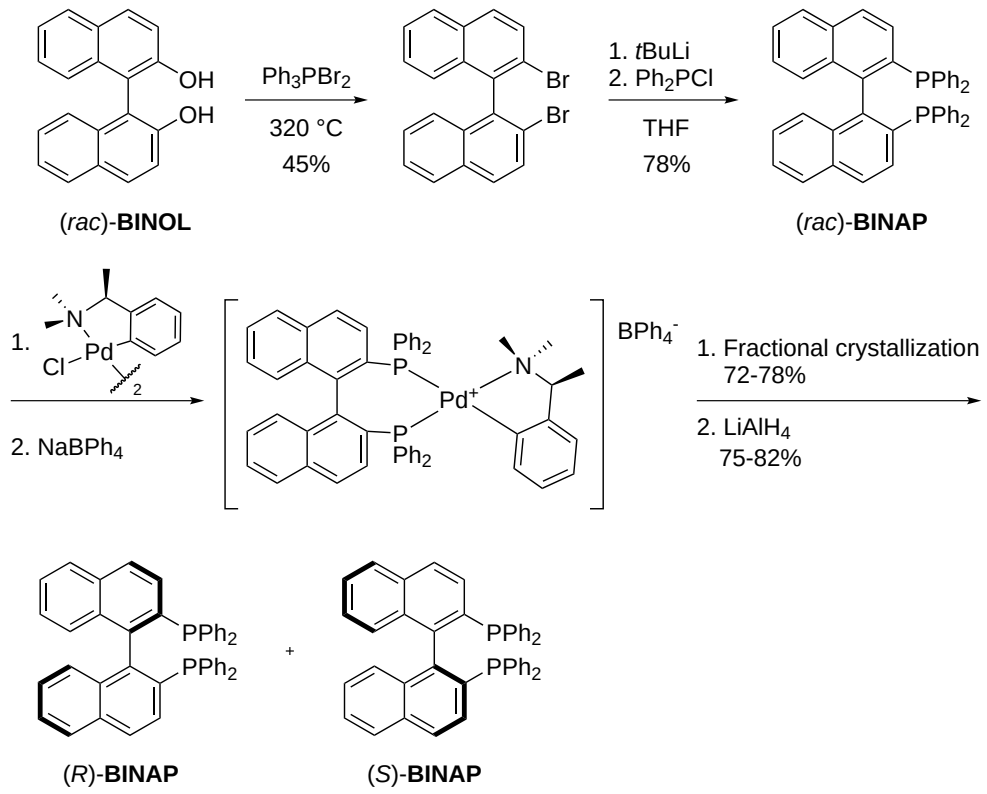

Scheme 11: Synthetic route to BINAP enantiomers, as first published by Noyori *et al.*.[44]

BINAP is one of the rare chiral ligands produced on industrial scale, and is used in a few large scale syntheses.[47] Perhaps one of the most famous industrial applications of BINAP is in the synthesis of (–)-menthol by Takasago International Corporation.[48] Takasago, which also first patented the industrial synthesis of BINAP by modifying Noyori's procedure, produces a few thousand tons of (–)-menthol per year from myrcene, originally using BINAP in the catalytic isomerization of diethylgeranylamine to (3*R*)-citronellal enamine in 96-99% enantiomeric excess (see scheme 12).

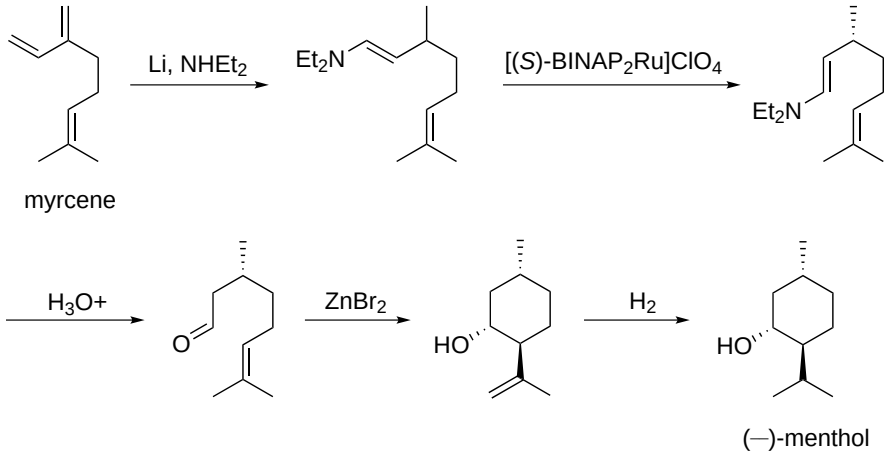

Scheme 12: Takasago's industrial process towards (–)-menthol using BINAP as chiral ligand.[48]

After later developing a new axially chiral ligand with smaller dihedral angle called SEGPHOS,[49] Takasago patented an alternate synthesis of (–)-menthol using SEGPHOS instead of BINAP,[48] as the corresponding Ru complex was found to surpass BINAP in efficiency.[49]

BINAP's modularity and versatility made Jacobsen coin it a *privileged* ligand,[50] and it is still today not only one of the rare chiral ligands produced on industrial scale, but also one used for many large scale reactions.[47]

1.4.2 The golden age of backbone-chiral ligands

As BINAP was found to be an exceptional ligand not only for hydrogenation but other stereoselective C-C bond forming reactions, the development of backbone-chiral ligands was in full swing. One of the next big hits occurred with the development of Josiphos,[51] a bidentate diphosphane ligand possessing a planar chiral ferrocene backbone. This new ligand not only showed high enantioselectivities in various reactions, but also allowed the introduction of various phosphanyl substituents, making the synthesis extremely modular and allowing for easy variation of electronic and steric properties, the only limiting factor being the availability of the secondary phosphane reagents.[51][52]

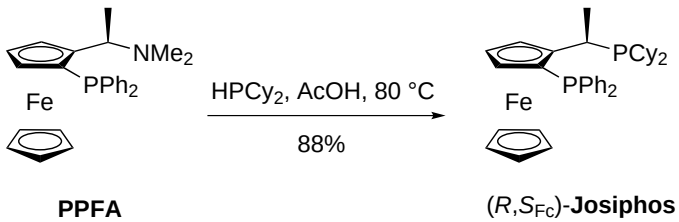

Scheme 13: Synthetic pathway to Josiphos as first published by Togni *et al.*.[51]

Josiphos and its derivatives went on to be used in important industrial processes,[53] such as the synthesis of a biotin intermediate (Lonza),[54] a water-soluble B-vitamin, metolachlor (Solvias),[55] an important herbicide used in maize and other crops, and methyl dihydrojasmonate (Paradisone, Firmenich),[56] a jasmin fragrance (see scheme 14).

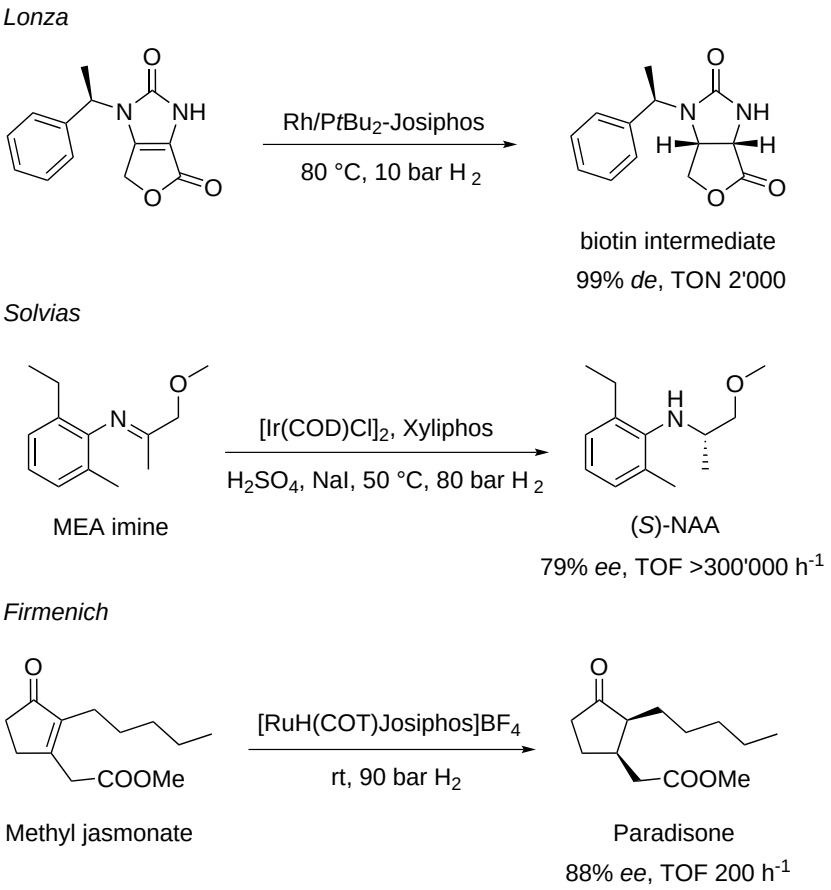

Scheme 14: Representative industrial applications of Josiphos ligands.[53]

This new type of chirality led to active further development of such 1,2 substituted ferrocene ligands for asymmetric catalysis.[57] The two step methodology developed for the synthesis of Josiphos could be extended to *P,N* ligands.[58] These new ligands developed by Togni *et al.* comprised of a phosphane and a pyrazole moiety, which was unprecedented in asymmetric catalysis (see scheme 15).

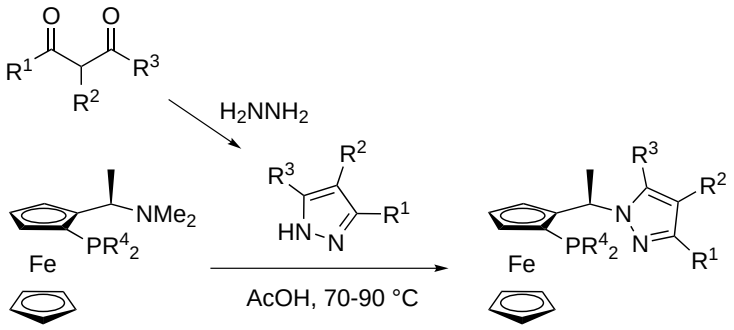

Scheme 15: *P,N* ferrocenylpyrazole ligand synthesis following the Josiphos methodology.[58]

It was shown that these *P,N* ferrocenyl chelating ligands are very active in the asymmetric rhodium-catalyzed hyroboration of styrene with catecholborane (see scheme 16) and showed the highest enantioselectivity known for this particular reaction.[59]

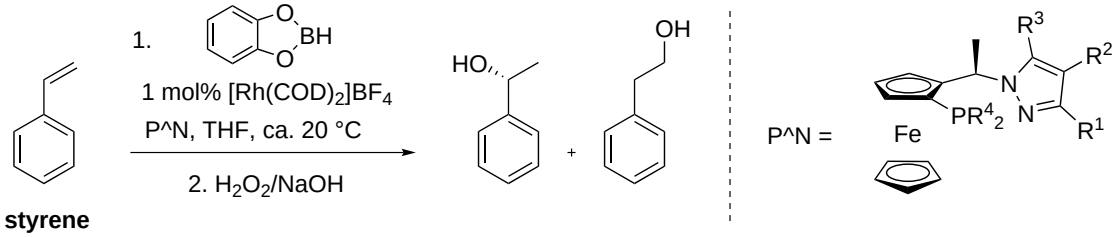

R^1	R^2	R^3	R^4	Yield (%)	branched:linear	*ee* (%, *R*)
Me	H	Me	Ph	91	66:34	95.1
CF_3	H	CF_3	Ph	78	61:39	33.4
Me	Me	Me	Ph	90	79:21	95.6
CF_3	H	Me	Ph	79	46:54	43.8
iPr	H	iPr	Ph	55	36:64	91.6
Me	Br	Me	Ph	80	65:35	95.7
H	H	H	Ph	71	41:59	65.2
Ph	H	Me	Ph	92	47:53	79.6
Me	H	Me	4-CF_3-C_6H_4	68	60:40	98.0
Me	H	Me	4-MeO-C_6H_4	61	61:39	90.0

Scheme 16: Rh-catalyzed hydroboration with electronically-varied ferrocenylpyrazoles.[59]

In the same decade, three groups independently reported the preparation and catalytic activity of phenyloxazoline (PHOX) ligands.[60][61][62] These compounds present a very broad scope of asymmetric reactions in which they are efficient ligands.[63][64] Their versatility, due to the high modularity of the phosphorus and nitrogen donor atoms present, makes them a class of privileged ligands which can be specifically modified sterically and electronically.[65] The particularity of this ligand class is that in contrast to many other privileged chiral ligand classes they do not possess a C_2 axis of symmetry. This allows a potentially favorable interaction with the metal which can consequently induce a preferential substrate-metal conformation.[65]

Helmchen *et al.* were the first to demonstrate the enantiodiscriminating potential of PHOX ligands in the iridium-catalyzed alkylation of allylic acetates (scheme 17).[66] Excellent branched to linear ratios were obtained, as well as enantioselectivities up to 95% in the case of a PHOX ligand possessing an electron-withdrawing group on the phenyl substituents of the phosphane.

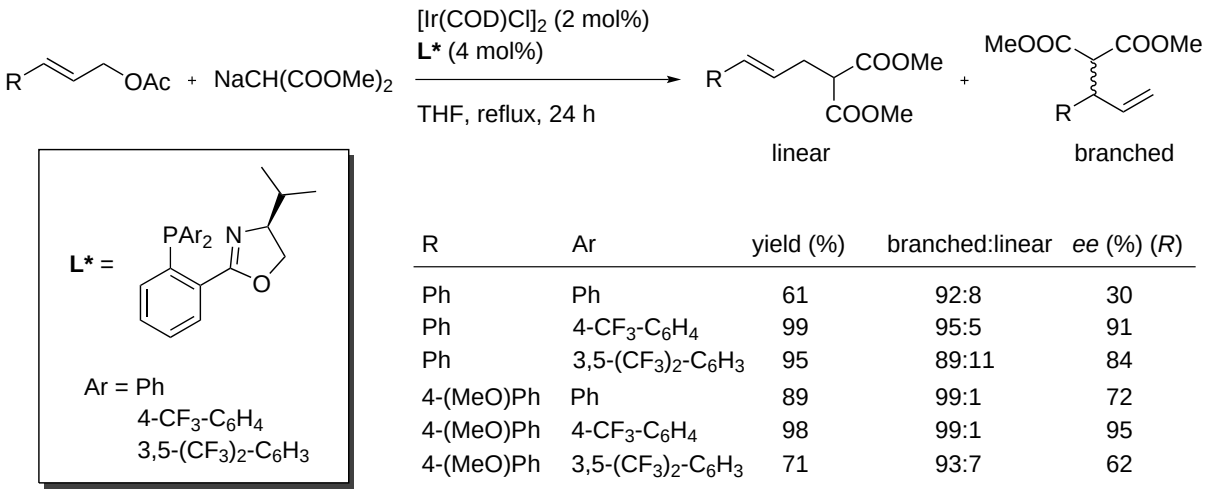

R	Ar	yield (%)	branched:linear	*ee* (%) (*R*)
Ph	Ph	61	92:8	30
Ph	4-CF_3-C_6H_4	99	95:5	91
Ph	3,5-$(CF_3)_2$-C_6H_3	95	89:11	84
4-(MeO)Ph	Ph	89	99:1	72
4-(MeO)Ph	4-CF_3-C_6H_4	98	99:1	95
4-(MeO)Ph	3,5-$(CF_3)_2$-C_6H_3	71	93:7	62

Scheme 17: First enantioselective iridium-catalyzed alkylation of monosubstituted allylic acetates using PHOX ligands.[66]

Backbone-modified oxazoline ligands have went on to also become part of successful catalytic systems, particularly ferrocenyloxazolines.[67] Although the first report on the synthesis of 1,2-ferrocenyloxazoline derivatives dates from 1982,[68] it took well over a decade before this seminal work was taken up and used to prepare a new type of *P,N* ligand. Three groups investigated the synthesis of such ligands independently. Richards *et al.*[69][70] and Uemura *et al.*[71] described the synthesis of phosphanylferrocenyloxazolines starting from carboxyferrocene, and the structure of their rhodium(I) complexes was investigated by the latter group.[72] Uemura *et al.* were the first to demonstrate the applicability of such ligands in the hydrosilylation of ketones,[73][74] whilst Sammakia *et al.* focused on the mechanism of the diastereoselective lithiation of ferrocenyloxazolines (scheme 18). They found that a number of factors influence the directed *ortho*-metalation of such substrates, including bulk and aggregation of the lithium reagent, solvent, additives, and size of the side chain at the oxazoline.[75][76][77]

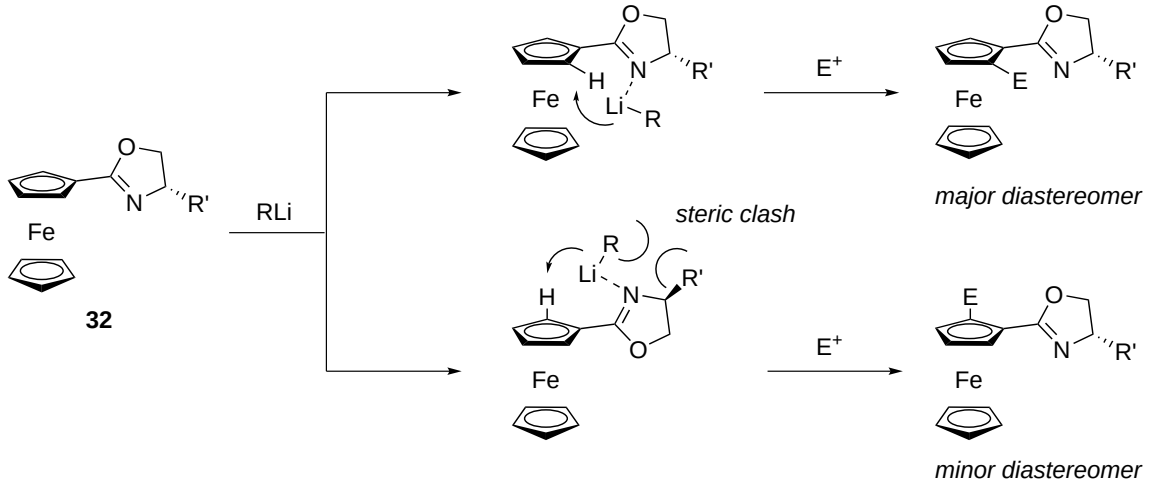

Scheme 18: Nitrogen-directed diastereoselective lithiation of ferrocenyloxazolines.[76][77]

1,2-Ferrocenyloxazolines combine the central chirality of the oxazoline side chain with the planar chirality of the ferrocene backbone, and the matching of these chirality elements has

been shown to be essential for excellent asymmetric induction.[78]

Oxazoline ligands have furthermore been shown to be useful in the hydrogenation of various aryl ketones at an industrial level. A range of ferrocenyl-, phenyl-, and thiophenyloxazoline ligands in combination with $[Ru(PPh_3)_3Cl_2]$ were able induce high enantioselectivities, the highest being achieved by ferrocenyloxazolines (>98% *ee*).[79] This triggered the development of a pilot process for the hydrogenation of 3,5-bistrifluoromethyl acetophenone (BTMA), which allows the preparation of an important chiral precursor for pharmaceutically relevant molecules such as the antiemetic aprepitant.[80][81]

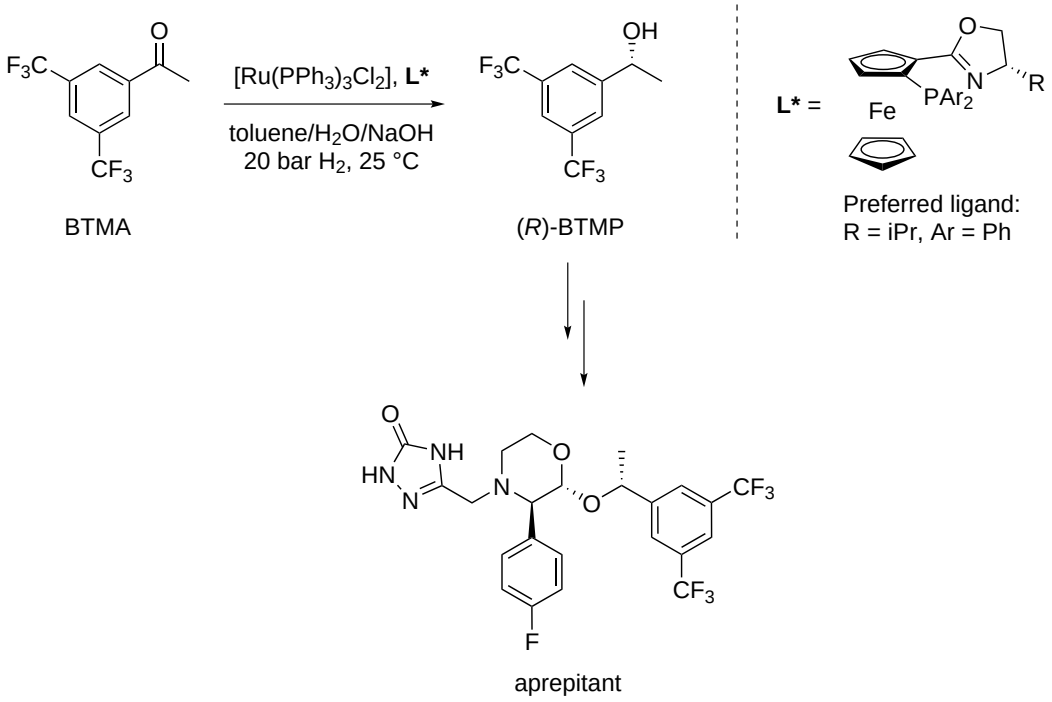

Scheme 19: Enantioselective hydrogenation of BTMA using a 1,2-ferrocenyloxazoline ligand.[80][81]

For further reading on chiral ferrocenes and their use in catalysis[82][83][84][85] as well as other privileged ligands,[86] the cited references are recommended.

1.4.3 The potential of *P*-stereogenic ligands

Backbone chiral ligands have generally gained more attention since the development of ligands such as DIOP, Chiraphos and especially BINAP (see sections 1.4.1 and 1.4.2) in part due to the excellent enantioselectivities achieved with such ligands in homogeneous catalysis. But probably the main reason why *P*-stereogenic ligands have been less investigated, is the tedious synthetic pathways towards such compounds (see section 1.3.2). Furthermore, the potential for epimerization of *P*-stereogenic phosphanes has hampered their extensive development. *P*-stereogenic ligands are nonetheless valuable compounds as they have shown in certain catalytic transformations superior results to their non *P*-stereogenic analogues. Many groups have thus pursued such motifs, and a few relevant examples will be presented hereafter.

Van Leeuwen *et al.* investigated the electronic effect of ligands in catalysis, by applying *P*-stereogenic ligands in the hydroformylation of styrene (table 3).[87] This is a very important

catalytic process, due to the high value of aldehydes in the chemical industry. The desired ligands were prepared following the Jugé methodology (see section 1.3.2).[32]

Table 3: Rhodium-catalyzed enantioselective hydroformylation of styrene with *P*-stereogenic 1,1'-ferrocenyl ligands.[87]

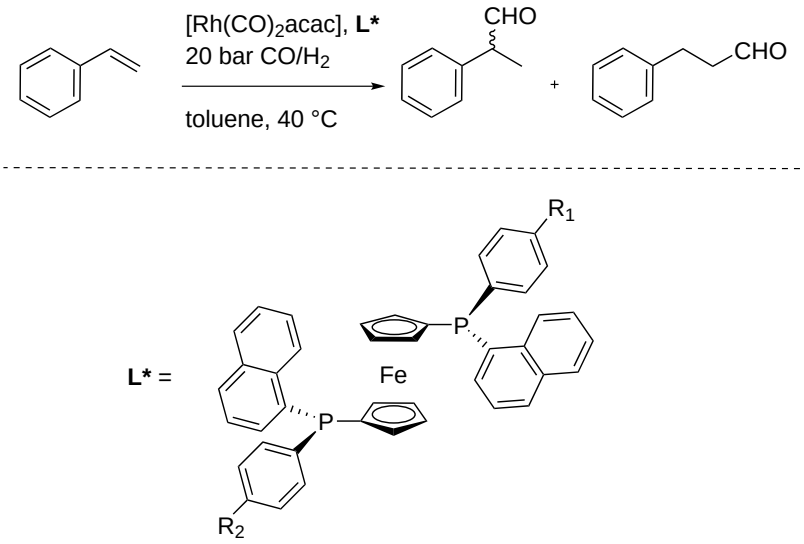

Entry	R_1	R_2	TOF	branched:linear	*ee* (%)
1	H	H	7	1.7	46
2	OMe	OMe	6	1.7	46
3	CF_3	CF_3	12	1.5	50
4	CF_3	OMe	11	1.7	41
5	dppf		11	2.4	-

Although the enantioselectivities observed are in general relatively low, it can be noted that the *P*-stereogenic ligands (entries 1-4) exert more enantioinduction than the C_1 parent ligand dppf (entry 5). Although the low branched to linear ratios are indicative of a sterically congested active catalyst species, all ligands nevertheless promoted the reaction at 40 °C. The presence of a *para*-trifluoromethyl group on the phenyl rings influenced the reactivity as well as the enantioselectivity positively (entry 3). The turnover frequency is nearly doubled in this case compared to the ligand possessing the electron-donating methoxy group (entry 2 vs. entry 3). Investigation of the ligand coordination mode to the metal center allowed to demonstrate the correlation between the binding mode and enantiodiscrimination performance of the diphosphane, and that the best π-acceptor ligand affords the highest enantioselectivities.[87]

Chen *et al.* reported in 2006 synthetic pathways to access various *P*-stereogenic planar chiral ferrocenyl ligands analogous to Taniaphos,[88] BoPhoz[89] and Josiphos[89] (scheme 20). The *P*-stereogenic derivatives of second generation Taniaphos (which were named PingFer) could be accessed with about 9:1 diastereoselectivity.[88] The *P*-stereogenic BoPhoz and Josiphos ligands were accessed at room temperature to avoid epimerization at the phosphorus. A single diastereomer (S_P) was exclusively obtained in both cases, although the other diastereomer

could be obtained via inversion of the order of addition of the reagents or, alternatively, by recrystallization of the (S_P) diastereomer.[89]

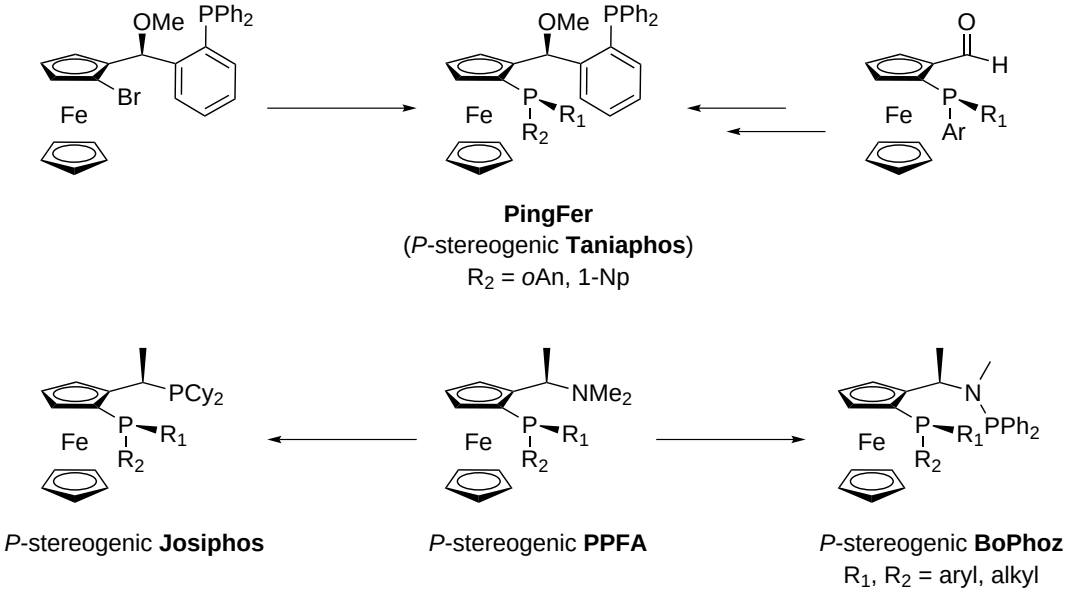

Scheme 20: Synthetic pathways towards *P*-stereogenic Taniaphos, BoPhoz and Josiphos ligands, as reported by Chen *et al.*.[88][89]

The obtained ligands were tested in the rhodium-catalyzed asymmetric hydrogenation of α-dehydroamino acid derivatives (see table 4). All *P*-stereogenic ligands showed higher enantioselectivities than their parent ligands in this catalytic process (entry 1 vs. entry 2 and entry 4 vs. entry 5). The matching of chirality elements was demonstrated to be essential in obtaining high enantioselectivities (entry 2 vs. entry 3 and entry 5 vs. entry 6). The (S_P) diastereomers were thus shown to induce the most enantioselectivity (entries 2 and 5), whereas the (R_P) diastereomers were less enantiodiscriminating (entries 3 and 6).

Table 4: Rhodium-catalyzed enantioselective hydrogenation of α-dehydroamino acid derivatives.[88][89]

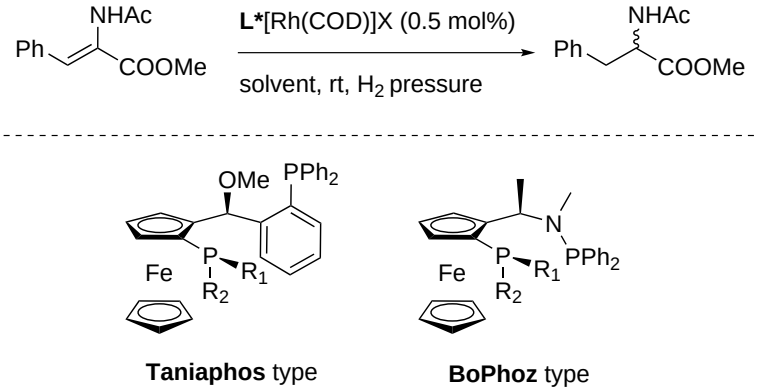

Entry	Ligand type	R_1	R_2	X	solvent	*ee* (%)
1	Taniaphos	Ph	Ph	BF_4	MeOH	90.5
2	Taniaphos	Ph	1-Np	BF_4	MeOH	99.6
3	Taniaphos	1-Np	Ph	BF_4	MeOH	69.3
4	BoPhoz	Ph	Ph	OTf	THF	95.7
5	BoPhoz	Ph	1-Np	OTf	THF	97.0
6	BoPhoz	1-Np	Ph	OTf	THF	92.4

In 2002, Buchwald *et al.* demonstrated the synthesis of the first *P*-stereogenic axially chiral BINAP-derived ligand **1**.[90] It however took more than half a decade before its use as chiral ligand could be demonstrated to be superior than that of the parent ligand.[91] Ligand **1** was then found to catalyze the C-C coupling of oxindoles with aryl and vinyl bromides in a highly stereoselective fashion, furnishing products with enantioselectivities up to 97% (scheme 21).

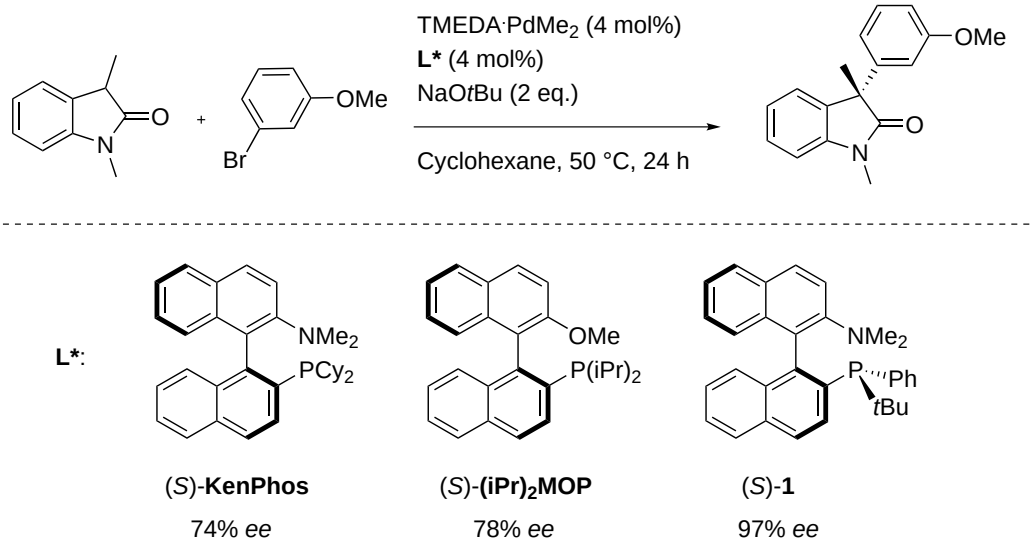

Scheme 21: Pd-catalyzed enantioselective α-arylation of 1,3-dimethyloxindoles with binaphthyl ligands.[91]

These results illustrate in this case the importance of the combination of *P*-stereogenicity with another chirality element.

For further examples, the two book chapters by Grabulosa dedicated to the use of *P*-stereogenic ligands in catalysis are recommended.[92]

1.5 Electron-poor phosphanes

The investigation of electronic properties of ligands is often performed by simply comparing them to the standard electron-rich analogue or by calculating the Tolman Electronic Parameter (TEP) value.[93] Phosphane ligands bearing two phenyl rings at the phosphorus are the most established, well known systems. Electron-poor phosphanes have received comparatively little attention, mostly due to their difficult syntheses, handling, or lack of inertness under the conditions required for catalysis. It is however clear that the electronic nature of a ligand will influence its coordination behavior and catalytic performance.

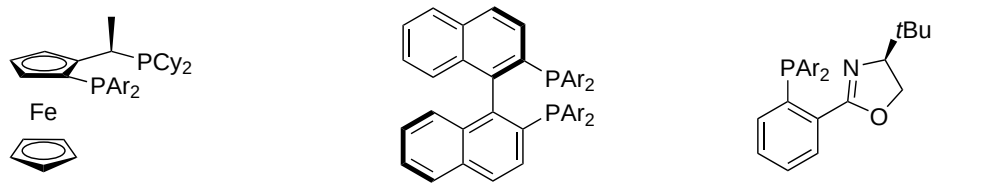

Ar = Ph = **Josiphos**
Ar = 2-CF_3-C_6H_4, Togni (2001)

Ar = Ph = **BINAP**
Ar = 4-CF_3-C_6H_4, Wu (2011)

Ar = Ph = **PHOX**
Ar = C_6F_5, Stoltz (2011)

Figure 13: Examples of electron-poor Josiphos,[94] BINAP,[95] and PHOX ligands.[96]

Electron-withdrawing substituents at the phosphorus usually comprise of trifluoromethyl-bearing or fluorinated phenyl groups (see figure 13). The presence of a trifluoromethyl or perfluorinated substituent at the phosphorus could allow more specific tuning of steric and electronic properties of such ligands. Perfluoroalkylphosphanes are however not simple targets. There nevertheless has been a renewed interest in such species, and a comprehensive review on fluoroalkylphosphanes has recently appeared.[97] Most of the original preparative methods involved hazardous, toxic or impractical reagents such as elemental phosphorus (white or red), mercury, phosphane gas (PH_3) or hydrofluoric acid (HF) and gave low product yields, mixtures of products, and in some cases explosive side products.[97]

One of the first breakthroughs concerning the preparation of trifluoromethylphosphanes probably occurred with the report of Volbach and Ruppert, who showed in 1983 that $P(NEt_2)_2CF_3$ could be directly synthesized from a mixture of $P(NEt_2)_3/PCl_3/CF_3Br$. Addition of HX (X = F, Cl, Br, I) furnished $P(CF_3)X_2$ in quantitative yield.[98] However, CF_3Br, also known as halon 1301, is an ozone-depleting agent and its use has essentially been suppressed due to its very high ozone depletion potential and being the halon with the longest atmospheric lifetime.[99] In the meantime, other viable methods, which circumvent the use of this reagent, have also been developed, and will be briefly discussed in the next section. Some more or less recent applications that are relevant to this thesis will also be shown later on.

1.5.1 Synthesis of trifluoromethylphosphanes

Hoge *et al.* reported in 2001 that cyanophosphanes react with $TMSCF_3$ (known as Ruppert or Ruppert-Prakash reagent), under cyanide ion activation (scheme 22).[100] Catalytic amounts of $[NEt_4]CN$, [18−crown−6 K]CN or NaCN were found to initiate the perfluoroorganylation reaction. PPh_2CF_3 was formed within 30 minutes in 70% yield. $PPh(CF_3)_2$ could also be prepared, however conversion was much slower due to trapping of the cyanide ion by the starting material, generating the phosphoranide species $[PPh(CN)_3]^-$, reducing the amount of free cyanide available. Tris(trifluoromethyl)phosphane could not be accessed by this method.

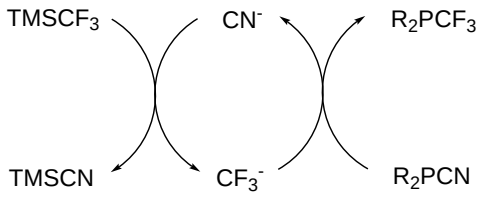

Scheme 22: Cyanide-catalyzed synthesis of trifluoromethylphosphanes from cyanophosphanes.[100]

The same year, Michalski *et al.* reported that fluorophosphanes, which they had previously shown to be accessible from phosphinites via nucleophilic substitution with a fluoride ion, could be converted to their trifluoromethyl analogues using the Ruppert-Prakash reagent under fluoride catalysis (scheme 23).[101] This method allowed the preparation of mono- and bistrifluoromethylphosphanes in good to excellent yields.

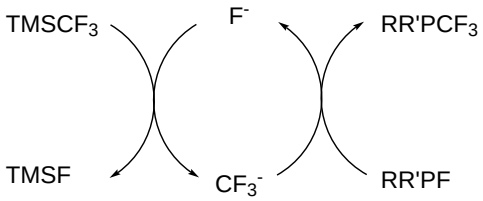

Scheme 23: Fluoride-catalyzed synthesis of trifluoromethylphosphanes from fluorophosphanes.[101]

A few years later, in 2005, Caffyn *et al.* simplified Michalski's procedure, by showing that phosphinites as well as phosphonites and phosphites can be directly converted to the corresponding trifluoromethylphosphanes (scheme 24).[102] They additionally demonstrated that not only trifluoromethyl- but also higher perfluoroalkylphosphanes could be generated in this manner.

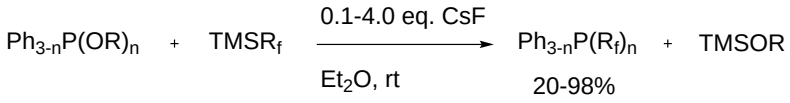

R = Ph, *p*-C_6H_4CN

$R_f = CF_3, C_2F_5, C_3F_7, C_4F_9, C_6F_{13}$

Scheme 24: Fluoride-catalyzed synthesis of trifluoromethylphosphanes from phosphinites, phosphonites and phosphites.[102]

This strategy was applied a few years later by Caffyn *et al.* in the synthesis of two electron-poor ferrocenyldiphosphanes bearing trifluoromethyl and pentafluoroethyl substituents (dfmpf and dfepf, scheme 25).[103]

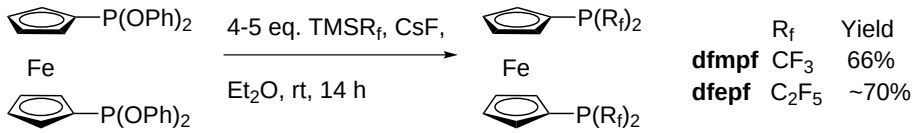

Scheme 25: Synthesis of trifluoromethyl and pentafluoroethyl substituted ferrocenyldiphosphanes.[103]

The corresponding platinum and molybdenum complexes were prepared (scheme 26). Their X-ray structures were determined and their carbonyl stretching frequencies analyzed. The estimated cone angles showed that these strongly electron-withdrawing phosphanes are some of the bulkiest diphosphanes ever prepared. The increased CO stretching frequencies compared to e.g. dppe or dppf illustrate the increased back bonding to the phosphane ligand and lowered electron density at the metal center.[103]

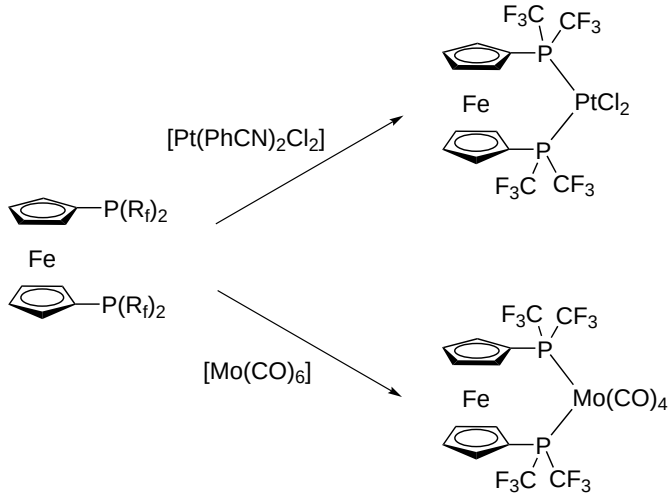

Scheme 26: Platinum and molybdenum complexes of ligands dfmpf and dfepf.[103]

Applying Caffyn's methodology, Roddick *et al.* prepared a pincer-type ligand bearing two bistrifluoromethylphosphanes (scheme 27) and subsequently investigated their corresponding Pt(II) chemistry.[104]

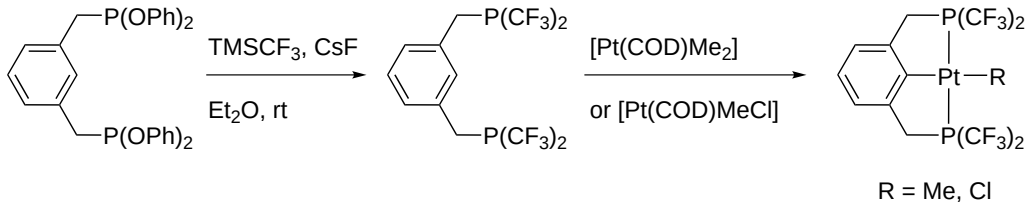

Scheme 27: Roddick's pincer-type bistrifluoromethylphosphane ligand and its corresponding platinum complexes.[104]

Since this original report, Roddick *et al.* have also the studied the coordination chemistry of this ligand with other transition metals such as iridium,[105] ruthenium,[106] and osmium.[107] The catalytic alkane dehydrogenation activity of these PCP acceptor ligands was also determined in the course of this work.

In 2006, Togni *et al.* reported the preparation of λ^3-iodanes for electrophilic trifluoromethylation.[108] The two reagents can be easily accessed from 2-iodobenzoic acid, and

their preparation has been efficiently optimized since their first development.[109] Reagent **2** (*acid* reagent) can be prepared in a convenient one-pot synthesis directly from 2-iodobenzoic acid, whereas reagent **3** (*alcohol* reagent) can be prepared in three steps from the corresponding methyl ester (see scheme 28).[109]

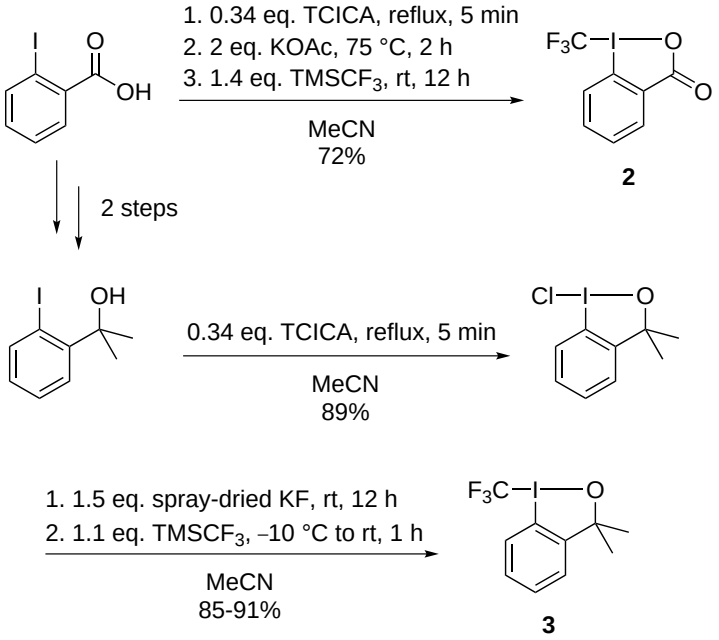

Scheme 28: One-pot synthesis of electrophilic trifluoromethylation reagents **2** (*acid* reagent) and optimized synthesis of **3** (*alcohol* reagent).[109]

The trifluoromethyl transfer to various organic nucleophiles was investigated, and it was found that both reagents allow trifluoromethylation of primary and secondary phosphanes as well as trimethylsilylated phosphanes under mild reaction conditions and in high yields (scheme 29).[110] It was later found that primary phosphanes can also undergo a second trifluoromethylation by employing an appropriate base such as DBU (scheme 29).[111]

Later applications for phosphorus trifluoromethylation mostly focused on the use of the acid reagent **2**, as it generally gives higher yields, the separation of the side-product 2-iodobenzoic acid from the desired product is usually easier, and the preparation of the acid reagent is more straightforward. Last but not least, the acid reagent is an air-stable crystalline solid which can be stored indefinitely at room temperature and does not decompose, which is not the case of the alcohol reagent **3**.

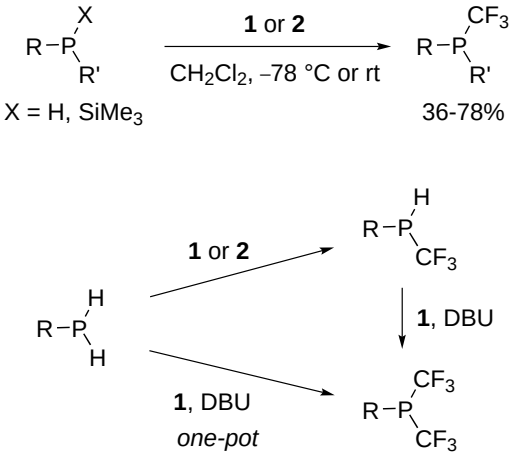

Scheme 29: Mono- and bistrifluoromethylation of primary phosphanes using reagents **2** and **3**.[110][111]

This newfound methodology could be used to prepare synthetically useful secondary and tertiary trifluoromethylphosphanes. The secondary phosphanes were subsequently found to be suitable nucleophiles to introduce a *P*-stereogenic trifluoromethyl phosphane on a ferrocene scaffold (scheme 30), allowing the preparation of the first examples of trifluoromethyl *P*-stereogenic Josiphos-derived ligands.[112][113]

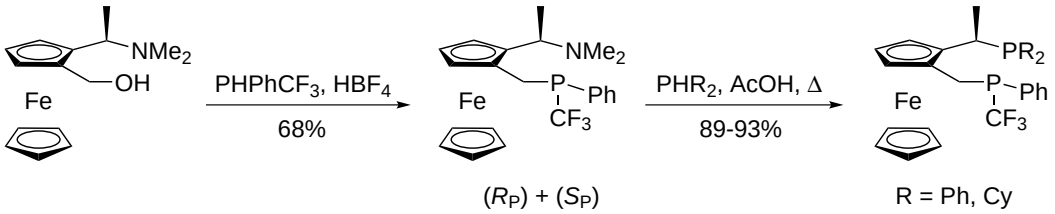

Scheme 30: Synthesis of trifluoromethyl *P*-stereogenic Josiphos analogues containing a methylene spacer between P1 and Cp.[112][113]

Further work in the Togni group was oriented towards the synthesis of bistrifluoromethyl ferrocenyl ligands. It was found that the bistrifluoromethyl PPFA analogue could be accessed in good yield following the Caffyn methodology, as the electrophilic pathway proved to be inadequate (scheme 31), although further screening of the base was not performed.[114]

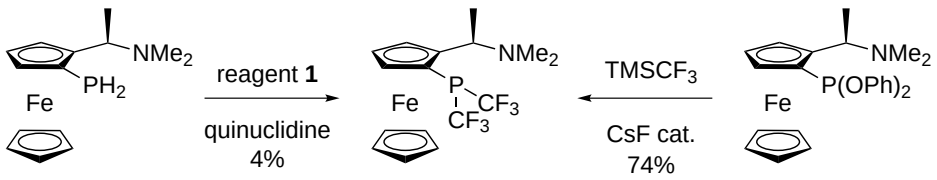

Scheme 31: Synthesis of bistrifluoromethyl PPFA analogue.[114]

Using this ligand as precursor allowed the subsequent preparation of Josiphos, ferrocenylpyrazole and Pigiphos bistrifluoromethyl analogues in very good yields (scheme 32).[114]

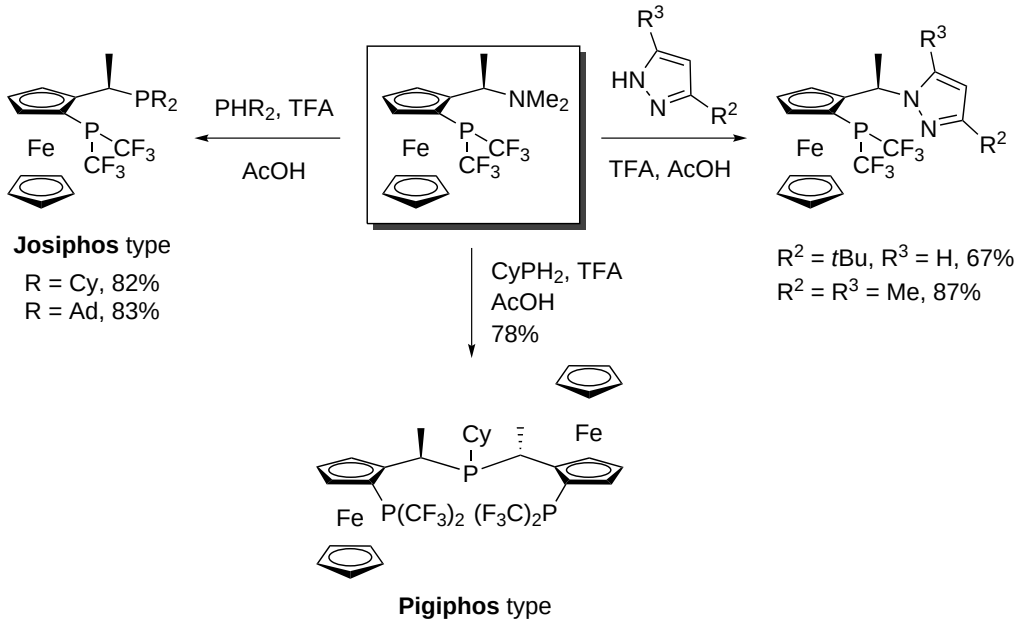

Scheme 32: Synthesis of bistrifluoromethyl Josiphos, ferrocenylpyrazole and Pigiphos derivatives.[114]

Further work in our group aiming towards the preparation of trifluoromethyl *P*-stereogenic ferrocenyl ligands allowed the development of a new synthetic methodology (scheme 33). It was found that treating lithiated Ugi amine with 0.5 eq. of $PPh(CF_3)_2$ yielded the monotrifluoromethyl *P*-stereogenic PPFA analogues. The diastereoselectivity could however not be controlled and in all cases was close to 1:1. It was also found essential to apply an excess of nucleophile to isolate the product diastereomers in reasonable amounts, as the reaction never reached full conversion.

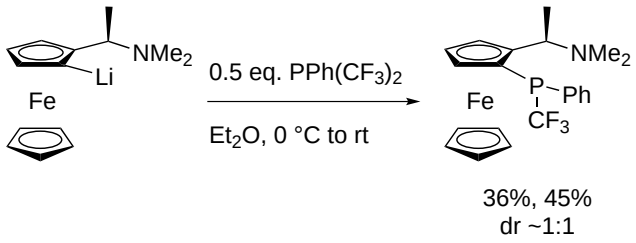

Scheme 33: Synthesis of monotrifluoromethyl *P*-stereogenic PPFA analogue.[115][116]

The trifluoromethyl *P*-stereogenic PPFA intermediate could be further transformed in a manner analogous to the bistrifluoromethyl congener to form the corresponding monotrifluoromethyl *P*-stereogenic analogues of Josiphos, ferrocenylpyrazole and Pigiphos (scheme 34).[115] The coordination behavior of the ligands to various transition metals was subsequently investigated.[115]

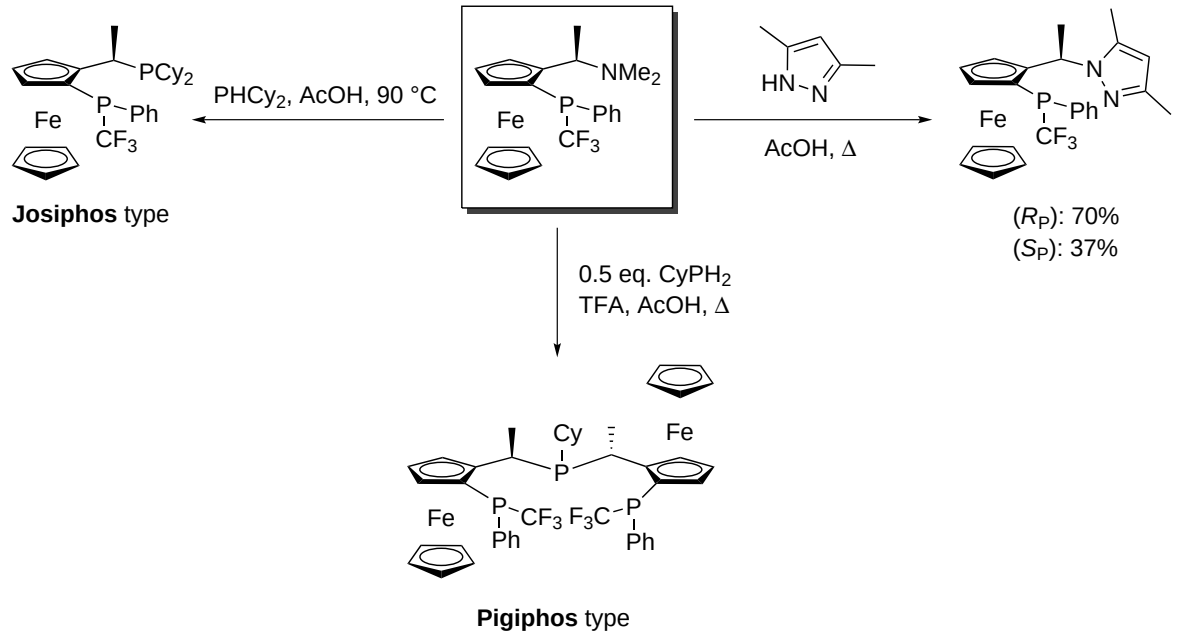

Scheme 34: Synthesis of monotrifluoromethyl *P*-stereogenic Josiphos, ferrocenylpyrazole and Pigiphos derivatives.[115]

This methodology was later applied in our group and found to be reproducible to prepare Xyliphos derivatives (scheme 35). These ligands were found to be more stable to air compared to the Josiphos analogues, but nevertheless had to be stored under argon.[117]

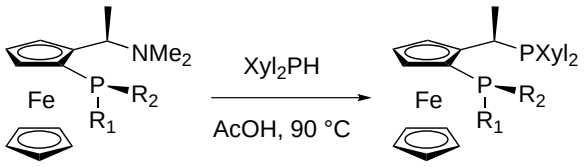

R_1	R_2	Yield (%)
Ph	CF_3	71
CF_3	Ph	49
Mes	CF_3	64
*o*An	CF_3	48
CF_3	*o*An	68
Cy	CF_3	87

Scheme 35: Synthesis of monotrifluoromethyl *P*-stereogenic Xyliphos derivatives.[117][118]

The final relevant question is, how do such ligands behave in catalysis? The next section will present a few relevant examples of trifluoromethylphosphanes used as ligands in various asymmetric transformations.

1.5.2 Trifluoromethylphosphanes in asymmetric catalysis

The activity of the bistrifluoromethyl Josiphos analogue prepared in our group (section 1.5.1) was tested in three different catalytic processes (see scheme 36).[114] In a first instance it was applied in the benchmark Rh-catalyzed enantioselective hydrogenation of dimethyl itaconate (DMI). The ligand was found to react much slower as the original Josiphos, displaying full conversion only after 13 hours at room temperature and exhibiting only 37% enantioselectivity. It was even less active in the Pd-catalyzed allylic alkylation of 1,3-diphenylallyl acetate, as it yielded only 11% racemic product.

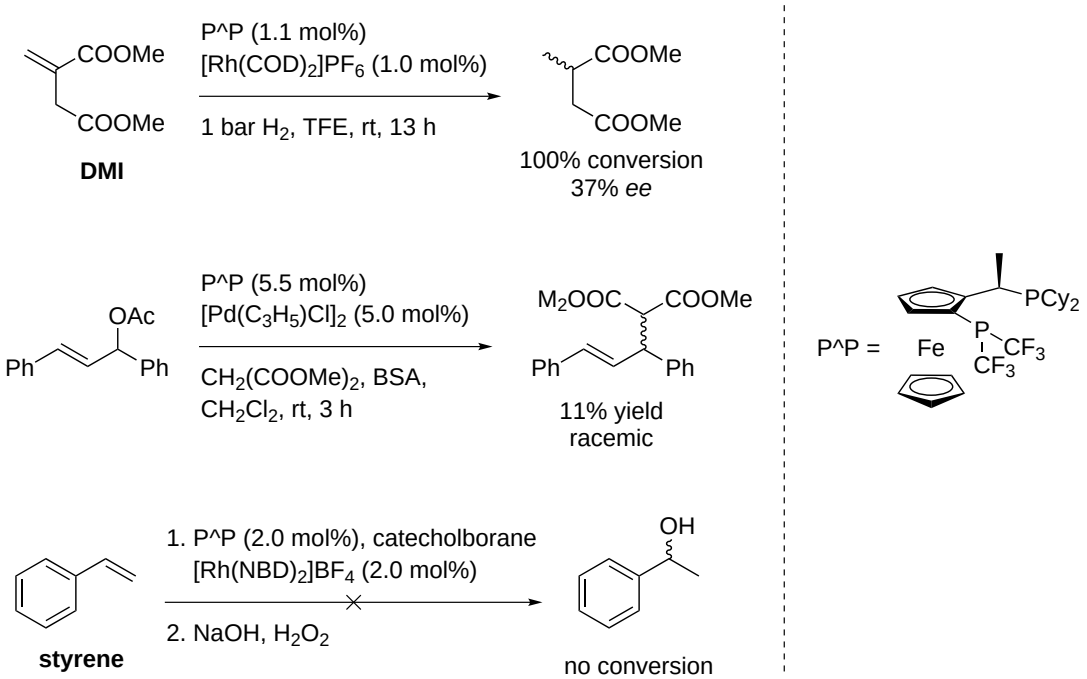

Scheme 36: Asymmetric catalytic trials using the bistrifluoromethyl Josiphos ligand.[114]

As a last attempt to display the ligand's possible ability induce enantioselectivity, the ligand was used in the Rh-catalyzed hydroboration of styrene. The parent Josiphos ligand displayed 92% *ee* and 65% product, but disappointingly the bistrifluoromethyl analogue did not allow any conversion to product at all.

After these first disappointing results, it was rationalized that the increased back bonding to the bistrifluoromethylphosphane stabilizes lower oxidation states and might therefore possibly decelerate the oxidative addition of a substrate. The low enantioselectivities compared to the diphenyl analogues can possibly be accounted for by the reduced steric demand of the trifluoromethyl substituents. The increased pyramidalization of such phosphanes (see section 1.2) also reduces the steric demand around the phosphorus, which might lead to reduced enantiodiscriminating ability in catalysis.

Undeterred by these results, it was thought that the combination of a single trifluoromethyl substituent with a more bulky, electron-rich aryl group might lead to preferential catalytic activity in contrast to bistrifluoromethyl ligands. The first example of a monotrifluoromethyl *P*-stereogenic Josiphos ligand was thus tested in the asymmetric hydrogenation of DMI as shown below. The results were very pleasing, as high enantioselectivities were achieved (see table 5). A relatively significant solvent dependency was observed (entry 1 vs. entry 2, entry 5 vs. entry 7 and entry 6 vs. entry 8). The nature of the counterion had a much smaller influence on the outcome (entry 2 vs. entry 3). In most cases the absolute configuration at phosphorus did not significantly influence the enantioselectivity, except when $[Rh(NBD)_2]BF_4$ was used as rhodium precursor (entry 5 vs. entry 6).

Table 5: Hydrogenation of DMI using *P*-trifluoromethyl Josiphos derivatives.[115][116]

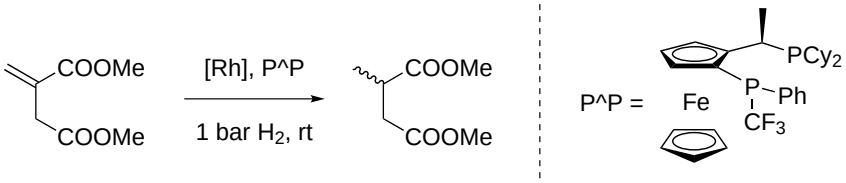

Entry	Ligand	$[RhL_2]X$	Solvent	Conversion (%)	*ee* (%)
1	(S_P)	$[Rh(COD)_2]SbF_6$	MeOH	95	58
2	(S_P)	$[Rh(COD)_2]SbF_6$	TFE	100	91
3	(S_P)	$[Rh(COD)_2]PF_6$	TFE	100	95
4	(R_P)	$[Rh(COD)_2]PF_6$	TFE	100	97
5	(S_P)	$[Rh(NBD)_2]BF_4$	MeOH	90	74
6	(R_P)	$[Rh(NBD)_2]BF_4$	MeOH	84	80
7	(S_P)	$[Rh(NBD)_2]BF_4$	TFE	100	95
8	(R_P)	$[Rh(NBD)_2]BF_4$	TFE	100	97

The promising results of these trifluoromethyl *P*-stereogenic ligands promoted further work in this direction. Analogous Xyliphos derivatives were thus prepared (see section 1.5.1), and their activity in the asymmetric hydrogenation of various substrates evaluated.[117] Cationic rhodium(I) complexes of Xyliphos ligands were found to hydrogenate DMI in less than an hour with up to >99% *ee* under 1 bar H_2 at room temperature. Corresponding iridium(I) catalysts were found to be active in the hydrogenation of 1-substituted 3,4-dihydroisoquinolinium chlorides (DHIQs). 1-Phenyl-3,4-dihydroisoquinolinium chloride was thus reduced in less than 3 hours under 100 bar H_2 reaching enantioselectivities up to 96% (table 6). Under the same conditions, the parent ligand yielded the product in only 84% *ee*.

Table 6: Hydrogenation of a DHIQ using *P*-trifluoromethyl Xyliphos derivatives.[117][118]

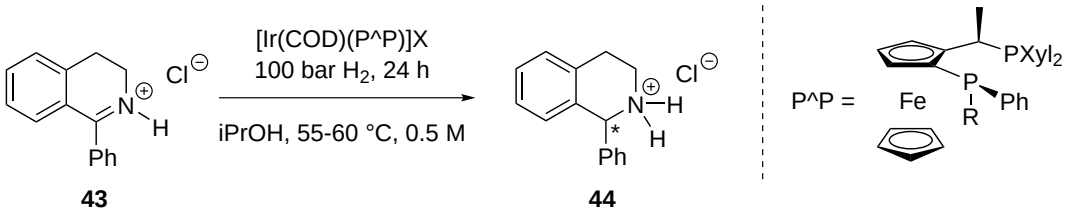

43 **44**

Entry	R	X	Yield (%)	*ee* (%)
1	Ph	Cl	>99	84
2	Ph	I	>99	93
3	CF_3	Cl	>99	96
4	CF_3	I	>99	82

An example of a bistrifluoromethyl *P*,*N* ligand successfully used in asymmetric catalysis appeared in 2012. Shen *et al.* reported the synthesis of bistrifluoromethyl analogues of phenyl- and ferrocenyloxazoline ligands.[119] They were subsequently tested in the Pd-catalyzed allylic alkylation of cinnamyl acetate (table 7).

Table 7: Palladium-catalyzed allylic alkylation of cinnamyl acetate using bistrifluoromethyl oxazoline ligands.[119]

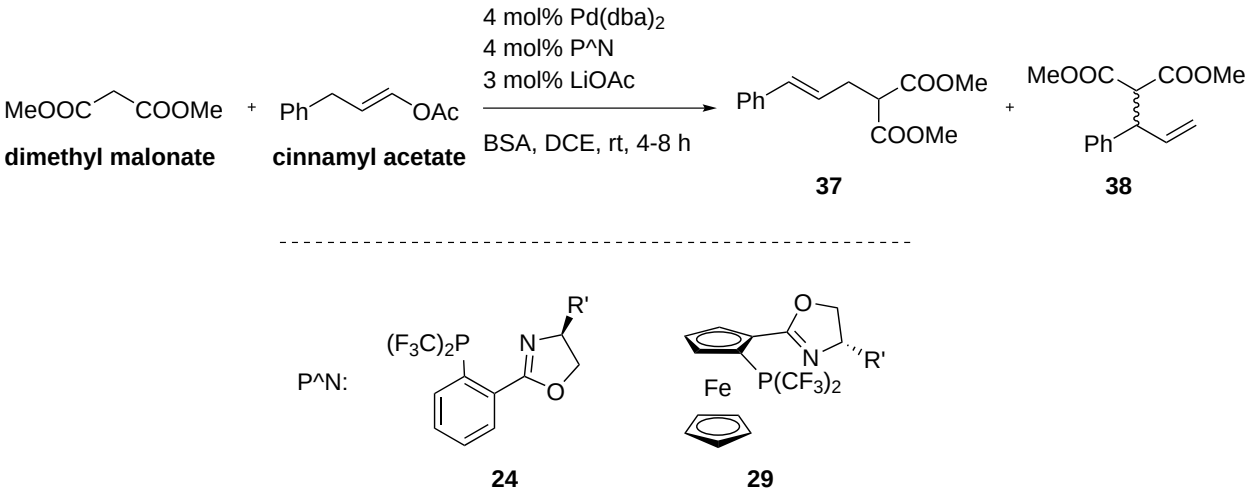

Entry	Ligand	R	Time (h)	**38**:**37**	*ee* (%)
1	**24**	Ph	8	1:1	72
2	**24**	Bn	8	3.4:1	92
3	**24**	iPr	8	5:1	88
4	**24**	*t*Bu	8	11.5:1	94
5	**29**	Ph	4	0.64:1	77
6	**29**	Bn	4	1:1	91
7	**29**	iPr	4	1.4:1	87
8	**29**	*t*Bu	4	4:1	93

The ligands were found to catalyze the reaction under 8 hours, and high enantioselectivities were observed (table 7). The most notable result is the high regioselectivity of certain ligands, as favorable branched to linear ratios were observed. In general the regioselectivity was better when using a phenyloxazoline ligand than a ferrocenyloxazoline ligand (entries 1-4 vs. entries 5-8). The oxazoline side chain seems to influence this strongly, as the regioselectivity varies significantly depending on the side chain present (e.g. entry 1 vs. entry 4). As comparison, in a control experiment under the same conditions, the parent ligand *t*BuPHOX was found to furnish solely the linear product (!).[5][119]

[5]Although this catalytic system has been extensively studied and is known to be sensitive to the reaction conditions,[120] it seems highly unlikely that this ligand, which has proven to be one of the best in this type of transformation,[64] would furnish no branched product at all under these conditions.

In 2014, You *et al.* have shown that the analogous 1,1' substituted ferrocenyloxazolines also demonstrate high enantioselectivity in the Pd-catalyzed allylic alkylation of monosubstituted allyl substrates (scheme 37).[121]

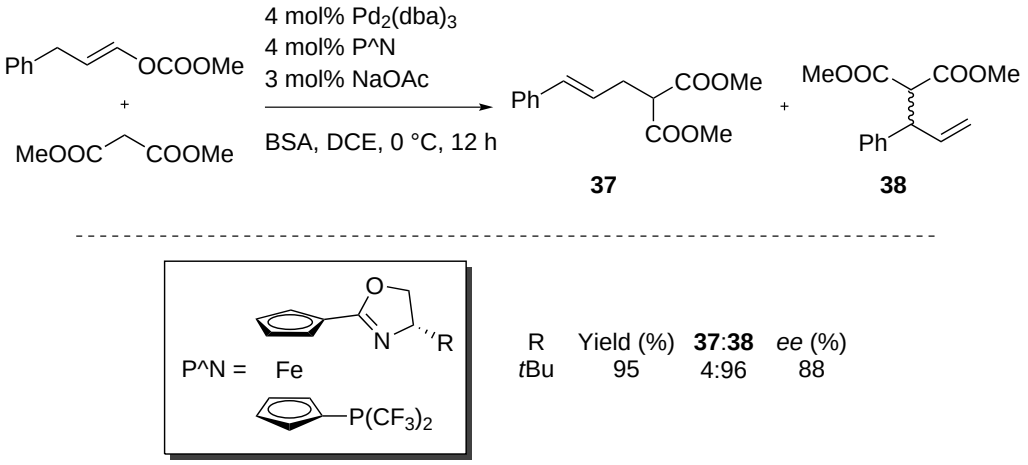

Scheme 37: Palladium-catalyzed allylic alkylation using 1,1'-ferrocenyloxazoline bistrifluoromethyl ligands.[121]

As in Shen's case (see table 7),[119] the oxazoline bearing a *t*Bu side chain was found to be the one exhibiting the most enantioinduction (scheme 37). Similar results were obtained using cinnamyl acetate as substrate.[121]

1.6 Aim of the thesis

Considering the importance of phosphorus-based ligands in asymmetric catalysis and the considerable potential of *P*-stereogenic ligands, research in this direction is definitely not futile. As much of the historical work has focused on electron-rich, backbone-chiral ligands, parallel research focusing on electron-poor, *P*-stereogenic compounds has been neglected to some extent.

The relatively new but mostly underrepresented class of perfluoroalkylphosphanes has been gaining some momentum in the last decade since the development of more reliable preparative methods,[97] but the combination of *P*-stereogenic phosphanes with a trifluoromethyl substituent is still quite rare and, to the best of our knowledge, all examples come from our research group.[112][115][117] Although some new methods have emerged for the preparation of such compounds, the synthetic protocols are still neither fully developed nor established as routinely used and reproducible methods. This calls for the development of reliable preparative methods and further motivates research in this direction.

To carry out these ideas, four main ligand backbones were selected (figure 14): binaphthyl (chapter 2), phenyl- and ferrocenyloxazoline (chapter 3), and finally phenylethylferrocene (chapter 4).

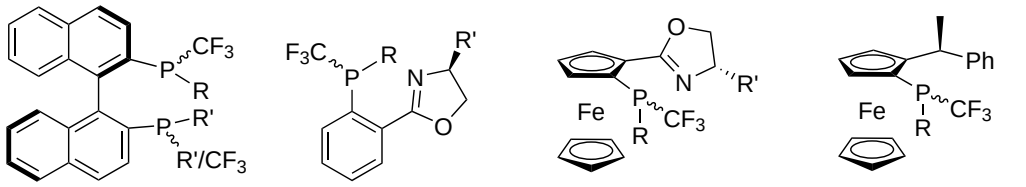

binaphthyl phenyloxazoline ferrocenyloxazoline phenylethylferrocene

Figure 14: Target ligand classes.

First the preparation of *P*-stereogenic trifluoromethyl derivatives will be investigated, the crucial step being the development of efficient and reliable synthetic protocols to prepare the target ligands. With the compounds in hand, it will then be possible to study their coordination behavior as well as investigate their use as chiral ligands in asymmetric transformations. This will allow to assess not only the steric but also the electronic effect of the electron-withdrawing trifluoromethyl group on the ligand and potential catalysts arising from transition metal complexes.

2 Biaryl ligands

2.1 Introduction

A major breakthrough occurred with the development of the axially chiral ligand BINAP (see section 1.4.2).[44] This ligand created a revolution in asymmetric catalysis and changed the approach to chemical synthesis.[45] BINAP is considered a privileged ligand not only for asymmetric hydrogenation, but also for other important chemical transformations such as C-C bond forming reactions. For further reading, a detailed review on BINAP and its modifications is recommended,[47] as well as a comprehensive book chapter on BINAP's applications.[122]

2.1.1 Previous work[111][114][123]

The success of BINAP in numerous stereoselective transformations prompted the development of a plethora of derivatives.[47] However, as already mentioned previously, the lack of synthetic methods for efficient preparation of trifluoromethylphosphanes hindered the development of such electron-poor derivatives. After the development of hypervalent iodine electrophilic trifluoromethylation agents,[108] it was found that primary phosphanes cleanly undergo mono- or bistrifluoromethylation under mild conditions (see section 1.5.1).[110] It was then thought that this new methodology should be applied to the synthesis of a new BINAP-type ligand, which would bear a bistrifluoromethyl electron-poor phosphane and a standard electron-rich diphenylphosphane (scheme 38). The binding behavior of these two antipodal moieties could then be directly compared in the same structure, and the catalytic activity of this unique compound could also be investigated.

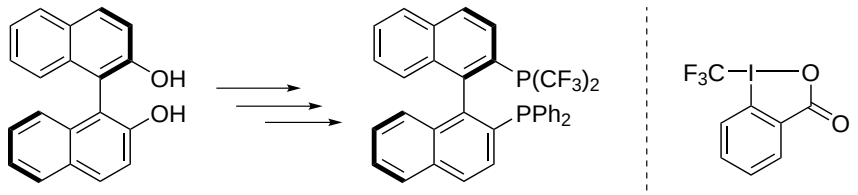

(*R*)-**BINOL** **5** **2**

Scheme 38: Synthesis of bistrifluoromethyl BINAP-type ligand **5** from BINOL, using **2** in a key step.[114][123]

Two approaches were envisioned for the preparation of ligand **5** (see scheme 39). Although both approaches would use BINOL triflate **9** as starting material, the main difference in the two pathways would be the sequence in which the two phosphane groups are introduced. In the first approach, the diphenylphosphanyl is introduced first, by cross-coupling of one triflate moiety with diphenylphosphane oxide to yield **8** and subsequent reduction to the tertiary phosphane. The second phosphane would then be introduced via the phosphonate **7**, followed by reduction to primary phosphane **6**. The desired ligand **5** would be obtained by bistrifluoromethylation of the primary phosphane.

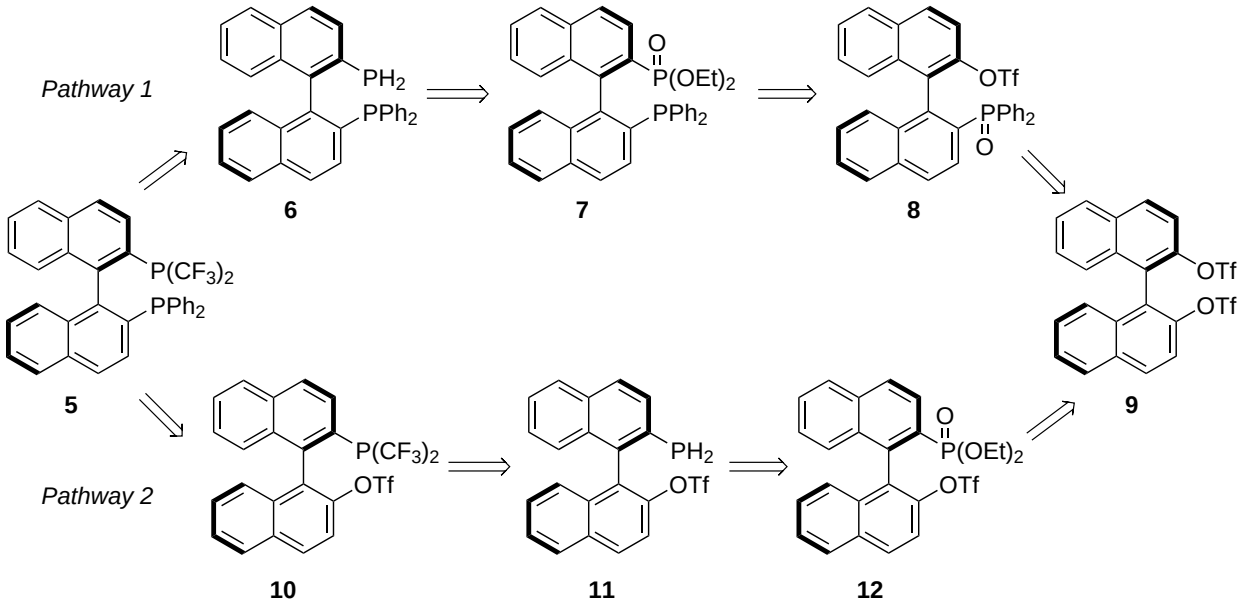

Scheme 39: Retrosynthesis of the two possible pathways to ligand **5**.[114][123]

In the second approach, the bis(trifluoromethyl)phosphanyl is introduced first by bistrifluoromethylation of the corresponding primary phosphane. The primary phosphane is obtained by reduction of the phosphonate, which is easily obtained by palladium-catalyzed cross-coupling of one triflate moiety with diethyl phosphite. The diphenylphosphanyl group is then introduced in the last step by nickel-catalyzed cross-coupling of the triflate with diphenylphosphane. These two approaches would involve the formation of to date unknown intermediates, the only one known (apart from BINOL triflate **9**) being compound **8**, therefore also allowing more insight in the chemistry of 2,2'-binaphthyl derivatives.

When Armanino[123] and Koller[114] set out to synthesize this ligand, they discovered a limitation of the trifluoromethylation reagent. It came to light that primary phosphanes would not undergo trifluoromethylation in the presence of a tertiary phosphane. This means that if the diphenylphosphanyl unit was installed on the binaphthyl backbone before the trifluoromethylated one, the primary phosphane could not be further substituted using the hypervalent iodine reagent **2**. The first pathway was then discarded, and the desired ligand **5** could be prepared in acceptable yield via the second pathway, as shown in scheme 40, with subsequent introduction of the bistrifluoromethylphosphane and the diphenylphosphane.

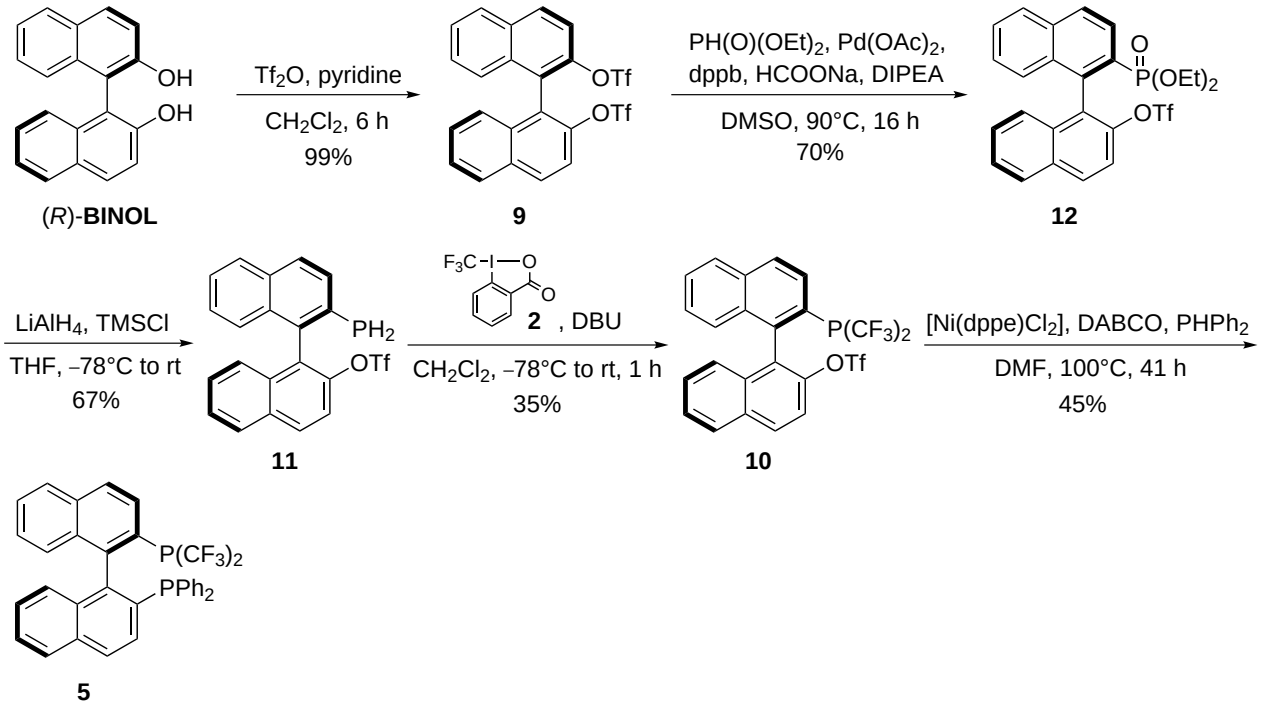

Scheme 40: Synthesis of the target BINAP-type ligand **5**.[111][114][123]

With the ligand in hand, its coordination behavior to palladium(II) was investigated. Ligand **5** was stirred with a suitable Pd(II) precursor, which reacted cleanly under an hour at room temperature to the corresponding Pd(II) dichlorido complex **13** in high yield (scheme 41).

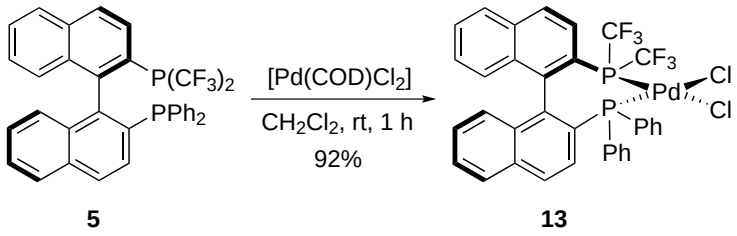

Scheme 41: Synthesis of Pd(II) dichlorido complex **13** from ligand **5**.[111]

Crystals suitable for X-ray diffraction were obtained by slow diffusion of pentane in a CD_2Cl_2 solution. An overlay of complex **13** with parent BINAP complex [Pd((*R*)−BINAP)Cl_2] is shown below.

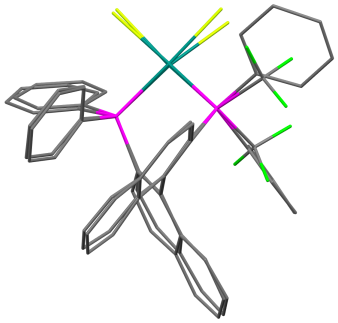

Figure 15: Overlay of complex **13**[123] and [Pd((*R*)−BINAP)Cl_2] (CCDC number 1172182, identifier HAPBIJ).

The X-ray structure of complex **13** shows similar features to the parent [Pd((*R*)−BINAP)Cl_2] complex. The most notable aspect is the bond angles around the phosphorus atoms. Whereas they deviate at most by 5° from a perfectly tetrahedral structure in the case of the PPh_2 substituent, this deviation reaches 14° in the case of the $P(CF_3)_2$ moiety, exhibiting a high degree of pyramidalization. This illustrates the electronic effect of the trifluoromethyl substituents, and is in agreement with the model put forward by Bent.[13]

2.1.2 Aim of the project

The goals of this project part are divided in two main parts. The first part deals with the preparation of ligand **5** and its application in an asymmetric catalytic transformation, in order to compare this unique ligand to its parent ligand (BINAP). The second part is focused on the attempted synthesis of further trifluoromethyl BINAP-type derivatives, which fulfill the initial goals of the thesis (see section 1.6). The idea would be to prepare new electron-poor ligands, some possessing stereogenic phosphorus atoms, in order to also compare them to their electron-rich congener.

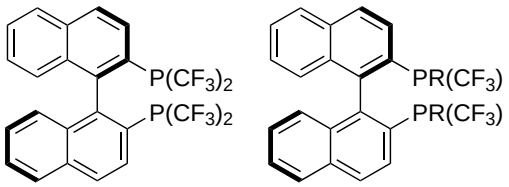

14 **15**

Figure 16: Target BINAP-type ligands.

Finally, all new phosphanes should be tested in a standard metal-catalyzed transformation, in order to assess their usefulness as chiral ligands and the possible influence of *P*-stereogenicity.

2.2 Results and discussion

2.2.1 Synthesis of BINAP-type ligand 5

Following the synthetic pathway developed in our research group described in section 2.1.1 (scheme 40), preparation of ligand **5** was started. The first two steps were carried out smoothly. The triflation of BINOL was run using DIPEA as base instead of pyridine, and yielded the product quantitatively. The Pd-catalyzed cross-coupling of the triflate with diethyl phosphite was selective in one position as expected[124] and yielded 75% phosphonate **12**. The yield could however not be improved, as reduction of the triflate substituent occurs under these reaction conditions, probably by oxidative addition to the Pd(0)-phosphane complex. This is known to occur in the presence of a hydrogen donor such as ammonium formate.[125]

The next stop of the synthesis was nevertheless carried out, but reduction of phosphonate **12** to the primary phosphane **11** did not go as smoothly as expected, as side products in non neglectable amounts were formed. Usually a mixture of three products was observed, and it was discovered that a mixture of the desired product, the hydrolyzed triflate and reduced triflate was obtained. As it is known that the triflate group can undergo reduction with $LiAlH_4$,[126] different reducing conditions exempt of $LiAlH_4$ were tested, summarized in table 8.

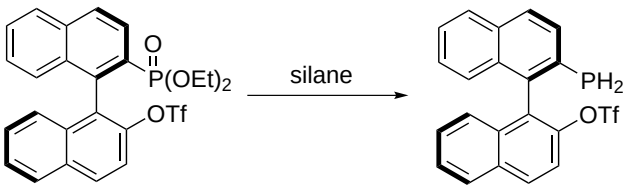

12 **11**

Table 8: Alternative reduction attempts towards primary phosphane **11**.

Silane	Conditions	Conversion (%)	Products
TMSCl[114]	$LiAlH_4$, THF, –78 °C	100	Mixture of 3 products, 1 isolated
Si_2Cl_6[127]	toluene, 100 °C	100	Mixture of >3 products
$HSiCl_3$[127]	NEt_3, toluene, 100 °C	0	Starting material recovered
TMDS[128]	$Ti(OiPr)_4$, MeCy[a], 100 °C	0	Starting material recovered

[a] MeCy = methylcyclohexane.

Unfortunately, the alternate methods either did not yield any product, or were unselective and yielded intractable mixtures. During experimentation with the reduction conditions, it was discovered that the primary phosphane was actually quite air-stable, at least in pure form, which correlates nicely with the findings of Higham *et al.*, who attribute the stability of certain primary phosphanes to delocalization in the aryl backbone.[129][130] This compound can thus be indefinitely stored at room temperature in an argon-flushed closed vessel without any apparent oxidation. A sample of a few hundred milligrams was stored in this manner, and the ^{31}P NMR spectrum recorded after three years did not show any sign of oxidation or decomposition.

Considering the unfavorable reaction conditions with respect to the presence of the triflate moieties, an idea to circumvent this easily reduced functional group came up. Having a less

labile leaving group, such as a bromide for example, would certainly be advantageous. The question is, how could one introduce it? Enantiomerically pure 2,2'-dibromo-1,1'-binaphthalene (DBBN) is not available, and the methods to synthesize it traditionally use toxic chemicals such as mercury salts.[131] An optimized procedure, in which zinc bromide is used instead of the original mercury bromide seemed promising,[132] but a recent report showed it to proceed in low yield.[133] Moreover, the necessary optically pure starting material 2,2'-diamino-1,1'-binaphthalene (DABN), although commercially available, is relatively expensive. We therefore preferred to investigate another possibility.

There are various reports concerning the metal-catalyzed conversion of triflate groups to bromides, and some have also been reported for aryl triflates as substrates. We thus selected three different methods, which have been described by Buchwald *et al.*[134] and Hayashi *et al.*.[135][136] To test the conditions, either naphthyl-2-triflate **16**, BINOL triflate **9**, or binaphthyl monotriflate **17** was used, as they are easily accessible in one step from the corresponding alcohols. If one of the methods would appear to be efficient, the functional group tolerance of the method would of course need to be compatible with the substituent in the 2 position of the binaphthyl backbone. We will however see later that we will not need to worry about this.

As summarized in table 9, no conversion of BINOL triflate **9** occurred using either Pd-catalyzed coupling with KBr or Ru-catalyzed coupling with LiBr (entries 1–3). Binaphthyl monotriflate **17** also did not react under Ru catalysis (entry 4). Actually, the only substrate that showed some conversion to the bromide is naphthyl-2-triflate **16**, using Hayashi's conditions[136] (entry 5). However, no full conversion was achieved even after heating at 100 °C for 80 h, although this substrate is reported to react in 6 h under these conditions. The further investigation of this pathway was therefore abandoned.

Table 9: Attempted conversion of triflate to bromide.

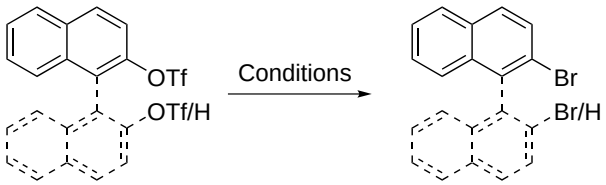

9/16/17

Entry	Substrate	Catalyst/Ligand system	Br source	Conversion (%)
1	BINOL triflate **9**	$[Pd_2(dba)_3]$/*t*BuBrettPhos[134]	KBr	0
2	BINOL triflate **9**	$[Ru(acac)_3]$/3,4,7,8-Me_4-phen[135]	LiBr	0
3	BINOL triflate **9**	$[Cp^*Ru(MeCN)_3OTf]$[136]	LiBr	0
4	Monotriflate **17**	$[Ru(acac)_3]$/3,4,7,8-Me_4-phen[135]	LiBr	0
5	Monotriflate **16**	$[Cp^*Ru(MeCN)_3OTf]$[136]	LiBr	~30

After these disappointing results, it was concluded that the steric hindrance of the binaphthyl backbone does not allow for conversion of the 2,2'-substituents in this manner,[6] and no further

[6]The conversion of F_8-substituted BINOL ditriflate to dibromide has also been observed to be unsuccessful.[137]

experiments were done in this direction.

2.2.2 Catalysis with BINAP-type ligand 5

The alkylative ring opening of oxabicyclic alkenes is a powerful method to access cyclic alcohols in a stereoselective fashion. Of particular interest is the ring opening of 7-oxabenzonorbornadiene **18**, providing functionalized dihydronaphthalenols, which are important structural motifs in medicinal chemistry.[138] The pioneering work by Lautens *et al.* directed towards an asymmetric version of this type of ring-opening reaction has shown that palladium complexes with chiral phosphane ligands can catalyze such reactions in a highly stereoselective manner.[139] Further work by Lautens' and other groups has greatly expanded the scope of this reaction, which has been shown to proceed under catalysis by a broad range of transition metals such as rhodium,[140] copper,[141], iridium,[142] and recently cobalt,[143] providing complementary selectivities and allowing the use of a wide range of nucleophiles.

In 2000, Lautens *et al.* showed that BINAP-derived ligands furnish *cis*-dihydronaphthalenols in a highly enantioselective manner, via Pd(II) catalysis[139] (scheme 42). The best results were obtained when combining (*R*)-tol-BINAP as ligand and diethylzinc as alkylating reagent, and all reactions gave high conversion at room temperature.[7]

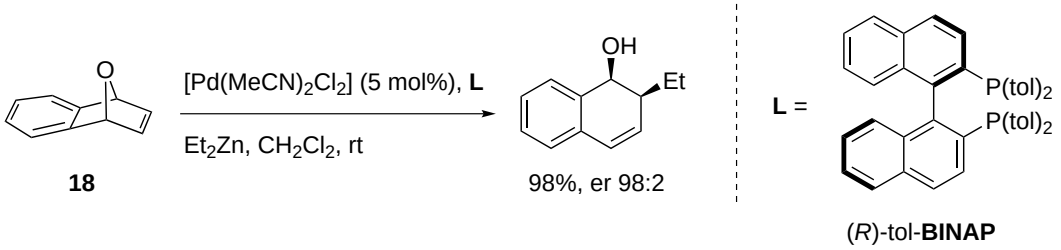

Scheme 42: Enantioselective Pd-catalyzed ring opening of oxabenzonorbornadiene **18** using BINAP ligands.[139]

We thus decided to test our ligand **5** in the ring opening of bicycle **18**, using diethylzinc as alkylating agent. The procedure by Lautens *et al.* was followed.[139] The precatalyst was formed *in situ* by first stirring the Pd(II) precursor and ligand in CH_2Cl_2 for 2 h. A solution of substrate **18** was then added, followed by a solution of diethylzinc in hexanes (1 M). The reaction mixture was then stirred at room temperature and monitored by GC-MS analysis.

Usually nearly full conversion was observed after 2 h. A few drops of water were then added to the reaction mixture, which was then stirred under air at least 30 min. The resulting suspension was filtered over silica gel, eluting with hexane:Et_2O 10:1, yielding the products as a colorless oil. The resulting products were then subjected to analytical HPLC to determine the enantiomeric ratio. The results are shown in table 10.

[7] Reaction times are however never mentioned.

Table 10: Pd(II)-catalyzed ring opening of oxabenzonorbornadiene **18** with diethylzinc.

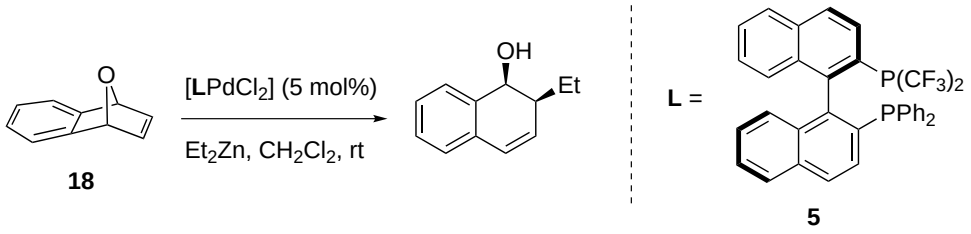

18 **5**

Entry	Ligand	Yield (%)	er[a]	(*ee*[b] (%))
1	**5**	n.d.[c]	91:9	(*82*)
2	**5**	n.d.[c]	92:8	(*84*)
3	(*R*)-BINAP	n.d.[c]	66:34	(*32*)
4	(*rac*)-BINAP	n.d.[c]	50:50	(*rac*)
5[139]	(*R*)-tol-BINAP	98	98:2[d]	(*96*)
6[139]	(*R*)-BINAP	91	94.5:5.5[d]	(*89*)

[a] Determined by analytical HPLC on a Chiracel OD-H column.
[b] Enantiomeric excesses below 5% are considered racemic.
[c] n.d. = not determined.
[d] er values were derived mathematically from the *ee*.

Interestingly enough, electron-poor ligand **5** yielded enantioselectivities in the same range as those reported by Lautens *et al.*.[139] The two runs with ligand **5** provided *ee* values between 82-84% (entries 1 and 2). However, to our surprise, parent ligand (*R*)-BINAP induced much less enantioselectivity than reported.[139] Although an experimental error can never be excluded, we tried to rationalize this discrepancy. The quality of our commercially acquired (*R*)-BINAP was checked and found to be immaculate. The same palladium precursor was used, namely $[Pd(MeCN)_2Cl_2]$, and the palladium precatalyst was formed *in situ* in the same manner. The only obvious difference in our system is the solvent in which the diethylzinc solution was present. Ours was in hexanes, whereas the reported catalysis makes use of diethylzinc in toluene, although this does not allow to easily rationalize the difference in enantioselectivity. As time constraints did not allow us to perform further catalytic trials, this issue was put to rest here. The influence of the solvent of the alkylating agent solution however remains to be elucidated.

These catalytic results are nevertheless exciting, as they present the first example of ligand **5** being used in an asymmetric transformation, with high enantioinduction nonetheless. Further catalytic trials will allow more insight in the application of a mixed electron-poor/electron-rich diphosphane ligand and further assessment of the role of increased electronic-withdrawing effect and reduced steric demand of the trifluoromethyl group.

2.2.3 Towards new trifluoromethyl BINAP derived ligands

Considering the goal of synthesizing further trifluoromethyl BINAP derivatives, a simple experiment was carried out. Starting with DBBN as substrate, it was subjected to lithiation, followed by electrophilic substitution with phosphane $PPh(CF_3)_2$ **4**. This procedure developed

in our group was previously shown to function best with an excess of nucleophile, and is accompanied by elimination of a trifluoromethyl group.[115] This protocol however quickly exposed itself as being unsatisfactory.

Table 11: Attempts towards trifluoromethyl *P*-stereogenic binaphthyl derivatives.

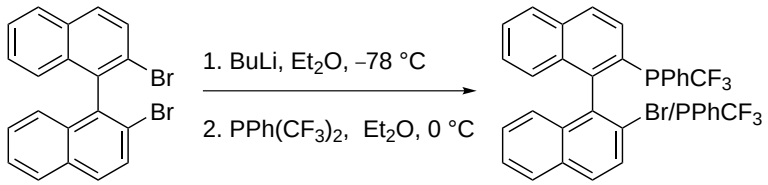

DBBN **19**

Entry	Li base	Eq.	T_1	T_2	T_3	Products
1	*t*BuLi	1.1	–78 °C	rt (15 min)	–78 °C	DBBN
2	*n*BuLi	2.2	–78 °C	–78 °C (30 min)	–78 °C	DBBN and DBBN–Br
3	*n*BuLi	2.2	–78 °C	rt (1 h)	0 °C	$PPh(CF_3)_2$:**19** 1:0.55

Reaction conditions: Li base added at –78 °C (T_1). T_2 = stirring T. $PPh(CF_3)_2$ (1.2 eq.) added at T_3.

When lithiation was performed with *t*BuLi, mostly starting materials were visible after stirring overnight (table 11, entry 1). Lithiation with *n*BuLi proved to be more promising, as a slight amount of debrominated DBBN was visible via GC-MS, however no desired product was detected and a major DBBN peak occurred (entry 2). Finally, a last run was carried out using *n*BuLi under similar conditions as entry 2, but the reaction mixture was stirred during 1 h at room temperature before addition of the electrophile. This allowed observation of a signal in ^{19}F NMR which may well correspond to the desired product (d, –58.6 ppm, $J_{F\text{-}P} = 64.4$ Hz). Although no more DBBN was observed after stirring overnight, conversion to the desired product was however very low (ratio **4**:**19** 1:0.55 by ^{19}F NMR). This pathway was at this point left aside.

As the 'forward' approach to new binaphthyl ligands was relatively unsatisfactory, another approach was envisioned. Since enantiomerically pure BINAP is commercially available, it was thought that a 'backward' or 'reverse' approach should be considered. This method would consist of the cleavage of the BINAP P-C_{Ph} bonds using an alkali metal, leading to the secondary (or possibly primary) diphosphane intermediate shown in scheme 43. Simple trifluoromethylation of this intermediate using reagent **2** would furnish new electron-poor BINAP derivatives. This would theoretically allow obtention of the desired ligands with *P*-stereogenic centers in only two steps, which would be very convenient.

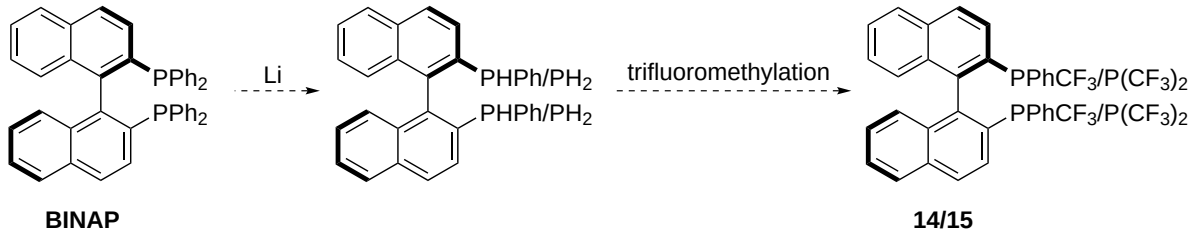

Scheme 43: Reverse strategy towards trifluoromethyl BINAP-derived ligands.

The cleavage of P-C bonds using alkali metals has been researched, although this synthetic pathway towards the preparation of new tertiary or secondary phosphanes is applied relatively sparsely. There are mostly reports dealing with the use of metallic lithium in THF or ammonia, although sodium and in some cases potassium have also been used (scheme 44). The drawback of the sodium in liquid ammonia reductive method, is that Birch reduction products (i.e. phosphanylcyclohexadienes) can be formed as side products. Studies by Meijboom *et al.* have shown that this highly depends on the choice of solvent, and that this does not occur in the aprotic solvent THF.[144]

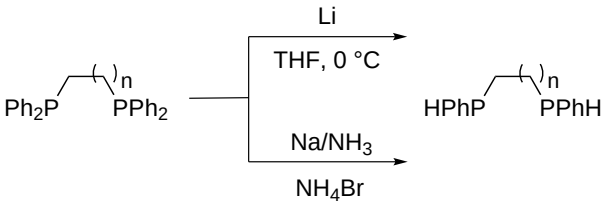

Scheme 44: P-C_{Ph} bond cleavage using alkali metals.[8]

There are, to our knowledge, very few reports dealing with the reductive cleavage of BINAP P-C bonds. A publication by Hayashi *et al.* from 2001 reports the use of *n*BuLi, showing selective bond cleavage between the binaphthyl moiety and the diphenylphosphanyl group.[151] Two other reports appeared in 2013 during the course of this work, disclosing the use of lithium metal.[152][153] A few experiments of our own were thus initiated.

The ease of handling of metallic lithium compared to sodium or potassium made it a candidate of choice for the experiments. Table 12 summarizes the reductive attempts. The quality of the lithium metal was shown to be crucial for reactivity. If the topmost layer of the lithium was blackened, indicative of a passivated layer consisting of lithium nitride, it had to be removed (e.g. by scratching with a sharp blade), otherwise no conversion was detected (entries 1 and 3). However, when unpassivated lithium wire was used, a complex mixture of phosphane oxides was obtained (entry 2).

[8] For examples see:[145][146][147][148][149][150].

Table 12: BINAP reduction attempts using lithium metal.

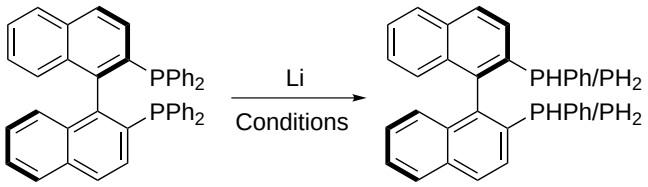

BINAP

Entry	Lithium species	Conditions	Conversion?	Products
1	Li wire	0 °C then reflux	no	starting material recovered
2	Li wire (scratched)	0 °C then reflux	yes	intractable mixture of oxides
3	Li wire + DBB	0 °C	no	starting material recovered
4	Li granules[b]+ DBB[a]	0 °C then –78 °C	yes	major product $PHPh_2$

[a] DBB = 4,4'-Di-tert-butylbiphenyl. The lithium metal and DBB were first reacted together, until a deep turquoise solution was obtained.
[b] The Li granules were stored in a glovebox.

We therefore considered enhancing the reactivity of lithium, by first forming lithium 4,4'-di-tert-butylbiphenylide (LDBB),[9] a powerful reducing agent that preferentially leads to electron transfer and to little or no radical combination.[155] Temperature is an important factor when using LDBB, and it was found that although the addition of a BINAP solution to the LDBB solution at –78 °C allowed conversion (entry 4), only diphenylphosphane was recovered. This left us with very little room for adjustment of reaction conditions. We rationalized that if primarily diphenylphosphane is formed already at –78 °C, going to lower temperatures would probably not change the outcome of the reaction.

As this pathway proved to be somewhat of a dead end and considering the general failure to access new trifluoromethyl BINAP ligands, no further time was invested in this strategy and the project was halted at this point.

2.2.4 A simple biphenyl ligand

Considering the synthetic difficulties encountered with the binaphthyl backbone, our strong desire to obtain a *P*-stereogenic axially chiral ligand remained nevertheless unabated. Wanting to demonstrate the possibility to easily access a P-CF_3 ligand with an unhindered torsion axis, we decided to make an attempt with the simplest biaryl backbone we could think of. We thus chose 2-bromo-1,1'-biphenyl as substrate, which is commercially available. It was subjected to lithiation followed by quenching with bistrifluoromethyl phosphane **4**, thereby eliminating a trifluoromethyl substituent, following the protocol previously developed in our group[115] (see section 1.5.1). We were delighted as desired ligand **20** was indeed obtained on the first attempt in reasonable yield (scheme 45).

[9] For details concerning LDBB see:[154]

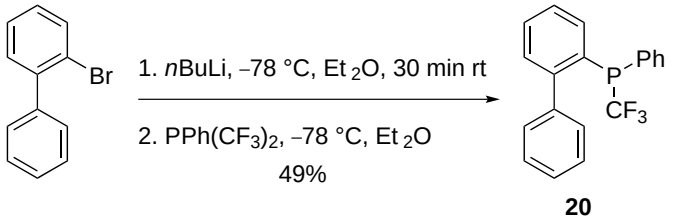

20

Scheme 45: Synthesis of trifluoromethyl P-stereogenic biphenyl ligand **20**.

The coordination ability of ligand **20** to Au(I) was subsequently tested, by stirring it with a suitable gold precursor as shown below. This complexation test was successful, yielding a coordination compound with ^{19}F and ^{31}P chemical shifts and coupling constants similar to other P-CF_3 gold complexes (table 13).

Table 13: Selected NMR data for gold(I) complex **21** and free ligand **20**

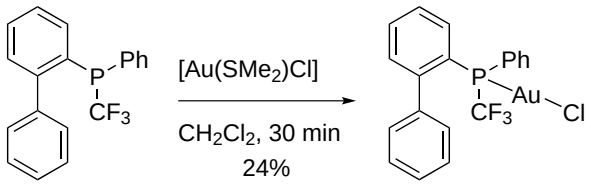

20 **21**

	Complex **21**	Free ligand **20**
^{31}P shifts (ppm)	33.9	–5.7
Multiplicity, $J_{P\text{-}F}$ (Hz)	q, 86.8	q, 76.3
^{19}F shifts (ppm)	–56.7	–54.0
Multiplicity, $J_{F\text{-}P}$ (Hz)	d, 86.9	d, 75.6

The structure of the complex was however not determined, as only a few milligrams were obtained and they did not yield crystals suitable for analysis by X-ray diffraction. As the goal of this side project was simply to illustrate the possibility of preparing a biaryl ligand with a freely rotating backbone and displaying its coordination ability, these reactions were not repeated, and no further experiments were carried out.

2.3 Conclusion

The forward route to ligand **5** was investigated, but no major optimization could be made. The conversion of the triflate groups to the corresponding bromide, projected in order to introduce a leaving group less prone to hydrolysis and reduction, proved unsuccessful. The attempted improvement of the reduction protocol of phosphonate **12** to primary phosphane **11** was also in vain. The direct introduction of P-CF_3 substituents via lithiation of DBBN followed by electrophilic substitution with phosphane **4** was unsatisfactory, as either no reaction or very little conversion was observed. A reverse synthetic strategy consisting of the cleavage of the BINAP P-C_{phenyl} bonds by lithium metal was tested. It was however found to favor the

cleavage of the P-$C_{binaphthyl}$ bonds, yielding mostly diphenylphosphane.

The electron-poor ligand **5** was tested in the Pd-catalyzed alkylative ring opening of oxabicyclic derivative **18** (scheme 46). Enantioselectivities in the same range as (*R*)-tol-BINAP were observed, albeit slightly lower, with values between 82 and 84%.

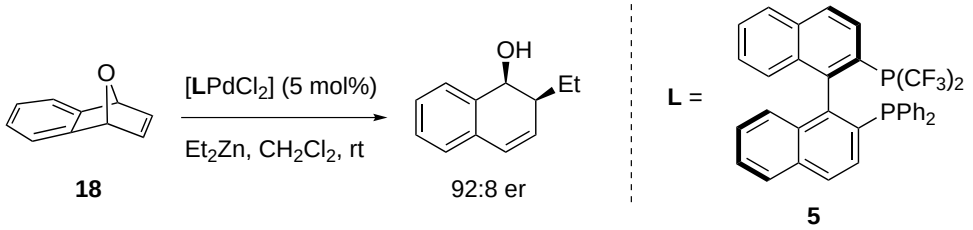

18 92:8 er **5**

Scheme 46: Pd-catalyzed ring opening of 7-oxabenzonorbornadiene **18** using ligand **5**.

Finally, as a proof-of-principle, we decided to synthesize a simple monodentate ligand with a freely rotating biaryl backbone. Biphenyl ligand **20** was thus directly obtained in good yield by lithiation of bromobiphenyl, followed by nucleophilic substitution of phosphane **4** (scheme 47).

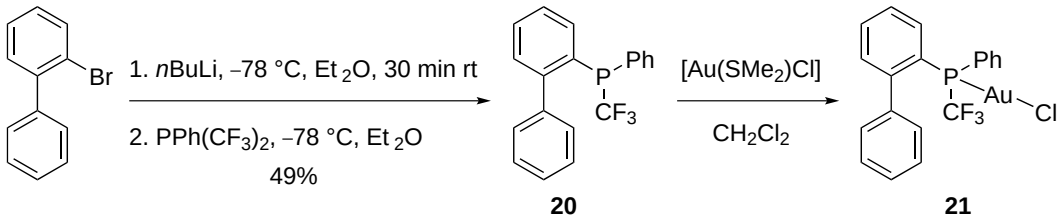

20 **21**

Scheme 47: Biphenyl ligand **20** and its corresponding gold(I) complex **21** prepared in this work.

The corresponding gold(I) complex **21** was prepared (scheme 47), and coordination was ascertained by multinuclear NMR. The exact structure of the complex was however not determined.

2.4 Outlook

Considering the hindered rotational barrier of the binaphthyl backbone, which makes derivatization in the 2,2' positions difficult, perhaps another synthetic approach should be considered. Transition metal-catalyzed coupling of naphthyl derivatives has been shown to occur under various conditions, yielding the corresponding binaphthyl compounds (scheme 48).

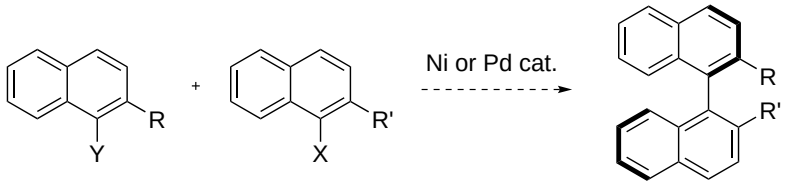

Scheme 48: Transition metal-catalyzed aryl-aryl coupling towards binaphthyl derivatives.

Asymmetric variants, making use of palladium or nickel combined with diverse chiral ligands, have also been reported, with modest to excellent enantioselectivities.[156][157][158][159][160]

However, one must think of functional group tolerance when selecting a method, as P-CF_3 derivatives may decompose under certain reaction conditions. A way to circumvent this would be late stage trifluoromethylation, after the binaphthyl backbone is formed.

Finally, thinking of a simpler binaphthyl system, an electron-poor MOP derivative can be envisioned. As it has been observed that the triflate group in the 2' position of compound **12** undergoes cleavage under reductive conditions (section 2.2.1), the conditions could possibly be adjusted to allow access to primary phosphane **22** as shown in scheme 49.

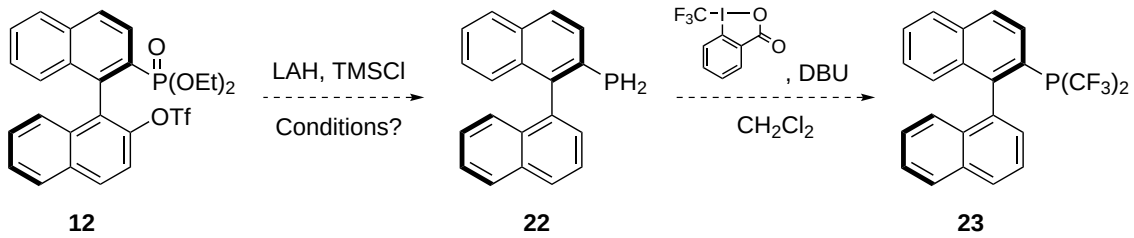

Scheme 49: Possible pathway to a simple bistrifluoromethyl-MOP derivative.

A preparative route to phosphane **22** has been published recently, which could also be used as alternative.[161] It however possesses a major drawback, as it consists of five steps starting from BINOL to access the primary phosphane (versus three with our projected pathway). With the primary phosphane in hand, simple bistrifluoromethylation with reagent **2** would yield the target ligand, which may well prove useful in catalysis, as many MOP congeners. Finally, if ligand **23** is accessible, one can envisage to selectively remove one trifluoromethyl substituent, for example by nucleophilic substitution with phenyllithium, in order to obtain an electron-poor *P*-stereogenic MOP analogue, which might as well prove useful in catalysis.

3 Oxazoline ligands

3.1 Phenyloxazoline ligands

3.1.1 Introduction

Since the simultaneous discovery of phosphane-based phenyloxazoline (PHOX) ligands by Pfaltz,[60] Helmchen,[61] and Williams[62] in 1993, these ligands have found numerous applications in asymmetric catalysis.[162][163] Their modular synthesis allows for easy variation of the phosphane functionality, making them a very attractive ligand to work with. Although *P*-stereogenic PHOX derivatives are known,[164] *P*-trifluoromethyl ligands are strictly limited to bistrifluoromethylphosphanes. Such derivatives have been described in 2012 by Shen *et al.*[119] (figure 17) The synthesis of *P*-perfluoroalkylated analogues of phenyl- and ferrocenyloxazoline derivatives has been shown, as well as successful application in catalysis (for more details see section 1.5.2). Encouraged by these results and being active in this chemistry niche, we set out to synthesize monotrifluoromethyl *P*-stereogenic derivatives of this ligand class.

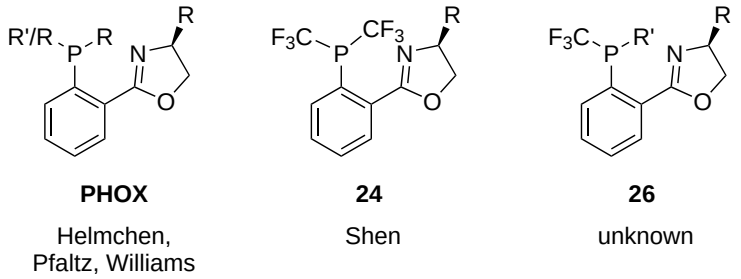

PHOX — Helmchen, Pfaltz, Williams

24 — Shen

26 — unknown

Figure 17: Parent phenyloxazoline PHOX, Shen's bistrifluoromethyl variant **24**, and monotrifluoromethyl analogue **26**.

3.1.2 Synthesis of *P*-trifluoromethyl phenyloxazolines

Following the standard zinc-catalyzed synthesis of bromophenyloxazolines of type **25** developed by Witte and Seeliger in the 70s,[165] a set of ligand precursors **25a–c** with various side chains at the oxazoline were obtained in good yields (scheme 50). Although the conditions did not have to be strictly anhydrous, $ZnCl_2$ was activated by heating under high vacuum. The resulting compounds were purified by column chromatography over silica gel, yielding colorless oils in 52-60% yields. Unreacted 2-bromobenzonitrile could be easily recycled by recrystallization after column chromatography and reused.

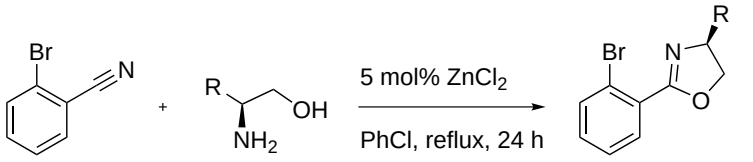

	R:	Yield
25a	iPr	52%
25b	Ph	60%
25c	*t*Bu	60%

Scheme 50: Preparation of bromophenyloxazolines **25a–c** via zinc catalysis.

The question of how to introduce the phosphane with a single trifluoromethyl substituent then arose. As Shen *et al.* have shown that bistrifluoromethyl derivatives **24** can be prepared via the Caffyn method[119] (see section 1.5.1), we thought that this established pathway should be used, and one trifluoromethyl substituent could be subsequently eliminated by using an appropriate nucleophile, such as phenyllithium.

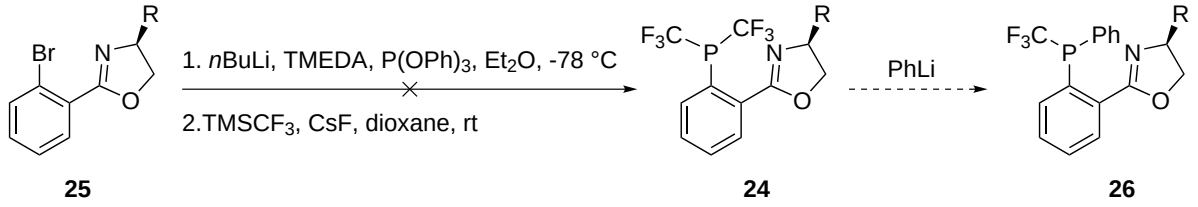

Scheme 51: Attempted synthesis of desired ligand **26** via bistrifluoromethyl oxazoline **24**, following Shen's procedure.[119]

However, when Shen's protocol was employed, the desired product **24** was not obtained, only a mixture of many compounds. Another approach was therefore chosen. As a previous group member had shown that $PPh(CF_3)_2$ can undergo nucleophilic substitution thereby eliminating a CF_3 substituent (see section 1.5.1),[115] it was decided to lithiate the bromoaryloxazoline precursor **25** and quench it with $PPh(CF_3)_2$ (scheme 52).

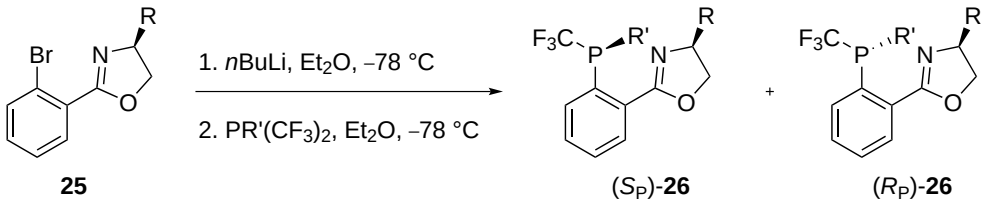

Scheme 52: Synthesis of trifluoromethyl *P*-stereogenic oxazoline ligands **26** using $PR(CF_3)_2$ as electrophile for quenching of the lithiated species.

To our delight, this procedure allowed the obtention of the desired ligands in a one-pot procedure, with yields ranging from 8 to 94% (see table 14). However, the yields did not appear to be reproducible, as the same conditions were used in all cases except entries 3 and 5, and the yields range from 19 to 59% under those constant conditions. There is also a big discrepancy in conversion between entries 3 and 5, although both make use of TMEDA. In entry 3, TMEDA was added before the electrophile, whereas in entry 5, TMEDA was added days after the electrophile. However, with substrate **26b** (entry 5), very little conversion was observed, even after heating for two days at reflux, whereas substrate **26a** converted much faster to the desired product and to a higher degree.

Table 14: Obtained trifluoromethyl *P*-stereogenic phenyloxazoline ligands.

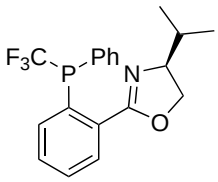

26a

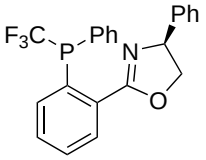

26b

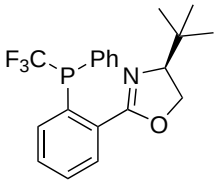

26c

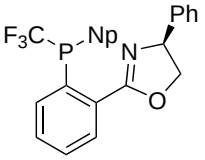

26d

Entry	Compound	R'	R	Yield (%)	dr[a]
1	**26a**	Ph	iPr	n.d.	1:2.0
2	**26a**	Ph	iPr	n.d.	1:1.6
3[b]	**26a**	Ph	iPr	94	1:1.5
4	**26a**	Ph	iPr	59	1:2.0
5[c]	**26b**	Ph	Ph	8	1:1.4
6	**26c**	Ph	*t*Bu	56	1:1.6
7	**26c**	Ph	*t*Bu	48	1:5.7
8	**26d**	Np[d]	Ph	19	1:6.5

[a] The diastereomeric ratios were determined by ^{19}F NMR spectroscopy.
[b] TMEDA (1 eq.) was used as additive.
[c] TMEDA (1 eq.) was added after 3 d since conversion was low, but no major change occurred.
[d] Np = Naphthalen-2-yl.

Concerning diastereoselectivity, the side chain does not appear to play a major role. Throughout entries 1 to 6, the diastereoselectivity is quite similar, although three different side chains with various bulks are present (isopropyl, phenyl and *tert*-butyl). Furthermore, in the case of substrate **26c** (entries 6 and 7), the diastereomeric ratio varied significantly under the same reaction conditions. Finally, the role of the aryl substituent of the electrophile can also be debated. When $PNp(CF_3)_2$ was used (entry 8), the highest diastereoselectivity was observed, although it remains comparable to that observed in entry 7, where $PPh(CF_3)_2$ was used as electrophile. Perhaps a specific matching between side chain and aryl substituent is needed to achieve higher diastereomeric ratios.

3.1.3 X-ray structures of *P*-trifluoromethyl oxazoline ligands

In an attempt to gain more insight into the structure of the new ligands **26a–c**, crystals suitable for analysis by X-ray diffraction were obtained from ligands **26a** and **26d** (figure 18).[10] An interesting feature is the torsion angle between the plane formed by the oxazoline moiety and the phenyl group (C1–C2–C7–N1 plane), which is close to zero in both cases. This is probably due to conjugation of the aromatic ring with the double bond of the oxazoline moiety. There are also no steric repulsions which would legitimate a distortion of the phenyloxazoline plane. It would be of interest to compare this to the parent ligand, however this structure does not

[10] The X-ray structures were determined by Lukas Sigrist.

exist in the Cambridge Structural Database.[11]

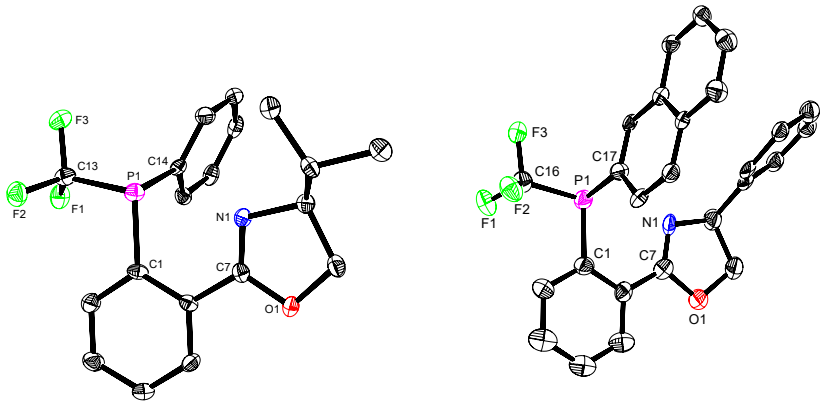

Figure 18: *ORTEP* representation of ligands **26a** (left) and **26d** (right). H atoms are omitted for clarity. Thermal ellipsoids are set to 50% probability.

The angles around the phosphorus atom in compound **26a** are consistent with the postulations of Bent[13] (see section 1.2.1), as they deviate to a large extent from perfect tetrahedral angles. This is due to the presence of the electron-withdrawing trifluoromethyl substituent (see table 15 for relevant data[12]).

Table 15: Selected solid-state angles of compound **26a**.

	C1–P1–C13	C1–P1–C14	C13–P1–C14	C1–C2–C7–N1
Bond angle (°)	100.47	103.42	94.32	-
Torsion angle (°)	-	-	-	2.44

Another noteworthy feature is the orientation of the naphthalenyl substituent in ligand **26d** (see figure 19). It lies on the same side as the phenyl ring from the oxazoline side chain, and it is not excluded that an edge-to-face interaction favors this conformation. On the contrary, this is not the case in ligand **26a**, as the phenyl substituent lies on the opposite side of the isopropyl side chain, which further corroborates the idea of stabilizing C–H$\cdots\pi$ interaction[166] in ligand **26d**.

[11] Search performed on 07.09.2016.

[12] As the X-ray data of compound **26d** is not sufficient enough, this structure can only be used qualitatively, that is why no numerical data is given.

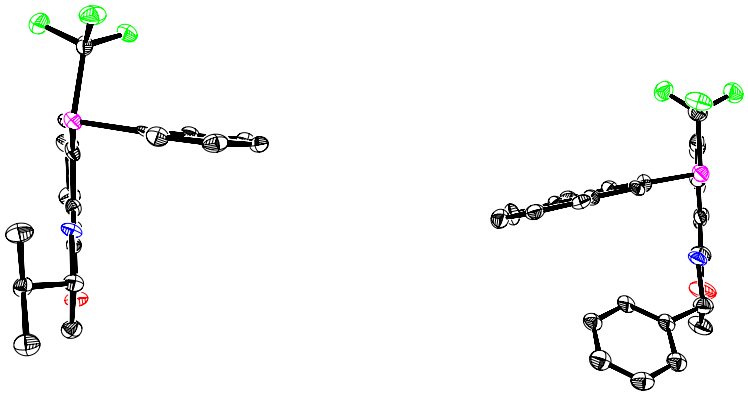

Figure 19: Plane view of X-ray structures of ligands **26a** (left) and **26d** (right).

3.1.4 Palladium(II) complex of ligand 26a

In order to investigate the coordination ability of compound **26a**, it was reacted with the Pd(II) precursor [Pd(COD)Cl_2] as shown in scheme 53.

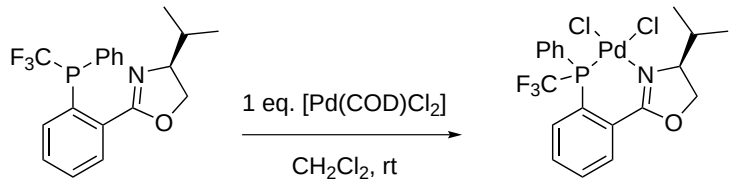

26a **27**

Scheme 53: Coordination of ligand **26a** to a Pd(II) center.

NMR analysis of the resulting bright yellow solid showed two new sets of signals, due to the two diastereomers, indeed corresponding to the *P,N* coordinated compound **27**. Table 16 summarizes the ^{19}F and ^{31}P NMR data of both afforded products and the free ligand. Coordination of the phosphorus is clear due to the significant high frequency shift of the ^{31}P NMR signals by 30–40 ppm compared to the free ligand. The $J_{P\text{-}F}$ and $J_{F\text{-}P}$ coupling constants are also slightly larger, indicative of coordination.

Table 16: Selected NMR data of complexes **27** and free ligands **26a**.

	Complex **27** (min)	Complex **27** (maj)	Ligand **26a** (min)	Ligand **26a** (maj)
^{31}P shifts (ppm)	35.0	25.0	–4.4	–5.0
Multiplicity, $J_{P\text{-}F}$ (Hz)	q, 76.2	q, 78.6	q, 71.8	q, 71.8
^{19}F shifts (ppm)	–52.1	–56.2	–55.0	–55.1
Multiplicity, $J_{F\text{-}P}$ (Hz)	d, 79.0	d, 79.0	d, 71.5	d, 71.5

As no suitable crystals were obtained for analysis by X-ray diffraction, the question remains how the geometry of the ligand is modified upon coordination. A slight distortion of the phenyloxazoline plane probably occurs in order to accommodate the square planar geometry of the metal, as it has been observed in solid state structures of similar complexes.[13]

3.1.5 Attempted isolation of single diastereomers

Since the synthesis of the ligands is not diastereoselective and modification of the conditions did not influence this (section 3.1.2), the next step was to find a way to separate the diastereomers, in order to be able to test the diastereopure ligands in catalysis.

In a first instance, chromatographic techniques were tested for the separation of the diastereomers. TLC runs with binary mixtures did not show any separation, and only the ternary eluent hexane:CH_2Cl_2:Et_2O 20:1:1 showed very limited resolution. Preparative TLC was then attempted with these conditions with ligand **26c**, but no separation was achieved, even after a few runs. Normal column chromatography on silica gel also did not result in any modification of diastereomeric ratio. Separation of the diastereomers by analytical HPLC was tested on different columns (Chiralcel AD-H, OD-H, OJ), to no avail.

In a second instance, crystallization was attempted, in the hopes that only one diastereomer would crystallize. Unfortunately, this was unsuccessful. The next attempt consisted of making a coordination compound, and then either crystallizing one diastereomer or, if the complex would be stable enough, separate them chromatographically. The dichlorido Pd(II) complex was thus formed, yielding nice yellow crystals. Unfortunately, the diastereomers could also not be separated as coordination compounds.

In a final endeavour, a different type of experiment was devised. Since the two species are diastereomers, they have different physical thus thermodynamic properties. This means that one of the diastereomers may be more stable than the other, and could possibly be accessed by epimerizing the phosphorus center. Ligand **26c** was therefore dissolved in two different high boiling solvents, diglyme and decane, in a Young NMR tube sealed under argon. The samples were then heated in an oil bath, and the reaction was monitored by ^{19}F NMR spectroscopy. In both cases, no change in diastereomeric ratio was observed after 3.5 days at 160 °C. Further heating at 200 °C for 4 days did not show any significant change, although some minor decomposition was observable (~9% in decane, ~5% in diglyme). Heating at maximum temperature of the stirring plate (230-240 °C) only showed slightly more decomposition. It was thus concluded that the ligands are kinetically inert, and cannot be epimerized in this manner. The stability of these compounds is actually a remarkable feature, as it is contrary to non fluorinated *P*-stereogenic analogues which are quite unstable and readily undergo epimerization at temperatures higher than 80 °C.[164] This may well be the window of opportunity for the potential of these ligands to be used and recognized.

Since the diastereomers were found to be inert, we envisaged the possiblity of rendering them labile, by lowering the energy barrier for thermal racemization. A recent publication has shown that pyramidal inversion of trivalent phosphanes can be catalyzed by single electron oxidation.[167] A series of *P*-stereogenic arylmethylphenylphosphanes underwent rapid racemization at room

[13] WebCSD search performed on 07.09.2016.

temperature when exposed to catalytic amounts of a single electron oxidant. The transient phosphoniumyl radical cation is formed under these conditions, and calculations indicate that the inversion barrier for such species is around 5 kcal/mol. Ligand **26c** was thus dissolved in acetonitrile, and ferrocenium hexafluorophosphate (0.25 eq) was added. The reaction mixture was stirred at room temperature overnight, and equilibration was monitored by ^{19}F NMR spectroscopy.

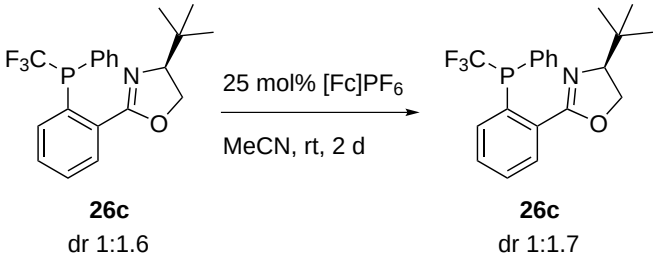

26c
dr 1:1.6

26c
dr 1:1.7

Scheme 54: Attempted epimerization of **26c** via single electron oxidation.

After stirring overnight, some signals due to decomposition products could be detected, mainly around –70 ppm, and the diastereomeric ratio had only slightly changed (1:1.7). The solution was further stirred for 2 days, and no further change in diastereomeric ratio was observed, only more decomposition was seen. This pathway was thus also abandoned, and a change in the ligand backbone was envisioned, as shown in the next sections.

3.1.6 Variation of the side chain architecture

After the disappointment of the unsuccessful separation of the ligand diastereoisomers, it was rationalized that bringing modifications to the ligand structure could possibly allow the obtention of separable diastereoisomers. For example, the introduction of a group with a different size and polarity on the ligand could influence the behavior of the diastereoisomeric mixture upon separation. Aiming towards this goal, the synthesis of a ligand containing an extra ring fused to the oxazoline moiety was envisaged, as shown in scheme 55.

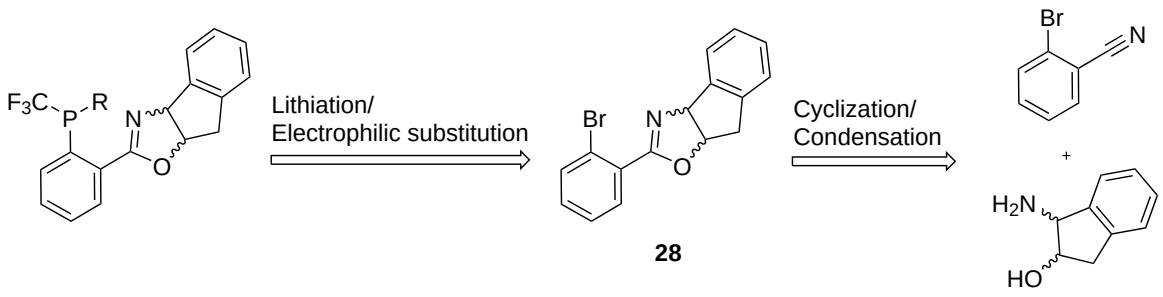

Scheme 55: Retrosynthetic pathway to an oxazoline-based trifluoromethyl ligand with a fused indane side chain.

The corresponding parent ligand has been reported in 1998 by Helmchen *et al.*.[168] They demonstrated its use in a Pd-catalyzed allylic alkylation, obtaining at best 82% *ee* with 1,3-dimethyl acetate as substrate.

As both pure enantiomers of *cis*-1-amino-2-indanol are commercially available, the two corresponding bromophenyloxazolines **28** were prepared using the standard zinc-catalyzed reaction of bromobenzonitrile with the amino alcohol in refluxing chlorobenzene. The two compounds were isolated in 35 and 40% yield respectively and the analytical data corresponds to literature.[169]

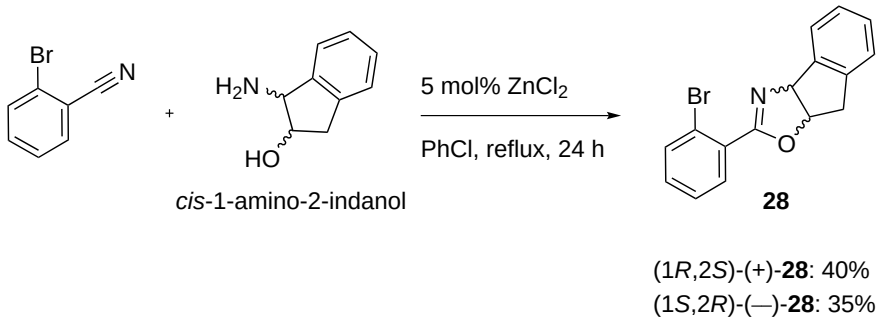

Scheme 56: Synthesis of bromophenyloxazolines with a fused indane side chain.

The next step, namely lithiation and subsequent electrophilic substitution with $PPh(CF_3)_2$, was however not successful. Many unidentifiable side products were formed, and no significant amounts of desired compound were observed. The further pursuit of phenyloxazoline ligands was thus stopped.

3.2 Ferrocenyloxazoline ligands

Thinking about the further development of oxazoline-based ligands, it was rationalized that replacement of the phenyl ring by a ferrocene backbone could possibly lead to separable diastereomers, as it has been shown that certain phosphanylferrocene diastereomers can be separated by column chromatography.[112][117] Ferrocene derivatives are furthermore very successful ligands for homogeneous catalysis (see section 1.4.2) and are being actively researched by various groups, although *P*-trifluoromethyl derivatives are very rare and usually limited to bistrifluoromethyl variants.[119][121] The investigation of ferrocenyloxazolines was thus instigated and is the topic of the second half of this chapter.

3.2.1 Introduction

Ferrocenyloxazoline ligands are without doubt an important class of ligands for asymmetric homogeneous catalysis. Many synthetic methods have been reported as well as a plethora of catalytic applications, which have been summarized in a comprehensive review.[67] Electron-poor derivatives remain rare, and usually only consist of phosphanes bearing trifluoromethyl-substituted aryl groups. Some examples of bistrifluoromethyl oxazolines exist, such as Shen's 1,2 ferrocenyl ligand **29**[119] or You's 1,1' ferrocenyl ligand **30**[121] (figure 20), which have both shown excellent enantioselectivities in Pd-catalyzed asymmetric allylic alkylations (see section 1.5.2).

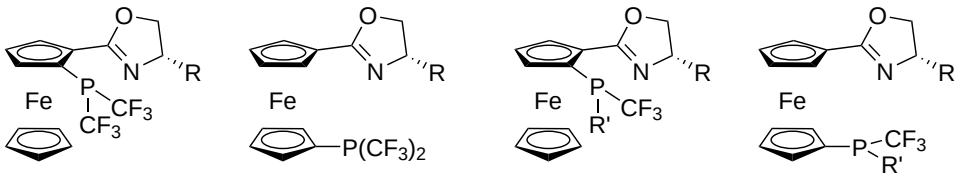

Figure 20: Shen's 1,2 ferrocenyl ligand **29**[119], You's 1,1' variant **30**[121] and the monotrifluoromethyl analogues.

3.2.2 Synthesis of 1,2-ferrocenyloxazolines

Following a standard procedure, the 1,2-ferrocenyloxazoline precursors were synthesized starting from ferrocene, which was first deprotonated using Schlosser's base,[170] and subsequently carboxylated using carbon dioxide, yielding carboxyferrocene **31**.[14] The oxazoline ring was then formed in a one-pot procedure consisting of acylation of the carboxylic acid, condensation to the amide, and finally cyclization to the heterocycle, forming ferrocenyloxazolines **32a–c**.

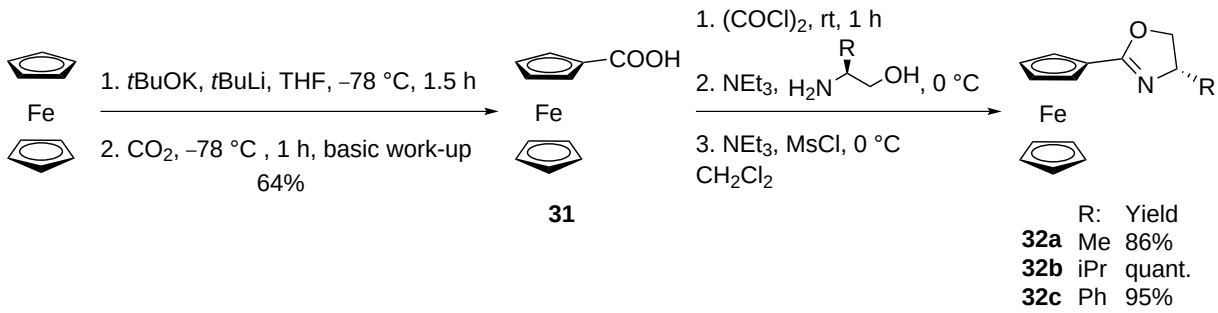

Scheme 57: Preparation of ferrocenyloxazoline ligand precursors **32a–c** via a one-pot procedure from carboxyferrocene **31**.

The desired products were obtained in high yields, making use of an efficient one-pot procedure adapted from literature[171] to transform the carboxylic acid to the oxazoline. The obtained ferrocenyloxazolines **32** were then used as substrates for electrophilic substitution with $PPh(CF_3)_2$, using the conditions previously developed in our group for introduction of a $P-CF_3$ moiety on the Josiphos backbone.[115]

[14] Higher yields were obtained when gaseous CO_2 was used.

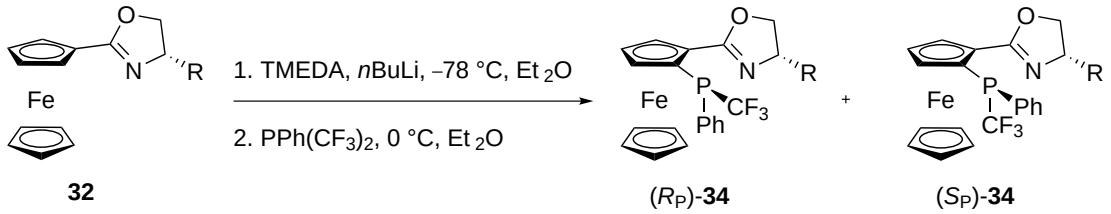

	R:	Yield
34a	Me	26% (R_P), 47% (S_P)
34b	iPr	0%
34c	Ph	0%

Scheme 58: Synthesis of *P*-trifluoromethyl ferrocenyloxazolines ligands **34a–c** from oxazoline precursors **32a–c**.

In the case of the alaninol derivative **34a**, the ligands were obtained in reasonable yields, and the diastereomers could be simply separated by flash column chromatography on silica gel. However, when another oxazoline side chain was present (precursors **32b** and **32c**), no conversion to the desired products was observed. Variation of the reaction conditions did not show any improvement in conversion (see Appendix D: Lithiation screening table for details). Synthesis of compounds **34b** and **34c** was then left aside.

Due to the difficulty of this reaction, it was attempted to gain more insight by investigating various reactions parameters. During the screening of the conditions, some experiments were performed using other electrophiles instead of $PPh(CF_3)_2$ (details of the screening can be found in Appendix D: Lithiation screening table). However, major difficulties also arose, irrespective of the electrophile, and no conversion to product could be observed in most attempts. Although this particular step has been reported by various groups, yields are not that high and not reproducible. The diastereoselectivity of the lithiation has also been investigated,[76][77] and it has been hypothesized that the size of the oxazoline side chain plays an important role in diastereoselectivity. Considering that our system possesses a methyl side chain, this can explain why the diastereoselectivity of lithiation was suboptimal in the synthesis of the parent ligand **33**. If one pushes this line of thought further, we could ask ourselves if the side chain is possibly hindering the lithiation step. This would allow an explanation for the failed syntheses of ferrocenyloxazolines **34b** and **34c** bearing larger side chains. It nevertheless does not explain the change in color from light yellow or orange (depending on the concentration) to red upon addition of the butyllithium solution, which would otherwise be visual proof of successful lithiation. However, even a synthesis attempt with a ferrocenyloxazoline bearing no side chain did not yield any desired product. It can thus be concluded that the side chain bears no role in the success (or failure) of lithiation of the ferrocenyl backbone.

It was then hypothesized that these lithiated species may be quite unstable and either undergo rapid quenching by traces of water present in the reaction vessel,[15] or simply decomposition due to instability in solution. However, even rapid quenching of the lithiated species with various electrophiles or use of different solvents or additives to supposedly stabilize the lithiated species did not allow conversion to product in a reasonable manner. PMDTA,[16] which has been shown to stabilize the lithiated cycloheptatrienyl-cyclopentadienyl titanium sandwich

[15] Even working under strict anhydrous conditions does not exclude the presence of a few ppms of water which can readily react with such species.

[16] PMDTA = *N,N,N′,N″,N″*-Pentamethyldiethylenetriamine.

compound (troticene) before quenching with the desired chlorophosphane,[172] did not allow clean conversion to product in our case.[17]

As a final attempt to obtain proof that lithiation is indeed taking place, a ^{7}Li NMR experiment was setup.[18] Ferrocenyloxazoline **32a**, TMEDA, and *n*BuLi were dissolved in dry THF (0.2 M), and a ^{7}Li NMR spectrum was measured at –40 °C. However, this experiment was inconclusive, as only one minor signal was visible, and it could not be determined to what it corresponds. Warming to room temperature did not increase the signal-to-noise ratio, and no additional signals could be uncovered. Since sufficient amounts of ligand **34a** were obtained and no reasonable solution was found for the ligand synthesis, no further experiments in this direction were performed at this point.

Ligand **34a** could be fully characterized, and one of the diastereomers as well as the 1,5 diastereomer of parent ligand **33** yielded suitable crystals for X-ray diffraction.[19] This allowed determination of the absolute configuration at phosphorus of ligand **34a**.

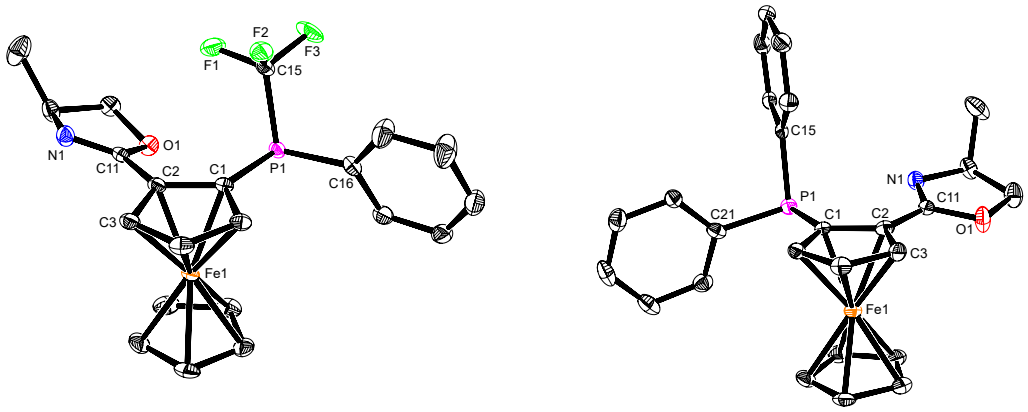

Figure 21: *ORTEP* representation of ligands (R_P,S_{Fc})-**34a** and (R_{Fc})-**33**. H atoms are omitted for clarity. Thermal ellipsoids are set to 50% probability.

Although only the crystal structure of the (R_{Fc}) isomer of parent ligand **33** is available, some comparisons with the trifluoromethyl analogue (R_P,S_{Fc})-**34a** can be made. The bond angles around the phosphorus atom are given in table 17 (entries 1–3). As in the case of the phenyloxazolines (section 3.1.3), the average bond angle around the phosphorus atom is smaller when a trifluoromethyl substituent is present (99.91° for **34a** vs. 100.45° for **33**), in accordance with Bent's rule (section 1.2.1).[13] The torsion of the oxazoline with respect to the phosphane is higher in **34a** (entry 4).

[17] Minor signals around –21 ppm were observed in ^{31}P NMR in the crude reaction mixture, however no desired product could be isolated after column chromatography on silica gel.

[18] This experiment was carried out by Franziska Elterlein in the context of her Master thesis.[173] NMR assistance was provided by Alex Lauber.

[19] The X-ray structures were determined by Lukas Sigrist.

Table 17: Selected solid state angles of compounds (R_P,S_{Fc})-**34a** and (R_{Fc})-**33**.

Entry	Angle (°)	Atoms	(R_P,S_{Fc})-**34a**	(R_{Fc})-**33**
1	Bond	C1–P1–C16/C21	101.66	99.44
2	Bond	C1–P1–C15	97.04	100.59
3	Bond	C15–P1–C16/C21	101.02	101.35
4	Torsion	P1–C1–C2–O1/N1	21.42	12.00
5	Torsion	C1–C2–C11–N1	27.00	10.80
6	Torsion	C3–C2–C11–O1	25.38	10.97

The oxazoline moiety is also much more distorted with respect to the cyclopentadienyl plane in the case of **34a** compared to **33** (entries 5 and 6). This is probably due to the orientation of the oxazoline. It is inverted in the case of the trifluoromethyl ligand **34a** with respect to a standard orientation, as the nitrogen is pointing away from the phosphorus. This orientation allows the oxazoline side chain to point upwards, in the same plane as the trifluoromethyl substituent, away from the ferrocene backbone.

3.2.3 Coordination compounds of ligand 34a

With ligand **34a** in hand, its complexation with different metals was investigated, in order to gain some insight on its coordination behavior. Two d^8 metals with suitable labile ligands were selected.

First, the coordination to Pd(II) was investigated. The ligand reacted cleanly at room temperature with 1 eq. of [Pd(COD)Cl_2] in CH_2Cl_2. Coordination was clearly visible by NMR spectroscopy. The ^{31}P signals were shifted to higher frequencies, and the $J_{P\text{-}F}$ and $J_{F\text{-}P}$ coupling constants were larger than those of the free ligands. The complexes however did not crystallize, so no insight on their solid state structure could be gained.

Table 18: Selected NMR data of complex **35** and free ligand **34a**.

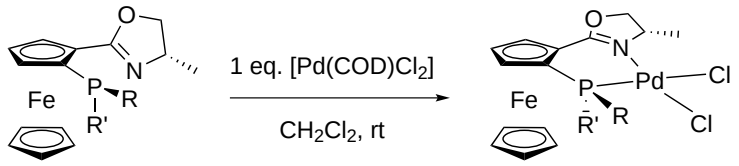

34a **35**

	R:	R':
(R_P)-**35**	CF_3	Ph
(S_P)-**35**	Ph	CF_3

	(R_P)-**35**	(R_P)-**34a**	(S_P)-**35**	(S_P)-**34a**
^{31}P shifts (ppm)	22.7	–11.0	25.7	–10.5
Multiplicity, $J_{P\text{-}F}$ (Hz)	q, 77.4	q, 65.4	q, 75.0	q, 69.0
^{19}F shifts (ppm)	–54.5	–56.3	–51.3	–55.2
Multiplicity, $J_{F\text{-}P}$ (Hz)	d, 75.2	d, 64.9	d, 75.0	d, 67.7

In an attempt to obtain a complex that would possibly crystallize in a suitable fashion for X-ray analysis, a Pt(II) complex was also prepared. The chosen precursor was a *cis*/*trans* mixture of $[Pt(SMe_2)_2Cl_2]$. Ligand **34a** was stirred with the Pt(II) precursor in CH_2Cl_2 at room temperature. (R_P)-**34a** reacted cleanly, yielding a brown solid after evaporation of the volatiles. The NMR signals are reported in table 19, with comparison to Pd(II) complex (R_P)-**35** and free ligand (R_P)-**34a**. Complex **36** however did not crystallize in a suitable fashion for X-ray analysis.

Table 19: Selected NMR data of complex (R_P)-**36** compared to complex (R_P)-**35** and free ligand (R_P)-**34a**.

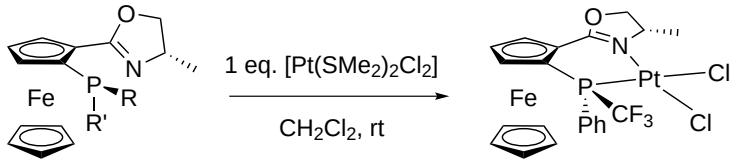

34a (R_P)-**36**

	(R_P)-**36**	(R_P)-**35**	(R_P)-**34a**
^{31}P shifts (ppm)	0.3	22.7	–11.0
Multiplicity, $J_{P\text{-}F}$ (Hz)	q, 77.8	q, 77.4	q, 65.4
^{19}F shifts (ppm)	–56.6	–54.5	–56.3
Multiplicity, $J_{F\text{-}P}$ (Hz)	d, 77.7	d, 75.2	d, 64.9
$J_{F\text{-}Pt}$ (Hz)	25.6	-	-

3.2.4 Allylic alkylation[20]

With sufficient amounts of ligands **34a** in hand and preliminary information on their coordination behavior, we moved towards the investigation of their catalytic applications. The first catalysis selected was the palladium-catalyzed asymmetric allylic alkylation of a monosubstituted allyl substrate.

The procedure Shen *et al.* used with their bistrifluoromethyl ligand **29** was applied.[119] The reactions were monitored by TLC until the starting materials had been consumed. All ligands showed high activity, and full conversion was observed in less than 4 hours. The (R_P) and (S_P) ligand diastereomers behaved similarly, the absolute configuration of the phosphorus atom influencing neither the regio- nor the enantioselectivity in a significant way.

Table 20: Palladium-catalyzed allylic alkylation of cinnamyl acetate.[174]

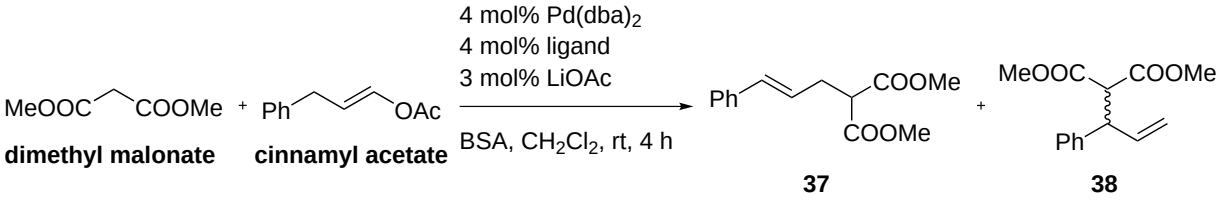

dimethyl malonate **cinnamyl acetate** **37** **38**

Entry	Ligand	Conversion (%)[a]	Ratio **37**:**38**[a]	er[b] (S:R)	(*ee* (%))
1	**33**	>99	89:11	74:26	(*48*)
2	(R_P)-**34a**	>99	63:37	81:19	(*62*)
3	(S_P)-**34a**	>99	63:37	79:21	(*58*)
4[119]	**29**	-	42:58	93.5:6.5[c]	(*87*)

[a] Determined by ^{1}H NMR spectroscopy.
[b] Determined by analytical HPLC.
[c] er values were derived mathematically from the *ee*.

We were encouraged when we observed that our trifluoromethyl ligands **34a** both showed higher enantioselectivities than the parent ligand **33**. It is also interesting to note that the *P*-stereogenic ligands **34a** showed a higher preference for the (S) enantiomer of the branched product compared to the parent ligand **33**, which could possibly be a direct consequence of the reduced steric bulk at the phosphorus, favoring coordination of the substrate with the phenyl residue pointing away. This effect is even more pronounced in the bistrifluoromethyl case (entry 4), which corroborates this hypothesis.

The reduced steric bulk at the phosphane could also give a possible explanation why the parent ligand has a higher preference for the linear compound compared to the *P*-trifluoromethyl derivatives. This trend is also followed when comparing to Shen's bistrifluoromethyl ligand **29**, as it shows an even more pronounced preference for the branched product (entry 4). It also exhibits the highest enantioselectivity, but this effect could be due to the larger steric bulk at the oxazoline side chain (iPr vs. Me),

[20] Allylic alkylation experiments were carried out by Marius Lutz during his semester project.[174]

which is better suited in exerting enantioinduction. To assess the electronic influence of the trifluoromethyl groups, a comparison with alkyl substituents is surely necessary in the future.

With these first promising results, we decided to further test ligands **34a** in catalysis. The next transformation chosen was the hydrosilylation of alkenes and subsequent transformation to the corresponding alcohols.

3.2.5 Hydrosilylation

The conversion of olefins to alcohols via hydrosilylation with trichlorosilane is a powerful tool in organic synthesis. It was pioneered by Tamao and Kumada[175] and Fleming,[176] who developed the stereospecific oxidation of trisubstituted silyl molecules. The retention of configuration at the carbon atom makes this synthetic method towards alcohols very valuable.[177]

As ferrocenylpyrazole ligands of type **40** have been shown to be very effective in the hydrosilylation of norbornene and styrene,[178] we thought it would be interesting to test our ferrocenyloxazoline ligands **34a** in such transformations to have a direct comparison of *P*,*N* ligands. Towards this end, three trifluoromethyl ligands were chosen (figure 22): ferrocenyloxazolines **34a** and an electron-poor bistrifluoromethyl ferrocenylpyrazole **40b** previously prepared in our group.

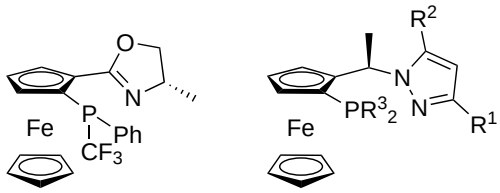

(R_P)/(S_P)-**34a** **40**

	R^1	R^2	R^3
40a	3,5-$(CF_3)_2$Ph	H	Ph
40b	Mes	H	CF_3
40c	Me	Me	Ph
40d	Mes	H	Ph

Figure 22: Ligands used for the hydrosilylation experiments.

In a first instance, the reaction of norbornene with trichlorosilane was studied. After oxidative work-up, *exo*-norborneol **39a** and **39b** were obtained. The precatalyst was prepared *in situ* by first mixing all components except trichlorosilane for 30 min (the mixture turning slightly orange). Trichlorosilane was then added, and after complete conversion, the oxidative work-up procedure was carried out (see experimental section 6.3.3 for details).

Table 21: Hydrosilylation of norbornene.

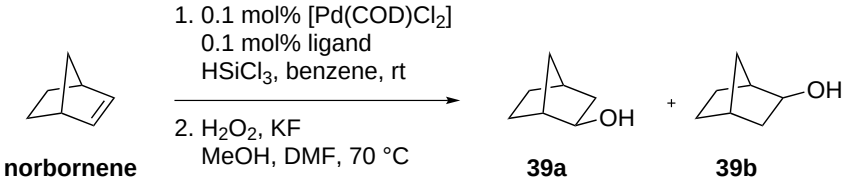

norbornene **39a** **39b**

Entry	Ligand	Conversion (%)	Yield (%)	er[a]	(*ee*[b] (%))
1[178]	**40a**	-	59	99.75:0.25[c]	(>*99.5*)
2	**40b**	>99	83	70:30	(*40*)
3	(R_P)-**34a**	>99	19	46:54	(*8*)
4	(S_P)-**34a**	>99	27	49:51	(*rac*)
5	**40c**	>99	52	50:50	(*rac*)
6[178]	**40d**	-	56	95.5:4.5[c]	(*91*)

[a] Determined by capillary GC on a Supelco β-dex 120 chiral column.
[b] Enantiomeric excesses below 5% are considered racemic.
[c] er values were derived mathematically from the *ee*.

The results obtained confirm what had already been previously observed,[178] namely that the electronic nature at the phosphorus has an important effect on the enantioselective outcome of the reaction. It had been observed that a ligand containing phenyl substituents bearing two trifluoromethyl groups in the *meta* positions at the phosphorus (**40a**) allow nearly perfect enantioselection (entry 1). The ferrocenylpyrazole ligand **40b** bearing a bistrifluoromethylphosphane led to higher enantioselectivity (entry 2) than the ferrocenyloxazolines which, disappointingly, yielded neglectable enantioinduction (entries 3 and 4), although they performed marginally better than the electron-rich pyrazole **40c** (entry 5). As the steric bulk on the side chain is also a crucial factor for enantioinduction (*cf.* entries 5 and 6), this may explain the behavior of the ferrocenyloxazolines. Experimenting with ligands with larger side chain is definitely necessary. The absolute configuration at phosphorus also seems to have a minor influence on stereoselection (entries 3 and 4).

Moving towards a non cyclic aromatic alkene, styrene was used as second hydrosilylation substrate. The catalyst precursor was also formed *in situ* by first stirring the ligand and catalyst precursor [Pd(COD)Cl_2] together for approximately 1 h. Styrene and trichlorosilane were subsequently added, followed by oxidative work-up after complete conversion.[21]

[21] No conversion was detected by GC-MS after 1 h, so stirring was continued for 2 d over the week-end.

Table 22: Hydrosilylation of styrene.

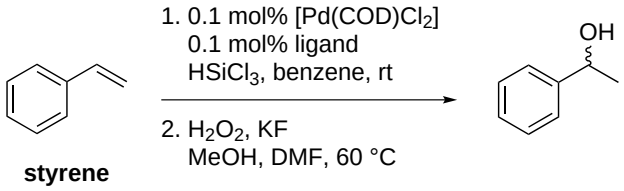

Entry	Ligand	Conversion (%)	Yield (%)	er[a] (*R*:*S*)	(*ee*[b] (%))
1	**40c**	>99	44	49:51	(*rac*)
2	**40b**	>99	4	51:49	(*rac*)
3	(R_P)-**34a**	>99	3	38:62	(*24*)
4	(S_P)-**34a**	>99	47	33:67	(*34*)
5[179]	**40d**	-	63	32:68[c]	(*63*)
6[179]	**40a**	-	40	42.5:57.5[c]	(*15*)

[a] Determined by analytical HPLC on a Chiracel OD-H column.
[b] Enantiomeric excesses below 5% are considered racemic.
[c] er values were derived mathematically from the *ee*.

In this case, the steric bulk of the ligand side chain was shown to have a much lesser influence on enantioselectivity. Ferrocenylpyrazole **40c** yielded racemic product (entry 1), whereas the corresponding ligand with mesityl side chain **40d** showed some enantioinduction (entry 5). Ligand **40a** gave only 15% *ee* (entry 6), contrary to the case of norbornene, where the influence of the bulky side chain and electron-withdrawing substituents was much larger. The electron-poor analogue **40b** did not show any stereoselectivity at all in this case (entry 2). However, the *P*-stereogenic trifluoromethyl derivatives **34a** gave promising results in this case with enantioselectivities up to 34% (entry 4) although, once again, the absolute configuration at phosphorus played only a minor role (*cf.* entries 3 and 4).

3.2.6 Hydrogenation

Moving towards a different type of catalysis, we also wanted to test our ligands in transition-metal-catalyzed hydrogenation reactions. We first wanted to try a standard substrate, namely dimethylitaconate (see scheme 59). Using conditions previously applied in the group,[117] hydrogenations were run with ligands **33** and **34a**. As no conversion was observed under 1 bar H_2, the catalyses were rerun under identical conditions in an autoclave under 10 bar H_2 pressure. This also did not lead to any conversion, so the reactions were discarded and another substrate class was chosen, in which ferrocenyloxazolines have been shown to be active.

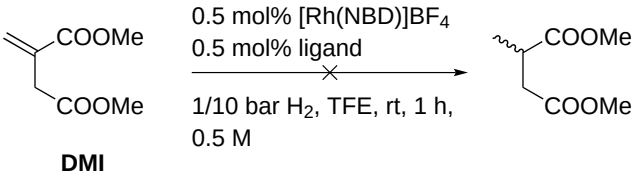

Scheme 59: Hydrogenation of dimethylitaconate (DMI).

Ferrocenyloxazolines can catalyze the hydrogenation of quinoline derivatives with high enantioselectivities,[180] so 2-methylquinoline was chosen for further hydrogenation experiments (see table 23). The reactions were run in autoclaves under 100 bar H_2 pressure, at 0.2 M concentration. Conversion was satisfactory in 12-16 h, in all cases >95%.

Table 23: Hydrogenation of 2-methylquinoline.

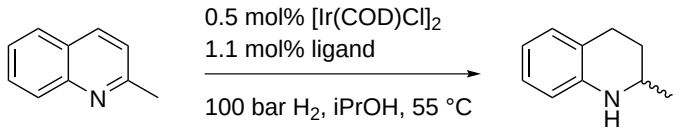

2-methylquinoline **42**

Entry	Ligand	Conversion (%)	Yield (%)	er[a]	(*ee* (%))
1	(R_P)-**34a**	>99	n.d.[b]	54:46	(*8*)
2	(S_P)-**34a**	>95	n.d.	50:50	(*rac*)
3	**33**	>99	n.d.	50:50	(*rac*)
4[180][c]	**41**	>95	-	-	(*51*)

[a] Determined by analytical HPLC.
[b] n.d. = not determined.
[c] The reaction was run under ~40 bar H_2 pressure at rt.[180]

However, ligands **33** and (S_P)-**34a** did not induce any enantioselectivity at all (entries 2 and 3), and ligand (R_P)-**34a** provided only very little enantiodiscrimination (entry 1). As the corresponding iridium complexes could not be isolated, it remains unclear if coordination of the ferrocenyl ligand actually takes place and what the structure of the precatalyst is. Comparing to the parent ligand **41** with a *tert*-butyl side chain Zhou *et al.* used (entry 4),[180] 51% enantioselectivity is obtained under 40 bar hydrogen pressure. The enantioinduction can once again probably be attributed to the larger steric bulk of the oxazoline side chain (*t*Bu vs. Me).

As *P*-trifluoromethyl ferrocenyl ligands have shown excellent activities and enantioselectivities in the hydrogenation of the challenging substrates dihydroisoquinolines (DHIQs),[117] we finally moved to this type of quinoline. The screening previously performed by R. Schwenk in our group showed that 1-phenyl-3,4-dihydroisoquinolinium chloride gave the best enantioselectivities,[117] so it was chosen as substrate. The catalysis was run using ligands **34a** and **33** in an autoclave under 40 bar H_2 in toluene at 0.5 M concentration (scheme 60).[22] Under these conditions, no conversion was observed after 24 h reaction time. Due to time constraints, the reproduction of the catalyses at higher hydrogen pressure was not possible, so at this point catalytic screening was stopped.

[22] Initially, the same conditions as described by R. Schwenk were planned (*i.e.* 100 bar H_2, 2-propanol as solvent),[117] unfortunately the substrate was inadvertently switched with another reaction when setting up different catalyses in parallel.

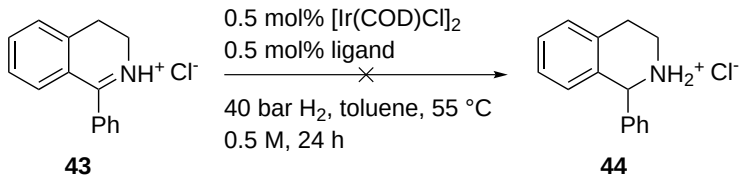

43 **44**

Scheme 60: Hydrogenation of DHIQ **43**.

After these catalytic trials yielding modest results and the failure to access 1,2-ferrocenyloxazolines with side chains other than methyl, we thought that variation of the ferrocene substitution pattern would be necessary. We rationalized that if steric hindrance is an issue, this could be circumvented by having a 1,1' substitution pattern at the ferrocene backbone, which would allow the introduction of oxazolines with bulkier side chains. We then moved to the synthesis of such molecules, which will be the topic of the next section.

3.2.7 Synthesis of 1,1'-ferrocenyloxazolines[23]

1,1'-Ferrocenyloxazolines have been investigated as bidentate chelating ligands by various groups, and have shown good enantioselectivities in selected asymmetric reactions (see section 1.5.2). In contrary to 1,2 disubstituted ferrocenes which possess planar chirality, 1,1' derivatives do not. However, such derivatives form two distinct rotameric forms upon coordination, due to the rotation of the Cp rings. The chirality triggered is considered to be axial.[181]

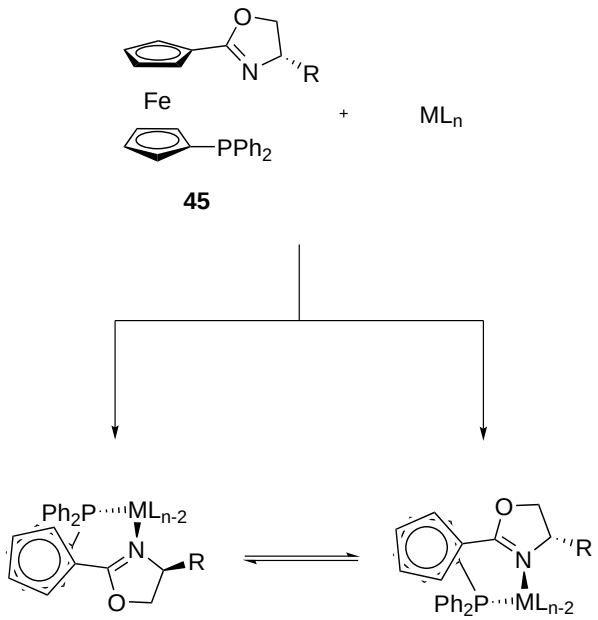

45

Scheme 61: Ligand **45** and its two rotameric forms upon coordination.[181]

With the goal of synthesizing *P*-trifluoromethyl derivatives as well as the parent ligand **45**, the synthetic pathway as shown in scheme 62, analogous to that for the 1,2-ferrocenyloxazolines, was projected.

[23] Most of the experimental work from this project was carried out by Franziska Elterlein during her Master thesis.[173]

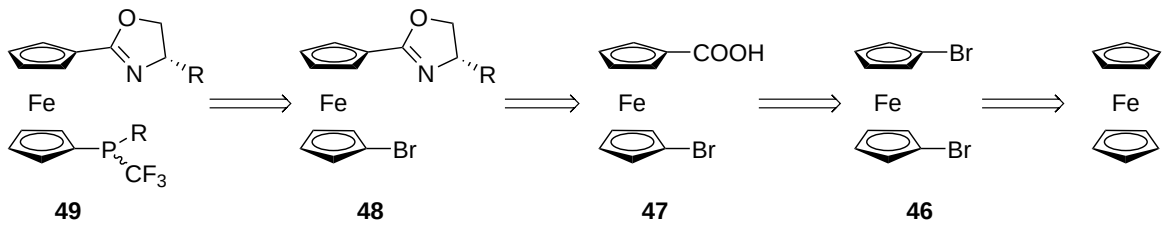

Scheme 62: Retrosynthetic pathway to 1,1'-ferrocenyloxazoline ligands.

1,1'-Dibromoferrocene **46** is accessible from ferrocene, and it can undergo selective carboxylation in one position upon treatment with one equivalent of lithium base and subsequent quenching with carbon dioxide to yield **47**. The carboxylic acid can then be transformed to the oxazoline **48**. Finally, lithiation followed by quenching with a phosphorus-based electrophile would yield the desired ligands **49**.

Following this pathway, the ligand precursors **48a–c** were prepared in modest to excellent yields. Dibromination of ferrocene was shown to work best using 1,2-dibromotetrachloroethane as bromine source, and two purifications by flash column chromatography were necessary to obtain product of sufficient purity.[24] Subsequent carboxylation was achieved by selective lithiation in one position using 1 eq. of *n*BuLi, followed by quenching with carbon dioxide. We found that it was critical that the lithiation be run at –25 °C, as other temperatures yielded less or absolutely no product. The precipitation of 1-bromo-1'-lithioferrocene was usually visible and allowed visual determination of successful lithiation (generally achieved in under 20 min). Finally, the formation of the oxazoline moiety was carried out using the same conditions applied for the singly substituted ferrocenes as described in section 3.2.2.

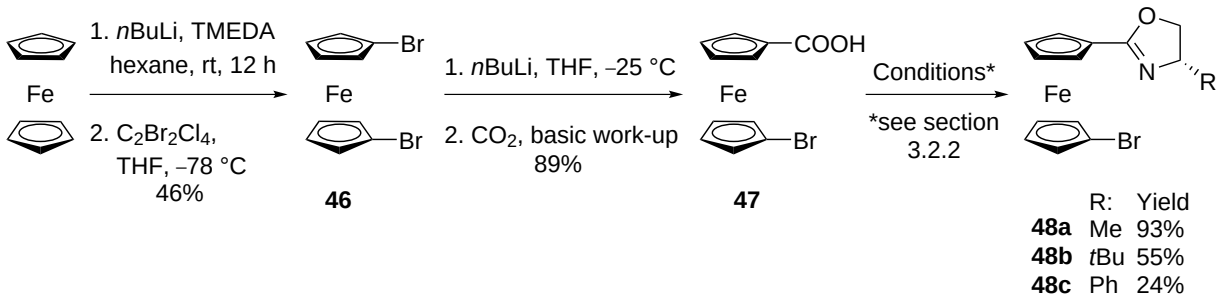

Scheme 63: Synthesis of 1,1'-ferrocenyloxazolines **48a–c**.[173]

The conversion of the bromo derivative **48** to the phosphane **49** was then attempted as shown in scheme 64. Disappointingly, this did not go as smoothly as expected. The lithiation step is highly temperature dependent and the nature of the electrophile is crucial. After several attempts using various lithium bases and electrophiles, this step was abandoned and another synthetic route to the parent ligand **45** was devised.

[24] The oxidative work-up procedure developed by Long *et al.*[182] was successful in removing monobrominated and unsubstituted side products; it was however a very long and arduous process as it required several washings with a saturated $FeCl_3$ solution and the resulting black opaque mass in the separatory funnel was difficult to process. See experimental section for more details.

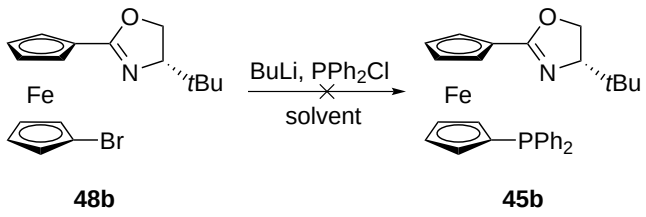

48b **45b**

Scheme 64: Attempted conversion of **48b** to **45b**.[173]

Considering the fact that problems always arise when lithiation of the ferrocenyloxazoline followed by quenching with a phosphane are attempted, we thought that this may be circumvented by introducing the phosphane at the beginning, where lithiation is bound to be successful, and forming the oxazoline moiety in a later stage (see scheme 65). To this end, 1,1'-dibromoferrocene **46** was thus lithiated at –78 °C, and was quenched after 2 h with PPh_2Cl, yielding 1-bromo-1'-phosphanylferrocene **50** in 52% yield. It was subsequently carboxylated using the same conditions as previously mentioned, and the resulting compound **51** could be transformed to the corresponding oxazoline using the standard conditions previously applied (see section 3.2.2). The phosphorus atom, however, underwent oxidation under the standard oxazoline forming conditions yielding compound **52a**, which had to be subsequently reduced to the desired ligand **45a**. Standard reduction with trichlorosilane was used. The conditions were not optimized, hence the low yield.

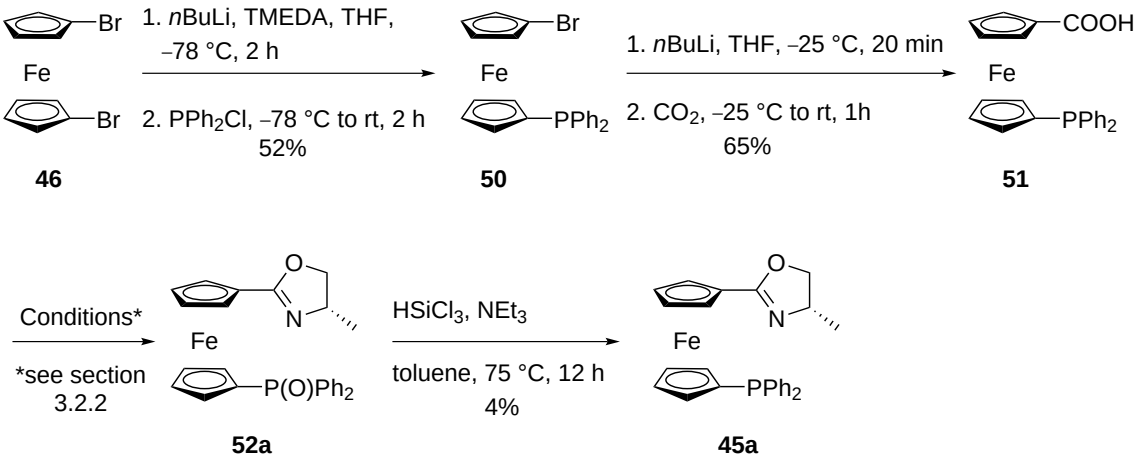

46 **50** **51**

52a **45a**

Scheme 65: Alternative route to parent ligand **45a**.[173]

With the preparation of ligand **45a** being dealt with, focus was once again turned to the *P*-trifluoromethyl analogues. The lithiation/quenching with $PPh(CF_3)_2$ conditions were then investigated with precursor **48**, as it was found out that this protocol was also problematic as was the case for the 1,2-ferrocenyloxazolines. As shown in scheme 66, these conditions allowed the obtention of the desired ligand **49a**.

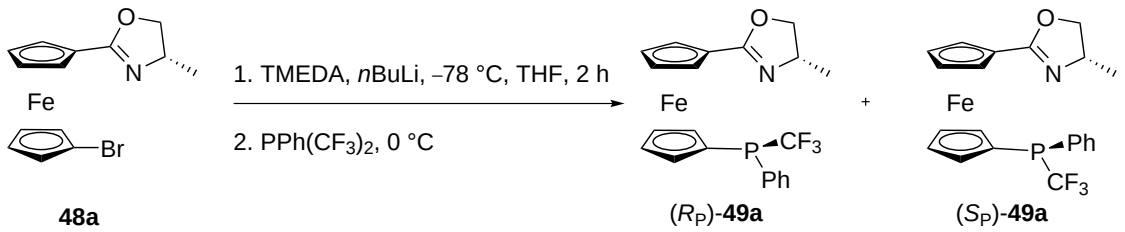

Scheme 66: Synthesis of *P*-trifluoromethyl 1,1'-ferrocenyloxazoline ligands **49a**.[173]

Unfortunately, a mixture of products was always obtained. Attempts to optimize the reaction conditions to attain a reproducible reaction proved fruitless.[173] Thus, with the small amount of **49a** obtained, the ligand diastereomers separation was attempted. However, separation by flash column chromatography was not successful, contrary to the 1,2 substituted ligands (see section 3.2.2). TLC assays with various binary and ternary eluents did not prove very helpful in determining better separation conditions, and as last resort, a preparative TLC was run several times, in order to be able to isolate at least part of a pure diastereomer. This was however also unsuccessful. Although these attempts did not yield separated diastereomers, the ^{19}F and ^{31}P NMR shifts of the ligands could be assigned and are reported in table 24 with the shifts of ligands **34a** as comparison.

Table 24: Selected NMR data of 1,1' ligands **49a** compared to 1,2 ligands **34a**.[173]

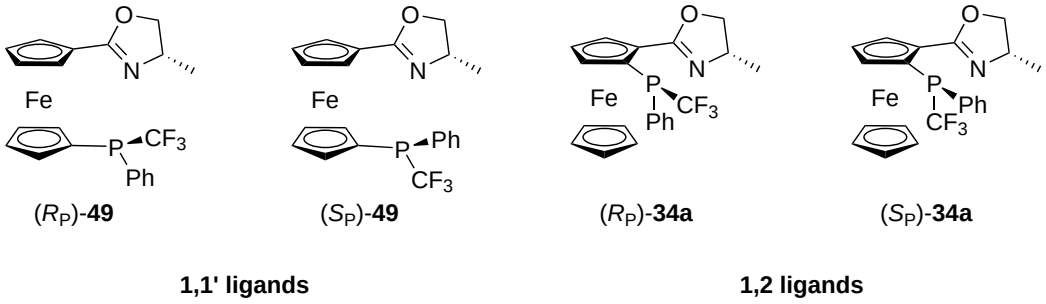

	(R_P)-**49a**	(S_P)-**49a**	(R_P)-**34a**	(S_P)-**34a**
^{31}P shifts (ppm)	–11.4	–10.6	–11.0	–10.5
Multiplicity, $J_{P\text{-}F}$ (Hz)	q, 64	q, 68	q, 65	q, 69
^{19}F shifts (ppm)	–55.8	–55.2	–56.3	–55.2
Multiplicity, $J_{F\text{-}P}$ (Hz)	d, 63	d, 68	d, 65	d, 68

The similarity between the two ligands is unsurprising, as the substitution pattern is not expected to have a major influence either on the ^{31}P or on ^{19}F NMR shifts.

3.2.8 Coordination test of ligand 49a

With the diastereomeric mixture of ligand **49a** in hand, a coordination attempt was carried out, as simple proof-of-principle that these compounds can also effectively act as ligands. [Pd(COD)Cl_2] was chosen as metal precursor, and it was stirred with the ligand in CH_2Cl_2

at room temperature for 1 h before evaporation of the volatiles and analysis of the residual brown solid. Coordination is indeed observed, with the characteristically larger $J_{F\text{-}P}$ coupling constants and the slight low frequency displacement of the ^{19}F NMR shifts. The presence of the complex was also confirmed by HRMS.[25]

Table 25: NMR data of complex **53** and free ligand **49a**.

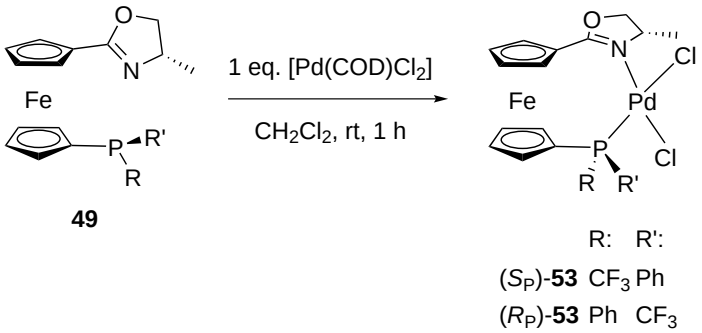

	(R_P)-**53**	(S_P)-**53**	(R_P)-**49a**	(S_P)-**49a**
^{31}P shifts (ppm)	-[a]	-[a]	–11.4	–10.6
Multiplicity, $J_{P\text{-}F}$ (Hz)	-	-	q, 64	q, 68
^{19}F shifts (ppm)	–52.8	–51.3	–55.8	–55.2
Multiplicity, $J_{F\text{-}P}$ (Hz)	d, 72	d, 73	d, 63	d, 68

[a] The ^{31}P NMR shifts of the complex could not be determined due to too little sample available.

As the amount remaining for the coordination attempt was so little (1 mg), full characterization of the complexes was not possible. The separation of the diastereomers could also not be attempted on this scale, but since the polarity of the complex is modified compared to the free ligands, this would definitely be worth investigating on a larger scale in the future. The ligands were not applied in any transition-metal-catalyzed transformations, as using a mixture of diastereomeric ligands would not allow the investigation of the effect of absolute configuration of phosphorus on enantioselectivity, so at this point the project was stopped.

3.3 Conclusion

The synthesis of *P*-trifluoromethyl oxazolines was investigated, allowing the preparation of a range of new phenyl- and ferrocenyloxazoline ligands **26a**, **26b**, **26c**, **26d**, **34a** and **49a** using a lithiation/$PPh(CF_3)_2$ quenching protocol (see scheme 67). The phenyoxazoline **26** and 1,1'-ferrocenyloxazoline **49** ligand diastereomers could not be separated by various analytical, preparative and/or other methods. However, the 1,2-ferrocenyloxazoline ligand diastereomers **34a** could be separated by normal flash column chromatography on silica gel. An alternative route to parent ligand **45** was developed. X-ray structures of ligands **26a**, (R_P,S_{Fc})-**34a** and (R_{Fc})-**33** were successfully obtained.

[25] HRMS (MALDI): calcd. (m/z) for $C_{21}H_{19}Cl_2F_3FeNNaOPPd$: 643.8815 ($[M+Na]^+$), found: 643.8805 ($[M+Na]^+$).

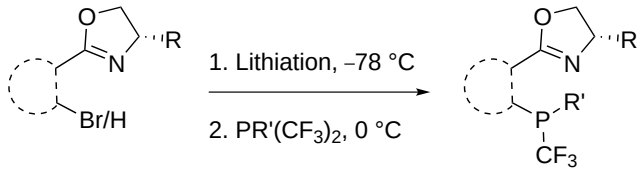

Phenyloxazoline ligands

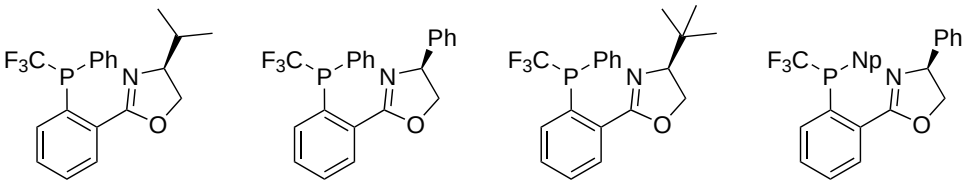

26a **26b** **26c** **26d**

Ferrocenyloxazoline ligands

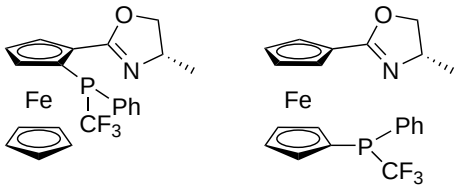

34a **49**

Scheme 67: Synthesis of trifluoromethyl *P*-stereogenic phenyl- and ferrocenyloxazoline ligands.

Ligands **26a**, **34a** and **49a** were coordinated to Pd(II) and in the case of **34a** also to a Pt(II) center. Unfortunately, none of them allowed to grow suitable crystals for analysis by X-ray diffraction, however coordination was confirmed for all complexes by NMR spectroscopy.

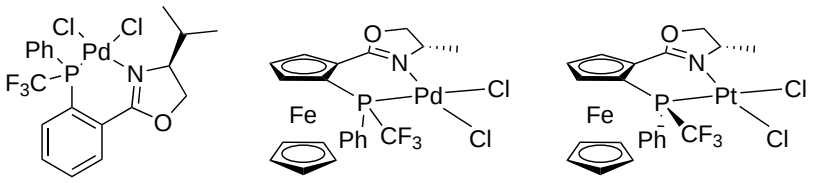

27 (R_P)/(S_P)-**35** (R_P)-**36**

Scheme 68: Pd(II) and Pt(II) complexes of trifluoromethyl *P*-stereogenic oxazoline ligands isolated during this work.

Ligand **34a** was used in various asymmetric transformations, namely allylic alkylation of cinnamyl acetate, hydrosilylation of norbornene and styrene, hydrogenation of DMI, 2-methylquinoline and a dihydroisoquinoline. The best results were obtained in the Pd-catalyzed asymmetric allylic alkylation, where ligands **34a** displayed higher enantioselectivities as well as a better branched to linear ratio than parent ligand **33**. The absolute configuration at phosphorus did not seem to have a major influence on the outcome of these catalyses. In general enantioselectivities were modest, but showed promising results compared to their diphenyl analogues, which is encouraging for further research of catalytic applications of such ligands.

3.4 Outlook

An alternative synthetic pathway is needed to access the ligands investigated, as the lithiation/$PPh(CF_3)_2$ quenching protocol was found to be neither reliable nor reproducible. In the case of the phenyloxazolines, although product formation was always observed, the conversion and diastereoselectivities were extremely variable. With the ferrocenyloxazolines as substrates, no conversion to the desired ligands occurred in the presence of an oxazoline with a side chain larger than methyl. The recurring issue with this lithiation/electrophilic substitution process remains poorly understood, and very few references mention this,[183] making rationalization difficult. The electrophilic substitution of the lithiated species is especially problematic and needs to be investigated properly from a mechanistic point of view to understand this process better, as screening of the reaction conditions allowed neither room for optimization nor more insight on how the reaction works.

Shown in scheme 69 are possible synthetic routes towards the target *P*-stereogenic ligands. Two majors pathways can be envisioned: either via a primary phosphane (PH_2), or via a protected phosphane ($PNEt_2$). Single substitution of both molecules should afford an intermediate which can be further functionalized via introduction of a second substituent. The major issue with these pathways is conversion and yields. Single substitution of such compounds may not be that efficient, especially depending on the species used. Moreover, if the trifluoromethyl group is introduced at an early stage, one must always consider the compatibility with subsequent reagents and reactions conditions.

Furthermore, most of the envisaged intermediates shown are quite labile and can readily undergo oxidation or hydrolysis, which impedes easy handling and possibly obtention of high yields. The relative instability of such species makes synthetic work on a small scale combined with multistep syntheses very difficult, as the amounts of product lost result in a significant decrease in materials available in the end. Scale-up of such reactions is not trivial and does not necessarily lead to higher conversions or yields. Much thought and experimenting still remain to be invested to discover appropriate synthetic pathways towards such ligands.

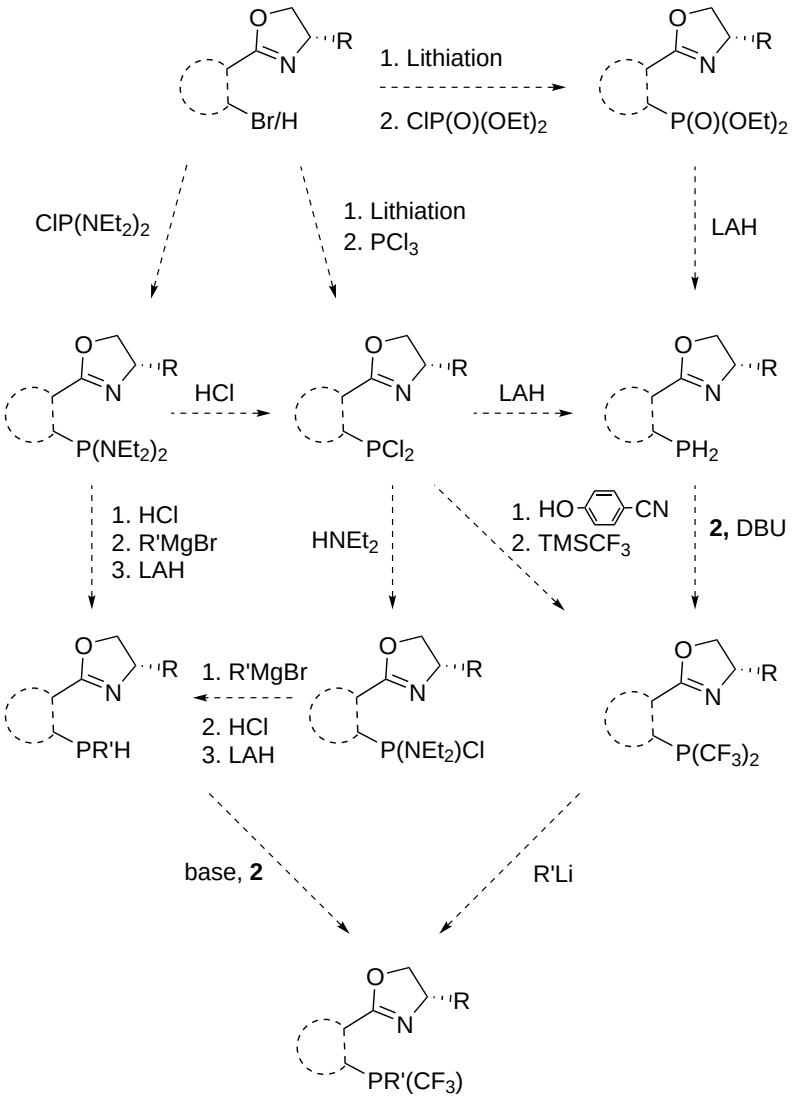

Scheme 69: Possible synthetic pathways towards trifluoromethyl *P*-stereogenic ligands.

Finally, when a reasonable method is found to access such ligands, analogues with bulkier side chains at the oxazoline and different substituents at the phosphorus (*e.g.* alkyl) should be prepared (figure 23). This should allow the continued comparison of not only sterics but also electronic effect of the substituents.

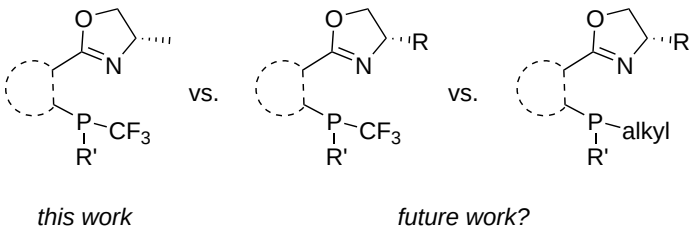

Figure 23: Ligands prepared in this work versus possible future ligands.

The full characterization as well as coordination behavior of such species should be investigated, ideally with comparisons of the solid state structures, to allow more insight on the electronic and steric effect of the trifluoromethyl substituent on the phosphane. Further applications in catalysis, with comparisons to the parent ligands, the corresponding bistrifluoromethyl ligands,

and the alkyl analogues, would help to gain insight on the effect of the trifluoromethyl moiety in catalysis as well as the influence of *P*-stereogenicity on stereoselective outcome.

4 Phenylethylferrocene ligands

4.1 Introduction

Chiral ruthenium(II) complexes are an important class of compounds, especially in the context of developing highly efficient systems for homogeneous catalysis. Since the development of Noyori's bifunctional Ru(II) catalyst system in 1995[184] (see figure 24), its excellent performance has made it a benchmark for asymmetric transfer hydrogenation.

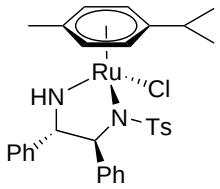

[Ru(TsDPEN)Cl]

Figure 24: Noyori's [Ru(TsDPEN)Cl] catalyst.[184]

4.1.1 Ruthenium(II) tethered ligands

The success of this catalyst system inspired many others to develop ligands specifically designed for bifunctional catalysis. Among these, tethered analogues have emerged as structures which are able to compete with Noyori's original catalyst. Examples of diamine tethered complexes have proven to be useful in catalysis, exhibiting faster rates and in most cases superior enantioselectivities compared to the untethered analogues in the asymmetric transfer hydrogenation of aromatic ketones (figure 25).[185][186]

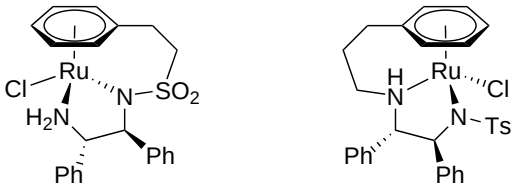

Figure 25: Wills' diamine tethered Ru(II) catalysts.[186]

The chelate effect of the tethering of the ligand generates a more rigid structure around the metal center, which may not only lead to a more stable complex, but also allows a better stereodiscrimination of prochiral substrates used in asymmetric catalysis.[187] Much focus has been given to complexes based on ligands containing phosphorus as donor atom, although analogues containing other pnictogens (N, As) and chalcogens (O, S) are also known.

Various subclasses of phosphorus-containing tethered complexes have been described, containing either planar chirality,[188] a stereogenic center in the bridge,[189] or a stereogenic phosphane substituent[190][191] (see figure 26).

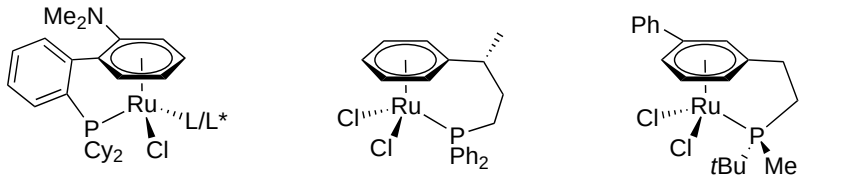

planar chiral — Faller (2003)

chiral backbone — Zenneck (2004)

stereogenic phosphorus — Muller (2013)

Figure 26: Examples of Ru(II) tethered complexes containing a phosphorus-based ligand.[188][189][191]

Being involved in this chemistry, recent work by Grabulosa *et al.* focused on the preparation of such tethered [Ru(η^6-arene)P*] complexes with *P*-stereogenic 2-biphenylylphosphanes.[192] They found that by using $[Ru(PhCOOMe)Cl_2]_2$ as Ru(II) precursor and simple irradiation with a desk lamp at room temperature, the aryl substituent of the phosphane displaces the benzoate moiety, yielding an intramolecularly tethered complex (see scheme 70). These complexes were tested in the transfer hydrogenation of acetophenone, the highest *ee* obtained being 47%. In this case, the tethered complexes however showed in general slightly lower enantioselectivities than the non tethered analogues.

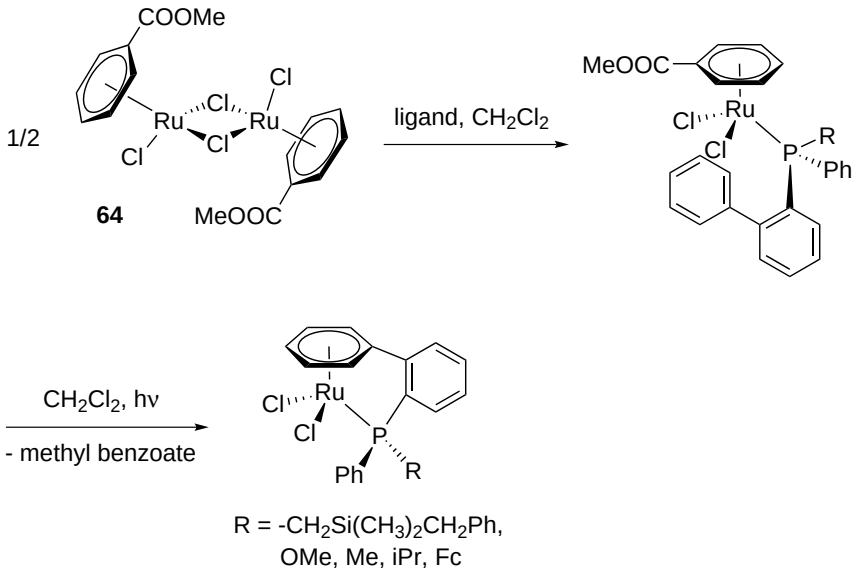

Scheme 70: Grabulosa's phenyl-tethered Ru(II) complexes.[192]

4.1.2 Previous work[193]

Parallel to this work, phenyethylferrocene derived ligands were being investigated in our group by R. Aardoom,[193] with the idea of making a ferrocenyl-tethered ruthenium(II) complex, analogous to Wills' tethered Ru(II) diamine catalysts.[185][186] The rationale was that the presence of a 1,2 susbtituted ferrocene backbone could possibly exert better enantioinduction due to planar chirality. The ferrocenyldiamines proved, however, to be inaccessible. The corresponding ferrocenylphosphanes were thus prepared, and it was found that they could indeed coordinate to Ru(II) in a tethered fashion via arene displacement as shown in scheme 71.

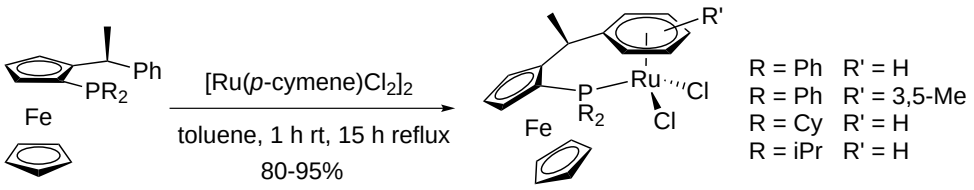

Scheme 71: Aardoom's ferrocenyl-tethered Ru(II) complexes.[193]

The solid state structure of the diphenyl complex [Ru(**54**)Cl_2] illustrates how the tethering to ruthenium modifies the geometry of the ligand (figure 27): whereas the orientation of the diphenylphosphanyl group did not substantially change compared to the free ligand, the side chain conformation is remarkably different. The ruthenium atom is positioned in an *endo* fashion with respect to the ferrocene backbone, and the ligand structure is very distorted, probably due to the steric demand of the $RuCl_2$ moiety. The cyclopentadienyl rings exhibit an interplanar angle of 6.8°.

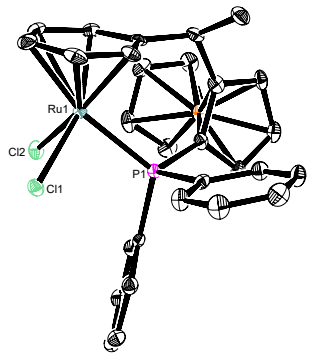

Figure 27: *ORTEP* representation of ferrocenyl-tethered Ru(II) complex from ligand **54**.[193]

The complexes were consequently applied in the reduction of acetophenone as hydride transfer agents, the catalyst composed of the all-phenyl ligand **54** giving the best yield (59%) and enantioselectivity (44%) after screening of reaction conditions and ligand substituents (scheme 72).

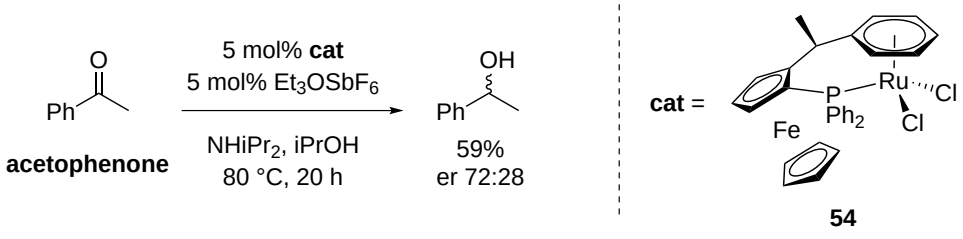

Scheme 72: Transfer hydrogenation of acetophenone using a ferrocenyl-tethered Ru(II) complex.[193]

Based on the promising work involving *P*-trifluoromethyl ligands (see section 1.5.2) and the previously outlined pioneering work of Aardoom concerning the preparation and catalytic

applications of phenylethylferrocenyl ligands,[193] it was thought of interest to prepare the trifluoromethyl analogues **59** and **60** (figure 28) in order to compare their coordination behavior and catalytic activity to the electron-rich analogues. These compounds would then fill the gap between Grabulosa's *P*-stereogenic phenyl-tethered ligands and Aardoom's non *P*-stereogenic planar chiral ferrocenyl-tethered ligands. Moreover, this would further the scope of planar chiral ferrocenylphosphanes, by introducing a new element of chirality at the phosphorus atom.

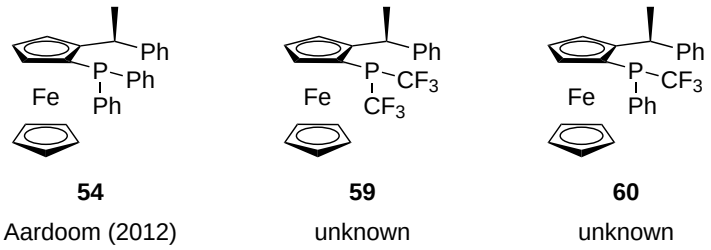

54 Aardoom (2012) **59** unknown **60** unknown

Figure 28: Parent ligand **54** versus mono- and bistrifluoromethyl ligands **60** and **59**.

In order to assess the properties of these ligands, it will be necessary to synthesize the mono- and the bistrifluoromethyl derivatives, in order to not only compare the electronic and steric effects, but also the influence (if any) of phosphorus stereogenicity in stereoselective transformations. This will lead to more insight in this unique class of ligands.

4.2 Results and discussion[26]

4.2.1 Synthesis of *P*-trifluoromethyl phenylethylferrocenes

Following the synthetic protocol developed by Aardoom utilizing a Taniaphos inspired synthesis,[193] the necessary ligand precursor **56** was accessed in two steps in high yield (overall yield 78%) starting from Ugi amine, as shown in scheme 73.

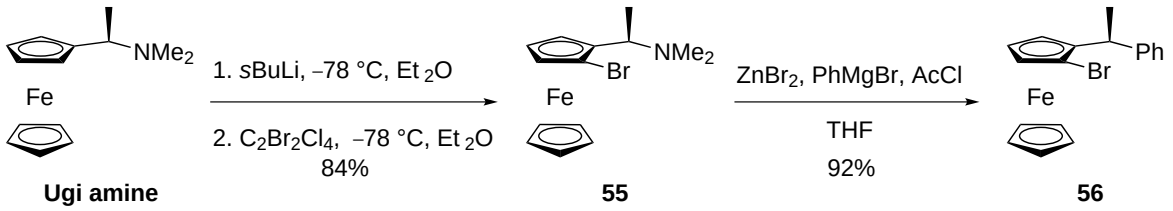

Ugi amine **55** **56**

Scheme 73: Synthesis of ligand precursor **56** starting from resolved Ugi amine following Aardoom's procedure.[193]

We first turned our attention to the monotrifluoromethyl ligands, and decided to apply the previously mentioned lithiation/$PPh(CF_3)_2$ quenching protocol. However, once again conversion issues arose with this method. We therefore needed to devise proper conditions for the lithiation/electrophile quenching protocol. Screening of the conditions and electrophile was then initiated. Various reaction parameters and electrophiles were tested, and the main results are summarized in table 26.

[26] Most of the experimental work from this chapter was carried out by Manuel Kober-Czerny during his research project.[194]

Table 26: Screening of conditions for electrophilic substitution of **56**.

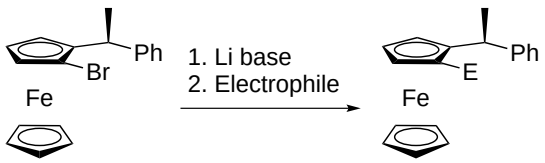

56

Entry	Li base[a]	Electrophile E^+	E^+ eq.	Concentration (M)	Product? (Yield[b])
1	*n*BuLi	$PPh(CF_3)_2$	0.5	0.27	no
2	*s*BuLi	PPh_2Cl	0.5	0.07	no
3	*n*BuLi	PPh_2Cl	1.0	0.07	no
4[c]	*n*BuLi	TMSCl	70.8	0.06	no
5	*n*BuLi	PPh_2Cl	3.0	0.07	no
6	*n*BuLi	PPh_2Cl	3.1	0.14	yes (44%)
7	*n*BuLi	$PPh(CF_3)_2$	3.0	0.13	no
8[d]	*n*BuLi	$P(O)(OEt)_2Cl$	1.1	0.17	yes (95%)

[a] 1.1-1.2 eq. of Li base were used.
[b] Isolated yields are given.
[c] This reaction was run in hexane.
[d] This reaction was run at room temperature.

Under standard conditions, the reaction mixtures were refluxed overnight following the procedure developed by Aardoom.[193] It became apparent very soon that these conditions were not suitable for electrophilic substitution with $PPh(CF_3)_2$. The major issue was not even the fact that $PPh(CF_3)_2$ is highly volatile so mostly unsuited for reactions at high temperatures. The need of an excess of electrophile (3 eq.) proved to be incompatible with the presence of butyllithium. Decomposition of $PPh(CF_3)_2$ by formation of many side products was always observed by ^{19}F NMR spectroscopy. It was hypothesized that $PPh(CF_3)_2$ reacts faster with *n*BuLi than with the lithiated ferrocene species, forming as major side product butyltrifluoromethylphosphane.[27] As the reaction did not work using a stoichiometric or even substoichiometric amount of electrophile, another pathway had to be projected for the preparation of the monotrifluoromethyl ligands.

Thinking along different lines, since the introduction of a phosphonate proved to be high yielding (table 26, entry 8), we decided to go forward with the synthesis of the bistrifluoromethyl derivative **59**. We thought that the monotrifluoromethyl analogues could be accessed directly from it in a second instance by nucleophilic substitution. Phosphonate **57** was thus reduced to the primary phosphane **58** in 84% yield, and it was subsequently bistrifluoromethylated in reasonable yield using reagent **2**, yielding the desired ligand **59** as a dark orange solid (scheme 74).

[27] This is supported by the signals observed in ^{31}P and ^{19}F NMR spectra (which can be found in appendix E). The structure of this product could however not be ascertained, as the deliberate preparation of PBu_2CF_3 was unsuccessful, and no comparable data exists for such compounds.

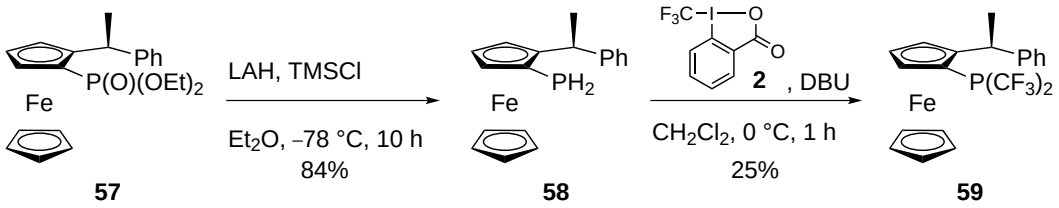

57 **58** **59**

Scheme 74: Synthesis of bistrifluoromethyl phenylethylferrocenyl ligand **59**.

With ligand **59** in hand, conditions for nucleophilic substitution to the monotrifluoromethyl analogue **60** were explored. As it has been shown that bistrifluoromethyl ferrocenylphosphanes can undergo nucleophilic substitution using phenyllithium,[115] we decided to examine this option. The results of the experiments (reported in table 27) showed that using an excess of phenyllithium was detrimental, as mostly doubly substituted parent ligand **54** was formed, although the diastereomeric ratio of monotrifluoromethyl ligands **60** was relatively high (entry 1).

Table 27: Screening of conditions for nucleophilic substitution of **59**.

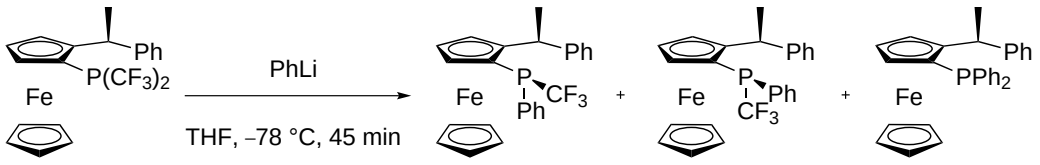

59 (*R*P)-**60** (*S*P)-**60** **54**

Entry	Eq. PhLi[a]	d.r.[b] (*R*P)-**60**:(*S*P)-**60**	**54** observed?	**59** remaining[b]
1	4.5	1:4	yes	0%
2	2.0	1:2	yes	0%
3	1.5	1:1.5	no	51%

[a] 1.9 M solution in dibutylether.
[b] Determined by ^{19}F NMR spectroscopy.

The reaction was then run in a Young NMR tube, in order to be able to monitor conversion by ^{19}F NMR spectroscopy. When phenyllithium was used stoichiometrically, no conversion was observed after one hour. A second equivalent was subsequently added (a color change to dark brown was observed), and full conversion to the products was seen by NMR spectroscopy (entry 2). In a scale-up of this promising experiment, a total of 1.5 eq of phenyllithium were added in portions over a period of 45 min, with reaction control using GC-MS and NMR spectroscopy (entry 3). The reaction mixture was thus quenched before formation of parent ligand **54** could occur. The separation of the three ligands was then achieved first by a column chromatography on silica gel eluting with hexane:CH_2Cl_2 9:1, which allowed removal of part of ligand **59** and part of a diastereomer of **60**. The two remaining mixed fractions (one containing **59** and one diastereomer of **60**, the other containing both diastereomers of **60**) were further separated by preparative TLC eluting with hexane:CH_2Cl_2:Et_2O 20:1:1. This allowed the isolation of (*R*P)-**60** in 46% yield and of (*S*P)-**60** in 25% yield.

4.2.2 Solid state structures of the ligands

Ligands **59** and **60**, which were obtained as orange solids, are soluble in many solvents, and could easily be recrystallized by slow evaporation of a single or binary solvent solution (see appendix C for details). The absolute configuration at phosphorus of the ligand diastereomers **60** could thus be determined by X-ray diffraction analysis. All the solid state structures of this ligand subclass were therefore determined (figure 29).[28]

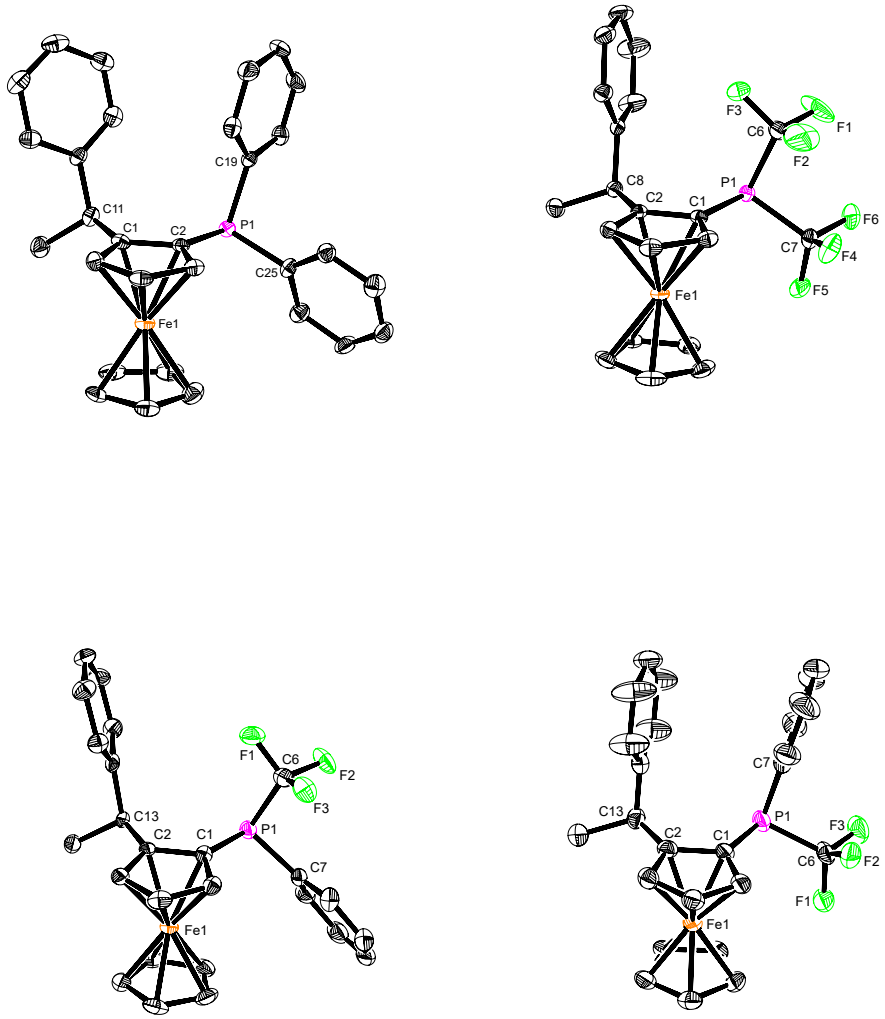

Figure 29: *ORTEP* representation of ligands **54** (top left), **59** (top right), (R_P)-**60** (bottom left), and (S_P)-**60** (bottom right). Phenyl ring disorder of ligand (S_P)-**60** as well as all H atoms are omitted for clarity. Thermal ellipsoids are set to 50% probability.

Ligand (S_P)-**60** seems to exhibit a π-π (face-to-face) interaction, as suggested by the apparent

[28] The X-ray structures of **59** and **60** were determined by Ewa Pietrasiak and Lukas Sigrist. Structure of **54** was determined by Raphael Aardoom.[193]

quasi parallel orientation of the two phenyl rings and an average plane-to-plane distance of 3.984 Å. However, a closer look and the determination of the deviation angle, which lies between 16.77-27.41° due to the disorder of the phosphorus phenyl ring, points towards a very weak or, if at all, non stabilizing interaction. This may be supported by the structure of the other diastereomer, where the phenyl rings are pointing in opposite directions. This could be due to an otherwise unfavorable steric interaction between the trifluoromethyl group and the ferrocene core that would arise in the other conformation. This corroborates the fact that the possible π-π interaction occurring in diastereomer (S_P)-**60** is probably very weak or not stabilizing enough that the other diastereomer would also prefer such a conformation. In the end, sterics seem to be the dominant influence.

The bistrifluoromethyl ligand typically shows smaller bond angles than its monotrifluoromethyl congeners, in conformity with the presence of two electron-withdrawing groups (table 28). They increase the pyramidalization degree of the phosphane due to higher s character of the phosphorus lone pair, in accordance with Bent's postulate.[13] Conversely, the increased p character of the bonds consequently leads to smaller bond angles.

Table 28: Selected solid state data of compounds **59** and **60** compared to parent ligand **54**.

Ligand	Bond angle (°)			Torsion (°)	
	C1–P1–C5	C1–P1–C6	C5–P1–C6	C1–C2–C3–C4	C2–C1–P1–C5
54	102.39	101.41	100.80	92.96	98.78
59	99.35	103.87	95.04	77.11	110.71
(R_P)-**60**	104.10	102.44	96.97	89.67	115.97
(S_P)-**60**	100.59	106.09	100.10	73.74	97.77

To gain more insight on the electronic and steric effects playing a role in these ligands, an overlay of the solid state structures of the parent ligand **54** (red), the bistrifluoromethyl analogue **59** (orange) and the two diastereomers of **60** (blue and green) is shown (figure 30).

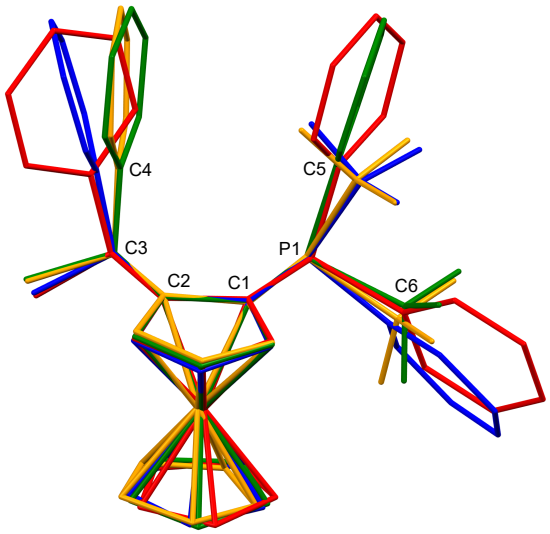

Figure 30: Overlay of **54** (red), **59** (orange), (R_P)-**60** (blue), and (S_P)-**60** (green).

A striking feature which catches the eye, is the relatively large difference in orientation of the pendant phenyl rings. Ligands **54** (red) and (R_P)-**60** (blue) both exhibit a quite large torsion angle around the C1–C2–C3–C4 atoms, around 90° (see table 28). Comparatively, the two other ligands possess values lower than 80°. Furthermore, the phenyl ring of ligand **54** displays the most distortion with respect to the plane of the phenyl substituent at the phosphorus, with a deviation of 26.65°. This distortion may be attributed to a preferential parallel displacement type of π interaction, which could be stabilizing this conformation. This is corroborated by the closest C–C distances of the phenyl rings, which amount to 3.349 and 3.874 Å. That such a conformation arises with the all-phenyl ligand may also illustrate the fact that the previously discussed face-to-face interaction is non existent or not stabilizing enough to enforce such an orientation of the phenyl rings.

4.2.3 Coordination studies

With the desired ligands in hand, the study of their coordination behavior was started. In a first instance, the coordination of ligands **59** and (S_P)-**60** to a Ru(II) center was investigated (see scheme 75). The ligands **59** and (S_P)-**60** were stirred with $[Ru(p\text{–cymene})Cl_2]_2$ at room temperature for an hour and then heated to reflux in toluene. Both reactions were monitored by ^{31}P NMR spectroscopy.

In the case of bistrifluoromethyl ligand **59**, it came to light that it would not coordinate to Ru(II) under these conditions. Refluxing for several days did not allow any conversion to complex **61a**. Work-up of the reaction mixture yielded mostly free ligand, and slight decomposition was

discernible by ^{19}F NMR and ^{31}P NMR spectroscopy.

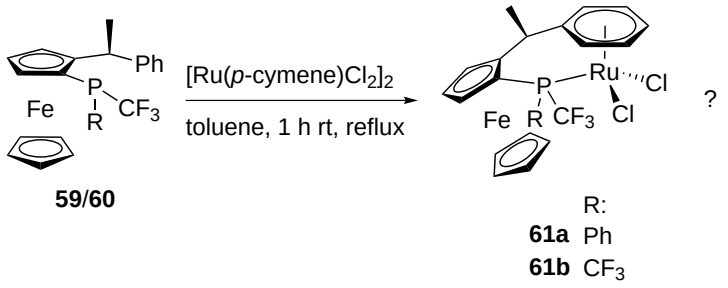

Scheme 75: Coordination of ligands **59** and (S_P)-**60** to an Ru(II) center.

Ligand (S_P)-**60** was much more promising. After refluxing overnight, a 1:1 ratio of coordination compound to free ligand was observed. After addition of an extra 0.5 eq. of Ru(II) precursor and further heating for 2 days, the reaction was stopped as only more decomposition was seen. After ensuring that the product was stable on silica, the complex was purified by column chromatography. The obtained ^{19}F NMR and ^{31}P NMR spectra clearly point to a *P*-coordinated complex (see table 29). It remains however unclear if the pendant phenyl group is coordinated to the Ru(II) atom in an η^6 fashion. Overlapping of the aromatic proton signals in the ^{1}H spectrum did not allow to ascertain unambiguously if this is indeed the case. Moreover, the small amount of product afforded did not allow for further characterization of the complex (e.g. by ^{13}C NMR or 2D experiments) which would allow more precise determination of the structure.

Table 29: Selected NMR data for complex **61b** and free ligand (S_P)-**60**

	Complex **61b**	Ligand (S_P)-**60**
^{31}P shifts (ppm)	27.4	–12.3
Multiplicity, $J_{P\text{-}F}$ (Hz)	q, 82.3	q, 68.8
^{19}F shifts (ppm)	–69.9	–53.8
Multiplicity, $J_{F\text{-}P}$ (Hz)	d, 84.8	d, 69.5

We considered the possibility that the electron-rich *p*-cymene fragment was perhaps not labile enough to be displaced. This has already been observed by other groups, and Grabulosa *et al.* also ran into this issue during their study with tethered *P*-stereogenic ligands.[192] A common precursor which has therefore been used instead of the standard *p*-cymene dimer comprises of an alkyl benzoate, which is more electron-poor and thus a more labile η^6 coordinating arene. We therefore set out to synthesize a Ru(II) dinuclear complex containing methyl benzoate as arene ligand.

Towards this end, different routes where attempted, as shown in scheme 76. We chose our predilection alkali metal lithium as electron source, as it is has been shown that it is better suited than sodium for reduction of double bonds under Birch conditions.[195][196] Its ease to use as a wire also makes it very convenient to work with. First, the direct reduction of methyl benzoate was attempted, as it has been described in literature.[197] Disappointingly, an intractable mixture of various reductions products and starting material was obtained. Since the reduction of benzoic acid has been more often described (see refs.[198][199][200][201]) and more thoroughly investigated,[198] we moved to this substrate.

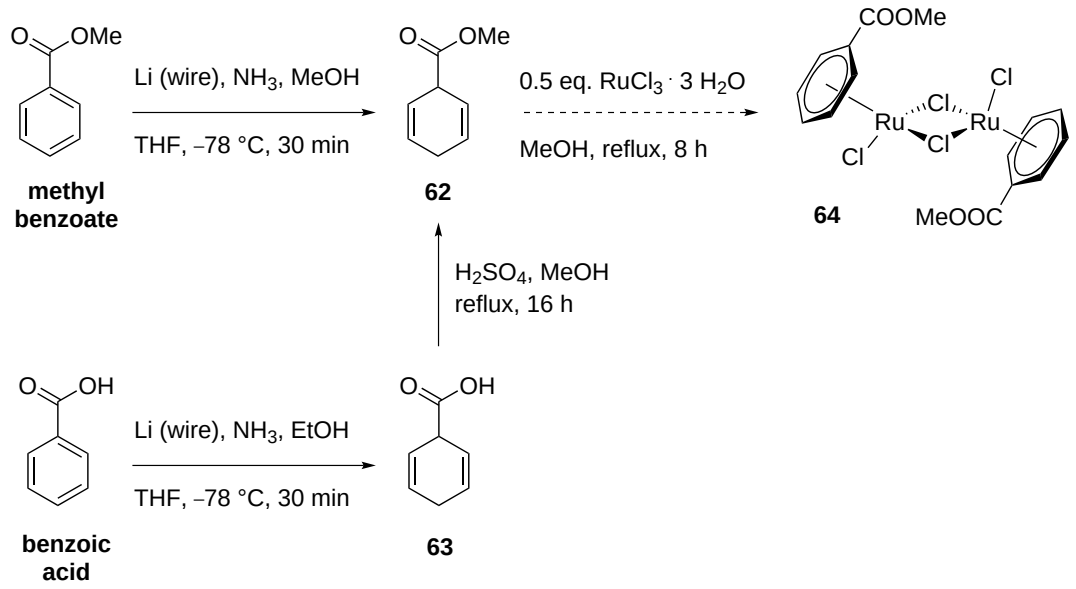

Scheme 76: Birch reduction attempts towards the synthesis of ruthenium(II) precursor **64**.

Regrettably, the reduction of benzoic acid with lithium metal did not provide clean conversion to desired product either. Mostly a mixture of many reduced and unreduced compounds was obtained, and the isolation of desired product from these mixtures via distillation proved to be impossible. As most of the gathered procedures are not described in detail, much room for experimental deviation is left. In most reported cases the crude is directly used in the next step or not properly characterized, so no yields or purity are available for the described conditions. The reactions were thus found to be unreproducible. After a few attempts, no optimization of the reduction towards the desired 1,5-dihydrocyclohexadiene could be achieved, and time constraints forced us to abort this synthesis. The investigation of the ruthenium chemistry of ligands **59** and **60** was then stopped here.

As the Ru(II) chemistry proved somewhat unsatisfactory, an effort to gain more insight on the coordination behavior of these ligands was furnished. A simple complexation to Au(I) was thus tested, as shown below. The gold(I) precursor [Au(SMe_2)Cl] was chosen, and it was stirred with the ligands **59** and (R_P)-**60** for 30 min at room temperature. The complexes, which were obtained as yellow oils, proved to be unstable in solution and in air, which aborted crystallization attempts. Complex **65a** was however (surprisingly) stable enough to be purified by column chromatography on silica gel.

Table 30: Selected NMR data for gold(I) complexes **65a** and **65b**.

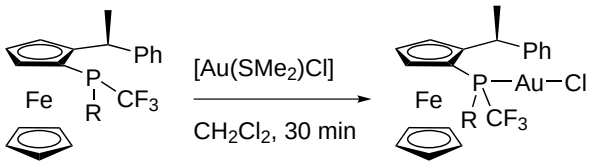

59/60

R:
65a Ph
65b CF_3

	Complex **65a**	Complex **65b**
^{31}P shifts (ppm)	39.0	31.1
Multiplicity, $J_{P\text{-}F}$ (Hz)	sept, 92.8	tq, 83.8
^{19}F shifts (ppm)	–52.6, –59.1	–60.5
Multiplicity, $J_{F\text{-}P}$ (Hz)	qd, 92.0	d, 84.8
$J_{F\text{-}F}$ (Hz)	8.2	12.0

The NMR data obtained (see table 30) confirm coordination of both ligands to gold(I), as observed by the significant shift of the ^{31}P signals and larger $J_{P\text{-}F}$ coupling constants. As no solid state structure was obtained, one can only speculate about the change in geometry upon coordination. Aardoom has observed in the case of the all-phenyl ligand **54** that the phenyl substituent of the phosphane and the pendant phenyl ring are much better aligned in the corresponding Au(I) complex, indicative of a π-π stacking interaction.[193] With the monotrifluoromethyl ligands, the question remains if this will also be observed, and if this has any influence on the behavior of these complexes in solution.

It was originally projected to perform catalytic tests with these ligands. It has for example been shown by Widenhoefer *et al.* that the intramolecular hydroamination of unactivated alkenes can be catalyzed by gold(I)-phosphane complexes.[202] Aardoom's hydroamination results with gold complex [Au(**54**)Cl] were however inconclusive, as it could not be ascertained if the necessary coordination site was available or not, and chloride abstraction experiments were unsatisfactory.[193] Furthermore, as the aforementioned complexes were found to not be stable in solution or in air, the idea of catalytic trials with the gold(I) complexes was abandoned.

4.2.4 Transfer hydrogenation

As the coordination of ligands **59** and **60** to ruthenium(II) proved to be successful, we set out to test their activity as catalysts in the transfer hydrogenation of acetophenone. The standard reaction conditions reported by Aardoom were used,[193] as shown in scheme 77.

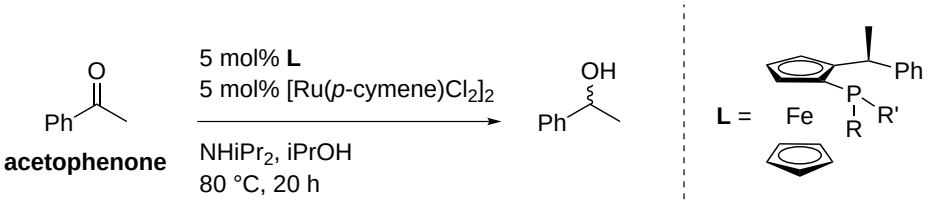

Scheme 77: Ru(II)-catalyzed transfer hydrogenation of acetophenone using ligands **54**, **59**, and **60**.

Under these conditions, none of the ligands showed any enantioselection. These first results confirm at least one aspect which had already been noted by Aardoom: without a free coordination site, no enantioselectivity is observed. This leaves much room for optimization of the conditions, as various halide abstractors, as well as other reaction parameters, still need to be tested. The possibility of stereoselective behavior of the trifluoromethyl ligands thus remains, and with this preliminary reactivity assessment, the project was halted here, as no further resources could be invested in catalytic screening.

4.3 Conclusion

With the idea of making trifluoromethyl *P*-stereogenic tethered ligands analogous to those reported by Aardoom,[193] the new ligands **59**, (R_P)-**60** and (S_P)-**60** were prepared (scheme 78). The common synthetic pathway to these ligands which was developed makes use of reagent **2** as trifluoromethyl source to access the bistrifluoromethyl ligand **59** from the primary phosphane **58**. As it was found that the lithiation/$PPh(CF_3)_2$ quenching protocol was ineffective in procuring the monotrifluoromethyl derivatives **60**, they were directly derived from **59** by nucleophilic substitution with phenyllithium. All obtained ligands afforded suitable single crystals for structure determination by X-ray diffraction, and their geometries in the solid state could be compared.

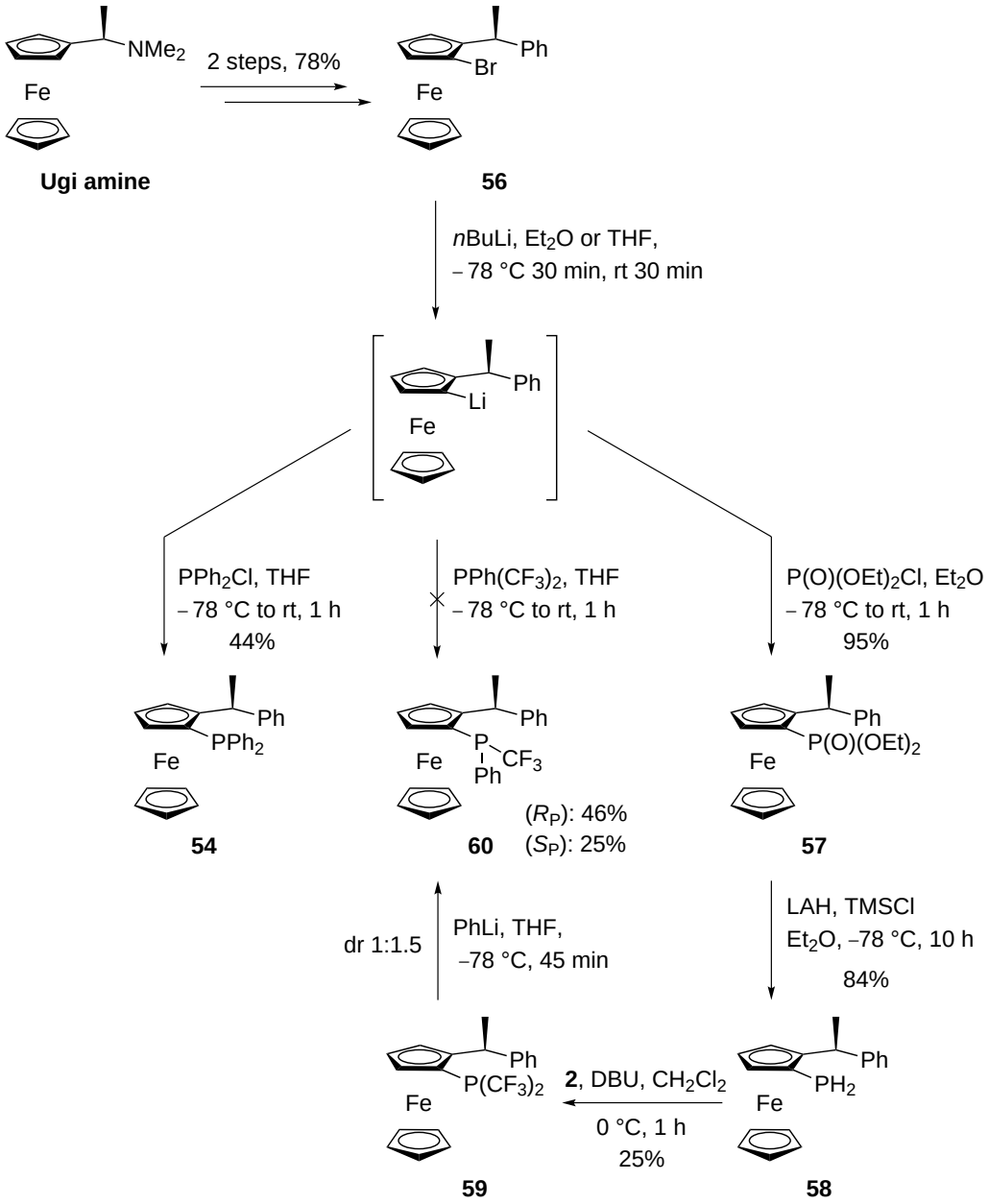

Scheme 78: Synthetic routes to ligands **54**, **59**, and **60**.

The coordination behavior of these ligands was investigated by complexation with the transition metal precursors $[Ru(p\text{−cymene})Cl_2]_2$ and $[Au(SMe_2)Cl]$ (figure 31). It was found that the very electron-poor ligand **59** does not coordinate to the Ru(II) ion, however this may be due to the low lability of the *p*-cymene Ru(II) precursor. On the other hand, ligand **60** does coordinate to Ru(II), however the η^6 coordination of the pendant phenyl group to the ruthenium atom remains to be confirmed. Both ligands coordinated to a gold(I) center and the structures were characterized by multinuclear NMR.

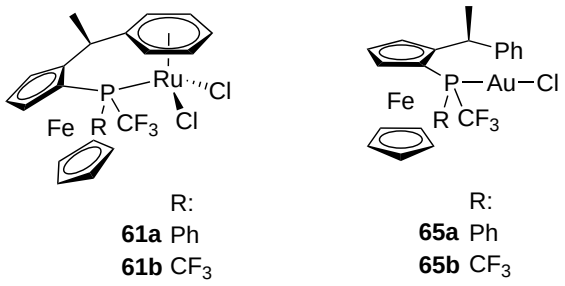

R:
61a Ph
61b CF_3

R:
65a Ph
65b CF_3

Figure 31: Complexes **61** and **65** investigated in this work.

Finally, the new ligands were tested in the transfer hydrogenation of acetophenone, and preliminary results showed them to not be better as parent ligand **54** in inducing stereoselectivity without a halogen abstractor, yielding racemic product. The ligands remain to be tested under optimized conditions, in order to assess their reactivity when exhibiting a free coordination site.

4.4 Outlook

The ruthenium(II) chemistry of ligands **60** remains to be further investigated. The coordination of the pendant aryl ring in an η^6 mode to the metal needs to be ascertained, to confirm an actual tethered nature of these species. The synthesis of Ru(II) precursor **64** still needs to be explored, as it could allow easier preparation of complexes **61** and possibly allow isolation and full characterization of these coordination compounds. Alternatively, another more labile ruthenium(II) precursor can be envisaged. Furthermore, the new ligands **59** and **60** still need to be screened in order to uncover their potential in asymmetric catalysis, and compare their reactivity to parent ligand **54**. Finally, if the ruthenium and gold chemistry of these compounds is unsatisfactory, the further scope of these ligands should be considered.

5 General conclusion and outlook

5.1 Summary

The present thesis mainly focused on the development of synthetic pathways towards *P*-trifluoromethyl phosphanes. Chapter 2 allowed to gain some insight on the catalytic activity of a bistrifluoromethyl BINAP derived ligand previously prepared in our group.[114][123] It was used in the Pd(II)-catalyzed alkylative ring opening of an oxabicycle and induced very high enantioselectivities, higher than the parent ligand BINAP (scheme 79).

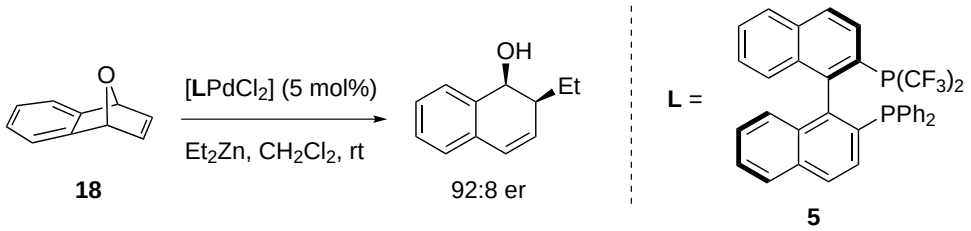

18 92:8 er **5**

Scheme 79: Pd-catalyzed enantioselective alkylative ring opening of 7-oxabenzonorbornadiene **18** using ligand **5**.

The binaphthyl backbone was shown to be a difficult substrate to derivatize in the 2,2' positions due to steric hindrance, and no new *P*-trifluoromethyl derivatives could be accessed. Subsequently, as proof-of-principle, a simple biphenyl ligand was successfully prepared and shown to coordinate to gold(I) (scheme 80).

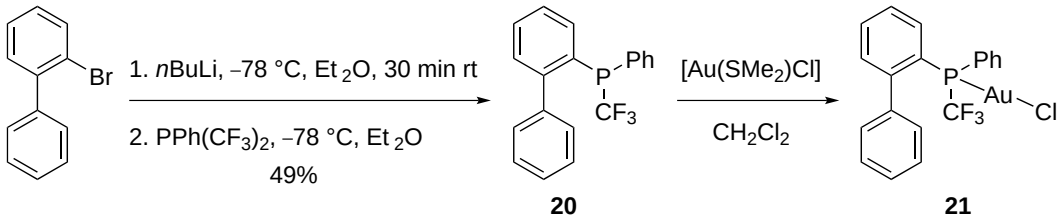

20 **21**

Scheme 80: Biphenyl ligand **20** and its corresponding gold(I) complex **21** prepared in this work.

In chapter 3, the preparation of phenyl- and ferrocenyloxazolines was investigated. The *P*-trifluoromethyl phenyloxazolines could be accessed via lithiation of the bromophenyl precursor and subsequent electrophilic substitution with $PPh(CF_3)_2$, during which a trifluoromethyl substituent acts as a leaving group (scheme 81).[115][117] The ligand diastereomers which arise due to phosphorus stereogenicity could however not be separated. Analytical and preparative methods were to no avail, as well as derivatization and epimerization of the structures. These ligands were thereby shown to be quite inert. They were furthermore shown to act as ligands by forming a Pd(II) complex. As the ligand diastereomers could not be separated, we moved towards a different ligand scaffold.

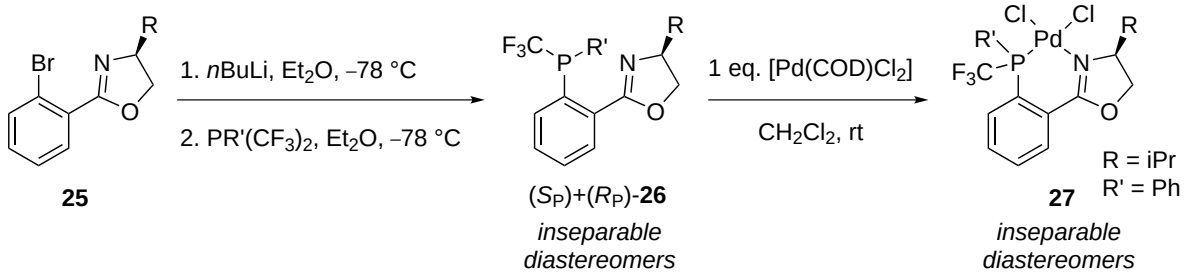

Scheme 81: Phenyloxazoline ligands **26a–d** and palladium(II) complex **27** prepared in this work.

1,2-Ferrocenyloxazolines were subsequently investigated (scheme 82). The lithiation/$PPh(CF_3)_2$ quenching protocol was shown not to be reproducible, and in general major synthetic problems arose as soon as an oxazoline side chain larger than methyl was present. A sufficient amount of *P*-trifluoromethyl ligands could nevertheless be obtained, and the diastereomers were shown to be separable by standard column chromatography on silica gel. Moreover, the ligand obtained allowed for coordination tests to Pd(II) and Pt(II) as well as catalytic trials.

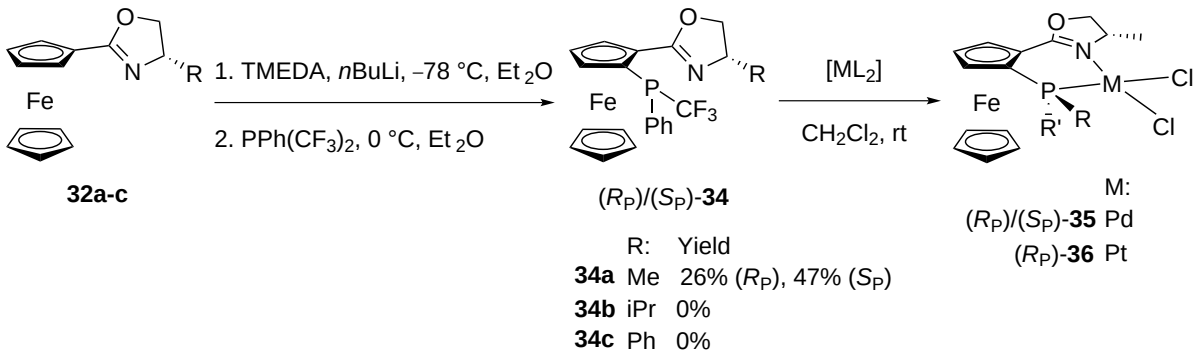

	R:	Yield
34a	Me	26% (R_P), 47% (S_P)
34b	iPr	0%
34c	Ph	0%

Scheme 82: 1,2-Ferrocenyloxazoline ligands **34a** and complexes **35** and **36** prepared in this work.

The ligand diastereomers were shown to be active in various asymmetric transformations. They however usually showed little enantioinduction, and in the reactions tested, the absolute configuration at phosphorus did not seem to play a role. The best catalytic result was obtained with the palladium-catalyzed allylic alkylation of cinnamyl acetate, where the *P*-trifluoromethyl ligands exhibited higher enantioselectivities as well as a preferential linear to branched ratio than the diphenyl parent ligand.

To assess the influence of steric hindrance in the lithiation/electrophilic substitution protocol, a different substitution pattern was subsequently chosen (scheme 83). The same synthetic procedures were applied to 1,1'-ferrocenyloxazolines, and it came to light that the preparative issue persisted with this substitution pattern. Once again, only minor amounts of an oxazoline ligand with a methyl side chain could be obtained. The obtained 1,1'-ferrocenyl diastereomers could moreover not be separated by column chromatography, contrary to the 1,2-ferrocenyl ligands. No preparative methods towards this end were found. The ligands could nonetheless be shown to coordinate to a Pd(II) center. In the course of this work, an alternate synthetic pathway to parent ligand **45** was developed, consisting of first the introduction of the phosphanyl moiety, and then the oxazoline ring formation.

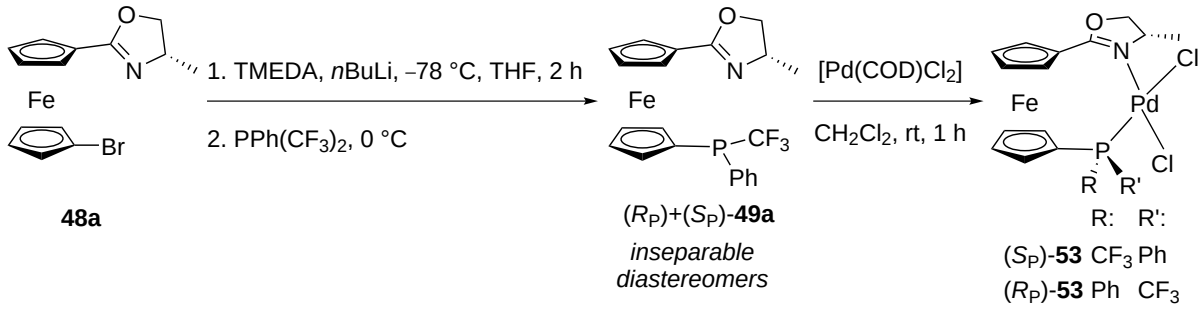

Scheme 83: 1,1'-Ferrocenyloxazoline ligands **49a** and Pd(II) complex **53** prepared in this work.

Finally, in chapter 4, *P*-trifluoromethyl derivatives of phenylethylferrocenyl ligands were considered (scheme 84). A synthetic pathway was developed to prepare the monotrifluoromethyl and the bistrifluoromethyl congeners via a primary phosphane intermediate. The monotrifluoromethyl ligands could be directly accessed by nucleophilic substitution of the bistrifluoromethyl ligand with phenyllithium. The preparative process could be scaled up on a laboratory scale.

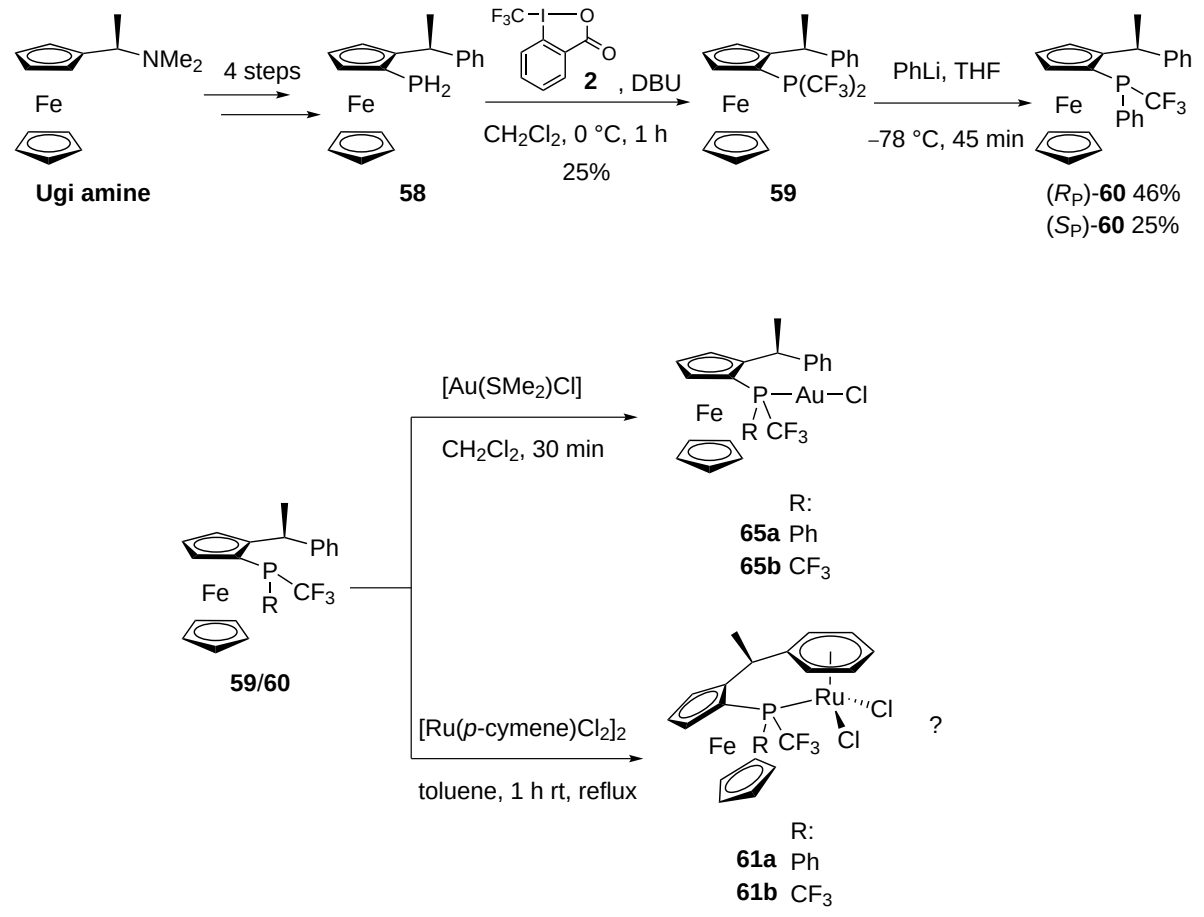

Scheme 84: Phenylethylferrocenyl ligands **59** and **60** and complexes **61** and **65** prepared in this work.

The coordination behavior to Ru(II) and Au(I) was assessed. It could not be determined if the Ru(II) complexes were coordinated in an η^6 fashion to the pendant phenyl ring, although *P*-coordination is evident. The gold(I) complexes were found to be quite unstable in air and in solution, but could nevertheless be characterized by multinuclear NMR spectroscopy. A

preliminary reactivity test was performed, by applying the ligands in the Ru(II)-catalyzed transfer hydrogenation of acetophenone. Under unoptimized conditions the ligands were all found to yield racemic product, however their catalytic behavior remains to be further assessed.

5.2 Outlook and closing remarks

Following the main goal of developing synthetic pathways towards trifluoromethyl *P*-stereogenic phosphanes, a few milestones were reached. New ligands could be prepared, bearing different types of chirality. Some were shown to be active in asymmetric catalysis and the activity of others remains to be assessed. Further investigation of the modification of BINAP-type ligands also promises to be an interesting topic, albeit challenging from a synthetic point of view. The major difficulty encountered during this work was the preparation of the compounds. Although some progress was made, robust synthetic protocols still need to be developed, especially towards the oxazoline ligands, as no reliable pathway was found.

Concerning synthetic pathways, many preparative experiments taken from literature were found to be unreproducible in the course of this work. This general, common problem in science has gained some attention in the last few years, but it however remains an issue than needs to be practically addressed and implemented. In a very recent publication (which appeared during the writing process of this thesis), Bergman and Danheiser have delivered some recommendations in this direction.[203] It is an issue that must not be ignored or taken lightly as, in the end, "reproducibility is a defining feature of science."[203][29]

Better understanding of catalytic mechanisms may also allow a more rational ligand design. This would certainly profit of collaborations with computer chemists as well as industrial chemists, and possibly allow the design of structures for specific catalytic challenges. However, as expressed by the esteemed Eric Jacobsen in his seminal paper coining the concept of *privileged chiral catalysts*[50]: "[...] the identification of new privileged ligands and catalysts remains enormously difficult and often requires a degree of serendipity. [...] The emergence of privileged classes of catalysts for asymmetric synthesis also presents a tantalizing opportunity on the mechanistic front. Efforts to understand the features that account for the broad applicability of these structures and to apply this understanding to the development of new privileged catalysts is an ongoing, exciting challenge for organic chemists today."

Electron-poor phosphanes remain a rare ligand type, and examples bearing a trifluoromethyl *P*-stereogenic phosphane are even more scarce. Such ligands have demonstrated their utility in asymmetric transformations, and as the field of enantioselective catalysis is boundless, there will always be a demand for chiral ligands. As a final thought, the words spoken by the respected William Knowles in his Nobel lecture speech[207] will remain a motivational base for chemists designing new ligands: "We can look on these catalysts as a labor-saving device for the laboratory. For this, they will have an impact for as long as chemists run reactions."

[29] For further reading on this topic, see:[204][205] as well as the IUPAC Gold Book entry for *reproducibility*.[206]

6 Experimental

6.1 General remarks

The procedures are not optimized for yields. If literature procedures were adapted or new analytical data was obtained it is compiled here in the synthetic part. In order to have a clear and consistent way of describing planar chirality and absolute configuration of stereogenic atoms, the following system was applied for generating stereodescriptors: phosphorus absolute configuration is denoted by a subscript capital P (R_P or S_P), whereas ferrocene planar chirality is denoted by a subscript Fc suffix (R_{Fc} or S_{Fc}). This is to avoid confusion with the IUPAC defined stereodescriptors for planar chirality (R_p) and (S_p). All stereodescriptors are placed at the beginning of the name.
All IUPAC names were generated using ACD/Name software (version 2015 2.5). Planar chiral and stereogenic phosphorus stereodescriptors were generated as previously mentioned.

6.1.1 Techniques

All moisture and/or air-sensitive reactions were carried out under an argon atmosphere using standard Schlenk techniques. Glassware was either heated in an oven at 150 °C for several hours or with a heat gun for several minutes under high vacuum before purging with argon.
Solvents for sensitive reactions were distilled under argon using an appropriate drying agent (toluene from sodium, hexane from sodium/benzophenone/tetraglyme, pentane from sodium/benzophenone/diglyme, MeOH, CH_2Cl_2 and CH_3CN from CaH_2, EtOH from sodium/diethyl phthalate, Et_2O and THF from sodium/benzophenone) or were purchased from Acros as bottled solvent over molecular sieves (CH_2Cl_2, Et_2O, hexane, THF). Thin layer chromatography, flash column chromatography and GC-MS measurements were performed with technical grade solvents.
Deuterated solvents were purchased from Armar Chemicals ($CDCl_3$) or Cambridge Isotope Laboratories (CD_2Cl_2, CD_3CN, D_2O). The solvents were used as received or distilled from CaH_2, degassed by several freeze-pump-thaw cycles and stored in a Young Schlenk over 3 Å or 4 Å molecular sieves under an argon atmosphere for sensitive samples ($CDCl_3$, CD_2Cl_2).

6.1.2 Chemicals

Chemicals were purchased from abcr, Acros, Apollo Scientific, Fluka, Fluorochem, Lancaster, PanGas, Sigma-Aldrich, Strem, TCI and VWR and used without further purification unless otherwise noted. TMEDA was filtered over neutral alumina and stored in a Young Schlenk flask. If necessary, *n*BuLi was titrated using *N*-pivaloyl-*o*-toluidine as reported by Suffert.[208]

1-Trifluoromethyl-1,2-benziodoxol-3(1*H*)-one **2**,[109] 1-bromo-2-(1-*N*,*N*-dimethylamino)-ethyl)ferrocene **55** ("Brugiamine"),[193] 1-bromo-2-(1-phenylethyl)ferrocene **56**,[193] 1-diphenylphosphanyl-2-(1-phenylethyl)ferrocene **54**,[193] ligand and metal precursors were prepared according to standard or cited procedures. [Pd(COD)Cl_2] was kindly provided by Peter Ludwig. *t*BuBrettPhos was synthesized and kindly provided by Barbara Czarniecki. [Fc]PF_6 and DHIQ **43** were prepared and kindly provided by Rino Schwenk. Resolved Ugi amine, [Au(SMe_2)Cl] and [Ir(COD)Cl]$_2$ were kindly provided by Lukas Sigrist. [Ru(*p*−cymene)Cl_2]$_2$ was kindly provided by Ewa Pietrasiak. *N*-Pivaloyl-*o*-toluidine was prepared and kindly provided by Raphael Bigler. [Pt(SMe_2)$_2$$Cl_2$] was prepared and kindly provided by Carl-Philipp Rosenau.

Ligand **5** was prepared according to Koller,[111] with two modifications: DIPEA was used instead of pyridine for the triflation of BINOL, and the LAH reduction of the phosphonate was worked-up using the Fieser protocol to avoid the formation of an intractable emulsion.[209] All PHOX precursors (4,5-dihydrooxazoles) were prepared from 2-bromobenzonitrile and the desired amino alcohol under $ZnCl_2$ catalysis in refluxing chlorobenzene.[210] Amino alcohols were prepared by reduction of commercially available amino acids with $LiAlH_4$ followed by basic work-up and recrystallization if necessary.[211]

6.1.3 Analytics

Thin layer chromatography (TLC) was run on Merck aluminium sheets covered with silica gel 60 F_{254} and were visualized by fluorescence quenching at 254 or 366 nm.

Preparative thin layer chromatography was performed on Merck 20x20 cm PLC glass plates covered with 2 mm silica gel 60 F_{254}. Bands were detected either visually (by color) or by fluorescence quenching at 254 or 366 nm.

Flash column chromatography (FC) was performed either manually on Fluka or SiliaFlash silica gel P60, both with 40-63 μm particle size (60 Å pore size/230-400 mesh) following the method published by Kahn *et al.*[212] where the solvents are given as volume ratios and the eluent flow was forced by 0.1-0.3 bar of air, or by an automated flash column chromatography system (Teledyne Isco Combiflash Rf+ 200 Lumen) with ELS and UV/vis detectors using universal RediSep silica gel cartridges and eluting with a pressure of a few bars.

Gas chromatography-mass spectrometry (GC-MS) used for reaction control was performed on an Agilent GC 7890A with an HP-5MS column (30 m x 250 μm x 0.25 μm), with a column flow of 1.7 ml/min using helium as carrier gas, and an Agilent mass spectrometer 5975C VL MSD operating in EI positive mode. Sample injection was done by an Agilent autosampler ALS 7693, 1 μl at $<$1 mg/ml in split mode (split ratio 100:1). The standard method used consisted of the following temperature program: 2 min at 50 °C, ramp of 20 °C/min with 2 min hold time at 300 °C (16.5 min total time). For heavy or not so volatile compounds, a high mass method was used consisting of the following temperature program: 2 min at 50 °C, ramp of 20 °C/min with 8 min hold time at 300 °C (22.5 min total time).

High performance liquid chromatography (HPLC) was performed on an Agilent 1100 series system with DAD detector at five different wavelengths (210, 220, 230, 254, 280 nm) or on a ThermoScientific Dionex UltiMate 3000 with DAD detector at 210, 230, 254, and 278 nm. Samples were dissolved in pure hexane or the given eluent composition at about 1 mg/ml. Retention times are given in minutes. Specific measurement parameters for each substance are cited.

Gas chromatography (GC) was performed on a Thermo Scientific Trace 1310 gas chromatograph with FID detector and β-dex 120 column (30 m x 0.25 mm x 0.25 μm film). Helium was used as carrier gas (1.4 ml/min), and the injector and detector were heated to 200 °C. The temperature programs are given for the corresponding substances. Retention times are given in minutes.

High resolution mass spectrometry (HRMS) was performed by the Mass Spec-

trometry Service Lab in the Laboratory of Organic Chemistry at ETH Zurich. The signals are given as mass-to-charge ratio (m/z).

Melting points (M.P.) were measured on a Büchi B-450 in an open capillary and are uncorrected.

For structure elucidation by **X-ray diffraction**, intensity data for single crystals mounted on MiTeGen MicroLoops were collected. The crystals were cooled to 100 K for measurement and the diffraction pattern was collected by a Bruker SMART APEX, APEXII platform with CCD detector or Venture D8. Graphite monochromated Mo-K_α-radiation (λ=0.71073 Å) was applied. The program SMART was used for data collection, integration was performed with SAINT.[213] The structures were solved by direct or heavy atom (Patterson) method, respectively, or by charge flipping, using the program SHELXS-97.[214] The refinement and all further calculations were carried out using SHELXL-97.[215] All non-hydrogen atoms were refined anisotropically using weighted full-matrix least-squares on F^2. The hydrogen atoms were included in calculated positions and treated as riding atoms using the SHELXL default parameters. An absorption correction was applied (SADABS)[216] and the weighting scheme was optimized in the final refinement cycles. The absolute configuration of chiral compounds was determined on the basis of the Flack parameter.[217][218] The standard uncertainties (s.u.) are rounded according to the "Notes for Authors" of Acta Crystallographica.[219] Detailed information about the crystal structures and their solutions is given in appendix C.

Nuclear magnetic resonance (NMR) spectra were recorded on a Bruker Avance AC-200, DPX-300, or DPX-700. All spectra were recorded at room temperature in the given solvent at the given frequency in non-spinning mode. Chemical shifts (δ) are given in ppm relative to the following external standards: tetramethylsilane (^{1}H, ^{13}C), $CFCl_3$ (^{19}F), 85% H_3PO_4 (^{31}P). Multiplicities are abbreviated as follows: s for singlet, d for doublet, t for triplet, q for quartet, quint for quintet, sext for sextet, sept for septet, and m for multiplet. The prefix br describes an obvious broadening of the signal. Coupling constants (J) are given in Hertz (Hz). Combined multiplicities with unresolvable coupling constants are cited as multiplets. Atoms were not assigned to signals if extensive broadening of signals was observed and assignments questionable.

6.2 Syntheses

6.2.1 Trifluoromethylated phosphanes and related compounds

((1,1'-Biphenyl)-2-yl)(phenyl)(trifluoromethyl)phosphane 20

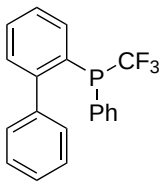

2-Bromo-1,1'-biphenyl (1 eq., 0.429 mmol, 0.073 ml) was dissolved in anhydrous Et_2O (3 ml) and cooled down to -78 °C. *n*BuLi (1 eq., 0.429 mmol, 0.295 ml, 1.6 M in hexanes) was then added, making the reaction mixture turn bright yellow. The reaction was warmed to rt and stirred for 30 min. The lithiated species was then added to a solution of $PPh(CF_3)_2$ in Et_2O (3 ml) cooled to -78 °C (yellowish-brown precipitate formed). It was then slowly warmed up to rt and further stirred overnight. The reaction mixture was quenched with sat. $NaHCO_3$, extracted once with Et_2O, dried over magnesium sulfate, filtered, and concentrated under

reduced pressure, yielding a yellowish-brown oil. The crude was filtered over a plug of silica gel eluting with hexane, yielding the title compound as an orange-brown oil (69.2 mg, 49%).

^{1}H NMR (300 MHz, $CDCl_3$): δ 7.69-7.66 (m, 1H, $H_{biphenyl}$), 7.62-7.59 (m, 2H, H_{PPh}), 7.48-7.33 (m, 10H, H_{Ar}), 7.24-7.18 (m, 1H, $H_{biphenyl}$); **^{19}F NMR** (282 MHz, $CDCl_3$): δ –54.0 (d, $J_{F\text{-}P}$ = 75.6 Hz, CF_3); **^{31}P{^{1}H} NMR** (121 MHz, $CDCl_3$): δ –5.7 (q, $J_{P\text{-}F}$ = 76.3 Hz, PCF_3).

Naphthalen-2-yl(trifluoromethyl)phosphane

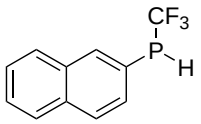

A suspension of 1-trifluoromethyl-1,2-benziodoxol-3(1*H*)-one (**2**) (1 eq., 8.43 mmol, 2.66 g) was added to a solution of naphthalen-2-ylphosphane (1 eq., 8.43 mmol, 1.35 g) in anhydrous CH_2Cl_2 (20 ml) at rt (the reaction was slightly exothermic). It was stirred for 4 h. The volatiles were then removed under reduced pressure using an external cooling trap yielding a slightly yellow oil (1.92 g, quant.). The product was used without further purification. The analytical data corresponds to literature.[117]

^{19}F NMR (282 MHz, $CDCl_3$): δ –51.2 (dd, $J_{F\text{-}P}$ = 59.2 Hz, $J_{F\text{-}H}$ = 11.3 Hz, PCF_3); **^{31}P{^{1}H} NMR** (121 MHz, $CDCl_3$): δ –40.3 (q, $J_{P\text{-}F}$ = 58.1 Hz, PCF_3).

Naphthalen-2-ylbis(trifluoromethyl)phosphane

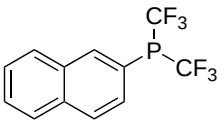

A suspension of 1-trifluoromethyl-1,2-benziodoxol-3(1*H*)-one (**2**) (1 eq., 3.51 mmol, 1.11 g) in anhydrous CH_2Cl_2 was added to a solution of naphthalen-2-yl(trifluoromethyl)phosphane (1 eq., 3.51 mmol, 0.801 g) in anhydrous CH_2Cl_2 (26 ml) at rt. The reaction mixture was cooled to –78 °C and DBU (1 eq., 3.51 mmol, 0.524 ml) was added dropwise. It was stirred 1 h at low temperature then brought to rt overnight (turned light yellow). The volatiles were removed under reduced pressure using an external trap yielding a highly viscous orange oil which was purified by column chromatography via Combiflash (40 g silica gel prepacked column) eluting with a pentane:ether gradient, yielding a colorless liquid. *Due to the high volatility of the product, the yield was not determined (conversion was 42% by ^{19}F NMR).* The analytical data corresponds to literature.[115]

^{19}F NMR (282 MHz, $CDCl_3$): δ –53.0 (d, $J_{F\text{-}P}$ = 79.7 Hz, PCF_3); **^{31}P{^{1}H} NMR** (121 MHz, $CDCl_3$): δ 0.0 (sept, $J_{P\text{-}F}$ = 79.3 Hz, PCF_3).

Phenyl(bis(trifluoromethyl))phosphane 4[115]

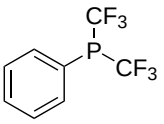

Method A: 4-Cyanophenol (2 eq., 50 mmol, 5.96 g) was suspended in anhydrous THF (80 ml) and triethylamine (2.1 eq., 52.5 mmol, 7.32 ml) was added. The reaction mixture was cooled to –78 °C, then dichlorophenylphosphane (1 eq., 25 mmol, 3.39 ml) was slowly added via syringe. The reaction mixture was brought to rt overnight, then the white solids were filtered off and the filtrate concentrated under reduced pressure yielding a yellow highly viscous oil (bis(4-cyanophenyl)phenylphosphonite, quant.) which was used without further purification. The oil was dissolved in Et_2O (50 ml) and MeCN (8 ml). $TMSCF_3$ (2.1 eq., 52.5 mmol, 7.76 ml) and a spatula tip of caesium fluoride were added at 0 °C. The reaction mixture was warmed up to rt and stirred for 5 h. Conversion

was checked by GC-MS and/or ^{31}P and ^{19}F NMR; if the reaction had not started, a further spatula tip of CsF was added. The volatiles were then removed using a cooling trap. The crude was filtered over a silica gel plug eluting with pentane, and the product was concentrated under reduced pressure (min. 750 mbar, 40 °C) yielding a clear, colorless, highly volatile liquid. **Method B**: To a suspension of $LiAlH_4$ (2 eq., 30 mmol, 1.14 g) in tetraglyme (40 ml) at 0 °C was slowly added a solution of dichlorophenylphosphane (1 eq., 15 mmol, 2.04 ml) in tetraglyme (10 ml). The reaction mixture was then stirred 1 h at rt. The product was distilled *in vacuo* ($1.5 \cdot 10^{-1}$ mbar, slight heating) in a Schlenk cooled to –78 °C, yielding a clear, colorless oil (phenylphosphane, quant.) which was used without further purification. To a solution of 1-trifluoromethyl-1,2-benziodoxol-3(1*H*)-one (2 eq., 30 mmol, 9.48 g) in anhydrous CH_2Cl_2 (15 ml) at 0 °C was added via syringe a solution of phenylphosphane in anhydrous CH_2Cl_2 (15 ml). DBU (4 eq., 60 mmol, 8.96 ml) was then added dropwise, making the reaction mixture turn reddish-brown; it was stirred and brought to rt overnight. The reaction mixture was adsorbed on silica gel, concentrated (750 mbar, 40 °C), and filtered over a silica gel plug eluting with pentane; the product eluted first. The fractions were collected and the solvent removed on the Rotavap (750 mbar, 35 °C) yielding a highly volatile, clear, colorless oil (1.7 g, 51%). The analytical data corresponds to literature.[115][117]

^{1}H NMR (300 MHz, $CDCl_3$): δ 7.85 (t, J = 9.0 Hz, 2H, H_{Ar}), 7.65 (td, J = 7.5 Hz, 3 Hz, 1H, H_{Ar}), 7.53 (td, J = 7.5 Hz, 3 Hz, 2H, H_{Ar}); **^{19}F NMR** (282 MHz, $CDCl_3$): δ –53.3 (d, $J_{F\text{-}P}$ = 79.0 Hz, PCF_3); **^{31}P{^{1}H} NMR** (121 MHz, $CDCl_3$): δ 0.0 (sept, $J_{P\text{-}F}$ = 79.7 Hz, PCF_3).

Chloroisopropylphosphane[220][221]

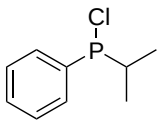

Isopropylmagnesium chloride (1.36 eq., 50 mmol, 2 M in THF, 25 ml) was added dropwise to a solution of dichlorophenylphosphane (1 eq., 36.8 mmol, 5 ml) in THF (20 ml) at –78 °C (1 h), then brought to rt. More THF (20 ml) was added to ensure proper stirring (the reaction mixture became quite thick). Conversion was checked by ^{31}P NMR (unlocked). When $PPhCl_2$ was completely consumed, the solution was filtered off via cannula filter and THF removed with an external cooling trap. The mixture was distilled under vacuum (T_{bath}=130 °C, 0.18 mbar), yielding a colorless liquid. Quite a lot of THF and side product were still present (seen in ^{1}H NMR). The crude was therefore redistilled using a 20 cm Vigreux column (T_{bath}=130 °C, T_{vapor}=75 °C, 0.3 mbar). 1 ml of clear, slightly yellow liquid was obtained (pure product, density unknown, not weighed, unknown yield). The analytical data corresponds to literature.

^{1}H NMR (300 MHz, $CDCl_3$): δ 7.75-7.65 (m, 2H, H_{Ar}), 7.47-7.43 (m, 3H, H_{Ar}), 2.25-2.10 (dsept, 1H, PC*H*), 1.11 (br d, 6H, $(CH_3)_2$); **^{13}C{^{1}H} NMR** (75 MHz, $CDCl_3$): δ 137.6 (d, $J_{C\text{-}P}$ = 35.8 Hz, 1C, PC_{Ar}), 131.4 (d, $J_{C\text{-}P}$ = 24.8 Hz, 2C, C_{Ar}), 130.5 (pseudo d, $J_{C\text{-}P}$ = 1.1 Hz, 1C, C_{Ar}), 128.5 (d, $J_{C\text{-}P}$ = 7.7 Hz, 2C, C_{Ar}), 34.3 (d, $J_{C\text{-}P}$ = 26.4 Hz, 1C, P*C*H), 17.6 (br d, $J_{C\text{-}P}$ = 17.6 Hz, 2C, CH_3); **^{31}P NMR** (121 MHz, $CDCl_3$): δ 102.0 (septs, $J_{P\text{-}H}$ = 7.5 Hz); **^{31}P{^{1}H} NMR** (121 MHz, $CDCl_3$): δ 102.0 (s).

6.2.2 Trifluoromethylated PHOX ligands

General procedure for the preparation of P-trifluoromethylated PHOX ligands 26a–d

The bromoarene precursor (1 eq.) was dissolved in anhydrous Et_2O and cooled to –78 °C (acetone/dry ice). *n*-Butyllithium (1.1 eq.) was added dropwise and the reaction mixture stirred at low temperature between 30 min and 2 h. A solution of bis(trifluoromethyl)phenylphosphane or naphthalen-2-ylbis(trifluoromethyl)phosphane in anhydrous Et_2O was then slowly added to the reaction mixture, which was subsequently stirred and brought to room temperature overnight. The volatiles were removed using a cooling trap (unreacted $PPh(CF_3)_2$ was recovered). The crude was dissolved in CH_2Cl_2 and filtered through a plug of silica gel eluting with hexane:EtOAc.

(4*S*)-2-(2-(phenyl(trifluoromethyl)phosphanyl)phenyl)-4-(propan-2-yl)-4,5-dihydro-1,3-oxazole
26a

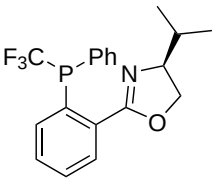

The title compound was prepared following the general procedure using TMEDA (1 eq., 0.373 mmol, 0.0563 ml) as additive and bis(trifluoromethyl)phenylphosphane (1.2 eq., 0.448 mmol, 110 mg) as electrophile, yielding the mixture of diastereomers (1:2) as a colorless oil (127 mg, 94%).

^{1}H NMR (300 MHz, CD_2Cl_2): δ 7.95-7.30 (m, 18H, H_{Ar}), 4.28 (t, J = 8.7 Hz, 1H, $NCHCH_2$), 4.21 (t, J = 8.9 Hz, 1H, $NCHCH_2$), 4.04-3.90 (m, 3H, $NCHCH_2$), 3.70 (q, J = 8.7 Hz, 1H, $NCHCH_2$), 1.66 (sext, J = 6.8 Hz, 1H, $CH(CH_3CH_3)$, diast1), 1.43 (sext, J = 6.8 Hz, 1H, $CH(CH_3CH_3)$, diast2), 1.01 (d, J = 6.6 Hz, 3H, $CH(CH_3CH_3)$, diast1), 0.91 (d, J = 6.8 Hz, 3H, $CH(CH_3CH_3)$, diast2), 0.61 (d, J = 6.6 Hz, 3H, $CH(CH_3CH_3)$, diast1), 0.50 (d, J = 6.8 Hz, 3H, $CH(CH_3CH_3)$, diast2); **^{19}F NMR** (282 MHz, $CDCl_3$): δ –55.0 (d, $J_{F\text{-}P}$ = 71.5 Hz, CF_3, diast1), –55.1 (d, $J_{F\text{-}P}$ = 71.5 Hz, CF_3, diast2); **^{31}P NMR** (121 MHz, $CDCl_3$): δ –4.4 (q, $J_{P\text{-}F}$ = 71.8 Hz, PCF_3, diast1), –5.0 (q, $J_{P\text{-}F}$ = 71.8 Hz, PCF_3, diast2); **HRMS** (MALDI) calcd. (m/z) for $C_{19}H_{20}F_3NOP$: 366.1229 ($[M+H]^+$), found: 366.1230 ($[M+H]^+$).

(4*S*)-4-phenyl-2-(2-(phenyl(trifluoromethyl)phosphanyl)phenyl)-4,5-dihydro-1,3-oxazole
26b

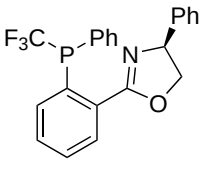

The title compound was prepared following the general procedure using TMEDA (1 eq., 0.48 mmol, 0.0724 ml) as additive and bis(trifluoromethyl)phenylphosphane (1.2 eq., 0.576 mmol, 142 mg) as electrophile, yielding the mixture of diastereomers (1:1.5) as a light yellow oil (15.8 mg, 8%).

^{1}H NMR (300 MHz, $CDCl_3$): δ 8.11-7.07 (m, 27H, H_{Ar}), 6.68 (d, J = 8.0 Hz, 1H, H_{Ar}), 5.35 (t, J = 9.0 Hz, 1H, $NCHCH_2$), 5.06 (t, J = 9.0 Hz, 1H, $NCHCH_2$), 4.69-4.54 (m, 2H, $NCHCH_2$), 4.08-3.95 (m, 2H, $NCHCH_2$); **^{19}F NMR** (282 MHz, $CDCl_3$): δ –55.1 (d, $J_{F\text{-}P}$ = 73.6 Hz, CF_3, diast1), –55.2 (d, $J_{F\text{-}P}$ = 72.6 Hz, CF_3, diast2); **^{31}P{^{1}H} NMR** (121 MHz, $CDCl_3$): δ –3.2 (q, $J_{P\text{-}F}$ = 73.3 Hz, $PPhCF_3$, diast1), –4.3 (q, $J_{P\text{-}F}$ = 73.3 Hz, $PPhCF_3$, diast2); **HRMS** (MALDI) calcd. (m/z) for $C_{22}H_{18}F_3NOP$: 400.1073 ($[M+H]^+$),

found: 400.1073 ([M+H]$^+$).

(4*S*)-4-tert-butyl-2-(2-(phenyl(trifluoromethyl)phosphanyl)phenyl)-4,5-dihydro-1,3-oxazole
26c

The title compound was prepared following the general procedure using bis(trifluoromethyl)phenylphosphane (0.6 eq., 0.57 mmol, 140 mg) as electrophile, yielding the mixture of diastereomers (1:1.6) as a yellow oil (200 mg, 56%).

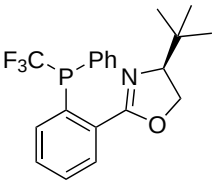

^{1}H NMR (300 MHz, $CDCl_3$): δ 7.97-7.28 (m, 18H, H_{Ar}), 4.37-4.01 (m, 5H, $NCHCH_2$), 3.70 (dd, J = 9.0 Hz, 1H, $NCHCH_2$), 0.95 (s, 18H, $C(CH_3)_3$); **^{19}F NMR** (282 MHz, $CDCl_3$): δ –54.5 (d, $J_{F\text{-}P}$ = 71.5 Hz, CF_3, diast1), –54.7 (d, $J_{F\text{-}P}$ = 71.5 Hz, CF_3, diast2); **^{31}P{^{1}H} NMR** (121 MHz, $CDCl_3$): δ –3.0 (q, $J_{P\text{-}F}$ = 71.4 Hz, PCF_3, diast1), –4.4 (q, $J_{P\text{-}F}$ = 71.4 Hz, PCF_3, diast2); **HRMS** (MALDI) calcd. (m/z) for $C_{20}H_{22}F_3NOP$: 380.1386 ([M+H]$^+$), found: 380.1386 ([M+H]$^+$).

(4*S*)-2-(2-((naphthalen-2-yl)(trifluoromethyl)phosphanyl)phenyl)-4-phenyl-4,5-dihydro-1,3-oxazole
26d

The title compound was prepared following the general procedure using naphthalen-2-ylbis(trifluoromethyl)phosphane (0.6 eq, 0.41 mmol, 122 mg) as electrophile, yielding the mixture of diastereomers (1:6.5) as a colorless oil which crystallized upon standing (82.1 mg, 19%).

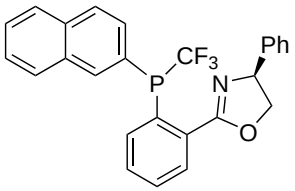

^{1}H NMR (300 MHz, $CDCl_3$): δ 8.41-7.31 (m, 32H, H_{Ar}), 6.90 (t, J = 9.0 Hz, 1H, $H_{oxazoline}$), 6.66 (t, J = 9.0 Hz, 1H, $H_{oxazoline}$), 6.46 (d, J = 9.0 Hz, 1H, $H_{oxazoline}$), 5.32 (t, J = 9.0 Hz, 1H, $H_{oxazoline}$), 4.63 (dd, J = 9.0 Hz, 1H, $H_{oxazoline}$), 3.98 (t, J = 9.0 Hz, 1H, $H_{oxazoline}$); **^{19}F NMR** (282 MHz, $CDCl_3$): δ –54.3 (d, $J_{F\text{-}P}$ = 72.6 Hz, CF_3, diast1), –54.4 (d, $J_{F\text{-}P}$ = 72.6 Hz, CF_3, diast2); **^{31}P{^{1}H} NMR** (121 MHz, $CDCl_3$): δ –2.7 (q, $J_{P\text{-}F}$ = 73.3 Hz, $PPhCF_3$, diast1), –3.9 (q, $J_{P\text{-}F}$ = 73.3 Hz, $PPhCF_3$, diast2); **HRMS** (MALDI) calcd. (m/z) for $C_{26}H_{20}F_3NOP$: 450.1229 ([M+H]$^+$), found: 450.1230 ([M+H]$^+$).

6.2.3 1,2-Ferrocenyloxazoline precursors and ligands

General procedure for the preparation of ferrocenyloxazolines 32[171]

Carboxyferrocene (1 eq.) was dissolved in anhydrous CH_2Cl_2 (15 ml) and oxalyl chloride (3 eq.) was added dropwise. The reaction mixture bubbled slightly and turned deep red. It was stirred at rt for 1 h. The volatiles were removed using an external cooling trap and the residue was redissolved in anhydrous CH_2Cl_2 (20 ml) and cooled to 0 °C. Triethylamine (2.5 eq.) was slowly added and the mixture was stirred for a few minutes. The amino alcohol (1.2 eq.) was then added dropwise. After 2 h stirring at 0 °C, methanesulfonyl chloride (2.5 eq.) and

triethylamine (2.5 eq.) were subsequently added dropwise. The reaction mixture was further stirred in the ice bath and gradually brought to rt overnight. It was then quenched with sat. $NaHCO_3$, extracted three times with CH_2Cl_2, washed with brine, dried over magnesium sulfate, filtered, and concentrated under reduced pressure.

(4*S*)-(4,5-Dihydro-4-methyl-2-oxazolyl)ferrocene 32a

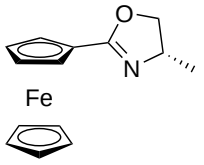

The title compound was obtained from (*S*)-2-aminopropan-1-ol (1.2 eq., 31.2 mmol, 2.44 ml) following the general procedure. The dark brown crude was adsorbed on silica gel and filtered through a silica gel column eluting with hexane:EtOAc 1:1, yielding a red solid (5.99 g, 86%).

^{1}H NMR (300 MHz, $CDCl_3$): δ 4.74 (s, 2H, Cp*H*), 4.41 (t, J = 8.5 Hz, 1H, CH_2), 4.33 (s, 2H, Cp*H*), 4.21 (m, 1H, C*H*), 4.18 (s, 5H, Cp*H*), 3.85 (t, J = 7.5 Hz, 1H, CH_2), 1.31 (d, J = 6.6 Hz, 3H, CH_3); **^{13}C{^{1}H} NMR** (75 MHz, $CDCl_3$): δ 166.1 (s, 1C, C*C*=N), 73.9 (s), 70.4 (s), 69.8 (s), 69.2 (s), 69.1 (s), 62.0 (s), 21.7 (s, *C*H_3); **HRMS** (MALDI) calcd. (*m/z*) for $C_{14}H_{16}FeNO$: 270.0576 ([M+H]$^+$), found: 270.0576 ([M+H]$^+$). **M.P.**: 79-81 °C.

(4,5-Dihydro-1,3-oxazol-2-yl)ferrocene 32d

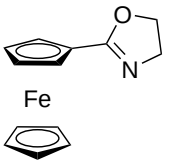

The title compound was obtained from ethanolamine (1.2 eq., 5.22 mmol, 0.315 ml) following the general procedure. The crude was first purified by column chromatography via Combiflash (24 g silica gel prepacked column) eluting with a hexane:EtOAc gradient, then recrystallized from hot hexane, yielding a bright orange microcrystalline solid (418 mg, 38%).

^{1}H NMR (300 MHz, $CDCl_3$): δ 4.74 (t, J = 1.9 Hz, 2H, Cp*H*), 4.37-4.31 (m, 4H, Cp*H* (2H) & CH_2 (2H)), 4.19 (s, 5H, Cp*H*), 3.90 (t, J = 9.0 Hz, 2H, CH_2); **^{13}C{^{1}H} NMR** (75 MHz, $CDCl_3$): δ 167.2 (s, 1C, C*C*=N), 70.4 (s), 69.8 (s), 69.1 (s), 67.4 (s), 55.0 (s, *C*H_2); **HRMS** (MALDI) calcd. (*m/z*) for $C_{13}H_{13}FeNO$: 255.0341 ([M]$^+$), found: 255.0341 ([M]$^+$); **M.P.**: 148-152 °C.

General procedure for the preparation of ferrocenyloxazoline ligands

The ferrocenyloxazoline precursor (1 eq.) and TMEDA (1.3 eq.) were dissolved in anhydrous THF and cooled to –78 °C (acetone/dry ice). *n*-Butyllithium (1.3 eq.) was added dropwise and the reaction mixture stirred at low temperature for 2 h, then brought to rt. The corresponding electrophile (2 eq.) was slowly added at 0 °C to the reaction mixture, which was subsequently stirred and brought to room temperature overnight. The reaction was diluted with diethyl ether and quenched with sat. $NaHCO_3$. The phases were separated and the aqueous phase extracted twice with Et_2O. The combined organics were dried over Na_2SO_4, filtered, and concentrated under reduced pressure.

(S_C,S_{Fc})-1-(Diphenylphosphanyl)-2-(4-methyl-4,5-dihydro-1,3-oxazol-2-yl)ferrocene 33

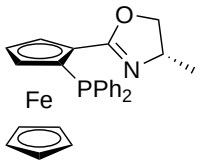

The title compound was prepared following the general procedure using $PPhCl_2$ (2 eq., 3.2 mmol, 0.574 ml) as electrophile and isolated by column chromatography via Combiflash with a 40 g silica gel prepacked column eluting with a hexane:EtOAc gradient yielding a brown solid (200 mg, 28%).

^{1}H NMR (200 MHz, $CDCl_3$): δ 7.54-7.18 (m, 10H, H_{Ar}), 4.23 (s, 5H, Cp*H*), 3.41 (t, J = 8.4 Hz, 1H, C*H*CH_3), 1.14 (d, J = 6.5 Hz, 3H, CHCH_3), CHCH_2 (2H) and Cp*H* (3H) could not be unambiguously assigned due to an obvious paramagnetic broadening of the spectrum; **^{31}P{^{1}H} NMR** (121 MHz, $CDCl_3$): δ –16.7 (s, *P*Ph_2); **HRMS** (MALDI) calcd. (*m*/*z*) for $C_{26}H_{24}FeNOP$: 453.0939 ($[M]^+$), found: 453.0935 ($[M]^+$).

General procedure for the preparation of P-trifluoromethylated Fcox ligands 34a

The ferrocenyloxazoline precursor (1 eq.) was dissolved in anhydrous solvent and cooled to –78 °C (acetone/dry ice). *n*-Butyllithium (1.3 eq.) was added dropwise and the reaction mixture stirred at low temperature between 30 min and 2 h. The low temperature bath was then replaced with an ice bath and the mixture stirred for approximately 5 min at 0 °C. A solution of bis(trifluoromethyl)phenylphosphane (0.5 eq.) in anhydrous solvent was then slowly added to the reaction mixture, which was subsequently stirred and brought to room temperature overnight. The reaction was diluted with diethyl ether and quenched with sat. $NaHCO_3$. The phases were separated and the aqueous phase extracted twice with Et_2O. The combined organics were dried over Na_2SO_4, filtered, and concentrated under reduced pressure. The diastereomers were separated via silica gel flash chromatography eluting with hexane:EtOAc.

(S_C,R_P,S_{Fc})-1-(4-methyl-4,5-dihydro-1,3-oxazol-2-yl)-2-(phenyl(trifluoromethyl)phosphanyl)ferrocene (R_P)-34a

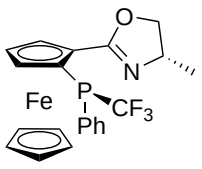

The title compound was prepared following the general procedure using $PPh(CF_3)_2$ (0.5 eq, 0.558 mmol, 137.3 mg) as electrophile and isolated on silica gel eluting with hexane:EtOAc 1:1, yielding a brown oil which crystallized upon standing (64 mg, 26%). The absolute configuration of the phosphorus atom was determined by using the Flack parameter obtained via X-ray diffraction of a single crystal.

^{1}H NMR (300 MHz, $CDCl_3$): δ 8.10 (dd, $J_{H\text{-}H}$ = 12.5 Hz, 7.6 Hz, 1H, H_{Ar}), 7.60-7.50 (m, 4H, H_{Ar}), 5.06 (br s, 1H, Cp*H*), 4.46 (br t, $J_{H\text{-}H}$ = 2.5 Hz, 1H, Cp*H*), 4.56 (br s, 1H, Cp*H*), 4.06 (s, 5H, Cp*H*), 1.34 (d, $J_{H\text{-}H}$ = 6.6 Hz, 3H, CH_3), C*H* and CH_2 not found (overlapping with Cp*H* signals); **^{19}F NMR** (282 MHz, $CDCl_3$): δ –56.3 (d, $J_{F\text{-}P}$ = 64.9 Hz, PCF_3); **^{31}P{^{1}H} NMR** (121 MHz, $CDCl_3$): δ –11.0 (q, $J_{P\text{-}F}$ = 65.4 Hz, *P*CF_3); **HRMS** (ESI) calcd. (*m*/*z*) for $C_{21}H_{20}F_3FeNOP$: 446.0579 ($[M+H]^+$), found: 446.0579 ($[M+H]^+$).

(S_C,S_P,S_{Fc})-1-(4-methyl-4,5-dihydro-1,3-oxazol-2-yl)-2-(phenyl(trifluoromethyl)-phosphanyl)ferrocene
(S_P)-34a

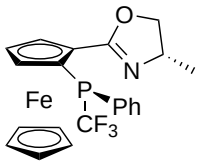

The title compound was prepared following the general procedure using $PPh(CF_3)_2$ (0.5 eq, 0.558 mmol, 137.3 mg) as electrophile and isolated on silica gel eluting with hexane:EtOAc 1:1, yielding a brown oil (117 mg, 48%). The P-stereogenicity was deduced from the X-ray structure of the other diastereoisomer.

^{1}H NMR (300 MHz, $CDCl_3$): the signals could not be assigned due to an obvious paramagnetic broadening of the spectrum; **^{19}F NMR** (282 MHz, $CDCl_3$): δ –55.2 (d, $J_{F\text{-}P}$ = 67.7 Hz, PCF_3); **^{31}P NMR** (121 MHz, $CDCl_3$): δ –10.5 (q, $J_{P\text{-}F}$ = 69.0 Hz, PCF_3); **HRMS** (ESI) calcd. (m/z) for $C_{21}H_{20}F_3FeNOP$: 446.0579 ($[M+H]^+$), found: 446.0574 ($[M+H]^+$).

6.2.4 1,1'-Ferrocenyloxazoline precursors and ligands

1,1'-Dibromoferrocene 46

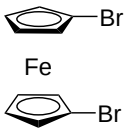

Method A: Tetrabromoethane as bromine source with oxidative work-up procedure[182]
To a stirred solution of ferrocene (1 eq., 53.8 mmol, 10 g) and TMEDA (2.33 eq., 125 mmol, 18.9 ml) in anhydrous hexane (50 ml) at 0 °C was added *n*BuLi (2.13 eq., 114 mmol, 1.6 M in hexanes, 2.13 ml). The reaction mixture was slowly brought to rt and stirred overnight. The next day, stirring was stopped, the suspension decanted and the solvent removed via cannula filtration. The solid was suspended in dry Et_2O and cooled to –78 °C. A solution of tetrabromoethane (2.15 eq., 116 mmol, 13.5 ml) in anhydrous Et_2O (50 ml) was added to the orange solution at –78 °C over 4 h, making the reaction mixture turn black. The solution was slowly warmed to room temperature overnight, yielding a liquid system with a black residue on the walls of the flask. The liquid layer was transferred to another flask (dark red with some black solids), quenched with water and separated, yielding a dark orange oil and some black residue after solvent removal. The crude was dissolved in hexane, filtered through Celite and washed with sat. aq. $FeCl_3$ (3x100 ml, until no more un- or monosubstituted products could be seen by GC-MS). The organic phase was then washed with water until colorless, dried over $MgSO_4$, filtered (30 g silica, eluting with hexane) and concentrated under reduced pressure yielding a dark orange liquid. Residual tetrabromoethane was removed by microdistillation ($4.5 \cdot 10^{-1}$ mbar, 80 °C) yielding the title compound as a dark brown-yellow microcrystalline solid (3 g, 16%).

Method B: 1,2-Dibromotetrachloroethane as bromine source
To a solution of ferrocene (1 eq., 19.5 g, 105 mmol) in dry hexane (195 ml) were added dropwise TMEDA (2.4 eq., 251 mmol, 37.9 ml) and *n*BuLi (2.2 eq., 230 mmol, 144 ml, 1.6 M in hexanes) at room temperature. The reaction mixture was stirred at room temperature overnight, during which it turned slightly red. The next day, stirring was stopped and the suspension decanted. The solvent was removed via cannula and syringe. The solid was washed once with dry hexane and then dissolved in dry THF (150 ml). The orange solution was added to a solution of 1,2-dibromotetrachloroethane (2.0 eq., 209 mmol, 25.1 ml) in THF (150 ml) via cannula at –78 °C (turned dark brown-greenish). The solution was slowly warmed to room temperature. The reaction was quenched after 3 h by addition of water then diluted with diethyl ether. After addition of brine, the layers were separated and

the aqueous phase was extracted with diethyl ether (2x). The combined organic fractions were dried over $MgSO_4$ and concentrated to give the crude product as a brown oil. The crude was purified twice by FC on silica gel, eluting with 100% hexane, yielding the title compound as a dark red crystalline solid (18.3 g, 45%, 90% purity and 11.4 g, 25%, 78% purity).

Method C: 1,2-Dibromotetrafluoroethane as bromine source[173]
Ferrocene (1 eq., 64.5 mmol, 12 g) was dissolved in dry hexane (120 ml). At room temperature, TMEDA (2.4 eq., 155 mmol, 23.4 ml) and *n*BuLi (2.2 eq., 142 mmol, 88.7 ml, 1.6 M in hexanes) were added via cannula. The reaction mixture was left to stir at room temperature overnight. The next day, stirring was stopped and the suspension decanted. The solvent was removed, the residue washed once with dry hexane and then dissolved in dry THF (100 ml). At –78 °C, the solution of 1,1'-dilithioferrocene in THF was carefully transferred via cannula into a solution of 1,2-dibromotetrafluoroethane (2.5 eq., 161 mmol, 19.3 ml) in THF (100 ml), making the reaction mixture turn dark brown. The solution was slowly warmed to room temperature and quenched after 3.5 h by addition of water. It was diluted with diethyl ether and the aqueous phase was extracted with diethyl ether (2x). The combined organic fractions were washed with brine, dried over $MgSO_4$ and the volatiles removed under reduced pressure yielding the crude product as a black oil. It was purified by flash column chromatography using a hexane:EtOAc eluent gradient yielding the title compound as a brown-yellow solid (9 g, 41%).

^{1}H NMR (300 MHz, $CDCl_3$): δ 4.43 (s, 4H, Cp*H*), 4.17 (s, 4H, Cp*H*); **^{13}C{^{1}H} NMR** (75 MHz, $CDCl_3$): δ 78.2 (s, *C*Br), 72.7 (s, *C*H), 69.9 (s, *C*H); **HRMS** (EI+) calcd. (*m/z*) for $C_{10}H_8Br_2Fe$: 341.8342 ($[M]^+$), found: 341.8346 ($[M]^+$); **M.P.**: 47-50 °C.

1-Bromo-1'-carboxyferrocene 47

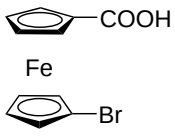

1,1'-Dibromoferrocene (1 eq., 8.58 mmol, 2.95 g) was dissolved in anhydrous THF (50 ml) and cooled with an acetone/dry ice bath. *n*BuLi (1 eq., 8.58 mmol, 1.6 M in hexanes, 5.36 ml) was added, and the reaction mixture stirred at low temperature for 20 min, during which the precipitation of 1-bromo-1'-lithioferrocene was clearly observable. CO_2(g) was then bubbled through the reaction mixture a few minutes, making it immediately turn deep red and homogeneous; it was further stirred at low temperature during 1 h. The mixture was warmed up to room temperature, extracted twice with a 10% NaOH solution, and the aqueous layers were combined. They were neutralized with HCl (1 M) until no further precipitate formed upon addition (pH<5). The filtrate was extracted three times with diethyl ether, dried over $MgSO_4$ and concentrated under reduced pressure, yielding a deep orange solid (2.2 g, 83%). The title compound was used without further purification.

^{1}H NMR (300 MHz, $CDCl_3$): δ 4.91 (t, J = 2.0 Hz, 2H, Cp*H*), 4.51 (t, J = 2.0 Hz, 2H, Cp*H*), 4.49 (t, J = 2.0 Hz, 2H, Cp*H*), 4.20 (t, J = 2.0 Hz, 2H, Cp*H*); **^{13}C{^{1}H} NMR** (75 MHz, $CDCl_3$): δ 176.9 (s, 1C, *C*OOH), 78.1 (s, 1C, *C*Br), 74.6 (s, Cp*C*), 72.7 (s, Cp*C*), 71.9 (s, Cp*C*), 70.1 (s, Cp*C*), 69.3 (s, Cp*C*); **HRMS** (MALDI) calcd. (*m/z*) for $C_{11}H_9BrFeO_2$: 307.9131 ($[M]^+$), found: 307.9129 ($[M]^+$); **M.P.**: 157-160 °C.

1-Bromo-1'-diphenylphosphanylferrocene 50[173]

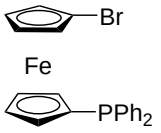

To a solution of 1,1'-dibromoferrocene (1 eq., 3.2 mmol, 1.1 g) in THF (5 ml) at –78 °C were added TMEDA (1 eq., 3.2 mmol, 0.483 ml) and *n*BuLi (0.95 eq., 3.04 mmol, 1.6 M in hexanes, 1.9 ml). After 2 h, chlorodiphenylphosphane (1 eq., 3.2 mmol, 0.574 ml) was added and the mixture was stirred for another 2 h at room temperature. The reaction mixture was then quenched with water (5 ml) and extracted with CH_2Cl_2. The combined organic phases were dried over $MgSO_4$, filtered, and concentrated under reduced pressure. The crude product was purified by automated column chromatography on a 40 g silica gel prepacked column with a hexane:EtOAc eluent gradient; the product eluted second with 35% EtOAc. (The first collected fractions contained a mixture of bromoferrocene and ferrocene.) The product fractions were collected and concentrated yielding a dark orange solid (742 mg, 52%).

^{1}H NMR (300 MHz, $CDCl_3$): δ 7.40-7.31 (m, 10H, H_{Ar}), 4.42 (pseudo t, J = 1.7 Hz, 2H, Cp*H*), 4.32 (pseudo t, J = 1.9 Hz, J = 1.7 Hz, 2H, Cp*H*), 4.16 (pseudo q, J = 1.9 Hz, J = 1.7 Hz, 2H, Cp*H*), 3.99 (pseudo t, J = 1.9 Hz, 2H, Cp*H*); **^{13}C{^{1}H} NMR** (75 MHz, $CDCl_3$): δ 139.0 (d, $J_{C\text{-}P}$ = 9.9 Hz, C_{Ar}), 133.5 (d, $J_{C\text{-}P}$ = 19.3 Hz, C_{Ar}), 128.5 (s, C_{Ar}), 128.3 (s, C_{Ar}), 128.2 (s, C_{Ar}), 76.9 (s, Cp*C*), 76.8 (s, Cp*C*), 73.8 (d, $J_{C\text{-}P}$ = 14.3 Hz, Cp*C*), 72.6-72.5 (m, Cp*C*), 69.3 (s, Cp*C*); **^{31}P NMR** (121 MHz, $CDCl_3$): δ –17.2 (pseudo s); **^{31}P{^{1}H} NMR** (121 MHz, $CDCl_3$): δ –17.6 (s).

1-Carboxy-1'-diphenylphosphanylferrocene 51[173]

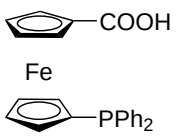

1-Bromo-1'-diphenylphosphanylferrocene **50** (1.0 eq., 8.24 mmol, 3.7 g) was dissolved in dry THF (18 ml). *n*BuLi (1 eq., 8.24 mmol, 1.6 M in hexanes, 5.15 ml) was added at –25 °C and the mixture was stirred at this temperature for 20 min. Then, CO_2 was bubbled through the reaction mixture, making it turn dark red. It was further stirred for 10 min at –25 °C, then at room temperature for 1 h. The mixture turned into an orange suspension. As quenched product was still observable by GC-MS, more CO_2 was bubbled through the mixture. The mixture was quenched with a 10% NaOH solution and left to stir overnight. The next day, the phases were separated and the organic phases was extracted twice with a 10% NaOH solution. The aqueous layers were combined and HCl (1 M) was added, until no more precipitation occurred ($\sim$ pH<5). The filtrate was extracted with diethyl ether (3x), dried over $MgSO_4$ and the solvents removed under reduced pressure, yielding the product as a brown-yellow solid (2.2 g, 65%).

^{1}H NMR (300 MHz, $CDCl_3$): δ 7.39-7.30 (m, 10H, H_{Ar}), 4.75 (pseudo t,J = 1.9 Hz, 2H, Cp*H*), 4.45 (pseudo t, J = 1.7 Hz, 2H, Cp*H*), 4.33 (pseudo t, J = 1.9 Hz, 2H, Cp*H*), 3.99 (pseudo q, J = 1.9 Hz, J = 1.7 Hz, 2H, Cp*H*); **^{31}P NMR** (121 MHz, $CDCl_3$): δ –18.1 (pseudo s); **^{31}P{^{1}H} NMR** (121 MHz, $CDCl_3$): δ –18.1 (s); **HRMS** (MALDI) calcd. (m/z) for $C_{23}H_{19}FeO_2P$: 414.0467 ($[M]^+$), found: 414.0469 ($[M]^+$).

General procedure for the preparation of 1-bromo-1'-oxazolinylferrocenes 48a–c

1-Bromo-1'-carboxyferrocene (1 eq.) was dissolved in anhydrous CH_2Cl_2 (15 ml) and oxalyl chloride (3 eq.) was added dropwise. The reaction mixture bubbled slightly and turned deep red. It was stirred at rt for 1 h. The volatiles were removed using an external cooling trap and the residue was redissolved in CH_2Cl_2 (20 ml) and cooled to 0 °C. Triethylamine (2.5 eq.)

was slowly added and the mixture was stirred for a few minutes. The aminoalcohol (1.2 eq.) was then added dropwise. After 2 h stirring at 0 °C, methanesulfonyl chloride (2.5 eq.) and triethylamine (2.5 eq.) were subsequently added dropwise. The reaction mixture was further stirred in the ice bath and gradually brought to rt overnight. It was then quenched with sat. $NaHCO_3$, extracted three times with CH_2Cl_2, washed with brine, dried over sodium sulfate, filtered, and concentrated under reduced pressure. The crude was dissolved in CH_2Cl_2 and filtered through a plug of silica gel eluting with hexane:EtOAc (10:1 to 4:1).

(4*S*)-1-Bromo-1'-(4-methyl-4,5-dihydro-1,3-oxazol-2-yl)ferrocene 48a

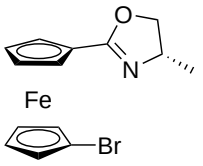

The title compound was obtained from (*S*)-2-aminopropan-1-ol (1.2 eq, 4.28 mmol, 0.33 ml) following the general procedure. The crude was first filtered over silica gel eluting with a hexane:EtOAc gradient (10:1→4:1), and the obtained brown solid recrystallized from hot hexane, yielding an orange semi-crystalline solid (product not weighed, yield unknown).

^{1}H NMR (700 MHz, $CDCl_3$): δ 5.01 (dsept, J = 5.1, 1.7 Hz, 1H, C*H*CH_3), 4.69 (pseudo t, J = 1.3 Hz, 2H, Cp*H*), 4.61 (pseudo t, J = 1.3 Hz, 2H, Cp*H*), 4.51-4.49 (m, 4H, Cp*H*), 4.27 (t, J = 10.7 Hz, 1H, *C*H_2), 3.72 (dd, J = 11.2, 5.1 Hz, 1H, *C*H_2), 1.54 (d, J = 7.3 Hz, 3H, CH*C*H_3); **^{13}C{^{1}H} NMR** (176 MHz, $CDCl_3$): δ 172.0 (s, 1C, C*C*=N), 75.5 (s, 1C, *C*Br), 75.1 (s, Cp*C*), 72.8 (s, Cp*C*), 72.7 (s, Cp*C*), 55.2 (s, 1C, *C*H_2), 46.6 (s, 1C, *C*H), 17.0 (s, 1C, CH*C*H_3); **HRMS** (MALDI) calcd. (*m/z*) for $C_{14}H_{15}BrFeNO$: 347.9682 ($[M+H]^+$), found: 347.9680 ($[M+H]^+$).

(4*S*)-1-Bromo-1'-(4–butyl-4,5-dihydro-1,3-oxazol-2-yl)ferrocene 48b

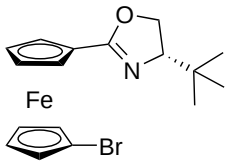

The title compound was obtained from (*S*)-*tert*-leucinol (1.2 eq., 4.28 mmol, 502 mg) following the general procedure followed by filtration over silica gel eluting with a hexane:EtOAc gradient (10:1→4:1). The obtained brown solid was then recrystallized from hexane and a little diethyl ether yielding a bright orange highly crystalline solid (740 mg, 53%). The substitution pattern was confirmed by X-ray analysis.

^{1}H NMR (300 MHz, $CDCl_3$): δ 4.81 (brs, 2H, Cp*H*), 4.43 (t, J = 1.9 Hz, 2H, Cp*H*), 4.37 (brt, J = 1.9 Hz, 2H, Cp*H*), 4.27 (d, J = 10.1 Hz, 1H, C*H*$_2$CH), 4.16 (d, J = 8.7 Hz, 1H, C*H*$_2$CH), 4.13 (t, J = 1.9 Hz, 2H, Cp*H*), 3.92 (dd, J = 10.2, 7.7 Hz, 1H, CH_2C*H*); **HRMS** (MALDI) calcd. (*m/z*) for $C_{17}H_{20}BrFeNO$: 389.0074 ($[M+H]^+$), found: 389.0072 ($[M+H]^+$); **M.P.**: 93 °C.

(4*S*)-1-Bromo-1'-(4-phenyl-4,5-dihydro-1,3-oxazol-2-yl)ferrocene 48c

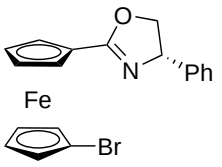

The title compound was obtained from (*S*)-phenylglycinol (1.2 eq., 7.00 mmol, 960 mg) following the general procedure yielding a brown oil which was not further purified (650 mg, 24%).

^{1}H NMR & ^{13}C{^{1}H} NMR : The signals could not be unambiguously assigned due to a paramagnetic appearance of the spectrum; **HRMS** (MALDI) calcd. (*m/z*) for $C_{19}H_{16}BrFeNO$: 408.9761 ($[M]^+$), found: 408.9758 ($[M]^+$); for $C_{19}H_{17}BrFeNO$: 409.9839

([M+H]$^+$), found: 409.9837 ([M+H]$^+$); for $C_{19}H_{16}BrFeNNaO$: 431.9658 ([M+Na]$^+$), found: 431.9658 ([M+Na]$^+$).

6.2.5 Phenylethylferrocene precursors and ligands

The following syntheses were performed with both (R)- and (S)-Ugi amine as starting materials, hence the stereochemistry is not specified in the compound names. For convenience only the (S_C,S_{Fc}) enantiomers are drawn.

1-(Diethoxyphosphoryl)-2-(1-phenylethyl)ferrocene 57

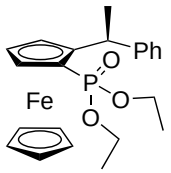

(S_{Fc})-1-Bromo-2-(1-phenylethyl)ferrocene (1 eq., 6.7 mmol, 2.5 g) was dissolved in anhydrous Et_2O (40 ml) and cooled down to –78° C. *n*-BuLi (1.1 eq., 7.42 mmol, 1.6 M in hexanes, 4.64 ml) was then added dropwise. The reaction was warmed to rt and stirred for 30 min; the reaction mixture turned light red in the meantime. A solution of diethyl chlorophosphate (1.7 eq., 11.5 mmol, 1.66 ml) in Et_2O (10 ml) was then added to the lithiated species cooled to 0 °C, which turned orangish-yellow. The reaction mixture was then slowly warmed up to rt and stirred overnight. It was washed with 5% HCl, brine, dried over sodium sulfate, filtered, and concentrated under reduced pressure yielding a yellowish-orange oil. The product was filtered over silica gel eluting hexane:EtOAc 4:1, furnishing the title compound as brown crystalline solid (2.72 g, 95%).

^{1}H NMR (200 MHz, $CDCl_3$): δ 7.20-7.06 (m, 5H, H_{Ar}), 4.59 (br s, 1H, Cp*H*), 4.45 (br s, 1H, Cp*H*), 4.41 (br s, 1H, Cp*H*), 4.32 (s, 5H, Cp'*H*), 3.93 (q, 1H, J = 7.0 Hz, C*H*CH_3), 3.55-3.38 (m, 4H, C$H_2$$CH_3$), 1.61 (d, J = 6.0 Hz, 3H, CHCH_3), 1.41 (t, 3H, J = 7.0 Hz, CH_2CH_3), 0.93 (t, 3H, J = 7.0 Hz, CH_2CH_3); **^{13}C{^{1}H} NMR** (50 MHz, $CDCl_3$): δ 147.8 (s, 1C, C_{Ar}), 128.1 (s, 2C, C_{Ar}), 127.4 (s, 2C, C_{Ar}), 125.8 (s, 1C, C_{Ar}), 97.2 (d, $J_{C\text{-}P}$ = 16.9 Hz, 1C, Cp*C*), 73.0 (d, $J_{C\text{-}P}$ = 14.3 Hz, 1C, Cp*C*), 70.6 (s, 5C, Cp'*C*), 69.9 (d, $J_{C\text{-}P}$ = 15.0 Hz, 1C, Cp*C*), 69.5 (d, $J_{C\text{-}P}$ = 13.6 Hz, 1C, Cp*C*), 65.1 (d, $J_{C\text{-}P}$ = 210.2 Hz, 1C, Cp*C*), 61.3 (d, $J_{C\text{-}P}$ = 17.6 Hz, 1C, *C*H_2), 61.2 (d, $J_{C\text{-}P}$ = 17.2 Hz, 1C, *C*H_2), 38.0 (s, 1C, *C*H), 23.7 (s, 1C, CH*C*H_3), 16.4 (d, $J_{C\text{-}P}$ = 6.6 Hz, 1C, CH_2*C*H_3), 16.1 (d, $J_{C\text{-}P}$ = 7.3 Hz, 1C, CH_2*C*H_3); **^{31}P{^{1}H} NMR** (81 MHz, $CDCl_3$): δ 25.3 (s); **HRMS** (MALDI) calcd. (*m/z*) for $C_{22}H_{27}FeO_3P$: 426.1042 ([M]$^+$), found: 426.1041 ([M]$^+$).

1-(1-Phenylethyl)-2-phosphanylferrocene 58

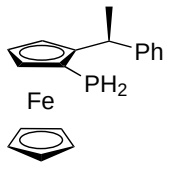

$LiAlH_4$ (3.3 eq., 4.22 mmol, 160 mg) was suspended in anhydrous diethyl ether and cooled down to –78 °C. TMSCl (3.1 eq., 3.96 mmol, 0.503 ml) was added dropwise, then the cold bath was removed and the reducing mixture stirred at rt 30 min. It was then cooled again to –78 °C, and a solution of phosphonate/RD193 (1 eq., 1.28 mmol, 545 mg) in diethyl ether was added dropwise (turned slightly greenish-yellow). The reaction mixture was stirred at rt overnight. The next day, the reaction was cooled to 0 °C, and 0.16 ml water, 0.16 ml 15% NaOH, and 0.48 ml water were added subsequently. The organic phase was dried over magnesium sulfate, filtered, and the volatiles removed using an external cooling trap yielding an orange oil or solid (quant.). *The title compound is highly sensitive to oxygen. A pure isolated sample in a Schlenk under argon was completely oxidized at the phosphorus atom after a week.*

^{1}H NMR (300 MHz, $CDCl_3$): δ 7.42-7.23 (m, 5H, H_{Ar}), 4.66 (br s, 1H, Cp*H*), 4.45 (br s, 1H, Cp*H*), 4.42 (br s, 1H, Cp*H*), 4.33 (s, 5H, Cp*H*), 4.32 (q, 1H, J = 7.2 Hz, C*H*), 3.95 (dd, $J_{H\text{-}P}$ = 203.4 Hz, $J_{H\text{-}H}$ = 12.3 Hz, 1H, PH_2), 3.27 (dd, $J_{H\text{-}P}$ = 203.4 Hz, $J_{H\text{-}H}$ = 12.3 Hz, 1H, PH_2), 1.84 (d, J = 7.18 Hz, 3H, CH_3); **^{13}C{^{1}H} NMR** (75 MHz, $CDCl_3$): δ 147.4 (s, 1C, C_{Ar}), 128.4 (s, 2C, C_{Ar}), 127.2 (s, 2C, C_{Ar}), 125.9 (s, 1C, C_{Ar}), 98.3 (d, $J_{C\text{-}P}$ = 9.4 Hz, 1C, Cp*C*), 76.1 (d, $J_{C\text{-}P}$ = 14.9 Hz, 1C, Cp*C*), 69.9 (s, 5C, Cp'*C*), 68.6 (d, $J_{C\text{-}P}$ = 13.2 Hz, 1C, Cp*C*), 68.5 (d, $J_{C\text{-}P}$ = 15.4 Hz, 1C, Cp*C*), 64.4 (d, $J_{C\text{-}P}$ = 6.6 Hz, 1C, Cp*C*), 39.2 (d, $J_{C\text{-}P}$ = 3.3 Hz, 1C, *C*H), 23.0 (s, 1C, *C*H_3); **^{31}P NMR** (121 MHz, $CDCl_3$): δ –152.0 (t, $J_{P\text{-}H}$ = 204.5 Hz, *P*H_2); **^{31}P{^{1}H} NMR** (121 MHz, $CDCl_3$): δ –152.0 (s, *P*H_2).

1-(Bis(trifluoromethyl)phosphanyl)-2-(1-phenylethyl)ferrocene 59

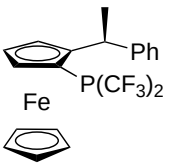

To a stirred solution of (S_C,S_{Fc})-1-(1-phenylethyl)-2-phosphanylferrocene (1 eq., 4.56 mmol, 1.47 g) in anhydrous CH_2Cl_2 (20 ml) at rt was added 1-trifluoromethyl-1,2-benziodoxol-3(1*H*)-one (2 eq., 9.13 mmol, 2.88 g). DBU (4 eq., 18.3 mmol, 2.73 ml) was then slowly added dropwise at 0° C via syringe making the reaction mixture turn dark orange-red. It was further stirred in the ice bath and slowly brought to rt overnight. The next day, the reaction mixture was directly purified via FC on silica gel eluting with hexane:CH_2Cl_2 9:1, yielding the product as a red solid which crystallized from a hexane:CH_2Cl_2 mixture (516 mg, 25%).

^{1}H NMR (300 MHz, $CDCl_3$): δ 7.22-7.01 (m, 5H, H_{Ar}), 4.79 (br s, 1H, Cp*H*), 4.64 (t, J = 2.6 Hz, 1H, Cp*H*), 4.50 (br s, 1H, Cp*H*), 4.33 (s, 5H, Cp*H*), 1.67 (d, J = 7.0 Hz, 3H, CH_3), CH not found, overlap with CpH signal; **^{13}C{^{1}H} NMR** (75 MHz, $CDCl_3$): δ 146.9 (s, 1C, C_{Ar}), 128.5 (s, 2C, C_{Ar}), 127.0 (pseudo d, J = 1.7 Hz, 2C, C_{Ar}), 126.4 (s, 1C, C_{Ar}), 102.0 (d, J = 34.1 Hz, 1C, Cp*C*), 72.54-72.46 (m, 2C, Cp*C*), 71.7 (d, J = 2.2 Hz, 1C, Cp*C*), 70.6 (d, J = 6.6 Hz, 1C, Cp*C*), 70.5 (pseudo d, J = 1.1 Hz, 5C, Cp'*C*), 39.5 (d, J = 9.4 Hz, 1C, *C*H), 23.8 (s, 1C, *C*H_3), CF_3 signals not found; **^{19}F NMR** (282 MHz, $CDCl_3$): δ –50.7 (dq, $J_{F\text{-}P}$ = 76.2 Hz, $J_{F\text{-}F}$ = 8.5 Hz, 3F, PC*F*$_3$), –56.1 (dq, $J_{F\text{-}P}$ = 70.5 Hz, $J_{F\text{-}F}$ = 8.5 Hz, 3F, PC*F*$_3$); **^{31}P{^{1}H} NMR** (121 MHz, $CDCl_3$): δ –4.6 (tsept, $J_{P\text{-}F}$ = 76.3 Hz, J = 7.5 Hz, *P*CF_3); **HRMS** (MALDI) calcd. (*m/z*) for $C_{20}H_{17}F_6FeP$: 458.0316 ([M]$^+$), found: 458.0315 ([M]$^+$).

1-(1-Phenylethyl)-2-(phenyl(trifluoromethyl)phosphanyl)ferrocene 60

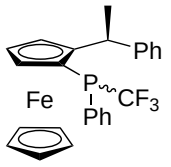

Method A: 1-Bromo-2-(1-phenylethyl)ferrocene (1 eq., 0.542 mmol, 200 mg) was dissolved in anhydrous THF (4 ml) and cooled to –78 °C. *n*-BuLi (1.1 eq., 0.596 mmol, 1.6 M in hexanes, 0.373 ml) was added dropwise, making the mixture turn from yellow to red. It was stirred 30 min at low temperature, then at rt for 1 h. It was then cooled down again, and a solution of bis(trifluoromethyl)phenylphosphane (1 eq., 0.542 mmol, 267 mg) was added dropwise, making the reaction mixture turn deep burgundy. It was left to stir 30 min at low temperature, then the cooling bath was removed and it was further stirred at 70 °C overnight (no color change). The solution was quenched with sat. $NaHCO_3$, the aqueous phase was extracted with Et_2O and the combined organic layers were dried over Na_2SO_4. The organic phase was then concentrated yielding a brown oil. The diastereomers were separated via preparative TLC eluting with hexane:CH_2Cl_2:Et_2O 20:1:1 (diast1: 57 mg, 23%, diast2: 15 mg, 6%).

Method B: To a solution of 1-(bis(trifluoromethyl)phosphanyl)-2-(1-phenylethyl)ferrocene (1 eq., 1.09 mmol, 499 mg) in anhydrous THF (20 ml) was slowly added at –78 °C PhLi (1.5 eq., 1.63 mmol, 0.86 ml, 1.9 M in dibutylether) via syringe. The reaction mixture turned dark brown immediately. After stirring for 1 h at low T, the reaction mixture was quenched with sat. $NaHCO_3$. The aqueous phase was extracted twice with CH_2Cl_2. The combined organic layers were dried over $MgSO_4$, filtered, and concentrated in vacuo, yielding a brown oil. The crude was purified by column chromatography eluting with hexane:CH_2Cl_2 9:1. The diastereomers were then separated by preparative TLC, eluting with hexane:Et_2O:CH_2Cl_2 20:1:1. Diast1 was obtained as first band (orange crystalline solid, 63.1 mg, 25%) and diast2 as second band (orange crystalline solid, 117 mg, 46%).

(S_C,S_P,S_{Fc})-1-(1-Phenylethyl)-2-(phenyl(trifluoromethyl)phosphanyl)ferrocene (S_P)-60

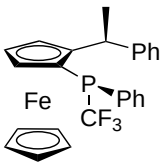

^{1}H NMR (300 MHz, $CDCl_3$): δ 7.12-7.06 (m, 1H, H_{Ar}), 6.97-6.87 (m, 4H, H_{Ar}), 6.71-6.65 (m, 5H, H_{Ar}), 4.68 (br q, J = 2.1 Hz, 1.7 Hz, 1H, Cp*H*), 4.55-4.53 (m, 2H, Cp*H*), 4.33 (s, 5H, Cp*H*), 4.14 (dq, J = 7.0 Hz, 2.3 Hz, 1H, C*H*), 1.62 (d, J = 7.0 Hz, 3H, CH_3); **^{13}C{^{1}H} NMR** (75 MHz, $CDCl_3$): δ 144.3 (s, 1C, C_{Ar}), 133.5 (d, $J_{C\text{-}P}$ = 20.9 Hz, 2C, PC_{Ar}), 129.3 (pseudo d, J = 1.1 Hz, 2C, PC_{Ar}), 127.9 (s, 2C, C_{Ar}), 127.7 (d, $J_{C\text{-}P}$ = 7.7 Hz, 2C, PC_{Ar}), 127.0 (br s, 2C, C_{Ar}), 125.7 (s, 1C, C_{Ar}), 99.8 (d, $J_{C\text{-}P}$ = 28.1 Hz, 1C, Cp*C*), 71.5 (d, $J_{C\text{-}P}$ = 26.4 Hz, 1C, Cp*C*), 70.7 (s, 1C, Cp*C*), 70.4 (s, 5C, Cp'*C*), 69.6 (s, 1C, Cp*C*), 69.5 (s, 1C, Cp*C*), 39.5 (d, $J_{C\text{-}P}$ = 10.5 Hz, 1C, *C*H), 23.4 (s, 1C, *C*H$_3$), CF_3 signals not found; **^{19}F NMR** (282 MHz, $CDCl_3$): δ –53.8 (d, $J_{F\text{-}P}$ = 69.5 Hz, C*F*$_3$); **^{31}P NMR** (121 MHz, $CDCl_3$): δ –12.3 (q, $J_{P\text{-}F}$ = 68.8 Hz, *P*CF_3); **HRMS** (MALDI) calcd. (*m/z*) for $C_{25}H_{22}F_3FeP$: 466.0755 ([M]$^+$), found: 466.0755 ([M]$^+$).

(S_C,R_P,S_{Fc})-1-(1-Phenylethyl)-2-(phenyl(trifluoromethyl)phosphanyl)ferrocene (R_P)-60

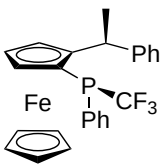

^{1}H NMR (300 MHz, $CDCl_3$): δ 7.98-7.92 (m, 2H, H_{Ar}), 7.54-7.47 (m, 3H, H_{Ar}), 7.29-7.09 (m, 5H, H_{Ar}), 4.62 (br s, 1H, Cp*H*), 4.50 (t, J = 2.6 Hz, 1H, Cp*H*), 4.48 (br s, 1H, Cp*H*), 4.29 (dq, J = 7.2 Hz,2.6 Hz, 1H, C*H*), 3.84 (s, 5H, Cp*H*), 1.68 (d, J = 7.2 Hz, 3H, CH_3); **^{13}C{^{1}H} NMR** (75 MHz, $CDCl_3$): δ 147.6 (s, 1C, C_{Ar}), 135.8 (d, $J_{C\text{-}P}$ = 25.3 Hz, 2C, PC_{Ar}), 131.2 (s, 2C, PC_{Ar}), 128.6 (d, $J_{C\text{-}P}$ = 9.9 Hz, 2C, PC_{Ar}), 128.3 (s, 2C, C_{Ar}), 127.2 (s, 2C, C_{Ar}), 126.0 (s, 1C, C_{Ar}), 101.8 (d, $J_{C\text{-}P}$ = 32.5 Hz, 1C, Cp*C*), 72.5 (d, $J_{C\text{-}P}$ = 4.4 Hz, 1C, Cp*C*), 70.7 (pseudo d, J = 1.1 Hz 2C, Cp*C*), 69.8 (s, 5C, Cp'*C*), 69.7 (s, 1C, Cp*C*), 38.9 (d, $J_{C\text{-}P}$ = 11.0 Hz, 1C, *C*H), 24.0 (s, 1C, *C*H$_3$), CF_3 signals not found; **^{19}F NMR** (282 MHz, $CDCl_3$): δ –56.9 (d, $J_{F\text{-}P}$ = 69.5 Hz, C*F*$_3$); **^{31}P NMR** (121 MHz, $CDCl_3$): δ –17.0 (tq, $J_{P\text{-}F}$ = 68.8 Hz, J = 9.0 Hz, *P*CF_3); **HRMS** (MALDI) calcd. (*m/z*) for $C_{25}H_{22}F_3FeP$: 466.0755 ([M]$^+$), found: 466.0753 ([M]$^+$).

6.2.6 Metal complexes

(((1,1'-Biphenyl)-2-yl)(phenyl)(trifluoromethyl)phosphane-κP)(chlorido)gold 21

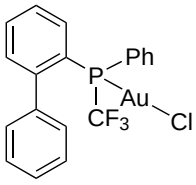

A solution of (dimethylsulfide)gold(I)chloride (1 eq., 0.0303 mmol, 8.92 mg) and **20** (1 eq., 0.0303 mmol, 10 mg) in dry CH_2Cl_2 (1 ml) was stirred at rt 30 min. The volatiles were then removed under reduced pressure yielding a greyish-brown solid. The residue was redissolved in CH_2Cl_2 and filtered over a silica gel filled pipette and concentrated under reduced pressure, yielding the two coordination isomers (1:1.32) as a light yellowish-brown solid (4 mg, 24%).

^{19}F NMR (188 MHz, $CDCl_3$): δ –56.7 (d, $J_{F\text{-}P}$ = 86.9 Hz); **^{31}P{^{1}H} NMR** (121 MHz, $CDCl_3$): δ 33.9 (q, $J_{P\text{-}F}$ = 86.8 Hz);

Dichlorido((4*S*)-2-(2-(phenyl(trifluoromethyl)phosphanyl-κP)phenyl)-4-(propan-2-yl)-4,5-dihydro-1,3-oxazole-κN)palladium 27

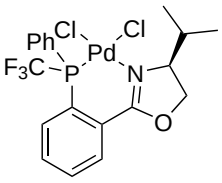

Ligand **26a** (1 eq., 0.17 mmol, 62.1 mg) was dissolved in anhydrous CH_2Cl_2 and $Pd(COD)Cl_2$ (1 eq., 0.17 mmol, 48.5 mg) was added to the solution. The reaction mixture was stirred at rt overnight. The volatiles were removed under reduced pressure yielding a bright yellow solid (116.7 mg, quant.).

^{1}H NMR : Due to overlapping of signals because of the presence of 2 diastereomers, unambiguous assignment of the signals was impossible. **^{19}F NMR** (282 MHz, $CDCl_3$): δ –52.1 (d, $J_{F\text{-}P}$ = 75.6 Hz, PCF_3, diast1), –56.3 (d, $J_{F\text{-}P}$ = 80.7 Hz, PCF_3, diast2); **^{31}P NMR** (121 MHz, $CDCl_3$): δ 35.6 (q, $J_{P\text{-}F}$ = 76.3 Hz, $J_{P\text{-}H}$ = 12.0 Hz, *P*CF_3, diast1), 25.0 (q, $J_{P\text{-}F}$ = 80.8 Hz, $J_{P\text{-}H}$ = 10.5 Hz, *P*CF_3, diast2); **^{31}P{^{1}H} NMR** (121 MHz, $CDCl_3$): δ 35.5 (q, $J_{P\text{-}F}$ = 76.3 Hz, *P*CF_3, diast1), 25.0 (q, $J_{P\text{-}F}$ = 79.3 Hz, *P*CF_3, diast2); **HRMS** (MALDI) calcd. (*m/z*) for $C_{19}H_{19}ClF_3NOPPd$: 505.9879 ([M-Cl]$^+$), found: 505.9873 ([M-Cl]$^+$).

(S_C,S_P,S_{Fc})-Dichlorido(1-(4-methyl-4,5-dihydro-1,3-oxazol-2-yl-2κN)-2-(phenyl(trifluoromethyl)phosphanyl-2κP)ferrocene)palladium (S_P)-35

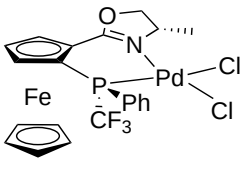

Ligand (S_P)-**32a** (1 eq., 0.0112 mmol, 4.99 mg) was dissolved in CH_2Cl_2 and $Pd(COD)Cl_2$ (1 eq., 0.0112 mmol, 3.53 mg) was added. The solution was shortly sonicated then left to stand at rt overnight. The volatiles were then removed under reduced pressure, yielding a reddish-brown semi-crystalline solid (6.96 mg, quant.).

^{1}H NMR No assignments could be made as the spectrum was very broadened by paramagnetic impurities; **^{19}F NMR** (188 MHz, $CDCl_3$): δ –51.3 (d, $J_{F\text{-}P}$ = 75.0 Hz, PCF_3); **^{31}P{^{1}H} NMR** (121 MHz, $CDCl_3$): δ 25.7 (q, $J_{P\text{-}F}$ = 75.0 Hz, *P*CF_3).

(S_C,R_P,S_{Fc})-Dichlorido(1-(4-methyl-4,5-dihydro-1,3-oxazol-2-yl-2κN)-2-(phenyl(trifluoromethyl)phosphanyl-2κP)ferrocene)palladium (R_P)-35

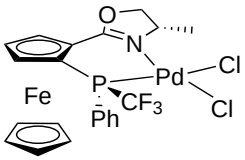

Ligand (R_P)-**32a** (1 eq., 0.372 mmol, 16.6 mg) was dissolved in CH_2Cl_2 and $Pd(COD)Cl_2$ (1 eq., 0.372 mmol, 11.7 mg) was added. The solution was shortly sonicated then left to stand at rt overnight. The volatiles were then removed under reduced pressure, yielding a reddish-brown semi-crystalline solid (23.2 mg, quant.).

^{1}H NMR No assignments could be made as the spectrum was very broadened by paramagnetic impurities; **^{19}F NMR** (188 MHz, $CDCl_3$): δ –54.5 (d, $J_{F\text{-}P}$ = 75.2 Hz, PCF_3); **^{31}P{^{1}H} NMR** (121 MHz, $CDCl_3$): δ 22.7 (q, $J_{P\text{-}F}$ = 77.4 Hz, PCF_3).

(S_C,R_P,S_{Fc})-Dichlorido(1-(4-methyl-4,5-dihydro-1,3-oxazol-2-yl-2κN)-2-(phenyl(trifluoromethyl)phosphanyl-2κP)ferrocene)platinum 36

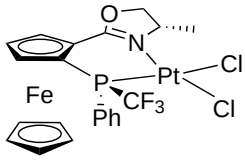

Ligand (R_P)-**32a** (1 eq., 0.0112 mmol, 5 mg) and *cis*/*trans*-$[Pt(SMe_2)_2Cl_2]$ (1 eq., 0.0112 mmol, 8.77 mg) were stirred in CH_2Cl_2 (1 ml, from bottle) in a vial at rt overnight. The volatiles were removed yielding a brown solid which was recrystallized from hexane.

^{1}H NMR (300 MHz, $CDCl_3$): δ 8.38 (dd, $J_{H\text{-}H}$ = 13.2 Hz, 6.6 Hz, 2H, H_{Ar}), 7.70-7.62 (m, 3H, H_{Ar}), 5.68 (br quint, $J_{H\text{-}H}$ = 7.2 Hz, 5.5 Hz, 1H, C*H*), 5.18 (br s, 1H, Cp*H*), 4.94-4.91 (m, 2H, Cp*H*), 4.44-4.43 (m, 1H, CH_2), 4.38-4.37 (m, 1H, CH_2), 3.91 (s, 5H, Cp*H*), 1.57 (d, $J_{H\text{-}H}$ = 6.6 Hz, 3H, CH_3); **^{19}F NMR** (282 MHz, $CDCl_3$): δ –56.6 (d, $J_{F\text{-}P}$ = 77.7 Hz, $J_{F\text{-}Pt}$ = 25.6 Hz, PCF_3); **^{31}P{^{1}H} NMR** (121 MHz, $CDCl_3$): δ 0.3 (q, $J_{P\text{-}F}$ = 77.8 Hz, PCF_3);

(S_C,S_{Fc})-(1-(Bis(trifluoromethyl)phosphanyl-2κP)-2-(1-phenylethyl)ferrocene)(chlorido)gold 65a

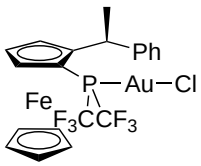

In a vial, a solution of (dimethylsulfide)gold(I)chloride (1.02 eq, 0.0564 mmol, 16.6 mg) and ligand **59** (1 eq., 0.0553 mmol, 25.3 mg) in CH_2Cl_2 (1 ml) was stirred for 2 days. All volatiles were removed under reduced pressure. The remaining solid was taken up in CH_2Cl_2 and filtered over silica gel eluting with hexane:EtOAc (3:1). The product was obtained as a yellow oil (7.1 mg, 19%).

^{1}H NMR (300 MHz, $CDCl_3$): δ 7.24-7.08 (m, 5H, H_{Ar}), 5.07 (br s, 1H, Cp*H*), 4.89 (br s, 1H, Cp*H*), 4.76 (br d, 1H, C*H*), 4.65 (br s, 1H, Cp*H*), 4.47 (br s, 5H, Cp*H*), 1.69 (br d, J = 5.1 Hz, 3H, CH_3); **^{13}C{^{1}H} NMR** (75 MHz, $CDCl_3$): δ 146.1 (s, 1C, C_{Ar}), 128.8 (s, 2C, C_{Ar}), 127.2 (s, 2C, C_{Ar}), 126.8 (s, 1C, C_{Ar}), 71.8 (br s, 5C, Cp'*C*), 39.9 (d, $J_{C\text{-}P}$ = 3.9 Hz, 1C, *C*H), 24.7 (s, 1C, *C*H_3), Cp*C* and *C*F_3 signals not observed; **^{19}F NMR** (282 MHz, $CDCl_3$): δ –52.6 (qd, $J_{F\text{-}P}$ = 92.0 Hz, $J_{F\text{-}F}$ = 8.2 Hz, 3F, CF_3), –59.1 (qd, $J_{F\text{-}P}$ = 92.0 Hz, $J_{F\text{-}F}$ = 8.2 Hz, 3F, CF_3); **^{31}P NMR** (121 MHz, $CDCl_3$): δ 39.0 (sept, $J_{P\text{-}F}$ = 92.8 Hz, $P(CF_3)_2$).

(S_C,R_P,S_{Fc})-Chlorido(1-(1-phenylethyl)-2-(phenyl(trifluoromethyl)phosphanyl-2κP)ferrocene)gold
65b

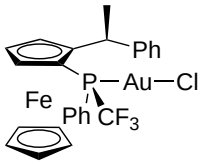

In an NMR tube, a solution of (dimethylsulfide)gold(I)chloride (1.02 eq., 0.022 mmol, 6.44 mg) and ligand (R_P)-**60** (1 eq., 0.021 mmol, 10 mg) in dry CD_2Cl_2 (0.5 ml) was stirred for 30 min. ^{19}F and ^{31}P NMR spectra confirm coordination. The product was not purified.

^{1}H NMR (300 MHz, CD_2Cl_2): δ 8.21-8.14 (m, 2H, H_{Ar}), 7.79-7.63 (m, 3H, H_{Ar}), 7.29-7.08 (m, 5H, H_{Ar}), 5.09 (q, J = 7.0 Hz, 1H, CH), 4.93 (q, J = 2.3 Hz, 1H, CpH), 4.71 (t, J = 2.3 Hz, 1H, CpH), 4.44-4.41 (m, 1H, CpH), 4.08 (s, 5H, CpH), 1.71 (d, J = 7.0 Hz, 3H, CH_3); **^{19}F NMR** (282 MHz, CD_2Cl_2): δ –60.5 (d, $J_{F\text{-}P}$ = 84.8 Hz, CF_3); **^{31}P NMR** (121 MHz, CD_2Cl_2): δ 31.1 (tq, $J_{P\text{-}F}$ = 83.8 Hz, J = 12.0 Hz, PCF_3).

6.2.7 Overview of described compounds

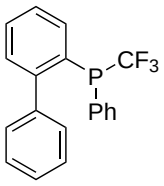

20

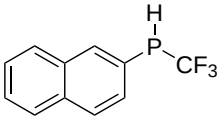

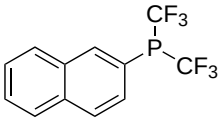

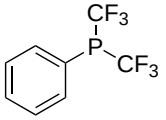

4

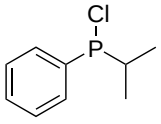

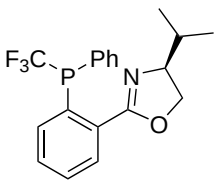

26a

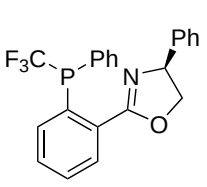

26b

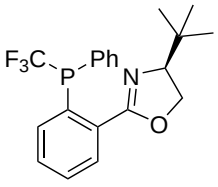

26c

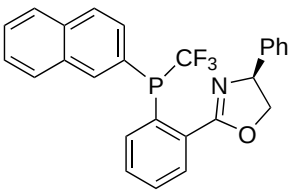

26d

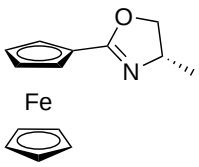

32a

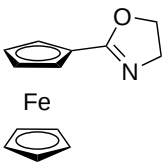

32d

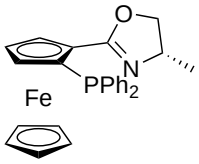

33

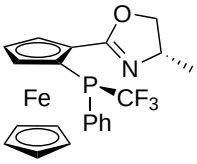

(R_P)-**34a**

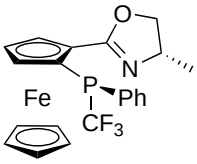

(S_P)-**34a**

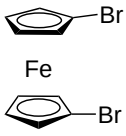

46

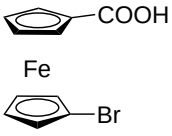

47

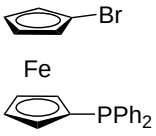

50

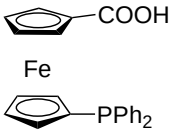

51

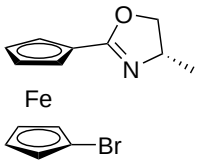

48a

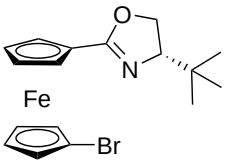

48b

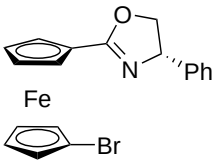

48c

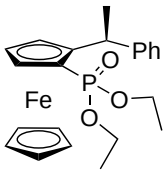

57

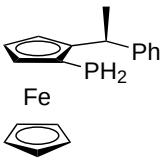

58

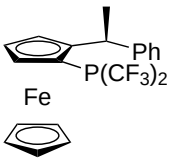

59

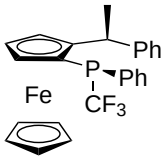

(S_P)-**60**

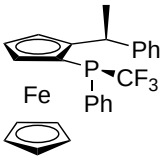

(R_P)-**60**

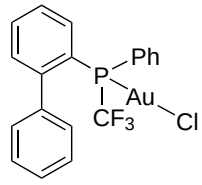

21

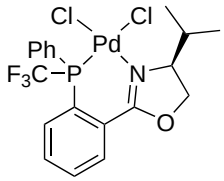

27

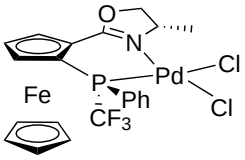

(S_P)-**35**

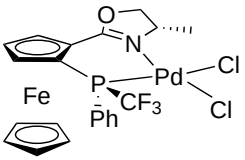

(R_P)-**35**

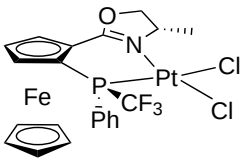

(R_P)-**36**

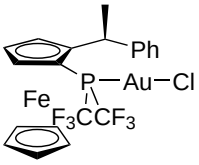

65b

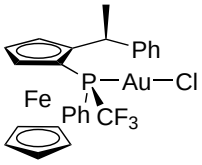

65a

6.3 Catalyses

6.3.1 Alkylative ring opening of 7-oxabenzonorbornadiene 18[139]

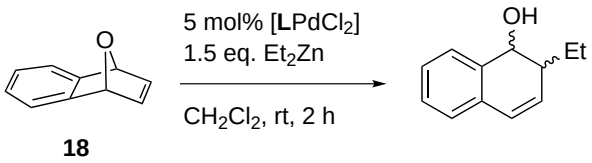

18

A 20 ml Schlenk tube was charged with ligand (0.05 eq., 0.00771 mmol, 4.8 mg) and $[Pd(MeCN)_2Cl_2]$ (0.05 eq., 0.00771 mmol, 2.0 mg) and stirred in dry CH_2Cl_2 (1 ml) for 2 h (bright yellow solution). Afterwards, a solution of bicycle **18** (1 eq., 0.154 mmol, 22.2 mg) in dry DCM (5 ml) was added, followed by a solution of diethyl zinc (1.5 eq., 0.231 mmol, 0.231 ml, 1 M in hexanes). The solution was stirred at rt until full conversion was observed by GC-MS (usually 2 h). The flask was opened to air and a few drops of water were added. The solution was stirred at rt 1 h (some solids formed), and purified on silica gel eluting with hexane:Et_2O 10:1, yielding the product as a clear oil.
The samples were dissolved in analytical grade hexane with a few drops 2-propanol and the enantiomeric ratio was determined by analytical HLPC (Agilent 1100, Chiralcel OD-H column, 0.5 ml/min, 5 μl injection, 25 °C, hexane:iPrOH 96:4, 254 nm). Enantiomer 1 = 16.251 min, enantiomer 2 = 17.663 min. Reference 7-oxabenzonorbornadiene (**18**): 21.777 min.

6.3.2 Allylic alkylation of cinnamyl acetate[174][119]

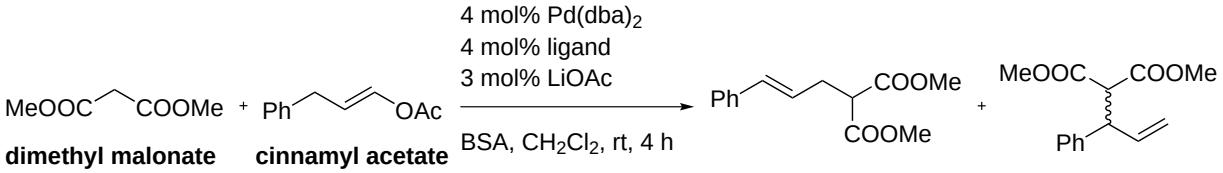

dimethyl malonate **cinnamyl acetate** **37** **38**

A glass vial charged with $Pd(dba)_2$ (0.04 eq., 0.02 mmol, 11.5 mg) and the ligand (0.04 eq., 0.02 mmol) was purged with argon, and anhydrous CH_2Cl_2 (2 ml) was added. To the solution were subsequently added cinnamyl acetate (1 eq., 0.5 mmol, 0.083 ml), dimethylmalonate (3 eq., 1.5 mmol, 0.17 ml), *N,O*-bis(trimethylsilylacetamide) (BSA) (3 eq., 1.5 mmol, 0.37 ml) and lithium acetate (0.03 eq., 0.015 mmol, 0.99 mg). The reaction mixture was stirred at rt and monitored by TLC. After disappearance of cinnamyl acetate, the mixture was diluted with CH_2Cl_2 (10 ml) and washed twice with saturated aqueous ammonium chloride. The organic phase was dried over $MgSO_4$ and concentrated under reduced pressure. The crude was purified by FC eluting with hexane:EtOAc 15:1 affording a clear oil.
The regioselectivity was determined by ^1H NMR spectroscopy and the enantiomeric ratio by analytical HPLC (ThermoScientific Dionex UltiMate 3000, Chiralcel OD-H column, 1.5 ml/min, hexane:iPrOH 90:10, 210 nm). Reference **38**: enantiomer 1 = 3.050 min, enantiomer 2 = 3.207 min.

6.3.3 Hydrosilylation of norbornene[179]

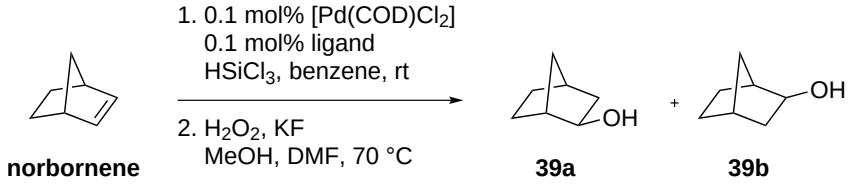

$Pd(COD)Cl_2$ (0.001 eq., 0.00637 mmol, 1.82 mg), ligand (0.001 eq., 0.00637 mmol), norbornene (1 eq., 6.37 mmol, 600 mg) and benzene (3 ml) were stirred until the solid $Pd(COD)Cl_2$ had dissolved (the mixture turned slightly orange, approx. 30 min.). Trichlorosilane (1.3 eq., 8.28 mmol, 0.837 ml) was added. After complete conversion (checked by norbornene smell), the reaction mixture was poured into a KF (10 eq., 63.7 mmol, 3.7 g) suspension in MeOH (10 ml) and stirred for 30 min. The solvent was removed, and DMF (6 ml)/H_2O_2 (10 eq., 30% solution in water, 6.51 ml) was added and the suspension heated for 1 h at 70 °C. 1 M NaOH (6 ml), TBME (6 ml), and NaCl sat. (4 ml) were then added. The organic phase was separated and the aqueous phase further extracted twice with TBME (2x4 ml). The combined organic layers were dried over magnesium sulfate and concentrated under reduced pressure yielding a slightly yellow oil.
The samples were dissolved in analytical grade ethyl acetate. The enantiomeric ratio was determined by GC (Supelco β-dex 120 column, 1.4 ml/min, 1 μl injection, 70 °C). Reference *exo*-norborneol **39**: enantiomer 1 = 74.127 min, enantiomer 2 = 77.927 min.

6.3.4 Hydrosilylation of styrene[179]

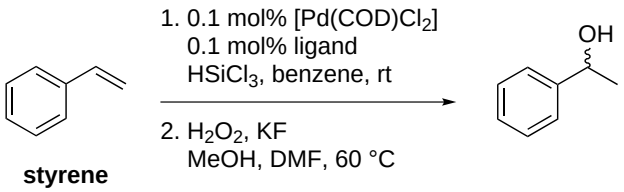

$Pd(COD)Cl_2$ (0.001 eq., 0.00524 mmol, 1.5 mg) and ligand (0.001 eq., 0.00524 mmol) were stirred in benzene (3 ml) until the solid $Pd(COD)Cl_2$ had dissolved (turned slightly orange, approx. 60 min). To the formed complex was added styrene (1 eq., 5.24 mmol, 0.6 ml) and trichlorosilane (1.3 eq., 6.81 mmol, 0.688 ml). After complete conversion (checked by GC-MS, no reaction after 1 h, stirred over the week-end), the reaction mixture was poured into a KF (10 eq., 52.4 mmol, 3.04 g) suspension in MeOH (10 ml) and stirred for 1 h. The solvent was removed, and DMF (6 ml)/H_2O_2 (10 eq., 30% solution in water, 5.35 ml) was added and the suspension heated for 1 h at 60 °C. 1 M NaOH (6 ml) and TBME (6 ml) were added. The organic phase was separated and the aqueous phase further extracted twice with TBME (2x4 ml). The combined organic layers were dried over magnesium sulfate and concentrated under reduced pressure yielding a yellow oil.
The samples were dissolved in analytical grade hexane with very little 2-propanol and the enantiomeric ratio was determined by analytical HLPC (Agilent 1100, Chiralcel OD-H column, 0.5 ml/min, 5 μl injection, 25 °C, hexane:iPrOH 90:10, 220 nm). Reference 1-phenylethanol: enantiomer 1 = 11.878 min, enantiomer 2 = 13.357 min.

6.3.5 Hydrogenation of dimethyl itaconate

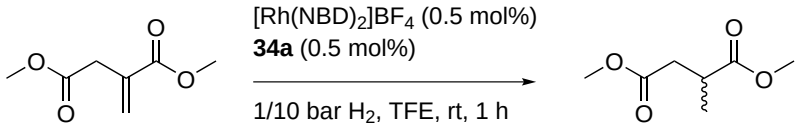

DMI

The ligand (0.005 eq., 0.00474 mmol) and metal precursor $[Rh(NBD)_2]BF_4$ (0.005 eq., 0.00474 mmol, 1.77 mg) were dissolved in trifluoroethanol (2 ml) in a vial purged with argon and stirred for 10 min. The substrate dimethyl itaconate (1 eq., 0.948 mmol, 150 mg) was then added, and the vial put under an H_2 atmosphere in an autoclave (3 cycles to inertize then exchange of the atmosphere to H_2) and stirred for 1 h under an H_2 atmosphere. The crude was filtered over a silica gel plug eluting with hexane:iPrOH 95:5 and concentrated under reduced pressure. Conversion was monitored by GC-MS (standard method).

6.3.6 Hydrogenation of 2-methylquinoline[222]

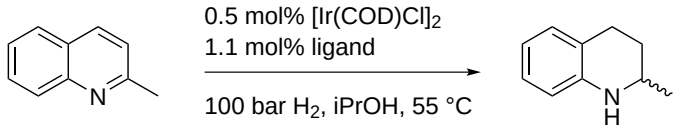

2-methylquinoline **42**

A screw cap vial purged with argon was charged with ligand (0.011 eq., 0.00461 mmol) and $[Ir(COD)Cl]_2$ (0.005 eq., 0.0021 mmol, 1.41 mg) was stirred in 2-propanol (1.2 ml) at rt for 30 min. The substrate 2-methylquinoline (1 eq., 0.419 mmol, 60 mg) was then added, and the vial was put under 100 bar H_2 in an autoclave for 24 h after the temperature was stabilized around 55 °C. The next day, NaOH (2 M solution, 4 ml) and hexane (6 ml) were added. The organic phase was separated, dried over magnesium sulfate, filtered and concentrated under reduced pressure.
The samples were dissolved in analytical grade hexane with very little 2-propanol and the enantiomeric ratio was determined by analytical HLPC (ThermoScientific Dionex UltiMate 3000, Chiralcel IB column, 1.0 ml/min, 1 μl injection, 25 °C, hexane:iPrOH 97:3). Reference 2-methyl-1,2,3,4-tetrahydroquinoline **42**: enantiomer 1 = 3.33 min, enantiomer 2 = 3.59 min.

6.3.7 Transfer hydrogenation of acetophenone[194][193]

Note: The ligands used are the (S_C,S_{Fc}) diastereomers.

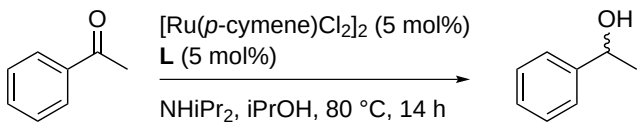

acetophenone **1-phenylethanol**

A Schlenk tube was charged with $[Ru(p\text{−cymene})Cl_2]_2$ (0.05 eq., 0.008 mmol, 4.74 mg) and ligand (0.05 eq., 0.008 mmol), and anhydrous CH_2Cl_2 (1 ml) was added. The solution was stirred for 3 h, then 2-propanol (1 ml), acetophenone (1 eq., 0.16 mmol, 0.02 ml) and

diisopropylamine (0.05 eq., 0.008 mmol, 0.002 ml) were added. The reaction mixture was stirred for 14 h at 80 °C. The reaction was quenched with sat. aq. NH_4Cl (1 ml) and extracted with Et_2O. The organic phase was dried with $MgSO_4$ and the product concentrated *in vacuo* . The samples were dissolved in analytical grade hexane with a drop of 2-propanol. GC conditions: Supelco β-dex 120 column, 1.4 ml/min, 1 μl injection, 80 °C. (R)= 61.118 min, (S)= 68.003 min. HPLC (Agilent 1100): Chiralcel OD-H column, 0.8 ml/min, 5 μl injection, 25 °C, 90:10 hexane:iPrOH, 210 nm. Reference 1-phenylethanol: enantiomer 1 = 7.120 min, enantiomer 2 = 7.963 min.

References

[1] R. E. Gawley, *J. Org. Chem.* **2006**, *71*, 2411–2416, DOI 10.1021/jo052554w.

[2] J. Emsley, *The 13th Element: The Sordid Tale of Murder, Fire, and Phosphorus*, John Wiley & Sons: New York, Chichester, England, **2000**.

[3] G. Bertrand, *Chem. Rev.* **1994**, *94*, 1161–1162, DOI 10.1021/cr00029a600.

[4] R. T. Sanderson in *Encyclopædia Britannica*, **2009**.

[5] J. Emsley, *Nature's Building Blocks: An A-Z Guide to the Elements*, Oxford University Press, Great Clarendon Street, Oxford, **2011**, pp. 389–398.

[6] D. A. Dixon, A. J. Arduengo III, *J. Am. Chem. Soc.* **1987**, *109*, 338–341, DOI 10.1021/ja00236a007.

[7] D. G. Gilheany, *Chem. Rev.* **1994**, *94*, 1339–1374, DOI 10.1021/cr00029a008.

[8] A. Rauk, L. C. Allen, K. Mislow, *Angew. Chem. Int. Ed.* **1970**, *9*, 400–414, DOI 10.1002/anie.197004001.

[9] C. C. Levin, *J. Am. Chem. Soc.* **1975**, *97*, 5649–5655, DOI 10.1021/ja00853a001.

[10] E. Magnusson, *J. Am. Chem. Soc.* **1990**, *112*, 7940–7951, DOI 10.1021/ja00178a014.

[11] E. Magnusson, *J. Am. Chem. Soc.* **1993**, *115*, 1051–1061, DOI 10.1021/ja00056a033.

[12] A. D. Walsh, *Discuss. Faraday Soc.* **1947**, *2*, 18–25, DOI 10.1039/df9470200018.

[13] H. A. Bent, *Chem. Rev.* **1961**, *61*, 275–311, DOI 10.1021/cr60211a005.

[14] D. A. Dixon, A. J. Arduengo III, T. Fukunaga, *J. Am. Chem. Soc.* **1986**, *108*, 2461–2462, DOI 10.1021/ja00269a063.

[15] A. J. Arduengo III, D. A. Dixon, D. C. Roe, *J. Am. Chem. Soc.* **1986**, *108*, 6821–6823, DOI 10.1021/ja00281a070.

[16] R. D. Baechler, K. Mislow, *J. Am. Chem. Soc.* **1970**, *92*, 3090–3093, DOI 10.1021/ja00713a028.

[17] A. L. Allred, A. L. Hensley JR, *J. Inorg. Nucl. Chem.* **1961**, *17*, 43–54, DOI 10.1016/0022-1902(61)80184-X.

[18] L. Horner, W. Hofer, *Tetrahedron Lett.* **1966**, *7*, 3323–3328, DOI 10.1016/S0040-4039(01)82786-6.

[19] G. W. Koeppl, D. S. Sagatys, G. S. Krishnamurthy, S. I. Miller, *J. Am. Chem. Soc.* **1967**, *89*, 3396–3405, DOI 10.1021/ja00990a004.

[20] K. Mislow, *Trans. N.Y. Acad. Sci.* **1973**, *35*, 227–242, DOI 10.1111/j.2164-0947.1973.tb01961.x.

[21] J. Meisenheimer, L. Lichtenstadt, *Chem. Ber.* **1911**, *44*, 356–359, DOI 10.1002/cber.19110440154.

[22] W. S. Knowles, M. J. Sabacky, *Chem. Commun.* **1968**, 1445–1446, DOI 10.1039/c19680001445.

[23] L. Horner, H. Siegel, H. Büthe, *Angew. Chem. Int. Ed.* **1968**, *7*, 942, DOI 10.1002/anie.196809422.

[24] A. Grabulosa, J. Granell, G. Muller, *Coord. Chem. Rev.* **2007**, *251*, 25–90, DOI 10.1016/j.ccr.2006.05.009.

[25] A. Grabulosa, *P-Stereogenic Ligands in Enantioselective Catalysis*, The Royal Society of Chemistry, Thomas Graham House, Science Park, Milton Road, Cambridge, UK, **2011**.

[26] L. Horner, H. Winkler, A. Rapp, A. Mentrup, H. Hoffmann, P. Beck, *Tetrahedron Lett.* **1961**, *2*, 161–166, DOI 10.1016/S0040-4039(01)84058-2.

[27] O. I. Kolodiazhnyi, *Tetrahedron: Asymmetry* **2012**, *23*, 1–16, DOI 10.1016/j.tetasy.2012.01.007.

[28] S. B. Wild, *Coord. Chem. Rev.* **1997**, *166*, 291–311, DOI 10.1016/S0010-8545(97)00046-5.

[29] J. Bayardon, S. Jugé in *Phosphorus(III) Ligands in Homogeneous Catalysis: Design and Synthesis*, (Eds.: P. C. J. Kamer, P. W. N. M. van Leeuwen), John Wiley & Sons, Ltd, Chichester, UK, **2012**, pp. 355–389, DOI http://doi.wiley.com/10.1002/9781118299715.ch12.

[30] K. Tani, L. D. Brown, J. Ahmed, J. A. Ibers, A. Nakamura, S. Otsuka, M. Yokota, *J. Am. Chem. Soc.* **1977**, *99*, 7876–7886, DOI 10.1021/ja00466a020.

[31] B. D. Vineyard, W. S. Knowles, M. J. Sabacky, G. L. Bachmann, D. J. Weinkauff, *J. Am. Chem. Soc.* **1977**, *99*, 5946–5952, DOI 10.1021/ja00460a018.

[32] S. Jugé, M. Stephan, J. A. Laffitte, J. P. Genet, *Tetrahedron Lett.* **1990**, *31*, 6357–6360, DOI 10.1016/S0040-4039(00)97063-1.

[33] E. J. Corey, Z. Chen, G. J. Tanoury, *J. Am. Chem. Soc.* **1993**, *115*, 11000–11001, DOI 10.1021/ja00076a072.

[34] F. Maienza, F. Spindler, M. Thommen, B. Pugin, C. Malan, A. Mezzetti, *J. Org. Chem.* **2002**, *67*, 5239–5249, DOI 10.1021/jo0201301.

[35] U. Nettekoven, P. C. J. Kamer, P. W. N. M. van Leeuwen, M. Widhalm, A. L. Spek, M. Lutz, *J. Org. Chem.* **1999**, *64*, 3996–4004, DOI 10.1021/jo982481z.

[36] A. R. Muci, K. R. Campos, D. A. Evans, *J. Am. Chem. Soc.* **1995**, *117*, 9075–9076, DOI 10.1021/ja00140a028.

[37] J. A. Osborn, G. Wilkinson, J. F. Young, *Chem. Commun. (London)* **1965**, 17, DOI 10.1039/C19650000017.

[38] J. F. Young, J. A. Osborn, F. H. Jardine, G. Wilkinson, *Chem. Commun. (London)* **1965**, 131–132, DOI 10.1039/c19650000131.

[39] W. S. Knowles, M. J. Sabacky, B. D. Vineyard, *Chem. Commun.* **1972**, 10–11, DOI 10.1039/C39720000010.

[40] W. S. Knowles, M. J. Sabacky, B. D. Vineyard, D. J. Weinkauff, *J. Am. Chem. Soc.* **1975**, *97*, 2567–2568, DOI 10.1021/ja00842a058.

[41] W. S. Knowles, *Acc. Chem. Res.* **1983**, *16*, 106–112, DOI 10.1021/ar00087a006.

[42] T. P. Dang, H. B. Kagan, *Chem. Commun.* **1971**, 481, DOI 10.1039/C29710000481.

[43] H. B. Kagan, T. P. Dang, *J. Am. Chem. Soc.* **1972**, *94*, 6429–6433, DOI 10.1021/ja00773a028.

[44] A. Miyashita, A. Yasuda, H. Takaya, K. Toriumi, T. Ito, T. Souchi, R. Noyori, *J. Am. Chem. Soc.* **1980**, *102*, 7932–7934, DOI 10.1021/ar00087a006.

[45] R. Noyori, *Angew. Chem. Int. Ed.* **2002**, *41*, 2008–2022, DOI 10.1002/1521-3773(20020617)41:12<2008::AID-ANIE2008>3.0.CO;2-4.

[46] R. Noyori, H. Takaya, *Chem. Scripta* **1985**, *25*, 83–89.

[47] M. Berthod, G. Mignani, G. Woodward, M. Lemaire, *Chem. Rev.* **2005**, *105*, 1801–1836, DOI 10.1021/cr040652w.

[48] N. Sayo, T. Matsumoto, U.S. Patent 6,342,644 B1, 2002, Takasago International Corporation, Tokyo, Japan.

[49] T. Saito, T. Yokozawa, T. Ishizaki, T. Moroi, N. Sayo, T. Miura, H. Kumobayashi, *Adv. Synth. Catal.* **2001**, *343*, 264–267, DOI 10.1002/1615-4169(20010330)343:3<264::AID-ADSC264>3.0.CO;2-T.

[50] T. P. Yoon, E. N. Jacobsen, *Science* **2003**, *299*, 1691–1693, DOI 10.1126/science.1083622.

[51] A. Togni, C. Breutel, A. Schnyder, F. Spindler, H. Landert, A. Tijani, *J. Am. Chem. Soc.* **1994**, *116*, 4062–4066, DOI 10.1021/ja00088a047.

[52] H.-U. Blaser, B. Pugin, F. Spindler, E. Mejía, A. Togni in *Privileged Chiral Ligands and Catalysts*, (Ed.: Q.-L. Zhou), Wiley-VCH Verlag GmbH & Co. KGaA, Weinheim, Germany, **2011**, pp. 93–136, DOI 10.1002/9781118299715.ch12.

[53] H.-U. Blaser, W. Brieden, B. Pugin, F. Spindler, M. Studer, A. Togni, *Top. Catal.* **2002**, *19*, 3–16, DOI 10.1023/A:1013832630565.

[54] J. McGarrity, F. Spindler, R. Fuchs, M. Eyer, Patent EP0624587, 1994, Lonza A.G., Gampel/Wallis, Switzerland.

[55] H.-U. Blaser, H.-P. Buser, K. Coers, R. Hanreich, H.-P. Jalett, E. Jelsch, B. Pugin, H.-D. Schneider, F. Spindler, A. Wegmann, *Chimia* **1999**, *53*, 275–280.

[56] D. Dobbs, K. Vanhessche, V. Rautenstrauch, Patent WO98/52687, 1998, Firmenich S.A., Geneva, Switzerland.

[57] H.-U. Blaser, W. Chen, F. Camponovo, A. Togni in *Ferrocenes: Ligands, Materials and Biomolecules*, (Ed.: P. Štěpnička), John Wiley & Sons, Ltd, Chichester, UK., **2008**, pp. 205–235, DOI 10.1002/9780470985663.ch6.

[58] U. Burckhardt, L. Hintermann, A. Schnyder, A. Togni, *Organometallics* **1995**, *14*, 5415–5425, DOI 10.1021/om00011a069.

[59] A. Schnyder, L. Hintermann, A. Togni, *Angew. Chem. Int. Ed.* **1995**, *34*, 931–933, DOI 10.1002/anie.199509311.

[60] P. von Matt, A. Pfaltz, *Angew. Chem. Int. Ed.* **1993**, *32*, 566–568, DOI 10.1002/anie.199305661.

[61] J. Sprinz, G. Helmchen, *Tetrahedron Lett.* **1993**, *34*, 1769–1772, DOI 10.1016/S0040-4039(00)60774-8.

[62] G. J. Dawson, C. G. Frost, J. M. J. Williams, S. J. Coote, *Tetrahedron Lett.* **1993**, *34*, 3149–3150, DOI 10.1016/S0040-4039(00)93403-8.

[63] G. Helmchen, A. Pfaltz, *Acc. Chem. Res.* **2000**, *33*, 336–345, DOI 10.1021/ar9900865.

[64] C. C. Bausch, A. Pfaltz in *Privileged Chiral Ligands and Catalysts*, (Ed.: Q.-L. Zhou), Wiley-VCH Verlag GmbH & Co. KGaA, Weinheim, Germany, **2011**, pp. 221–256, DOI 10.1002/9783527635207.ch6.

[65] M. P. Carroll, P. J. Guiry, *Chem. Soc. Rev.* **2014**, *43*, 819–833, DOI 10.1039/C3CS60302D.

[66] J. P. Janssen, G. Helmchen, *Tetrahedron Lett.* **1997**, *38*, 8025–8026, DOI 10.1016/S0040-4039(97)10220-9.

[67] O. B. Sutcliffe, M. R. Bryce, *Tetrahedron: Asymmetry* **2003**, *14*, 2297–2325, DOI 10.1016/S0957-4166(03)00520-2.

[68] G. Schmitt, P. Klein, W. Ebertz, *J. Organomet. Chem.* **1982**, *234*, 63–72, DOI 10.1016/S0022-328X(00)85702-2.

[69] C. J. Richards, T. Damalidis, D. E. Hibbs, M. B. Hursthouse, *Synlett* **1995**, *1995*, 74–76, DOI 10.1055/s-1995-4864.

[70] C. J. Richards, A. W. Mulvaney, *Tetrahedron: Asymmetry* **1996**, *7*, 1419–1430, DOI 10.1016/0957-4166(96)00159-0.

[71] Y. Nishibayashi, S. Uemura, *Synlett* **1995**, *1995*, 79–81, DOI 10.1055/s-1995-4881.

[72] Y. Nishibayashi, K. Segawa, Y. Arikawa, K. Ohe, M. Hidai, S. Uemura, *J. Organomet. Chem.* **1997**, *545-546*, 381–398, DOI 10.1016/S0022-328X(97)00368-9.

[73] Y. Nishibayashi, K. Segawa, K. Ohe, S. Uemura, *Organometallics* **1995**, *14*, 5486–5487, DOI 10.1021/om00012a012.

[74] Y. Nishibayashi, K. Segawa, H. Takada, K. Ohe, S. Uemura, *Chem. Commun.* **1996**, *2*, 847–848, DOI 10.1039/cc9960000847.

[75] T. Sammakia, H. A. Latham, D. R. Schaad, *J. Org. Chem.* **1995**, *60*, 10–11, DOI 10.1021/jo00106a005.

[76] T. Sammakia, H. A. Latham, *J. Org. Chem.* **1995**, *60*, 6002–6003, DOI 10.1021/jo00124a003.

[77] T. Sammakia, H. A. Latham, *J. Org. Chem.* **1996**, *61*, 1629–1635, DOI 10.1021/jo9515561.

[78] S.-L. You, X.-L. Hou, L.-X. Dai, Y.-H. Yu, W. Xia, *J. Org. Chem.* **2002**, *67*, 4684–4695, DOI 10.1021/jo016330z.

[79] F. Naud, C. Malan, F. Spindler, C. Rüggeberg, A. T. Schmidt, H.-U. Blaser, *Adv. Synth. Catal* **2006**, *348*, 47–50, DOI 10.1002/adsc.200505246.

[80] F. Naud, F. Spindler, C. J. Rueggeberg, A. T. Schmidt, H.-U. Blaser, *Org. Process. Res. Dev.* **2007**, *11*, 519–523, DOI 10.1021/op0601619.

[81] F. Naud, F. Spindler, C. Rueggeberg, A. T. Schmidt, H.-U. Blaser in *Asymmetric Catalysis on Industrial Scale: Challenges, Approaches and Solutions*, (Eds.: H.-U. Blaser, H.-J. Federsel), Wiley-VCH Verlag GmbH & Co. KGaA, Weinheim, Germany, **2010**, pp. 321–329, DOI 10.1002/9783527630639.ch19.

[82] *Ferrocenes: Homogeneous Catalysis, Organic Synthesis, Materials Science*, (Eds.: A. Togni, T. Hayashi), Wiley-VCH Verlag GmbH, Weinheim, Germany, **1994**, DOI 10.1002/9783527615599.

[83] A. Togni in *Metallocenes: Synthesis Reactivity Applications*, (Eds.: A. Togni, R. L. Halterman), Wiley-VCH Verlag GmbH, Weinheim, Germany, **1998**, pp. 685–721, DOI 10.1002/9783527619542.ch11.

[84] *Ferrocenes: Ligands, Materials and Biomolecules*, (Ed.: P. Štěpnička), John Wiley & Sons, Ltd, Chichester, UK., **2008**, DOI 10.1002/9780470985663.

[85] *Chiral Ferrocenes in Asymmetric Catalysis: Synthesis and Applications*, (Eds.: L.-X. Dai, X.-L. Hou), Wiley-VCH Verlag GmbH & Co. KGaA, Weinheim, Germany, **2009**, DOI 10.1002/9783527628841.

[86] *Privileged Chiral Ligands and Catalysts*, (Ed.: Q.-L. Zhou), Wiley-VCH Verlag GmbH & Co. KGaA, Weinheim, Germany, **2011**, DOI 10.1002/9783527635207.

[87] U. Nettekoven, P. C. J. Kamer, M. Widhalm, P. W. N. M. van Leeuwen, *Organometallics* **2000**, *19*, 4596–4607, DOI 10.1021/om0004489.

[88] W. Chen, S. M. Roberts, J. Whittall, A. Steiner, *Chem. Commun.* **2006**, 2916–2918, DOI 10.1039/b601952h.

[89] W. Chen, W. Mbafor, S. M. Roberts, J. Whittall, *J. Am. Chem. Soc.* **2006**, *128*, 3922–3923, DOI 10.1021/ja058531g.

[90] T. Hamada, S. L. Buchwald, *Org. Lett.* **2002**, *4*, 999–1001, DOI 10.1021/ol025563p.

[91] A. M. Taylor, R. A. Altman, S. L. Buchwald, *J. Am. Chem. Soc.* **2009**, *131*, 9900–9901, DOI 10.1021/ja903880q.

[92] A. Grabulosa, *P-Stereogenic Ligands in Enantioselective Catalysis*, The Royal Society of Chemistry, Thomas Graham House, Science Park, Milton Road, Cambridge, UK, **2011**, pp. 361–494.

[93] C. A. Tolman, *Chem. Rev.* **1977**, *77*, 313–348, DOI 10.1021/cr60307a002.

[94] C. Gambs, G. Consiglio, A. Togni, *Helv. Chim. Acta* **2001**, *84*, 3105–3126, DOI 10.1002/1522-2675(20011017)84:10<3105::AID-HLCA3105>3.0.CO;2-L.

[95] L. Liu, H.-C. Wu, J.-Q. Yu, *Chem. Eur. J.* **2011**, *17*, 10828–10831, DOI 10.1002/chem.201101467.

[96] D. C. Behenna, J. T. Mohr, N. H. Sherden, S. C. Marinescu, A. M. Harned, K. Tani, M. Seto, S. Ma, Z. Novák, M. R. Krout, R. M. McFadden, J. L. Roizen, J. A. Enquist, D. E. White, S. R. Levine, K. V. Petrova, A. Iwashita, S. C. Virgil, B. M. Stoltz, *Chem. Eur. J.* **2011**, *17*, 14199–14223, DOI 10.1002/chem.201003383.

[97] A. K. Brisdon, C. J. Herbert, *Coord. Chem. Rev.* **2013**, *257*, 880–901, DOI 10.1016/j.ccr.2012.07.028.

[98] W. Volbach, I. Ruppert, *Tetrahedron Lett.* **1983**, *24*, 5509–5512, DOI 10.1016/S0040-4039(00)94125-X.

[99] J. H. Seinfeld, S. N. Pandis, *Atmospheric Chemistry and Physics: From Air Pollution to Climate Change*, John Wiley & Sons, Inc., Hoboken, New Jersey, **2016**, pp. 167–168.

[100] P. Panne, D. Naumann, B. Hoge, *J. Fluor. Chem.* **2001**, *112*, 283–286, DOI 10.1016/S0022-1139(01)00513-9.

[101] I. Tworowska, W. Dąbkowski, J. Michalski, *Angew. Chem. Int. Ed.* **2001**, *40*, 2898–2900, DOI 10.1002/1521-3773(20010803)40:15<2898::AID-ANIE2898>3.0.CO;2-I.

[102] M. B. Murphy-Jolly, L. C. Lewis, A. J. M. Caffyn, *Chem. Commun.* **2005**, 4479–80, DOI 10.1039/b507752d.

[103] E. J. Velazco, A. J. M. Caffyn, X. F. Le Goff, L. Ricard, **2008**, 2402–2404, DOI 10.1021/om701244b.

[104] J. J. Adams, A. Lau, N. Arulsamy, D. M. Roddick, *Inorg. Chem.* **2007**, *46*, 11328–11334, DOI 10.1021/ic701426u.

[105] J. J. Adams, A. Lau, N. Arulsamy, D. M. Roddick, *Organometallics* **2011**, *30*, 689–696, DOI 10.1021/om1008633.

[106] J. J. Adams, B. C. Gruver, R. Donohoue, N. Arulsamy, D. M. Roddick, *Dalton Trans.* **2012**, *41*, 12601–12611, DOI 10.1039/c2dt31234d.

[107] J. J. Adams, A. Lau, N. Arulsamy, D. M. Roddick, *Organometallics* **2013**, *32*, 6468–6475, DOI 10.1021/om400823s.

[108] P. Eisenberger, S. Gischig, A. Togni, *Chem. Eur. J.* **2006**, *12*, 2579–2586, DOI 10.1002/chem.200501052.

[109] V. Matoušek, E. Pietrasiak, R. Schwenk, A. Togni, *J. Org. Chem.* **2013**, *78*, 6763–6768, DOI 10.1021/jo400774u.

[110] P. Eisenberger, I. Kieltsch, N. Armanino, A. Togni, *Chem. Commun.* **2008**, 1575–1577, DOI 10.1039/b801424h.

[111] N. Armanino, R. Koller, A. Togni, *Organometallics* **2010**, *29*, 1771–1777, DOI 10.1021/om100015s.

[112] A. Sondenecker, Doctoral thesis, ETH Zurich Dissertation No. 18681, **2009**, DOI 10.3929/ethz-a-005975151.

[113] A. Sondenecker, J. Cvengroš, R. Aardoom, A. Togni, *Eur. J. Org. Chem.* **2011**, *2011*, 78–87, DOI 10.1002/ejoc.201001162.

[114] R. Koller, Doctoral thesis, ETH Zurich Dissertation No. 19219, **2010**, DOI 10.3929/ethz-a-006354797.

[115] J. Bürgler, Doctoral thesis, ETH Zurich Dissertation No. 19513, **2011**, DOI 10.3929/ethz-a-006395663.

[116] J. F. Buergler, K. Niedermann, A. Togni, *Chem. Eur. J.* **2012**, *18*, 632–640, DOI 10.1002/chem.201102390.

[117] R. Schwenk, Doctoral thesis, ETH Zurich Dissertation No. 21772, **2014**, DOI 10.3929/ethz-a-010147107.

[118] R. Schwenk, A. Togni, *Dalton Trans.* **2015**, *44*, 19566–19575, DOI 10.1039/C5DT02019K.

[119] Z. Hu, Y. Li, K. Liu, Q. Shen, *J. Org. Chem.* **2012**, *77*, 206–210, DOI 10.1021/jo3011717.

[120] B. M. Trost, D. L. Van Vranken, *Chem. Rev.* **1996**, *96*, 395–422, DOI 10.1021/cr9409804.

[121] Z.-W. Lai, R.-F. Yang, K.-Y. Ye, H. Sun, S.-L. You, *Beilstein J. Org. Chem.* **2014**, *10*, 1261–1266, DOI 10.3762/bjoc.10.126.

[122] T. Ohkuma, N. Kurono in *Privileged Chiral Ligands and Catalysts*, (Ed.: Q.-L. Zhou), Wiley-VCH Verlag GmbH & Co. KGaA, Weinheim, Germany, **2011**, pp. 1–53, DOI 10.1002/9783527635207.ch1.

[123] N. Armanino, *Synthesis of a novel bis-trifluoromethyl-phosphine ligand of the binaphthyl class via electrophilic trifluoromethylation*, Master thesis, ETH Zurich, **2008**.

[124] L. Kurz, G. Lee, D. Morgans, M. J. Waldyke, T. Ward, *Tetrahedron Lett.* **1990**, *31*, 6321–6324, DOI 10.1016/S0040-4039(00)97053-9.

[125] S. Cacchi, P. G. Ciattini, E. Morera, G. Ortar, *Tetrahedron Lett.* **1986**, *27*, 5541–5544, DOI 10.1016/S0040-4039(00)85262-4.

[126] A. Garcia Martinez, I. Espada Rios, R. Martinez Alvarez, E. Teso Vilar, *An. Quím.* **1981**, *77*, 67–70.

[127] K. Naumann, G. Zon, K. Mislow, *J. Am. Chem. Soc.* **1969**, *91*, 7012–7023, DOI 10.1021/ja01053a021.

[128] M. Berthod, A. Favre-Réguillon, J. Mohamad, G. Mignani, G. Docherty, M. Lemaire, *J. Am. Chem. Soc.* **2007**, *2007*, 1545–1548, DOI 10.1055/s-2007-982536.

[129] R. M. Hiney, L. J. Higham, H. Müller-Bunz, D. G. Gilheany, *Angew. Chem. Int. Ed.* **2006**, *45*, 7248–51, DOI 10.1002/anie.200602143.

[130] B. Stewart, A. Harriman, L. J. Higham, *Organometallics* **2011**, *30*, 5338–5343, DOI 10.1021/om200070a.

[131] K. J. Brown, M. S. Berry, J. R. Murdoch, *J. Org. Chem.* **1985**, *50*, 4345–4349, DOI 10.1021/jo00222a029.

[132] T. Hoshi, H. Shionoiri, T. Suzuki, M. Ando, H. Hagiwara, *Tetrahedron: Asymmetry* **1999**, *28*, 1245–1246, DOI 10.1246/cl.1999.1245.

[133] M. Mešková, M. Putala, *Tetrahedron: Asymmetry* **2013**, *24*, 894–902, DOI 10.1016/j.tetasy.2013.06.007.

[134] J. Pan, X. Wang, Y. Zhang, S. L. Buchwald, *Org. Lett.* **2011**, *13*, 4974–4976, DOI 10.1021/ol202098h.

[135] E. Shirakawa, Y. Imazaki, T. Hayashi, *Chem. Commun.* **2009**, *7345*, 5088–5090, DOI 10.1039/b907761h.

[136] Y. Imazaki, E. Shirakawa, R. Ueno, T. Hayashi, *J. Am. Chem. Soc.* **2012**, *134*, 14760–14763, DOI 10.1021/ja307771d.

[137] B. Czarniecki, Doctoral thesis, ETH Zurich Dissertation No. 22254, **2014**, DOI 10.3929/ethz-a-010398240.

[138] M. Lautens, K. Fagnou, S. Hiebert, *Acc. Chem. Res.* **2003**, *36*, 48–58, DOI 10.1021/ar010112a.

[139] M. Lautens, J.-L. Renaud, S. Hiebert, *J. Am. Chem. Soc.* **2000**, *122*, 1804–1805, DOI 10.1021/ja993427i.

[140] M. Lautens, K. Fagnou, M. Taylor, T. Rovis, *J. Organomet. Chem.* **2001**, *624*, 259–270, DOI 10.1016/S0022-328X(00)00904-9.

[141] F. Bertozzi, M. Pineschi, F. Macchia, L. A. Arnold, A. J. Minnaard, B. L. Feringa, *Org. Lett.* **2002**, *4*, 2703–2705, DOI 10.1021/ol026220u.

[142] L. Yu, Y. Zhou, X. Xu, J. Li, Sifeng Xu, B. Fan, C. Lin, Z. Bian, A. S. C. Chan, *Tetrahedron Lett.* **2014**, *55*, 6315–6318, DOI 10.1016/j.tetlet.2014.09.089.

[143] B.-H. Tan, N. Yoshikai, *Org. Lett.* **2014**, *16*, 3392–3395, DOI 10.1021/ol501449j.

[144] J. A. van Doorn, J. H. G. Frijns, N. Meijboom, *Recl. Trav. Chim. Pays-Bas* **1991**, *110*, 441–449, DOI 10.1002/recl.19911101103.

[145] W. Hewertson, H. R. Watson, *J. Chem. Soc.* **1962**, 1490–1494, DOI 10.1039/JR9620001490.

[146] B. R. Kimpton, W. McFarlane, A. S. Muir, P. G. Patel, J. L. Bookham, *Polyhedron* **1993**, *12*, 2525–2534, DOI 10.1016/S0277-5387(00)83079-X.

[147] J. A. van Doorn, N. Meijboom, *Recl. Trav. Chim. Pays-Bas* **1992**, *111*, 170–177, DOI 10.1002/recl.19921110402.

[148] J. Dogan, J. B. Schulte, G. F. Swiegers, S. B. Wild, *J. Org. Chem.* **2000**, *65*, 951–957, DOI 10.1021/jo9907336.

[149] M. Ranocchiari, A. Mezzetti, *Organometallics* **2009**, *28*, 1286–1288, DOI 10.1021/om900028w.

[150] M. Bulbrook, M. Chu, K. Deane, R. J. Doyle, J. Hinc, C. Peterson, G. Salem, N. Thorman, A. C. Willis, *Dalton Trans.* **2010**, *39*, 8878–8881, DOI 10.1039/c0dt00648c.

[151] T. Shimada, Y.-H. Kurushima, Hiroaki Cho, T. Hayashi, *J. Org. Chem.* **2001**, *66*, 8854–8858, DOI 10.1021/jo010691x.

[152] C. W. D. Gallop, M. Bobin, P. Hourani, J. Dwyer, S. M. Roe, E. M. E. Viseux, *J. Org. Chem.* **2013**, *78*, 6522–6528, DOI 10.1021/jo4006393.

[153] A. Schira, Doctoral thesis, ETH Zurich Dissertation No. 21028, **2013**, DOI 10.3929/ethz-a-009939810.

[154] M. D. Ferguson in *e-EROS Encyclopedia of Reagents for Organic Synthesis*, **2001**, DOI 10.1002/047084289X.rl088.

[155] P. K. Freeman, L. L. Hutchinson, *Tetrahedron: Asymmetry* **1980**, *45*, 1924–1930, DOI 10.1021/jo01298a034.

[156] T. Hayashi, K. Hayashizaki, T. Kiyoi, Y. Ito, *J. Am. Chem. Soc.* **1988**, *110*, 8153–8156, DOI 10.1021/ja00232a030.

[157] A. N. Cammidge, K. V. L. Crépy, *Chem. Commun.* **2000**, 1723–1724, DOI 10.1039/b004513f.

[158] J. Yin, S. L. Buchwald, *J. Am. Chem. Soc.* **2000**, *122*, 12051–12052, DOI 10.1021/ja005622z.

[159] L. Benhamou, C. Besnard, E. P. Kündig, *Organometallics* **2014**, *33*, 260–266, DOI 10.1021/om4009982.

[160] S. E. Denmark, W.-t. T. Chang, K. N. Houk, P. Liu, *J. Org. Chem.* **2015**, *80*, 313–366, DOI 10.1021/jo502388r.

[161] A. Ficks, C. Sibbald, S. Ojo, R. Harrington, W. Clegg, L. Higham, *Synthesis* **2012**, *45*, 265–271, DOI 10.1055/s-0032-1316825.

[162] H. A. McManus, P. J. Guiry, *Chem. Rev.* **2004**, *104*, 4151–4202, DOI 10.1021/cr040642v.

[163] G. C. Hargaden, P. J. Guiry, *Chem. Rev.* **2009**, *109*, 2505–2550, DOI 10.1021/cr800400z.

[164] M. Peer, J. C. de Jong, Kiefer, Matthias, T. Langer, H. Rieck, H. Schell, P. Sennhenn, J. Sprinz, H. Steinhagen, B. Wiese, G. Helmchen, *Tetrahedron* **1996**, *52*, 7547–7583, DOI 10.1016/0040-4020(96)00267-0.

[165] H. Witte, W. Seeliger, *Liebigs Ann.* **1974**, *1974*, 996–1009, DOI 10.1002/jlac.197419740615.

[166] E. V. Anslyn, D. A. Dougherty in *Modern Physical Organic Chemistry*, University Science Books, Sausalito, CA, **2006**, pp. 180–186.

[167] K. D. Reichl, D. H. Ess, A. T. Radosevich, *J. Am. Chem. Soc.* **2013**, *135*, 9354–9357, DOI 10.1021/ja404943x.

[168] B. Wiese, G. Helmchen, *Tetrahedron Lett.* **1998**, *39*, 5727–5730, DOI 10.1016/S0040-4039(98)01173-3.

[169] T. Nol, K. Robeyns, L. Van Meervelt, E. Van der Eycken, J. Van der Eycken, *Tetrahedron: Asymmetry* **2009**, *17*, 1962–1968, DOI 10.1016/j.tetasy.2009.07.038.

[170] M. Schlosser, *Pure Appl. Chem.* **1988**, *60*, 1627–1634, DOI 10.1351/pac198860111627.

[171] S. A. Herbert, D. C. Castell, J. Clayden, G. E. Arnott, *Org. Lett.* **2013**, *15*, 3334–3337, DOI 10.1021/ol4013734.

[172] A. C. Tagne Kuate, S. Sameni, M. Freytag, P. G. Jones, M. Tamm, *Angew. Chem. Int. Ed.* **2013**, *52*, 8638–8642, DOI 10.1002/anie.201304252.

[173] F. Elterlein, *Trifluoromethylated P-stereogenic 1,1'-ferrocenyloxazoline ligands*, Master thesis, ETH Zurich, **2016**.

[174] M. Lutz, *Trifluoromethylated P-stereogenic ferrocenyloxazoline ligands*, Semester project, ETH Zurich, **2015**.

[175] K. Tamao, N. Ishida, T. Tanaka, M. Kumada, *Organometallics* **1983**, *2*, 1694–1696, DOI 10.1021/om50005a041.

[176] I. Fleming, R. Henning, H. Plaut, *J. Chem. Soc. Chem. Commun.* **1984**, 29–31, DOI 10.1039/c39840000029.

[177] G. R. Jones, Y. Landais, *Tetrahedron* **1996**, *52*, 7599–7662, DOI 10.1016/S0040-4020(96)00038-5.

[178] G. Pioda, A. Togni, *Tetrahedron: Asymmetry* **1998**, *9*, 3903–3910, DOI 10.1016/S0957-4166(98)00409-1.

[179] G. Pioda, Doctoral thesis, ETH Zurich Dissertation No. 13405, **1999**, DOI 10.3929/ethz-a-003846013.

[180] S.-M. Lu, X.-W. Han, Y.-G. Zhou, *Adv. Synth. Catal.* **2004**, *346*, 909–912, DOI 10.1002/adsc.200404017.

[181] L.-X. Dai, T. Tu, S.-L. You, W.-P. Deng, X.-L. Hou, *Acc. Chem. Res.* **2003**, *36*, 659–667, DOI 10.1021/ar020153m.

[182] M. S. Inkpen, S. Du, M. Driver, T. Albrecht, N. J. Long, *Dalton Trans.* **2013**, *42*, 2813–2816, DOI 10.1039/c2dt32779a.

[183] M. Kesselgruber, M. Lotz, P. Martin, G. Melone, M. Müller, B. Pugin, F. Naud, F. Spindler, M. Thommen, P. Zbinden, H.-U. Blaser, *Chem. Asian J.* **2008**, *3*, 1384–1389, DOI 10.1002/asia.200800186.

[184] S. Hashiguchi, A. Fujii, J. Takehara, T. Ikariya, R. Noyori, *J. Am. Chem. Soc.* **1995**, *117*, 7562–7563, DOI 10.1021/ja00133a037.

[185] J. Hannedouche, G. J. Clarkson, M. Wills, *J. Am. Chem. Soc.* **2004**, *126*, 986–987, DOI 10.1021/ja0392768.

[186] A. M. Hayes, D. J. Morris, G. J. Clarkson, M. Wills, *J. Am. Chem. Soc.* **2005**, *127*, 7318–7319, DOI 10.1021/ja051486s.

[187] R. Aznar, G. Muller, D. Sainz, M. Font-Bardia, X. Solans, *Organometallics* **2008**, *27*, 1967–1969, DOI 10.1021/om800076x.

[188] J. W. Faller, D. G. D'Alliessi, *Organometallics* **2003**, *22*, 2749–2757, DOI 10.1021/om030080q.

[189] P. Pinto, G. Marconi, F. W. Heinemann, U. Zenneck, *Organometallics* **2004**, *23*, 374–380, DOI 10.1021/om0305768.

[190] P. Pinto, A. W. Götz, G. Marconi, B. A. Hess, A. Marinetti, F. W. Heinemann, U. Zenneck, *Organometallics* **2006**, *25*, 2607–2616, DOI 10.1021/om050461z.

[191] R. Aznar, A. Grabulosa, A. Mannu, G. Muller, D. Sainz, V. Moreno, M. Font-Bardia, T. Calvet, J. Lorenzo, *Organometallics* **2013**, *32*, 2344–2362, DOI 10.1021/om3012294.

[192] M. Navarro, D. Vidal, P. Clavero, A. Grabulosa, G. Muller, *Organometallics* **2015**, *34*, 973–994, DOI 10.1021/acs.organomet.5b00018.

[193] R. M. Aardoom, Doctoral thesis, ETH Zurich Dissertation No. 20635, **2012**, DOI 10.3929/ethz-a-007579989.

[194] M. Kober-Czerny, *Preparation and first application of trifluoromethyl P-stereogenic phenylethylferrocene derived ligands*, Semester project, ETH Zurich, **2016**.

[195] A. L. Wilds, N. A. Nelson, *J. Am. Chem. Soc.* **1953**, *75*, 5360–5365, DOI 10.1021/ja01117a064.

[196] H. L. Dryden, G. M. Webber, R. R. Burtner, J. A. Cella, *J. Org. Chem.* **1961**, *26*, 3237–3245, DOI 10.1021/jo01067a049.

[197] H. Fujioka, N. Kotoku, Y. Sawama, H. Kitagawa, Y. Ohba, T.-L. Wang, Y. Nagatomi, Y. Kita, *Chem. Pharm. Bull.* **2005**, *53*, 952–957, DOI 10.1248/cpb.53.952.

[198] H. van Bekkum, C. B. van Den Bosch, G. van Minnen-Pathuis, J. C. de Mos, A. M. van Wijk, *Recl. Trav. Chim. Pays-Bas* **1971**, 137–149, DOI 10.1002/recl.19710900203.

[199] D. Kuck, J. Schneider, H.-F. Grützmacher, *J. Chem. Soc. Perkin Trans. 2* **1985**, 689–696, DOI 10.1039/P29850000689.

[200] D. Schröder, J. Loos, H. Schwarz, R. Thissen, O. Dutuit, *J. Phys. Chem. A* **2004**, *108*, 9931–9937, DOI 10.1021/jp0479973.

[201] S. Hirai, M. Nakada, *Tetrahedron* **2011**, *67*, 518–530, DOI 10.1016/j.tet.2010.10.076.

[202] X. Han, R. A. Widenhoefer, *Angew. Chem. Int. Ed.* **2006**, *45*, 1747–1749, DOI 10.1002/anie.200600052.

[203] R. G. Bergman, R. L. Danheiser, *Angew. Chem. Int. Ed.* **2016**, *55*, 12548–12549, DOI 10.1002/anie.201606591.

[204] M. Baker, *Nature* **2016**, *533*, 452–454, DOI 10.1038/533452a.

[205] S. Buck, *Science* **2015**, *348*, 1403–1403, DOI 10.1126/science.aac8041.

[206] A. D. McNaught, A. Wilkinson in *IUPAC. Compendium of Chemical Terminology, 2nd ed. (the "Gold Book")*, Blackwell Scientific Publications, Oxford, **1997**, DOI 10.1351/goldbook.R05305.

[207] W. S. Knowles, *Angew. Chem. Int. Ed.* **2002**, *41*, 1998–2007, DOI 10.1002/1521-3773(20020617)41:12<1998::AID-ANIE1998>3.0.CO;2-8.

[208] J. Suffert, *J. Org. Chem.* **1989**, *54*, 509–510, DOI 10.1021/jo00263a052.

[209] V. M. Mićović, M. L. Mihailović, *J. Org. Chem.* **1953**, *18*, 1190–1200, DOI 10.1021/jo50015a017.

[210] J. F. Bower, C. J. Martin, D. J. Rawson, A. M. Z. Slawin, J. M. J. Williams, *J. Chem. Soc. Perkin Trans. 1* **1996**, 333–342, DOI 10.1039/P19960000333.

[211] Y. Hsiao, L. S. Hegedus, *J. Org. Chem.* **1997**, *62*, 3586–3591, DOI 10.1021/jo962343e.

[212] W. C. Still, M. Kahn, A. Mitra, *J. Org. Chem.* **1978**, *43*, 2923–2925, DOI 10.1021/jo00408a041.

[213] *SAINT+*, Software for CCD Diffractometers, v. 6.01 and SAINT, v. 6.02; Bruker AXS, Inc., Madison, WI, **2001**.

[214] G. M. Sheldrick, *Acta Crystallogr. Sect. A* **1990**, *46*, 467–473, DOI 10.1107/S0108767390000277.

[215] G. M. Sheldrick, *SHELXL-97 Program for Crystal Structure Refinement* **1999**.

[216] R. H. Blessing, *Acta Crystallogr. Sect. A.* **1995**, *51*, 33–38, DOI 10.1107/S0108767394005726.

[217] H. D. Flack, *Acta Crystallogr. Sect. A* **1983**, *39*, 876–881, DOI 10.1107/S0108767383001762.

[218] G. Bernardinelli, H. D. Flack, *Acta Crystallogr. Sect. A* **1985**, *41*, 500–511, DOI 10.1107/S0108767385001064.

[219] *Acta Crystallogr. Sect. C-Cryst. Struct. Commun.* **2009**, *66*, e1–e8, DOI 10.1107/S0108270109047817.

[220] B. A. Chalmers, K. S. Athukorala Arachchige, J. K. D. Prentis, F. R. Knight, P. Kilian, A. M. Z. Slawin, J. D. Woollins, *Inorg. Chem.* **2014**, 8795–8808, DOI 10.1021/ic5014768.

[221] J. S. Han, W. Wolfsberger, *Z. Naturforsch. B* **1989**, *44*, 502–504.

[222] S.-M. Lu, X.-W. Han, Y.-G. Zhou, *Adv. Synth. Catal.* **2004**, *346*, 909–912, DOI 10.1002/adsc.200404017.

[223] C. A. Beevers, *J. Appl. Cryst.* **1970**, *3*, 45–49, DOI 10.1107/S0021889870005630.

Appendix A: Abbreviations and Acronyms

Ad	Adamantyl
aq.	Aqueous
Ar	Aryl
BINAP	1,1'-Binaphthalene-2,2'-diylbis(diphenylphosphane)
BINOL	1,1'-Binaphthalene-2,2'-diol
BSA	*N,O*-Bis(trimethylsilylacetamide)
BTMA	3,5-Bistrifluoromethyl acetophenone
BTMP	3,5-Bistrifluoromethyl phenylethanol
BuLi	Butyllithium
calcd.	Calculated
COD	Cycloocta-1,5-diene
COT	Cycloocta-1,3,5-triene
Cp	Cyclopentadienyl
Cy	Cyclohexyl
DABCO	1,4-Diazabicyclo[2.2.2]octane
DABN	2,2'-Diamino-1,1'-binaphthalene
DBBN	2,2'-Dibromobinaphthalene
DBU	1,8-Diazabicyclo[5.4.0]undec-7-ene
DCE	1,2-Dichloroethane
de	Diastereomeric excess
dfepf	1,1'-Bis(bis(pentafluoroethyl)phosphanyl)ferrocene
dfmpf	1,1'-Bis(bis(trifluoromethyl)phosphanyl)ferrocene
diglyme	Diethylene glycol dimethyl ether (1-methoxy-2-(2-methoxyethoxy)ethane)
DIPEA	*N,N*-Diisopropylethylamine
DMF	Dimethylformamide
DMI	Dimethyl itaconate
DMSO	Dimethylsulfoxide
dppb	1,2-Bis(diphenylphosphanyl)butane
dppe	1,2-Bis(diphenylphosphanyl)ethane
dppf	1,1'-Bis(diphenylphosphanyl)ferrocene
dr	Diastereomeric ratio
ee	Enantiomeric excess
EI	Electron Ionization
eq.	Equivalent
er	Enantiomeric ratio
ESI	Electrospray Ionization
Et	Ethyl
EtOAc	Ethyl acetate
EtOH	Ethanol
Fc	Ferrocenyl
FC	Flash Chromatography
Fcox	Ferrocenyloxazoline

GC	Gas Chromatography
h	Hour
hex	Hexane
HPLC	High Pressure Liquid Chromatography
iPr	Isopropyl
IUPAC	International Union of Pure and Applied Chemistry
LAH	Lithium Aluminium Hydride
LDA	Lithium diisopropylamide
M.P.	Melting point
m/*z*	Mass-to-charge ratio
MALDI	Matrix-Assisted Laser Desorption Ionization
Me	Methyl
MeCN	Acetonitrile
MeOH	Methanol
Ms	Mesyl (methanesulfonyl)
MS	Mass Spectrometry
NBD	2,5-Norbornadiene
*n*Bu	*n*-Butyl
NMR	Nuclear Magnetic Resonance
Np	Naphthalen-2-yl
Ph	Phenyl
PHOX	Phenyloxazoline
PMDTA	*N,N,N',N'',N''*-Pentamethyldiethylenetriamine
Pn	Pnictogen
quant.	Quantitative
rt	Room temperature
sat.	Saturated
*s*Bu	*sec*-Butyl
TBME	*tert*-Butylmethylether
*t*Bu	*tert*-Butyl
tetraglyme	Tetraethylene glycol dimethyl ether
Tf	Triflyl (trifluoromethanesulfonyl)
TFE	2,2,2-Trifluoroethanol
THF	Tetrahydrofuran
TLC	Thin Layer Chromatography
TMDS	Tetramethyldisiloxane
TMEDA	*N,N,N',N'*-Tetramethylethylenediamine
TMS	Trimethylsilyl
Tol	Tolyl (4-methylphenyl)
Ts	Tosyl (toluenesulfonyl)
TsDPEN	*N*-(*p*-Toluenesulfonyl)-1,2-diphenylethylenediamine
Xyl	Xylyl (3,5-dimethylphenyl)

Appendix B: Compound numbering

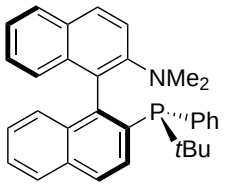

1

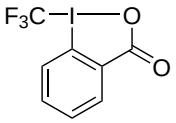

2

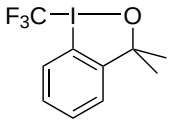

3

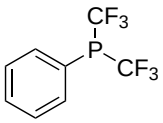

4

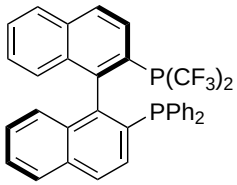

5

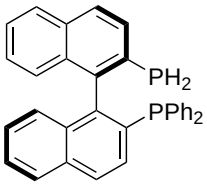

6

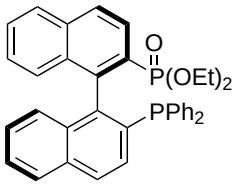

7

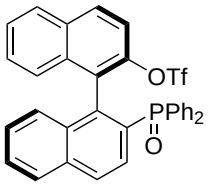

8

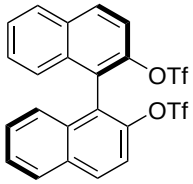

9

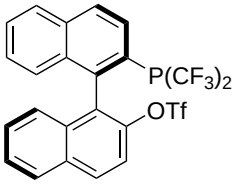

10

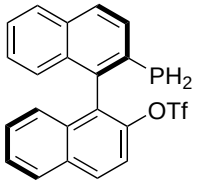

11

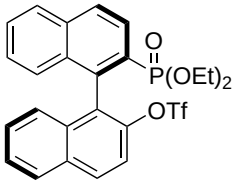

12

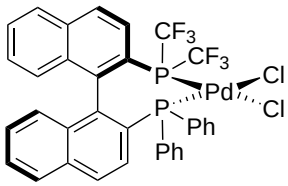

13

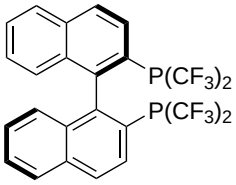

14

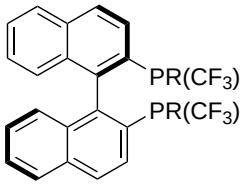

15

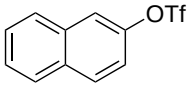

16

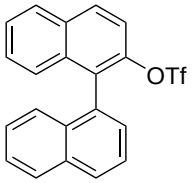

17

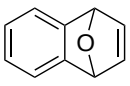

18

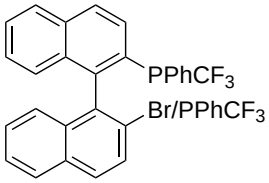

19

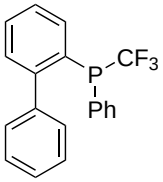

20

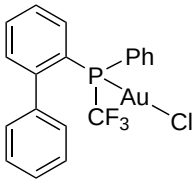

21

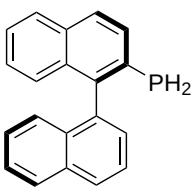

22

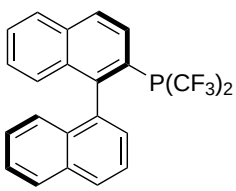

23

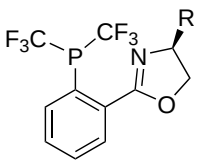

24

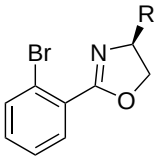

	R
a	iPr
b	Ph
c	*t*Bu

25

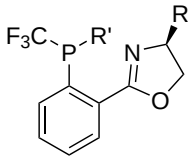

	R	R'
a	iPr	Ph
b	Ph	Ph
c	*t*Bu	Ph
d	Ph	2-Np

26

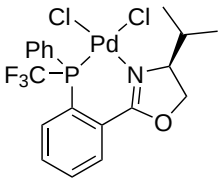

27

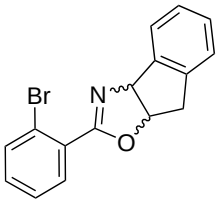

28

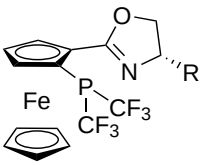

29

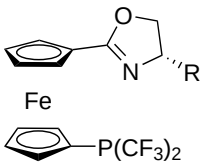

30

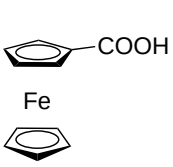

31

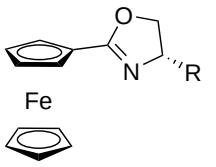

	R
a	Me
b	iPr
c	Ph
d	H

32

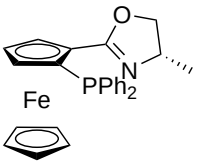

33

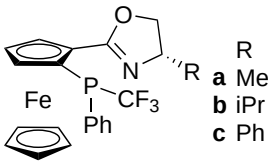

	R
a	Me
b	iPr
c	Ph

34

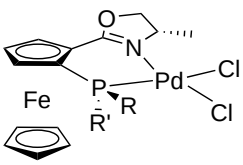

35

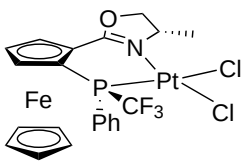

36

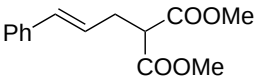

37

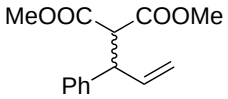

38

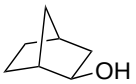

39a

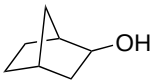

39b

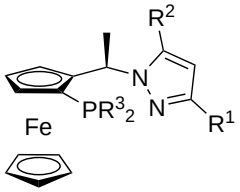

40

	R^1	R^2	R^3
40a	3,5-$(CF_3)_2$Ph	H	Ph
40b	Mes	H	CF_3
40c	Me	Me	Ph
40d	Mes	H	Ph

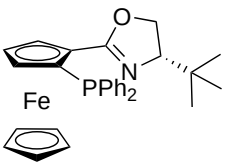

41

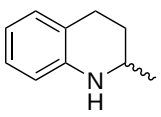

42

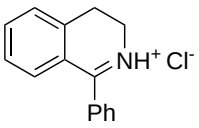

43

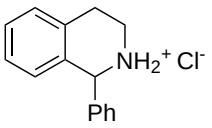

44

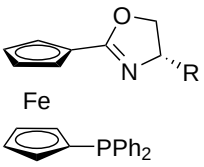

	R
a	Me
b	*t*Bu
c	Ph

45

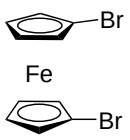

46

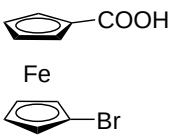

47

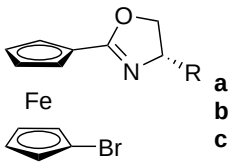

	R
a	Me
b	*t*Bu
c	Ph

48

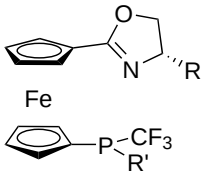

49

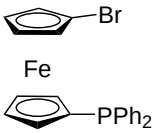

50

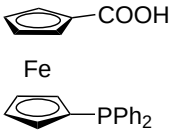

51

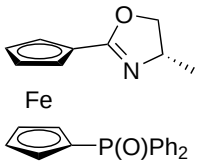

52

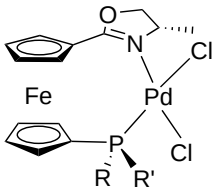

53

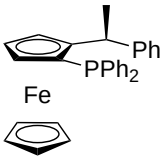

54

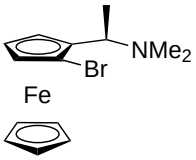

55

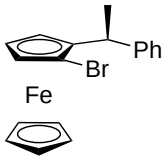

56

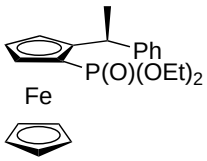

57

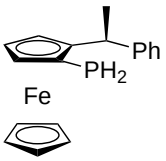

58

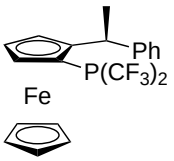

59

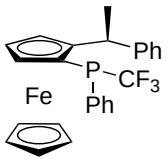

60

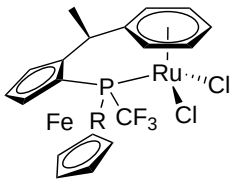

R:
61a Ph
61b CF_3

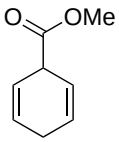

62

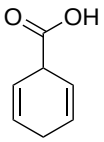

63

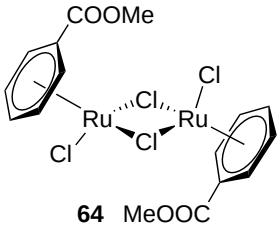

64

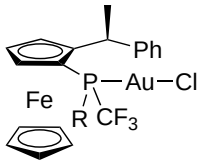

R:
65a Ph
65b CF_3

Appendix C: X-ray data[30]

(4*S*)-2-(2-(phenyl(trifluoromethyl)phosphanyl)phenyl)-4-(propan-2-yl)-4,5-dihydro-1,3-oxazole 26a

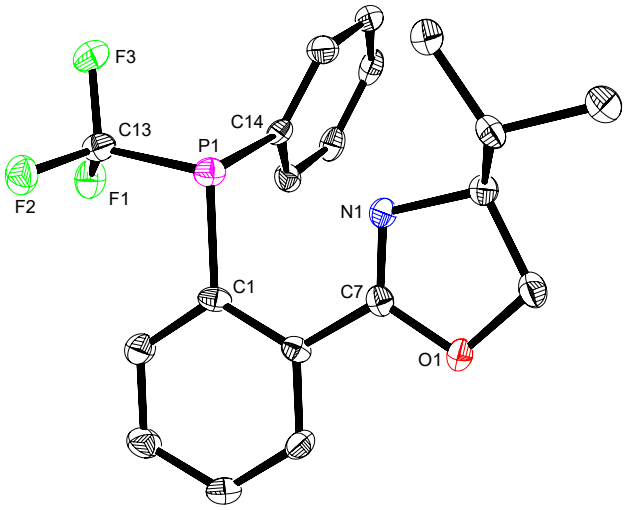

Identification code	RD107	CCDC number	1517362
Crystallization method	hexane/ether	Empirical formula	$C_{19}H_{19}NOF_3P$
Shape	prism	Moiety formula	$C_{19}H_{19}NOF_3P$
Color	clear colorless	Formula weight	365.32
Crystal size (mm)	0.147×0.125×0.075	Temperature (K)	100
Crystal system	orthorhombic	Space group	$P2_12_12_1$
a (Å)	8.4528(3)	α (°)	90
b (Å)	12.6776(5)	β (°)	90
c (Å)	16.8297(9)	γ (°)	90
Volume (Å^3)	1803.49(14)	Z	4
ρ_{calc} (g/cm^3)	1.345	μ (mm^{-1})	0.188
θ_{min}, θ_{max} (°)	2.90, 25.10	F_{000}	760
Limiting indices	$-10 \leq h \leq 11$	Data	4377
	$-9 \leq k \leq 16$	Restraints	0
	$-22 \leq l \leq 20$	Parameters	228
Collected/unique reflections	10181/4377	R_{int}	0.0750
Final R [I≥2σ(I)]	0.0452	$\Delta\rho_{max}$,$\Delta\rho_{min}$ (e·Å^{-3})	0.24, –0.25
Final R [all data]	0.0850	Flack parameter	–0.06(10)

[30] The color coding of the atoms is as follows (adapted from ref.[223]): black = carbon, red = oxygen, blue = nitrogen, magenta = phosphorus, orange = iron, green = fluorine, turquoise = bromine.

(S_C,R_P,S_{Fc})-1-(4-methyl-4,5-dihydro-1,3-oxazol-2-yl)-2-(phenyl(trifluoromethyl)-phosphanyl)ferrocene 34a

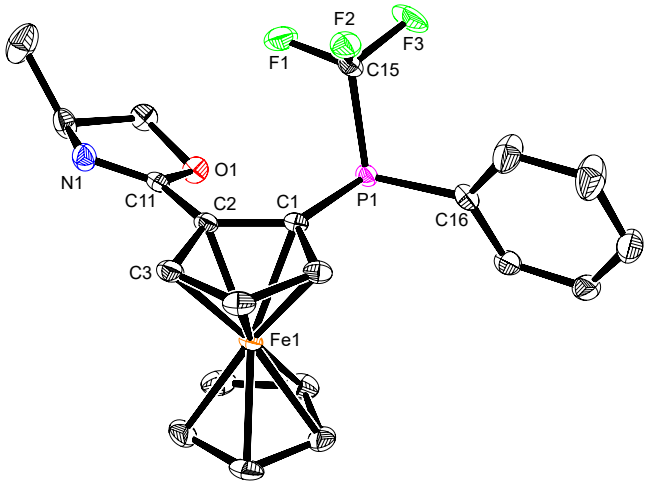

Identification code	RD152_F6-9	CCDC number	1517369
Crystallization method	acetone	Empirical formula	$C_{21}H_{19}NOF_3PFe$
Shape	prism	Moiety formula	$C_{21}H_{19}NOF_3PFe$
Color	clear orange	Formula weight	445.19
Crystal size (mm)	0.302×0.227×0.204	Temperature (K)	100
Crystal system	monoclinic	Space group	$P2_1$
a (Å)	8.0296(6)	α (°)	90
b (Å)	14.0525(10)	β (°)	110.771(2)
c (Å)	9.0786(7)	γ (°)	90
Volume (Å^3)	957.81(12)	Z	2
ρ_{calc} (g/cm^3)	1.544	μ (mm^{-1})	0.910
θ_{min}, θ_{max} (°)	2.71, 33.02	F_{000}	456.0
Limiting indices	$-12 \leq h \leq 12$	Data	6975
	$-21 \leq k \leq 21$	Restraints	1
	$-13 \leq l \leq 13$	Parameters	254
Collected/unique reflections	30145/6975	R_{int}	0.0509
Final R [I≥2σ(I)]	0.0409	$\Delta\rho_{max}$,$\Delta\rho_{min}$ (e·Å^{-3})	0.98, –0.36
Final R [all data]	0.1624	Flack parameter	–0.017(7)

(S_C,R_{Fc})-1-(Diphenylphosphanyl)-2-(4-methyl-4,5-dihydro-1,3-oxazol-2-yl)ferrocene 33

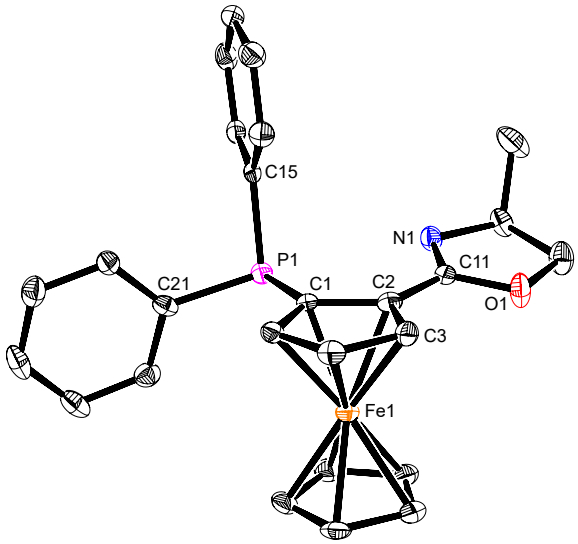

Identification code	RD191	CCDC number	1517347
Crystallization method	ethanol	Empirical formula	$C_{26}H_{24}FeNOP$
Shape	prism	Moiety formula	$C_{26}H_{24}FeNOP$
Color	clear colorless	Formula weight	453.28
Crystal size (mm)	0.255×0.228×0.163	Temperature (K)	100
Crystal system	orthorhombic	Space group	$P2_12_12_1$
a (Å)	10.3111(4)	α (°)	90
b (Å)	12.9167(4)	β (°)	90
c (Å)	16.0041(6)	γ (°)	90
Volume (Å^3)	2131.51(13)	Z	4
ρ_{calc} (g/cm^3)	1.413	μ (mm^{-1})	0.801
θ_{min}, θ_{max} (°)	2.35, 28.02	F_{000}	944.0
Limiting indices	$-14 \leq h \leq 14$	Data	6219
	$-17 \leq k \leq 18$	Restraints	0
	$-17 \leq l \leq 22$	Parameters	272
Collected/unique reflections	14246/6219	R_{int}	0.0677
Final R [I≥2σ(I)]	0.0439	$\Delta\rho_{max}$,$\Delta\rho_{min}$ (e·Å^{-3})	0.73, –0.42
Final R [all data]	0.0665	Flack parameter	–0.002(13)

(S_C,S_{Fc})-1-(Bis(trifluoromethyl)phosphanyl)-2-(1-phenylethyl)ferrocene 59

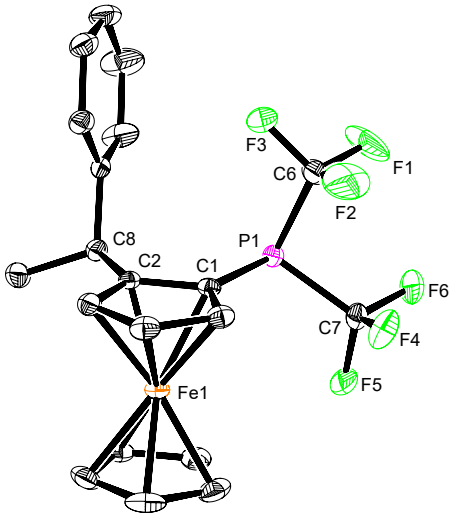

Identification code	MKZ11	CCDC number	1520990
Crystallization method	CH_2Cl_2/hexane	Empirical formula	$C_{20}H_{17}F_6PFe$
Shape	prism	Moiety formula	$C_{20}H_{17}F_6PFe$
Color	orange	Formula weight	458.15
Crystal size (mm)	0.169×0.168×0.071	Temperature (K)	100
Crystal system	orthorhombic	Space group	$P2_12_12_1$
a (Å)	9.4672(10)	α (°)	90
b (Å)	9.7884(10)	β (°)	90
c (Å)	20.566(2)	γ (°)	90
Volume (Å^3)	1905.8(3)	Z	4
ρ_{calc} (g/cm^3)	1.597	μ (mm^{-1})	0.934
θ_{min}, θ_{max} (°)	2.37, 28.63	F_{000}	928.0
Limiting indices	$-12 \leq h \leq 12$	Data	5096
	$-13 \leq k \leq 13$	Restraints	0
	$-28 \leq l \leq 28$	Parameters	254
Collected/unique reflections	21223/5096	R_{int}	0.0467
Final R [I≥2σ(I)]	0.0416	$\Delta\rho_{max}$,$\Delta\rho_{min}$ (e·Å^{-3})	0.52, –0.26
Final R [all data]	0.0340	Flack parameter	–0.013(6)

(S_C,R_P,S_{Fc})-1-(1-Phenylethyl)-2-(phenyl(trifluoromethyl)phosphanyl)ferrocene 60

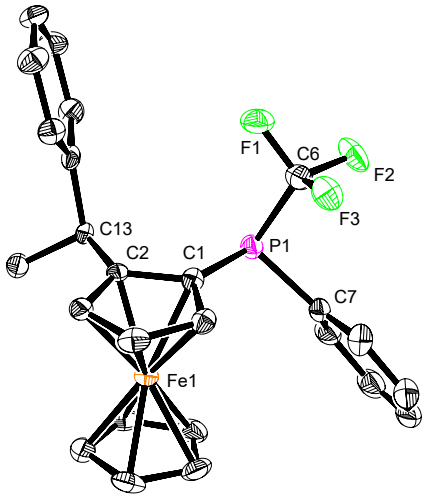

Identification code	MKZ43_B	CCDC number	1520992
Crystallization method	hexane	Empirical formula	$C_{25}H_{22}F_3PFe$
Shape	prism	Moiety formula	$C_{25}H_{22}F_3PFe$
Color	orange	Formula weight	466.24
Crystal size (mm)	0.281×0.211×0.192	Temperature (K)	100
Crystal system	orthorhombic	Space group	$P2_12_12_1$
a (Å)	11.3630(18)	α (°)	90
b (Å)	11.3974(18)	β (°)	90
c (Å)	16.248(3)	γ (°)	90
Volume (Å^3)	2104.3(6)	Z	4
ρ_{calc} (g/cm^3)	1.597	μ (mm^{-1})	0.828
θ_{min}, θ_{max} (°)	2.18, 23.85	F_{000}	960.0
Limiting indices	$-14 \leq h \leq 14$	Data	5008
	$-14 \leq k \leq 11$	Restraints	0
	$-21 \leq l \leq 21$	Parameters	272
Collected/unique reflections	16361/5008	R_{int}	0.1029
Final R [I≥2σ(I)]	0.1031	$\Delta\rho_{max}$,$\Delta\rho_{min}$ (e·Å^{-3})	0.57, –0.31
Final R [all data]	0.0681	Flack parameter	–0.016(17)

(S_C,S_P,S_{Fc})-1-(1-Phenylethyl)-2-(phenyl(trifluoromethyl)phosphanyl)ferrocene 60

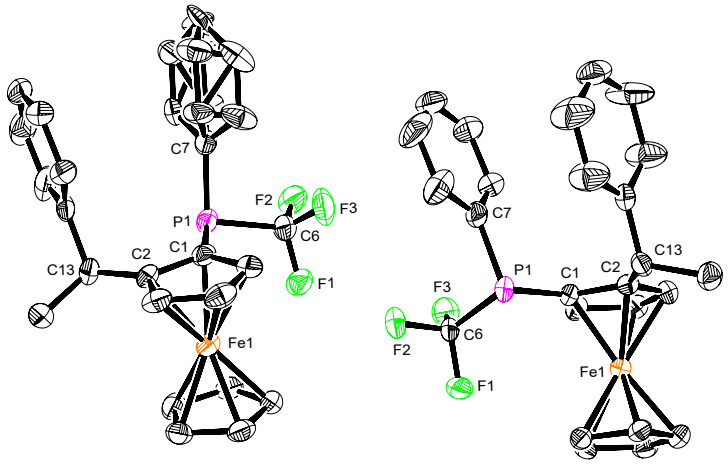

Identification code	MKZ43_A	CCDC number	1520993
Crystallization method	pentane	Empirical formula	$C_{25}H_{22}F_3PFe$
Shape	prism	Moiety formula	$C_{25}H_{22}F_3PFe$
Color	orange	Formula weight	466.24
Crystal size (mm)	0.305×0.302×0.168	Temperature (K)	100
Crystal system	monoclinic	Space group	$P2_1$
a (Å)	10.927(9)	α (°)	90
b (Å)	11.288(10)	β (°)	107.418(11)
c (Å)	18.161(15)	γ (°)	90
Volume (Å^3)	2138(3)	Z	4
ρ_{calc} (g/cm^3)	1.449	μ (mm^{-1})	0.815
θ_{min}, θ_{max} (°)	2.15, 28.20	F_{000}	960.0
Limiting indices	$-14 \leq h \leq 14$	Data	9685
	$-14 \leq k \leq 14$	Restraints	1
	$-23 \leq l \leq 23$	Parameters	590
Collected/unique reflections	33487/9685	R_{int}	0.0669
Final R [I≥2σ(I)]	0.0514	$\Delta\rho_{max}$,$\Delta\rho_{min}$ (e·Å^{-3})	1.33, –0.63
Final R [all data]	0.0912	Flack parameter	0.01(3)

Appendix D: Lithiation screening table

Various reaction conditions attempted towards ligands **34a–c**.*

Entry	Reaction	S.m.[a]	RLi	Electrophile	Solvent	T_1, t_1	T_2, t_2	T_3, t_3	Products?[b]
1[c]	RD104	**32a**	*t*BuLi	$PPh(CF_3)_2$	THF	–78 °C, 20 min	rt, 12 h	-	54% s.m., both diast. seen
2	RD144	**32a**	*n*BuLi	$PPh(CF_3)_2$	Et_2O	0 °C, 15 min	rt, 12 h	-	37% s.m., 23% diast1, 41% diast2
3	RD145	**32a**	*s*BuLi	$PPh(CF_3)_2$	Et_2O	0 °C, 15 min	rt, 12 h	-	44% s.m., 17% diast1, 39% diast2
4	RD146	**32a**	*n*BuLi	$PPh(CF_3)_2$	hexane	0 °C, 15 min	rt, 12 h	-	both diast. seen
5	RD147	**32a**	*s*BuLi	$PPh(CF_3)_2$	hexane	0 °C, 15 min	rt, 12 h	-	92% s.m., 2% diast1, 6% diast2
6	RD179	**32b**	*n*BuLi	$PPhCl_2$	Et_2O	–78 °C, 2 h	0 °C to rt, 2 h	-	s.m.
7	RD180	**32b**	*n*BuLi	$PPhCl_2$	Et_2O	–78 °C, 2 h	0 °C to rt, 16 h	-	s.m.
8	RD187	**32c**	*n*BuLi	PPh_2Cl	Et_2O:THF	–78 °C, 2 h	0 °C to rt, 48 h	50 °C, 1 d	s.m.
9	RD188	**32b**	*n*BuLi	PPh_2Cl	Et_2O:THF	–78 °C, 2 h	0 °C to rt, 48 h	50 °C, 1 d	s.m.
10	RD189	**32c**	*n*BuLi	$PPh(CF_3)_2$	Et_2O	0 °C to rt, 2 d	rt, 2 d	50 °C, 1 d	~90% s.m., no diast
11	RD190	**32b**	*n*BuLi	$PPh(CF_3)_2$	Et_2O:THF	0 °C to rt	rt, 2 d	50 °C, 1 d	~60% s.m., no diast
12	RD196	**32b**	*n*BuLi	PPh_2Cl	THF	–78 °C, 2 h	0 °C to rt, 16 h	-	s.m.
13	RD197	**32c**	*n*BuLi	PPh_2Cl	THF	–78 °C, 2 h	0 °C to rt, 16 h	-	ferrocene, s.m.
14	RD205	**32b**	*n*BuLi	$P(O)(OEt)_2Cl$	THF	–78 °C, 1 h	0 °C to rt, 16 h	-	unknown prod.
15	RD219	**32a**	*n*BuLi	PCl_3, then LAH	THF	–78 °C, 30 min	rt, 1.5 h	–78 °C to rt, 16 h	inconclusive
16	RD243	**32a**	*n*BuLi	PPhiPrCl	hex:THF	–78 °C, 2 h	0 °C to rt, 16 h	-	apparent product signals (^{31}P)
17	RD244	**32b**	*n*BuLi	PPhiPrCl	hex:THF	–78 °C, 2 h	0 °C to rt, 16 h	-	no
18	RD245	**32c**	*n*BuLi	PPhiPrCl	hex:THF	–78 °C, 2 h	0 °C to rt, 16 h	-	no
19	RD249	**32d**	*n*BuLi	$PPhCl_2$	THF	–78 °C, 1.5 h	0 °C to rt, 2 h	-	no
20	RD265	**32a**	*n*BuLi	PPh_2Cl	toluene	–78 °C, 2 h	0 °C to rt, 16 h	-	no
21[d]	RD266	**32a**	*n*BuLi	PPh_2Cl	THF	–78 °C, 20 min	rt, 15 min	–78 °C to rt, 16 h	apparent product signals (^{31}P)

*Conditions: RLi (1.3 eq), TMEDA (1.3 eq), E^+ (x.x eq.). [a] S.m. = Starting material. [b] Diast. = Diastereomer. [c] No TMEDA was used. [d] PMDTA was used instead of TMEDA.

Appendix E: ^{31}P and ^{19}F NMR spectra of the reaction of $PPh(CF_3)_2$ with *n*BuLi (RD271)